Retrospective Theses and Dissertations

Iowa State University Capstones, Theses and Dissertations

2006

Early age behavior of jointed plain concrete pavements subjected to environmental loads

Sunghwan Kim
Iowa State University

Early age behavior of jointed plain concrete pavements subjected to environmental loads

by

Sunghwan Kim

A dissertation submitted to the graduate faculty

in partial fulfillment of the requirements for the degree of

DOCTOR OF PHILOSOPHY

Major: Civil Engineering (Civil Engineering Materials)

Program of Study Committee:
Halil Ceylan, Co-major Professor
Kejin Wang, Co-major Professor
Charles T. Jahren
R. Chris Williams
Tomas J. Rudophi

Iowa State University

Ames, Iowa

2006

UMI Number: 3243549

UMI®

TABLE OF CONTENTS

LIST OF FIGURES

LIST OF TABLES

ABSTRACT

Studies on deformation characteristics of early-age Jointed Plan Concrete Pavements (JPCP) subjected to pure environmental loading has drawn significant interest as it is believed that the early-age deformation of Portland Cement Concrete (PCC) slab could result in the loss of pavement smoothness and the tensile stresses induced by these deformations could result in early-age cracking. However, the complex interaction of several environmental factors has resulted in difficulties in predicting the JPCP deformation characteristics under environmental loading. Also, the effect of the resulting slab distortion on the initial JPCP smoothness has not been adequately addressed by previous research studies.

In this study, two newly constructed JPCP test sections; one on highway US-34 near Burlington and the other on US-30 near Marshalltown, Iowa were instrumented and monitored during the critical time (seven days) immediately following construction during the summer of 2005. Temperature data and moisture data obtained from both sites were analyzed. The slab deformations associated with temperature and moisture were analyzed using measured vertical displacements and pavement surface profile measurements. Using the longitudinal surface profile measurements from different locations of the test section during the morning and afternoon diurnal cycles, the smoothness indices such as International Roughness Index (IRI) and Ride Number (RN) were computed.

The early-age deformation behavior of instrumented JPCP under environmental loading was simulated using ISLAB 2000 (2.5-D) and EverFE 2.24 (3-D) Finite Element

(FE) programs using the *equivalent temperature difference* concept. The changes in smoothness indices at different measurement times were investigated and compared with those obtained using FE simulations.

This study shows that the early-age deformation behavior of PCC is influenced not only by temperature variation but also by other environmental factors such as the moisture variation, drying shrinkage and temperature condition during pavement construction. Even though it is observed that measurable changes of early-age pavement smoothness do occur between morning and afternoon, these variations are not statistically significant.

CHAPTER 1. INTRODUCTION

1.1 Background

In simple words, the purpose of a road is to provide an open, public way for the passage of vehicles, people, and animals. To help make this road durable and capable of withstanding traffic and environment loading,, various combinations of aggregates and binding materials such as ordinary Portland Cement Concrete (PCC) and Hot Mix Asphalt (HMA) have been used over the years. These are primarily used to make a hard smooth surface (commonly referred to as pavement) for the conveyance of traffic.

Currently, over 3.99 million public centerline miles of road has been built in the United States and approximately 2.57 million miles of this (about 64 percent) are paved (FHWA, 2004). Approximately six percent of these pavements have been constructed using PCC wearing course or as a rigid pavement structure. The ability of PCC pavements to carry higher traffic loads and sustain harsher environments make them a better technical option; eventually manifesting themselves in approximately 40 % of the Federal – Aid Highways, which are segments of state and local road systems eligible for Federal-aid construction and rehabilitation funds because of their service value and importance (FHWA, 2004). Especially, over 87 % of the Federal – Aid Highways in Iowa are PCC pavements (FHWA, 2004). Considering the growth of traffic on the highway systems over times and our inability to predict this growth precisely, the use of PCC is a promising choice because of low maintenance costs.

The early-age behavior of PCC pavements (i.e. before opening to traffic) have drawn the attention of several researchers (Rasmussen, 1996; McCullough and Rasmussen, 1999) because of the growing need to expedite construction without compromising on pavement quality to minimize traffic delay and user cost. Even though the concrete pavements are subjected to only environmental loads including temperature (inducing curling) and moisture (inducing warping) during this period, the volumetric distortion of slab occurring in this period and the associated mechanical and environmental loadings after traffic opening could influence long-term performance of PCC pavement. In addition, there are very few studies directly addressing early age slab distortion behavior corresponding to environmental loads with the majority of studies focusing on theoretical analysis of temperature inducing curling stress (Westergaard, 1926; Thomlison, 1940; Ioannides and Salsili-Murua, 1989; Choubane and Tia, 1992; Lee and Dater, 1993; Harik, et. al., 1994; Massad and Taha, 1996; Mohamed and Hansen, 1997; Ioannides and Khazanovich, 1998).

Providing smoothness to traveling user is one of the important functions of a pavement. The initial smoothness immediately after construction can significantly affect the pavement service life (Janoff, 1990). Smith et al. (1997) reported that pavements constructed smoother stayed smoother over time provided all other factors affecting smoothness remained the same. Many agencies have established and implemented smoothness specifications for newly constructed pavements. Using these specifications, the agencies determine the bonuses or penalties to the contractor thereby encouraging the contractor to construct smoother pavements with smoothness levels higher than a specified value (Chou et. al., 2005). Even though it has been noticed that the change in

curvature of slab due to the temperature and moisture variation in climate could have significant influence on pavement smoothness measurements (Hveem, 1951; Karamihas et al., 1999), the effect of this distortion of slab on the initial smoothness have been very little discussed and studied in the literature.

1.2 Objectives

The objectives of this study are to:

- To understand the early-age behavior of Jointed Plain Concrete Pavement (JPCP) to environmental loads;
- To develop the pavement deformation model due to pure environmental loading at critical periods immediately after construction using Finite Element (FE) techniques; and
- To investigate the effect of slab curvature resulting from environmental loading on the initial smoothness of concrete pavements.

1.3 Research Approach

The newly constructed JPCP on US-34 near Burlington and US-30 near Marshall Town, Iowa were instrumented and monitored during the critical time immediately following construction (7 days after construction) to fulfill the objectives in this study. The information available including pavement design and mix design of these pavements were collected. Instrumentation consisted of the temperature and humidity sensors installed within the slab depth and the Linear Variable Differential Transducers (LVDTs) at the slab corner, center, and edges. In addition, surface profile measurements were

made during the early morning and late afternoon hours. A series of laboratory tests were undertaken to characterize the properties of paving material during controlled field evaluation.

Figure 1-1 shows the overall strategy schematically outlined used in this study. The research approach can be broken into three parts following the objectives;

1. In the first part, the slab deformation behavior corresponding to environmental loads including temperature variation were investigated using field collected data such as temperature, moisture, vertical movements and slab curvature profile.

2. Based on findings of first part, all the active environmental effects were quantified as equivalent temperature producing actual pavement deflection response at certain measured temperature difference. Using the quantified equivalent temperature difference combined with collected paving material properties and pavement design properties, the simulations of slab deformation behavior with two dimensional (2-D) and three dimensional (3-D) Finite Element (FE) programs (ISLAB 2000 and EverFE 2.24) were performed in second part.

3. Finally, the effect of slab curl behavior corresponding to environmental loads was identified using field measured smoothness indices variations and FEM predicted smoothness indices variation between morning and afternoon.
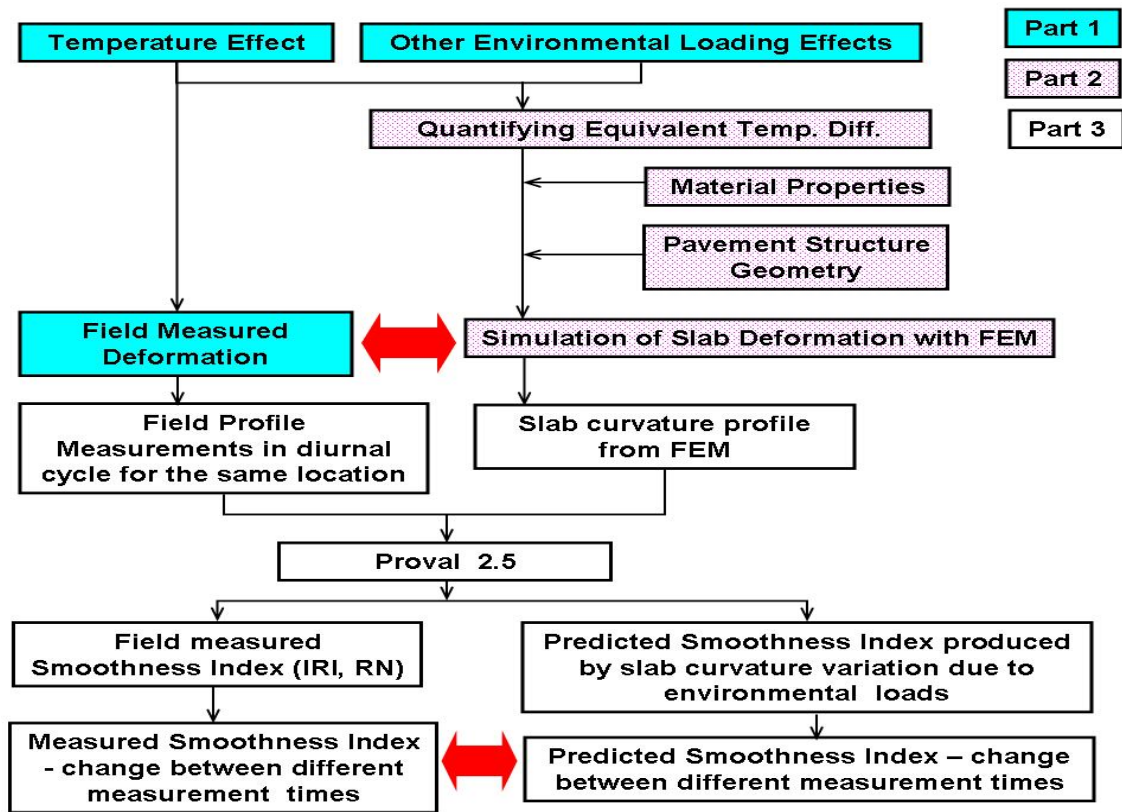
Figure 1-1 Flow chart of research approach

1.4 Dissertation Organization

Nine chapters, including five papers related with the experimental works and FE-simulations, are presented in this dissertation. The experimental studies include series of laboratory tests and instrumented pavements monitoring data. The FE-modeling include the simulation of slab curvature profile and of smoothness indices changes.

Chapter 1 presents the general background, research objectives and approach, and dissertation organization.

Chapter 2 contains general literature review, which serves to provide the necessary background and terminology on this study. PCC pavement systems used and various categories of environmental loads resulting in PCC slab deformation are also reviewed in this chapter. The application of FE method in the design and analysis of concrete pavement and the concept of pavement smoothness are provided.

Chapter 3 describes the laboratory test methods and the field measurement activities as experimental program. The laboratory test procedures are presented including compressive and split tensile strength, elastic modulus, and coefficient of thermal expansion (CTE) tests. Finally, field activities to measure temperature, moisture, vertical movement and surface profile in concrete pavements are summarized.

Chapter 4 presents paper 1: ***Early Age Response of Jointed Plain Concrete Pavements to Temperature and Moisture Variations***. The procedure and the results of data analysis using the collected data from the instrumented pavement in US-30 near Marshalltown, Iowa are discussed in this paper highlighting the important findings regarding the early-age curling and warping behavior of JPCP.

Chapter 5 contains paper 2: ***Characterization of the Early Age Jointed Plain Concrete Pavements Deformation under Environmental Loads Using Equivalent Temperature Difference Concept***. The procedures and the results of FE models based on the collected data and the quantified equivalent temperature differences using two different approaches are discussed. Comparisons between the field measured (US-30 near Marshalltown) and the FE computed slab deformations are presented in this paper.

Chapter 6 presents paper 3: ***The Effects of Slab Curvature due to Environmental Loading on Initial Smoothness of Jointed Plain Concrete Pavements***. The procedure

and the results of data analysis are discussed in this paper highlighting the important findings regarding the effect of slab curvature resulting from environmental loadings on the smoothness of newly constructed pavements in US-30 near Marshalltown at the critical time (7 days) immediately following construction.

Chapter 7 presents paper 4: *Evaluation of Finite Element Models for Studying Early-Age Deformation of Jointed Plain Concrete Pavements under Environmental Loading*. Sensitivity analyses of input parameters in ISLAB 2000 and EverFE 2.24 for rigid pavement deflection due to environmental effects were discussed to establish more realistic input parameter combinations based on field and laboratory test data collected from instrumented pavements on US 34 near Burlington, Iowa. The procedure and the results of the FE analysis are discussed. Comparisons between the field (US-34 near Burlington) measured and the FE computed slab deformations are presented in this paper.

Chapter 8 contains paper 5: *Environmental Effects on the Deformation and Smoothness Behavior of Early Age Jointed Plain Concrete Pavements*. The procedure and the results of data analysis using the colleted data from the tested pavement in US-34 near Burlington and FE-based model are discussed in this paper highlighting the important findings regarding the early-age curling and warping behavior and the effect of these behaviors on the initial smoothness of newly constructed pavement during 7days after paving.

Chapter 9 provides a summary of these research works, contributions of this study and recommendations for future research.

Six appendices are included at the end of this dissertation, which contain the complete sets of data collected from laboratory tests and field measurements in this study and graphs of the FE-simulation.

1.5 References

Choubane, B. and Tia, M., 1992, "Nonlinear Temperature Gradient Effect on Maximum Warping Stresses in Rigid Pavements," *Transportation Research Board*, Vol. 1370, Washington, D. C., pp. 14-24.

Chou, S. F. and Pellinen, T. K., 2005, "Assessment of Constriction Smoothness Specification Pay Factor Limits Using Artificial Neural Network Modeling," *Journal of Transportation Engineering*, Vol. 131, No.7, American Society of Civil Engineering, pp.563-570.

Federal Highway Administration (FHWA.), 2004, *Highway Statistics 2004*. Office of Highway Policy information, FHWA, Washington, D.C.

Harik, I. E., Jianping, P., Southgate, H., and Allen, D., 1994, "Temperature Effects on Rigid Pavements," *Journal of Transportation Engineering*, Vol. 120, No.1, American Society of Civil Engineering, pp.127-143.

Hveem, F. N., 1951, "Slap Warping Affects Pavement Joint Performance," *Proceedings of the American Concrete Institute*, Vol. 47, pp.797-808.

Ioannides, A. M. and Khazanovich, L., 1998, "Nonlinear Temperature Effects on Multilayered Concrete Pavements," *Journal of Transportation Engineering*, Vol.124, No.2, American Society of Civil Engineering, pp.128-136.

Ioannides, A. M. and Salsili-Murua, R. A., 1989, "Temperature Curling in Rigid Pavements: An Application of Dimensional Analysis," *Transportation Research Record*, Vol. 1227, Transportation Research Board, Washington, D. C., pp.1-10.

Janoff, M. S., 1990, "The Prediction of Pavement Ride Quality from Profile Measurements of Pavement Roughness," *Surface Characteristic of Roadways: International Research Technologies*, ASTM STP 1031, American Society of Testing and Materials, Philadelphia, Pennsylvania, pp.259-267.

Karamihas, S. M., Gillespie, T. D., Perera, R. W., and Kohn, S. D., 1999, *Guidelines for Longitudinal Pavement Profile Measurement*, National Cooperative Highway Research Program Report 434, Transportation Research Board, Washington. D.C.

Lee, Y. H. and Dater, M. I., 1993, "Mechanistic Design Models of Loading and Curling in Concrete Pavements," *Proceedings of Airport Pavement Innovations – Theory to Practice*, Vicksburg, MS.

McCullough, B. F. and Rasmussen, R. O., 1999, *Fast-Track Paving: Concrete Temperature Control and Traffic Opening Criteria for Bonded Concrete Overlays*, Volume I: Final Report, FHWA-RD-98-167, Washington, D.C.

Massad, E. and Taha, R., 1996, "Finite-Element Analysis of Temperature Effects on Plain – Jointed Concrete Pavements," *Journal of Transportation Engineering*, Vol.122, No.5, American Society of Civil Engineering, pp.388-398.

Mohamed, A. R. and Hansen, W., 1997, "Effect of Nonlinear Temperature Gradient on Curling Stress in Concrete Pavement," *Transportation Research Record*, Vol. 1568, Transportation Research Board, Washington, D. C., pp.65-71.

Rasmussen. R.O., 1996, *Development of An Early Age Behavior Model for Portland Cement Concrete Pavements*, Ph.D. Thesis, University of Texas at Austin, Austin, Texas.

Smith, K. L., Smith, K. D., Evans, L. D., Hoerner, T. E., Darter, M. I., and Woodstrom, J. H., 1997, *Smoothness Specifications for Pavements*. National Cooperative Highway Research Program Web Document No. 1, Transportation Research Board, Washington, D.C.

Thomlison, J., 1940, "Temperature Variations and Consequence Stress Produced by Daily and Seasonal Temperature Cycles in Concrete Slabs," *Concrete Constructional Engineering*, Vol. 36, No. 6, pp.298-307 and No.7, pp.352-360.

Westergaard, H. M., 1926, "Analysis of Stressed in Concrete Pavements due to Variations of Temperature," *Proceedings of Highway Research Board*, Vol. 6, National Research Council, Washington, D.C., pp.201-217.

CHAPTER 2. LITERATURE REVIEW

This chapter attempts to present a comprehensive literature review on the early-age deformation characteristics of Portland Cement Concrete (PCC) pavement systems resulting from pure environmental loading, the application of Finite Element (FE) methodology in the analysis and design of PCC pavements, and the concept of pavement smoothness. More specific literature reviews pertaining to each paper are provided in the individual chapters.

2.1 Concrete Pavement Systems

A concrete pavement is composed of PCC as the wearing surface with or without a base course on a prepared subgrade (Siddique, 2004). Early concrete pavements were constructed directly on subgrade without using a base course (referred to as slab-on-grade pavement systems). As the weight and volume of traffic increased over the years, the use of a base course became quite common to prevent pumping (Huang, 1993).

Concrete pavements built in the United States can be classified into three types in terms of their cracking control (Muench et al., 2003):

1. Jointed Plain Concrete Pavement (JPCP): JPCP controls cracks by dividing the pavement into individual slabs separated by contraction and expansion joints. Slabs are typically one lane wide (i.e., 3.7 m (12 ft.)) and 6.1 m (20 ft.) long. JPCP does not use any reinforcing steel but uses dowel bars and tie bars.

2. Jointed Reinforced Concrete Pavement (JRCP): JRCP controls cracks by dividing the pavement into individual slabs separated by contraction and

expansion joints. However, these slabs are much longer (as long as 15 m (50 ft.)) than JPCP slabs, so JRCP uses reinforcing steel within each slab to control cracking within the slab.

3. Continuous Reinforced Concrete Pavement (CRCP): CRCP uses reinforcing steel rather than joints for crack control. Cracks typically appear every 1.1 - 2.4 m (3.5 - 8 ft.) and are held tightly together by the underlying reinforcing steel.

As shown in Figure 2-1, JPCP selected in this research is the most common type of pavement in the United States with 43 states using it, while JRCP and CRCP have been built in only 9 and 6 states, respectively (Muench et al., 2003).

(a) States using JPCP   **(b) States using JRCP**   **(c) States using CRCP**
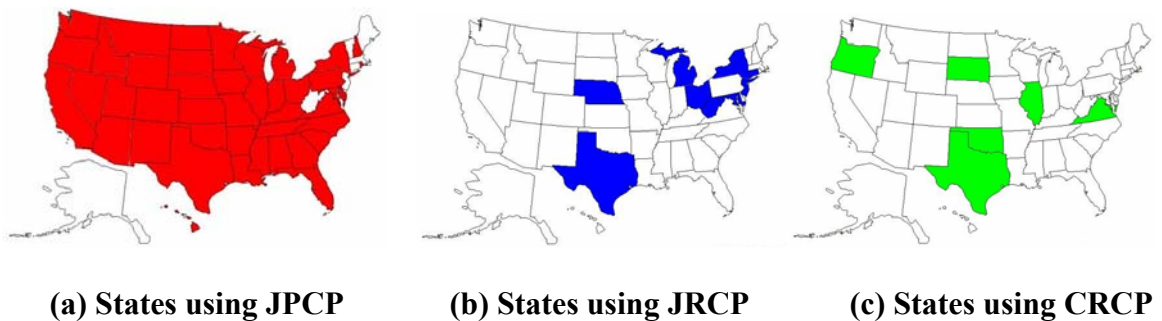
Figure 2-1 Concrete pavement type usage in the U.S. (adopted from Muench et al., 2003)

2.2 Early-Age Behavior of Concrete Pavements under Environmental Loads

The temperature and moisture variations across the depth of the PCC slab can generate a bending curvature with respect to horizontal plan in the PCC slab. In addition, many other environmental factors such as drying shrinkage, pavement temperature

gradient during the setting and curing of PCC, and the creep of the slab may cause this unique curvature behavior during the early age of concrete pavement, in which the concrete transforms from the plastic state to the solid state through a sequence of chemical reactions between the cement components, calcium, and water. Each environmental factor that has an influence on the early-age behavior and curvature of PCC slab is examined in detail and presented in this chapter.

2.2.1 Temperature Gradient

The PCC pavement response to temperature differences through the slab thickness has been recognized as curling. As shown in Figure 2-2, a positive temperature difference between the top and the bottom surfaces of the concrete slab during daytime causes the slab corners to curl downwards while a negative temperature difference during night time results in the upward curling of PCC. Since concrete can recover its original shape after the effects of temperature variation are removed, the curling due to temperature variation from daily or seasonal weather condition can be considered as a transient component of slab curvature behavior due to environmental loading (Yu et al., 2004).

(a) Temp. at top > Temp. at bottom (day-time)   **(b) Temp. at top < Temp. at bottom (night-time)**
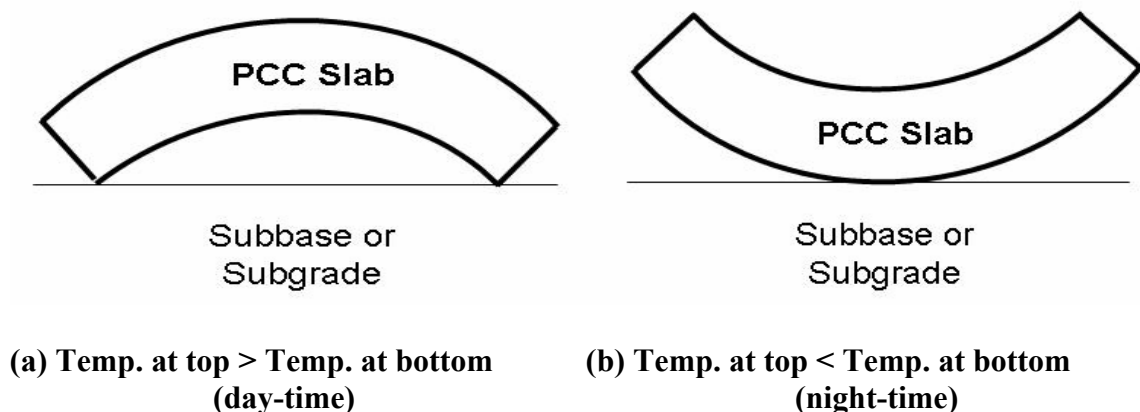
Figure 2-2 Typical slab curling behavior

Curling can create not only slab deformation but also internal stresses in the absence of traffic loading. Westergaard (1926) published the first well known closed–form theory for prediction of PCC slab curling deflections and stress on the basis of assumption of an infinite or semi-infinite slab over dense liquid foundation. Bradbury (1938) later expanded Westergaard's bending stress solutions for a slab with finite dimensions in both x and y directions.

Even though the assumption of linear temperature profile through the depth of PCC has been used in the analysis and design of concrete pavements, it is known that the temperature profile through the depth of PCC is nonlinear from the observation of field measurements (Thomlinson, 1940; Choubane and Tia, 1992). As shown in Figure 2-3 (Choubane and Tia, 1992), total nonlinear temperature profile in a slab can be thought of as having three components: (a) uniform component causing axial expansion or contraction, (b) a linear component causing bending of pavement slab, and (c) a zero – moment nonlinear component that remains after subtraction of the uniform and linear component from total nonlinear components.

| Total nonlinear temperature profile | (a) Uniform component | (b) Linear component | (C) Zero-moment nonlinear component |
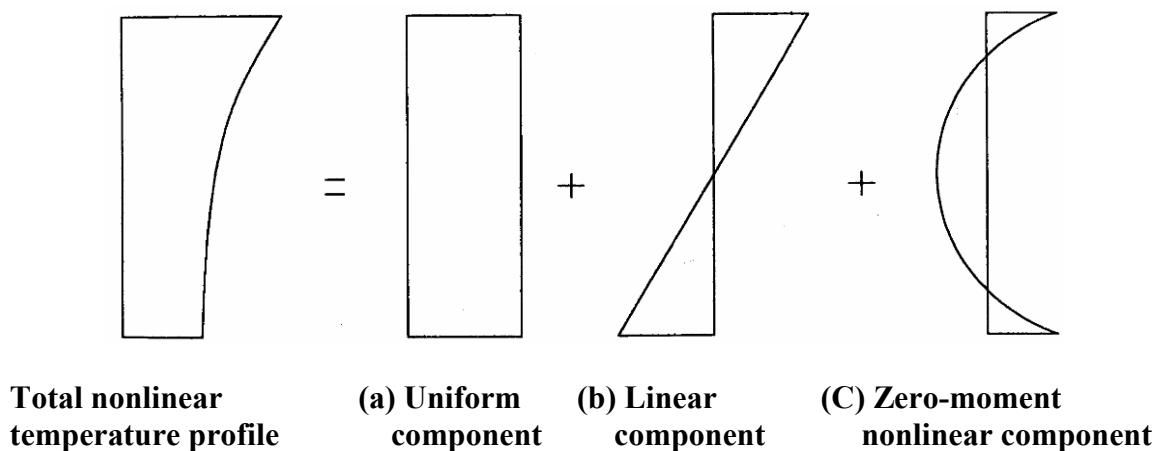
Figure 2-3 Typical temperature profile through the slab thickness (adopted from Choubane and Tia, 1992)

Even though the lack of knowledge of the zero–moment nonlinear component could lead to higher maximum computed tensile stress during day time and lower maximum computed tensile stress during night time (Choubane and Tia, 1992), the zero–moment nonlinear temperature component couldn't have a significant influence in the calculation of curling deflection since the curling deflection could be generated from external moment (Yu et al., 2004).

2.2.2 Moisture Gradient

The moisture gradient through the depth of PCC affects the reversible shrinkage which is recognized as warping. The moisture gradient is influenced by the daily and seasonal weather conditions and the pavement material such as permeable base and poor drainage soils (Rao and Roesler, 2005). Especially, it has been recognized that seasonal variations could be more influential than daily variations due to the low hydraulic conductivity of concrete (Vandenbossche, 2003; Yu, et al 2004). The reversible warping causing moisture variations from seasonal weather conditions are accounted for transient component of slab curvature behavior under environmental loads in the new Mechanistic-Empirical Pavement Design Guide (MEPDG) under the National Cooperative Highway Research Program Project 1-37 A (NCHRP, 2004)

As shown in Figure 2-4, a positive moisture difference between the top and the bottom surfaces of the concrete slab causes the slab corners to warp downwards while a negative moisture difference results in the upward warp of PCC. However, even in very dry area, the surface of the slab is typically only partially saturated while the bottom is usually saturated (Janssen, 1987; NCHRP, 2004). Therefore, upward warp of PCC caused

by negative moisture difference as shown in Figure 2-4 (b) is usually more obvious than the downward warp as shown in Figure 2-4 (a) (Jeong and Zollinger, 2005) .
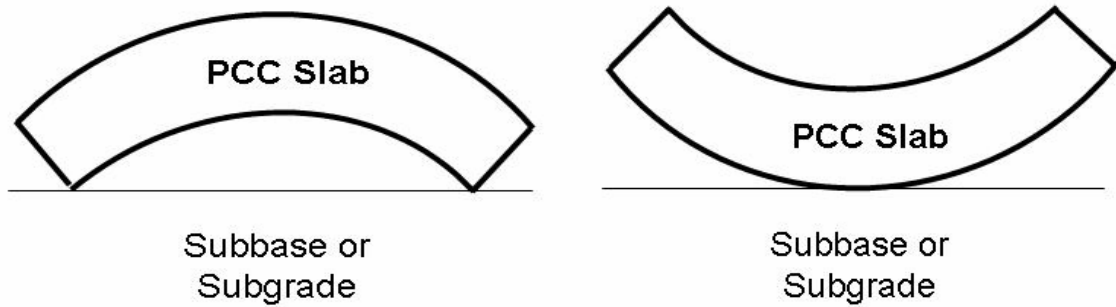
(a) Moisture at top > Moisture at bottom   (b) Moisture at top < Moisture at bottom

Figure 2-4 Typical warping behavior

2.2.3 Shrinkage

The shrinkage can be defined as decrease in either length or volume of a material resulting from changes in moisture content, temperature, or chemical changes (Kosmatka et al., 2002). The main volume change of concrete can be divided into early shrinkage (within 24 hours) and shrinkage of hardened concrete. Early shrinkage includes the chemical shrinkage, the autogenous shrinkage and the plastic shrinkage while shrinkage of hardened concrete includes the drying shrinkage resulting from moisture loss and the volume change due to temperature. The main cause of early shrinkage is the loss of moisture so that the early shrinkage could be considered as a special case of drying shrinkage in fresh concrete (Mindess and Young, 1981). In addition, the volume change due to temperature in hardened concrete should be related to curling behavior, which

makes the slab recover the original shape after removing the temperature effect. The

main types of shrinkage causing loss of moisture in concrete are summarized in Table 2-1.

Table 2-1 Main types of shrinkage in concrete

Type	Description	Reference
Chemical shrinkage	The reduction in absolute volume of solid and liquids in paste resulting from cement hydration in fresh concrete	Kosmatka et al. 2003
Autogenous shrinkage	The macroscopic volume reduction associating with the loss of water from the capillary pores due to the cement hydration in fresh concrete	Holt and Janssen,1998
Plastic shrinkage	The reduction of volume in surface of fresh concrete associating the loss of moisture from surface causing the evaporation and suction by the underlying dry concrete or soil.	Nevil, 1996.
Drying shrinkage	The volume change of hardened concrete resulting from the loss of moisture	Mindess and Young, 1981

As shown in Figure 2-5, most of the shrinkage, which is caused by the loss of

water, shows the significant irreversible deformation after rewetting. Mindess et al. (2003)

suggested that the origin of this irreversibility could be related to the unstable amorphous

nature of C-S-H, which could experience the rearrangement of their packing causing the

loss of moisture. This irreversibility of shrinkage could contribute to the permanent

deformation at zero temperature and moisture gradient (Yu, et al 2004; NCHRP, 2004).
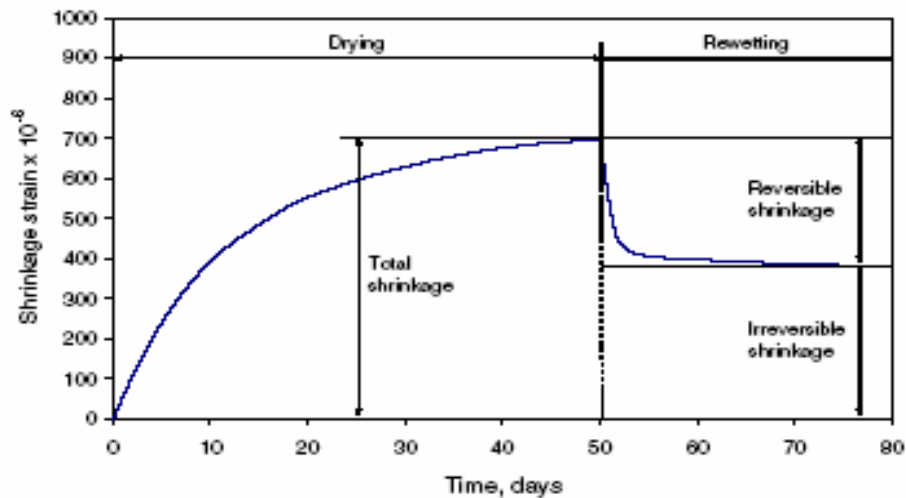
Figure 2-5 Typical behavior of concrete on drying and wetting (adopted from Mindess et al., 2003)

2.2.4 Temperature Condition during Setting of Concrete Pavement

The construction of concrete pavements is typically undertaken during the daytime in warmer months of the years. In this paving period, the top of the slab is typically warmer than the bottom of the slab during the concrete setting time (Rao and Roesler, 2005). The retained amount of heat generated from the cement hydration at the surface could also cause this positive temperature gradient (Vandenbossche et al., 2006). Since the concrete slab set under this condition, the flat slab condition is not associated with a zero temperature gradient but with the positive temperature condition as shown in Figure 2-6 (a). When the temperature gradient in the slab is zero after setting time, the slab curls upward rather than lies flat as shown in Figure 2-6 (b) (Yu, et al., 1998; Rao and Roesler, 2005). This curling up behavior at zero temperature gradient combined with unrecoverable shrinkage was defined as permanent curling and warping in the MEPDG (Yu, et al 2004; NCHRP, 2004).

(a) Temp. at top > Temp. at bottom **(b) Temp. at top = Temp. at bottom**
(during setting time)   **(after setting time)**
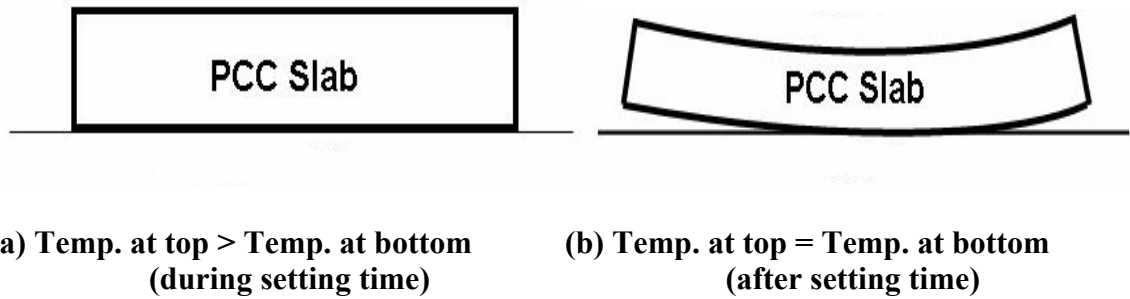
Figure 2-6 Typical slab curvature behavior during and after setting time

2.2.5 Creep

Creep in material can be defined as the time dependent deformation under a constant load while relaxation can be defined as the time dependent stress change under a constant strain condition. Because of the self weight of the slab and also the restraints from the shoulder or the adjacent slab as a constant load, the creep occurred in the already deformed slab can be recovered partially over the time as illustrated in Figure 2-7. (Rao et al., 2001).

(a) Time = 0   **(b) Time = ∞**
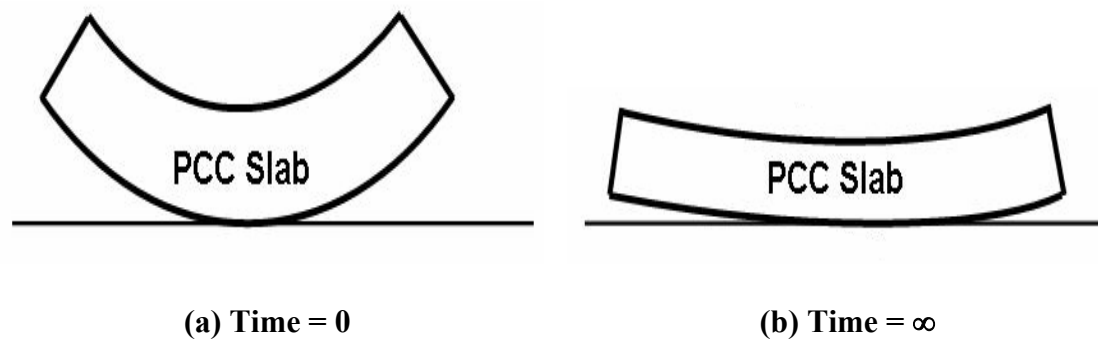
Figure 2-7 Typical creep behavior of deformed slab

2.3 Finite Element Method in the Design and Analysis of Concrete pavements

2.3.1 Finite Element Method

The Finite Element Method (FEM) can be described as a numerical method for solving problems of engineering and mathematical physics. Even though it is difficult to determine the origin of the FEM and the precise moment of its invention (Zienkiewicz and Taylor, 1987), it has been considered that the modern development of the FEM began in the 1940s in the field of structural engineering with the work by Hrennikoff (1941) and McHenry (1943). After their works, from the early 1950s to present, enormous advances have been made in the application of the FEM to complicated engineering problems including structural analysis, heat transfer, fluid flow, mass transport, and electromagnetic potential (Logan, 2002).

For problems involving complicated geometries, loadings, and material properties, it is generally not possible to solve these problems with mathematical expression (ordinary or partial differential equations) that yields the values of the desired unknown quantities at any location in a total structure and are thus valid for an infinite number of locations in a total structure (Logan, 2002). In the FEM, instead of solving the problem for the entire body in one operation, the formulation of the algebraic equations for each smaller bodies or units (finite elements) interconnected at points and the combination of equations yields the solution of a total structure. Although solution obtained by the FEM is an approximation, it is possible to enhance the accuracy of the

result by defining finer elements and providing accurate material properties (Siddique, 2004)

The general step involved in any FE-analysis consists of the following steps (Logan, 2002). Step 1 involves the division of the structure into the finite elements and the selection of the element types requires the decision of the analyst while the other steps, step 2 to step 7, usually are carried out automatically by a computer program.

Step 1. Discrete and select the element types (e.g. line element, two-dimensional element, three –dimensional element, axisymmetric-element, etc.);

Step 2. Select displacement function (e.g. linear, quadratic, cubic polynomials, and trigonometric series, etc.);

Step 3. Define the strain/displacement and stress/strain relationships;

Step 4. Derive the element stiffness matrix and equations with alternative methods such as direct equilibrium method, work/energy methods, and methods of weighted residuals

Step 5. Assemble the element equations to obtain the global or total equations and introduce boundary conditions

Step 6. Solve for the unknown degrees of freedom (or generalized displacements)

Step 7. Solve for the element strains and stresses

Step 8. Interpret the results

2.3.2 Application of FEM in Concrete Pavement Research

With the development of the high speed digital computers, the application of FEM in the design and analysis of concrete pavement has significantly increased over the

past decade (Hammons and Ioannides, 1997). The ability of FEM to solve a broad class of boundary value problems provide a better understanding of the critical aspects of pavements response, such as joint load transfer (Armaghani, et al. 1986; Ioannides and Korovesis, 1990; Ioannides and Korovesis, 1992; Davids, 2001), pavement response under dynamic loads (Chatti, et al, 1994; Vepa and George, 1997) and environmental loads (Ioannides and Salsili-Murua, 1989; Beckemeyer et al, 2002; Rao and Roesler, 2005) that couldn't have been captured with other analytical solutions.

This advantage of FEM has enabled many researchers to apply FE-based methodology for rigid pavement analysis either by using special-purpose software for rigid pavements or by using the commercially available general- purpose FE software. Table 2-2 presented an overview of certain key attributes of the more common FE-programs applied to concrete pavements as originally reported by Hammons and Ioannides (1997) and modified according to additional information based on latest information.

Table 2-2 Overview of FE-programs for concrete pavements (after Hammons and Ioannides, 1997)

Type	Program name	Slab model	Load transfer	Foundation model(s)	Reference
Special-purpose program	ILL-SLAB & ISLAB 2000	2-D medium-thick plate	Linear spring, beam element on spring foundation	Dense liquid, Boussinesq, nonlinear resilient, two and three parameter models	Tabatabaie et al., 1978; Khazanovich, et al., 2000
	JSLAB	2-D medium-thick plate	Linear spring, beam element on spring foundation	Dense liquid	Tayabji et al., 1986
	WESLIQID & KENSLABS	2-D medium-thick plate	Linear springs	Dense liquid	Chou,1981; Huang, 1993
	FEACONS III	2-D medium-thick plate	Linear springs and torsional springs	Dense liquid (linear and nonlinear spring)	Tia et al., 1987
	EverFE 2.24	3-D brick element	Linear and nonlinear springs, interface elements, gap elements, multipoint constraints, explicit models	Dense liquid	Davids, et al., 1998
General-purpose program	ABAQUS	2-D shell element 3-D brick element	Linear and nonlinear springs, interface elements, gap elements, multipoint constraints, explicit models	Dense liquid, 3-D brick element with linear and nonlinear elastic, plastic, and viscoelastic constitutive models, user-defined models	Kuo et al., 1995; Massad et al., 1996; Kim et al., 2003
	ANSYS	3-D brick element	Linear and nonlinear springs, interface elements, gap elements, multipoint constraints, explicit models	Dense liquid	Siddique, 2004 ; Mahboub et al., 2004

Most special-purpose FE programs, customized for concrete pavement modeling and analysis, such as ISLAB 2000, JSLAB, KENSLABS, and FEACONS III use two-dimensional (2-D) plate element, while the general–purpose FE software such as ABAQUS and ANSYS, and the EverFE 2.24 choose three-dimensional (3-D) continuum element as their representation of the slab model. The major advantages of using special-purpose FE software are that they are readily available, require only modest computer resources, and have user-friendly interfaces that can be easily accessed by the pavement designer. However, the general- purpose 3-D FE softwares have the advantage of the ability to more realistically model the pavement structure compared to the ready-made 2-D FE programs. The disadvantages of using the commercial 3-D FE software for rigid pavement modeling are that very few models have been validated and the various features of the software are not readily understood by the pavement designer.

Among the FE-programs applied to concrete pavements, ISLAB 2000 and EverFE 2.24 have some special advantages over other FE programs. These two programs have evolved from earlier versions with validation using field data (Tabatabaie and Barrenberg, 1978; Davids and Mahoney, 1999; Khazanovich et al., 2000; Davids et al., 2003) and can simulate field observed responses well (Wang et al., 2006). In addition, ISLAB 2000 was used as the main structural model cooperating with the neural network for generating pavement responses in the new MEPDG under the NCHRP Project 1-37 A (NCHRP, 2004), and EverFE 2.24 is the only available one of the 3-D FE program among the special-purpose FE programs which can be expected to overcome the disadvantage of 2-D FE programs.

2.4 Pavement Smoothness

The American Society for Testing and Material (ASTM) Standard E867 (1997) defines roughness of road as the deviations of a pavement surface from a true planer surface with characteristic dimensions that affect vehicle dynamics, ride quality, dynamic loads, and drainage. From a road user's point of view, pavement smoothness can de defined as a lack of noticeable roughness and a more optimistic view of the road condition (Sayers and Karamihas, 1998; Akhter et al., 2002). Pavement smoothness has been recognized as an important measurement in evaluating pavement performance because it is directly related to the serviceability of road for the traveling public (Ksaibatti et al., 1995).

Perera (2002) suggested that there are several factors that contribute to pavement roughness: built-in construction irregularities, traffic loading, environmental effects, and construction materials. The construction irregularity can result in poor initial smoothness due to variations in the pavement profile from the design profile and the repeated traffic loading can cause pavement distress such as cracking that result in increased roughness. The environmental effects such as frost heave and volume changes due to shrink and swell of subgarde can also contribute the propagation of roughness over time. In addition, the non-uniformities in the materials used for pavement construction as well as the non-uniform compaction of pavement layers and subgrade can cause roughness. Akhter et al. (2002) reported that the concrete modulus of rupture, subgrade material, number of wet days, and initial roughness could significantly affect the rate of roughness progression as was observed from the roughness index data collected from 21 concrete pavements constructed after 1992 in Kansas.

Even though it has been recognized that low initial roughness can prevent the developing roughness over time and provide the longer pavement life (Ma et al., 1995; Perera et al., 2002), the factors influencing the initial smoothness of a concrete pavement are not very well discussed in literature. However, it is believed that several factors are related to the initial smoothness of a concrete pavement. These include elements related to the pavement design, material selection, concrete uniformity, climate, and construction practices (Ramussen et al., 2002; Ramussen et al., 2004).

A variety of equipment has evolved over the year to measure the roughness of pavements for monitoring the conditions of a pavement network in a pavement management system (PMS) or evaluating the ride quality of newly constructed / rehabilitated pavement. The equipments that are used to measure roughness of pavements can be divided into the five categories (Perera et al., 2002) and presented in Table 2-3.

Because of different instruments for measuring roughness, a parameter representing the actual measuring roughness condition is needed as the same scale. Smoothness Index (or Roughness Index) has been developed and used for this demand. The most common profile indices in the current use can be divided into two categories; ride statistic and profile index. Ride statistic can be computed from a statistic model using measured pavement profile as input and include International Roughness Index (IRI) and Ride Number (RN). Profile Index (PI) can be directly obtained from profile trace measured by the profilograph. Currently, most state agencies use the PI for judging the quality of new pavements and a ride statistic such as IRI for monitoring the condition of their pavement network (Perera et al., 2002; Smith et al., 2002).

Table 2-3 The equipments used for measurement of roughness of pavements
(information were obtained from Perera et al., 2002)

Category	Type	Description
Response type road roughness measurement systems	Bureau of Public Roads (BPR) roughometer, Maysmeter, Portland Cement Association (PCA) roadmeter.	Measuring the response of the road on the vehicle or a special trailer using a transducer
High speed inertia profilers	Dynatest Road Surface Profiler (RSP), International Cybernetic Corporation (ICC) profiler, Infrastructure Management Services (IMS) Laser RST profiler, K.J. Law DNC 690 profiler, Pathway profiler, Roadware profiler.	Recording the true profile of a pavement surface at highway speed by height sensors
Profilographs	California truss type profilograph, Ames profilograph, Rainhart profilograph.	Recording the response of center wheel to road on a strip chart recorder linked to the center wheel
Lightweight profilers	Ames Lightweight Inertial Surface Analyzer (LISA), ICC dual track profiler, K.J. Law lightweight profiler	Installing similar profile system with inertia profiler on a light vehicle, such as a golf cart or an all terrain vehicle
Manual devices	Road and level, Dipstick, Australian Road Research Board (ARRB) walking profiler, ICC rolling profiler	Measuring true elevation of road and checking the accuracy of other profiler

2.5 Summary

Concrete pavements built in the United States could be classified into three types: JPCP, JRCP and CRCP. Among them, JPCP selected in this research has been used by most states in the United States. The JPCP shows the unique bending curvature behavior associated with temperature and moisture variations through the depth of PCC slab. In addition, this curvature behavior of early age JPCP is more complicated because several

other environmental factors such as shrinkage, pavement temperature condition during the setting, and creep of slab could be also involved.

A number of FE-programs have been developed to understand the critical aspects of concrete pavement responses. Among these FE-programs, ISLAB 2000 and EverFE 2.24 have some special advantages over other FE programs and would be able to help better comprehend the complicate behavior associating environment loads.

Even though it has been recognized that low initial roughness can prevent the developing roughness over time and provide the longer pavement life, the factors influencing the initial smoothness of a concrete pavement, especially the effect of environmental condition at early age, have not been very well understood.

2.6 References

Akhter, M., Hussain, M., Boyer, J., and Parcells, W. J., 2002, "Factors Affecting Rapid Roughness Progression on Portland Cement Concrete Pavements in Kansas," *Transportation Research Record*, Vol. 1809, Transportation Research Board, Washington, D.C., pp. 74-84.

Armaghani, J. M., Lybas, J. M., Tia, M., and Ruth, B. E., 1986, "Concrete Pavement Joint Stiffness Evaluation," *Transportation Research Record*, Vol.1099, Transportation Research Board, Washington, D.C., pp. 22-36.

ASTM Standard E867-97: Terminology Relating to Vehicle –Pavement Systems, *Annual Book of ASTM stand*ards, Vol. 04. 03., ASTM International, West Conshohocken, PA, 1998.

Beckemeyer, C. A., Khazanovich, L., and Yu, H. T., 2002, "Determining Amount of Built-in Curling in Jointed Plain Concrete Pavement: Case Study of Pennsylvania I-80," *Transportation Research Record*, Vol. 1809, Transportation Research Board, Washington, D.C., pp. 85-92.

Bradbury, R.D., 1938, *Reinforced Concrete Pavements.* Wire Reinforcement Institute, Washington, D.C.

Chatti, K., Lysmer, J., and Monismith, C. L., 1994, "Dynamic Finite Element Analysis of Jointed Concrete Pavement," *Transportation Research Record*, Vol. 1449, Transportation Research Board, Washington, D.C., pp. 79-90.

Chou, Y. T., 1981, *Structural Analysis Computer Programs for Rigid Multi-Component Pavement Structures with Discontinuities: WESLIQID and WESLAYER*, Technical Report GL 81-6, U.S. Army Engineer Waterways Experiment Station, Vicksburg, Mississippi.

Choubane, B. and Tia, M., 1992, "Nonlinear Temperature Gradient Effect on Maximum Warping Stresses in Rigid Pavements," *Transportation Research Board*, Vol. 1370, Washington, D.C., pp. 14-24.

Davids, W. G., 2001, "3D Finite Element Study on Load Transfer at Doweled Joints in Flat and Curled Rigid Pavements," *The International Journal of Geomechanics*, American Society of Civil Engineering, Vol.1, No.3, pp. 309-323.

Davids, W. G. and Mahoney, J. P., 1999, "Experimental Verification of Rigid Pavements Joint Load Transfer Modeling with EverFE," *Transportation Research Record*, Vol. 1684, Transportation Research Board, Washington, D.C., pp. 81-89.

Davids, W. G., Turkiyyah, G. M., and Mahoney, J. P., 1998, "EverFE: Rigid Pavement Three –Dimensional Finite Element Analysis Tool," *Transportation Research Record*. Vol. 1629, Transportation Research Board, Washington, D.C., pp. 41-49.

Davids, W.G., Wang, Z., Turkiyyah, G. M., Mahoney, J. P., and Bush, D., 2003, "Three-Dimensional Finite Element Analysis of Jointed Plan Concrete Pavement with EverFE2.2," *Transportation Research Record*, Vol. 1853, Transportation Research Board, Washington, D.C., pp. 92-99.

Hammons, M. I. and Ioannides, A. M., 1997, *Advanced Pavement Design:Finite Element Modeling for Rigid Pavement Joints Report I: Background Investigation*, Technical Report DOT- FAA- AR-95-85, Federal Aviation Administration, U.S. Department of Transportation.

Holt, E. and Janssen, D., 1998, "Influence of Early Age Volume Changes on Long Term Concrete Shrinkage," *Transportation Research Record*, Vol. 1610, Transportation Research Board, Washington, D.C., pp. 28-32.

Hrennikoff, A., 1941, "Solution of Problems in Elasticity by the Frame Work Method," *Journal of Applied Mechanics*, Vol. 8, No. 4, pp.169 – 175.

Huang, Y. H., 1993, *Pavement Design and Analysis*, 1st edition, Prentice Hall, Englewood Cliffs, NJ.

Ioannides, A. M. and Korovesis, G. T., 1990, "Aggregate Interlock: A Pure-Shear Load Transfer Mechanism," *Transportation Research Record*, Vol.1286, Transportation Research Board, Washington, D.C., pp. 14-24.

Ioannides, A. M. and Korovesis, G. T., 1992, "Analysis and Design of Doweled Slab-on-grade Pavement Systems" *Journal of Transportation Engineering*, Vol. 118, No. 6, American Society of Civil Engineering, pp. 745-768.

Ioannides, A. M. and Salsili-Murua, R. A., 1989, "Temperature Curling in Rigid Pavements : An Application of Dimensional Analysis," *Transportation Research Record*, Vol. 1227, Transportation Research Board, Washington, D.C., pp. 1-10.

Janssen, D.J., 1987, "Moisture in Portland Cement Concrete," *Transportation Research Record*, Vol. 1121, Transportation Research Board, Washington, D.C., pp. 40-44.

Jeong., J.H. and Zollinger, D.G., 2005, "Environmental Effects on the Behavior of Jointed Plain Concrete," *Journal of Transportation Engineering*, Vol.131, No.2, American Society of Civil Engineering, pp. 140-148.

Ksaibati, K., Staigle, R. and Adkins, T. M., 1995, "Pavement Construction Smoothness Specification in the United States," *Transportation Research Record*, Vol.1491, Transportation Research Board, Washington, D.C., pp. 27-32.

Khazanovich, L., Yu, H. T., Rao, S., Galasova, K., Shats, E., and Jones, R., 2000, *ISLAB2000-Finite Element Analysis Program for Rigid and Composite Pavements*, User's Guide, ERES Consultant, Champaign, Illinois.

Kim, J. and Hjelmstad, K. D., 2003, "Three-Dimensional Finite Element Analysis of Doweled Joints for Airport Pavements," *Transportation Research Record*, Vol.1853, Transportation Research Board, Washington, D. C., pp. 100-109.

Kosmatka, S. H., Kerkhoff, B., and Panarese, W. C., 2002, *Design and control of concrete mixtures*, 4th edition, Portland Cement Association, Skokie, Illinois.

Kuo, C. M., Hall, K. T., and Dater, M. I., 1995, "Three Dimensional Finite Element Model for Analysis of Concrete Pavement Support," *Transportation Research Record*, Vol.1505, Transportation Research Board, Washington, D.C., pp. 119-127.

Logan, D.L., 2002, *A First Course in the Finite Element Method*, 3rd edition, Thomson Learning, Inc., Pacific Grove, CA.

Ma, S. and Caprez, M., 1995, "The Pavement Roughness Requirement for WIM," *First European Conference on Weight –in –motion of Road Vehicle*, Switzerland.

Mahboub, K. C., Liu, Y., and Allen, D. L., 2004, "Evaluation of Temperature Responses in Concrete Pavement," *Journal of Transportation Engineering*, Vol.130, No.3, American Society of Civil Engineering, pp. 395-401.

Massad, E. and Taha, R.,1996, "Finite-Element Analysis of Temperature Effects on Plain – Jointed Concrete Pavements," *Journal of Transportation Engineering*, Vol.122, No.5, American Society of Civil Engineering, pp. 388-398.

McHenry, D., 1943, "A Lattice Analogy for the Solution of Plane Stress Problems," *Journal of Institution of Civil Engineers*, Vol. 21, pp. 59-82.

Mindess, S. and Young, J. F., 1981, *Concrete*. 1st edition, Prentice-Hall, Inc., Englewood Cliffs, NJ.

Mindess, S., Young, J. F. and Darwin, D., 2003, *Concrete*. 2nd edition, Prentice-Hall, Inc., Englewood Cliffs, NJ.

Muench, S. T, Mahoney, J.P. Pierce, L. M., 2003, *WSDOT Pavement Guide*. http://training.ce.washington.edu/wsdot, Washington State Department of Transportation.

National Cooperative Highway Research Program (NCHRP), 2004, *Guide for Mechanistic-Empirical Design of New and Rehabilitated Pavement Structures*, http://trb.org/mepdg., National Cooperative Highway Research Program 1-37A, Transportation Research Board, Washington, D.C.

Nevil, A.M., 1996, *Properties of Concrete*, 4th edition, John Wiley & Sons, Inc., New York, NY.

Perera. R. W and Kohn. S. D., 2002, *Issues in Pavement Smoothness*, National Cooperative Highway Research Program Web Document No. 42, Transportation Research Board, Washington, D.C.

Rao, C., Barenberg, E. J., Snyder, M. B., and Schmidt, S., 2001, "Effects of Temperature and Moisture on the Response of Jointed Concrete Pavements," *Proceedings of 7th International Conference on Concrete Pavements*, Orlando, Florida.

Rao, S., and Roesler, J. R., 2005, "Characterizing Effective Built in Curling from Concrete Pavement Field Measurements," *Journal of Transportation Engineering*, Vol. 131, No.4, American Society of Civil Engineering, pp. 320-327.

Rasmussen, R. O., Karamihas, S. K. and Chang, C. K., 2002, *Inertial Profile Data for Pavement Performance Analysis : Project Overview*, Tech Brief Number 1, Federal Highway Administration Contact DTFH 61-02-C-00077, Washington, D.C.

Rasmussen, R. O., Karamihas, S. K., Cape, W. R., Chang, C. K. and Guntert, R. M., 2004, "Stringline Effects on Concrete Pavement Construction," *Transportation Research Record*, Vol. 1900, Transportation Research Board, Washington, D.C., pp. 3-11.

Sayers, M. W. and Karamihas, S. M., 1998, *The Little Book of Profiling*. University of

Michigan, Ann Arbor. Michigan.

Siddique, Z. Q., 2004, *Finite Element Simulation of Curling on Concrete Pavement*. Ph.D.

Thesis, Kansas State University, Manhattan, Kansas.

Smith, K. L., and Clover, L. T., Evans, L. D., 2002, *Pavement Smoothness Index

Relationships*, Technical Report Feral Highway Administration- RD- 02-057,

Federal Highway Administration, U.S. Department of Transportation.

Tabatabaie, A. M. and Barrenberg, E. J., 1978, "Finite Element Analysis of Jointed or

Cracked Concrete Pavements," *Transportation Research Record*, Vol. 671,

Transportation Research Board, Washington, D. C., pp. 11-17.

Tayabji, S. D. and Colley, B. E., 1986, *Analysis of Jointed Concrete Pavements*,

Technical Report Federal Highway Administration- RD- 86-041, Federal

Highway Administration, U.S. Department of Transportation.

Thomlison, J., 1940, "Temperature Variations and Consequence Stress Produced by

Daily and Seasonal Temperature Cycles in Concrete Slabs," *Concrete

Constructional Engineering*, Vol. 36, No. 6, pp.298-307 and No.7, pp. 352-360.

Tia, M., Armaghani, J. M., Wu, C. L., Lei, S., and Toye, K. L., 1987, " FEACONS Ш,

Computer Program for Analysis of Jointed Concrete Pavements." *Transportation

Research Record*, Vol. 1136, Transportation Research Board, Washington, D. C.,

pp. 12-22.

Vandenbossche, J. M., 2003, *Interpreting Falling Weight Deflectometer Results for

Curled and Warped Portland Cement Concrete Pavements*, Ph.D. Thesis,

University of Minnesota, Minneapolis, Minnesota.

Vandenbossche, J. M., Wells, S. A. and Phillips, B.M., 2006, "Quantifying Built-in Construction Gradients and Early-Age Slab Shape to Environmental Loads for Jointed Plain Concrete Pavements," *CD-ROM Proceedings of the 85rd Annual Meeting of the Transportation Research Board*, Washington, D.C.

Vepa, T. S. and George, K. P.,1997, "Deflection Response Model for Cracked Rigid Pavements," *Journal of Transportation Engineering*, Vol. 123, No. 5, American Society of Civil Engineering, pp.377-384.

Wang, W., Basheer, I., and Petros, K., 2006, "Jointed Plain Concrete Pavement Models Evaluation," *CD-ROM Proceedings of the 85rd Annual Meeting of the Transportation Research Board*, Washington, D.C.

Westergaard, H. M.,1926, "Analysis of Stressed in Concrete Pavements Due to Variations of Temperature," *Proceedings of Highway Research Board*, Vol. 6, National Research Council, Washington, D.C., pp.201-217.

Yu, H. T., Khazanovich, L. Darter, M. I, and Ardani, A., 1998, "Analysis of Concrete Pavement Response to Temperature and Wheel Loads Measured from Instrumented Slab," *Transportation Research Record*, Vol. 1639, Transportation Research Board, Washington, D.C., pp.94-101.

Yu, H. T., Khazanovich, L., and Darter, M. I., 2004, "Consideration of JPCP Curling and Warping in the 2002 Design Guide," *CD-ROM Proceedings of the 83rd Annual Meeting of the Transportation Research Board*, Washington, D.C.

Zienkiewicz, O. C. and Taylor, R. L., 1987, *The Finite Element Method- Basic Formulation and Linear Problems*, Vol. 1, 4th edition, Mcgraw-Hill Book Company, London.

CHAPTER 3. EXPERIMENTAL PROGRAM

An experimental program was established to investigate the early-age curling and warping behavior of JPCP under environmental conditions and also to study the effect of this behavior on the initial smoothness of concrete pavement. All the activities summarized in Table 3-1 were conducted on the controlled test sections of two pavement sections under study during the critical time (seven days) immediately following the construction. This chapter presents the description of each activity in the experimental program.

Table 3-1 Summary of the experimental program

Laboratory testing	Field monitoring
Split tensile test	Slab temperature and moisture gradient
Compressive strength test	Vertical slab movement
Elastic modulus test	Pavement surface profiling for measuring slab curvature profile and smoothness index
Coefficient of thermal expansion	

3.1 Test Sections

Two pavement test sections, constructed during the summer of 2005, US-34 near Burlington and US-30 near Marshalltown in Iowa, were selected in this study. These pavements are typical JPCPs constructed in Iowa following the pavement design in Table 3-2.

The two test sections corresponding to different construction times in the travel lane of each project were utilized for laboratory testing and field evaluation, generally

following the schematic displayed in Figure 3-1. The test sections in US-34 near

Burlington were evaluated from June 7 to June 20, 2005 and the test sections in US-30

near Marshalltown were evaluated from July 13 to July 20, 2005.

Table 3-2 Summary of pavement design information for test sections

Slab	Type		JPCP
	Thickness		260 mm – 280mm (10.2 in. – 11 in.)
	Transverse joint spacing		6 m (20 ft)
	Width	Passing lane	3.6 m (12 ft)
		Travel lane	4.3 m (14 ft)
Base	Type		Open –grade granular
	Thickness		152 mm – 260 mm (6 in. – 10 in.)
Tie bar	Length		914 mm (36 in.)
	Diameter		12.7 mm (0.5 in.)
	Spacing		762 mm (29.5 in.)
Dowel bar	Length		457 mm (18 in.)
	Diameter		38 mm (1.5 in.)
	Spacing		305 mm (12 in.)
Joint depth	Transverse		32 mm (1.25 in.)
	Longitudinal		87 mm (3.4 in.)
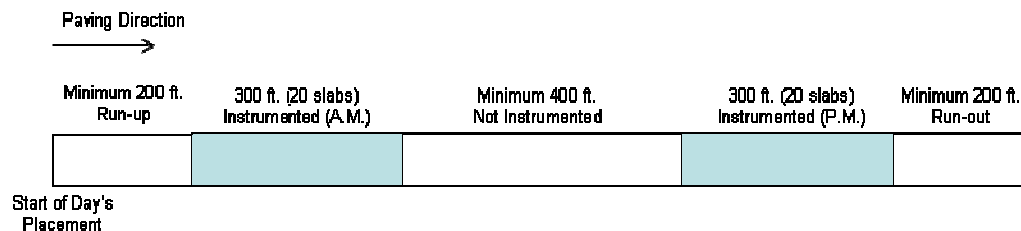
Figure 3-1 Typical test section layout in this study

3.2 Laboratory Testing

A series of laboratory tests at different ages were conducted in ISU's PCC mobile

laboratory and ISU's in-house PCC laboratory to characterize the fundamental physical

properties of the paving material. The concrete mixture designs used in each paving

project are summarized in Table 3-3.

Table 3-3 Summary of concrete mix design information for paving sites

Component	US-34 near Burlington		US-30 near Marshalltown	
	Description	Batch weight	Description	Batch weight
Portland cement	Lafarge - type 1 (SM)	263 kg/m^3	Ash Grove (Louisville, NE) - type I/II	266 kg/m^3
Fly ash	Chillicothe - type C (Spec. Grav. = 2.61)	66 kg/m^3	Ottumwa Generating Station - type C (Spec. Grav. = 2.61)	66 kg/m^3
Coarse aggregate 1	River products (Col. Jct.) - limestone (Spec. Grav = 2.55)	891 kg/m^3	Wendling - Montour #86002 (Spec. Grav = 2.61)	913 kg/m^3
Coarse aggregate 2	River products (Col. Jct.) - limestone (Spec. Grav = 2.55)	266 kg/m^3	Wendling - Montour #86002 (Spec. Grav = 2.61)	162 kg/m^3
Fine aggregate	Cessford (Spring Grove) - natural (Spec. Grav. = 2.66)	650 kg/m^3	Manatt - Flint #86502 (Spec. Grav. = 2.66)	755 kg/m^3
Admixture 1	Brett AEA 92 - Air entrainer	215 mL/m^3	WR Grace - Daravair 1400 - Air entrainer	152 mL/m^3
Admixture 2	Brett Euchon WR - Water reducer	857 mL/m^3	WR Grace - WRDA 82 - Water reducer	759 mL/m^3
Water	132 kg/m^3		133 kg/m^3	
W/C Ratio	0.4		0.4	
Air content	6.00 %		6.00 %	

Using the in-situ samples obtained from the paving site, the concrete specimens

were prepared according to ASTM C 192 (2000) specifications. Immediately following

the sampling, the concrete was placed into the four-inch by eight-inch cylinder in three

layers and rodded 25 times. The specimens were stored in the curing room with a

constant temperature around 25 °C (75 °F) and 100 % humidity. After one day of curing,

the specimens were demolded and stored in curing room again until the test date.

Compressive and split tensile strengths of various aged concretes are measured

according to ASTM C 39 (2001) and ASTM 496 (1996) as shown in Figure 3-2. Elastic

modulus testing of concrete, ASTM C 469(1994), was undertaken at different days as shown Figure 3-3. The average value of the three specimens for each test at different ages in each paving site are provided in Appendix 1.

(a) Compressive strength testing   **(b) Split tensile strength testing**

Figure 3-2 Strength testing of concrete

Figure 3-3 Elastic modulus testing

The Coefficient of Thermal Expansion (CTE) of concrete could be a critical property as input for simulation modeling of slab deformation due to environmental loads with Finite Element (FE) programs. The CTE of specimens for each paving site were measured using CTE apparatus shown in Figure 3-4. The CTE testing apparatus consists of three parts: water bath temperature controller, support frame measuring specimen length changes with submersible spring loaded Linear Variable Differential Transducer (LVDT), and data logger which can collect specimen length changes associated with temperature changes.
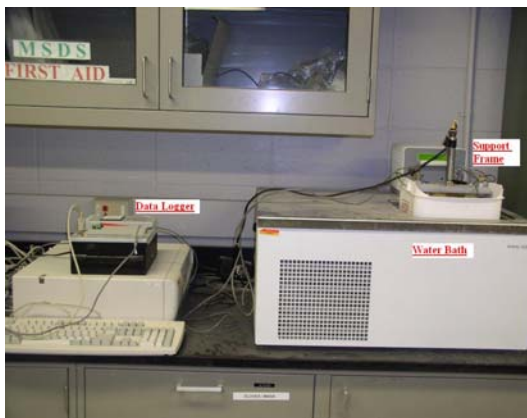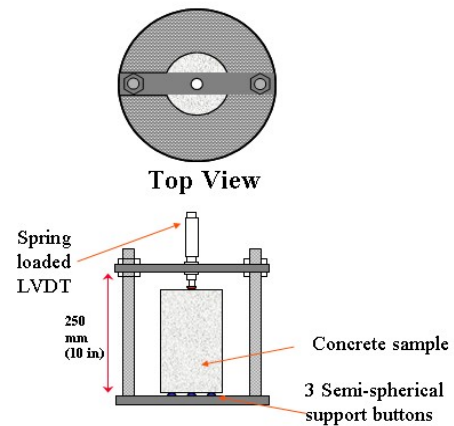
(a) Overview   **(b) Support frame**

Figure 3-4 CTE apparatus

The test procedure as specified in AASHTO T60 (2000) is summarized below:

1. Remove the specimen from the curing room and measure its length (Lo) at room temperature to the nearest 0.1 mm (0.004 inch).

2. Place the specimen in support frame located in the controlled temperature water bath, making sure that the lower end of the specimen is firmly seated

against the support buttons and that the LVDT tip is seated against the upper end of the specimen.

3. Set the temperature of the water bath to 10 ± 1 °C (50 ± 2 °F) as first setting temperature (T_1) and maintain this temperature until thermal equilibrium of water and specimen has been reached.

4. Record the LVDT reading as the first length reading (L1) after the temperature of water has been stabilized at 10 ± 1 °C.

5. Set the temperature of water bath to 50 ± 1 °C (122 ± 2 °F) as second setting temperature (T_2).

6. Record the temperature of water bath and the LVDT reading at every ten minute.

7. Record the LVDT reading as the second length reading (L_2) after the temperature of water has been stabilized at 50 ± 1 °C.

8. Set the temperature of water bath to 10 ± 1 °C (50 ± 2 °F) as third setting temperature (T_3).

9. Record the temperature of water bath and the LVDT reading at every ten minute.

10. Record the LVDT reading as the third length reading (L_3) after the temperature of water has been stabilized at 10 ± 1 °C.

11. Report CTE as average of CTE_1 and CTE_2 obtained from Equation 3-1 and Equation 3- 2.

$$CTE_1 = \frac{(L_2 - L_1) + [C_f \times L_0 \times (T_2 - T_1)]}{L_0 \times (T_2 - T_1)}$$ (Equation 3-1)

$$CTE_2 = \frac{(L_2 - L_3) + [C_f \times L_0 \times (T_2 - T_3)]}{L_0 \times (T_2 - T_3)}$$

(Equation 3-2)

Where, T_1 = the first setting temperature (10 ± 1 °C), T_2 = the second setting temperature (50 ± 1 °C), T_3 = the third setting temperature (10 ± 1 °C), L_0 = the initial length of specimen, L_1 = the first length reading, L_2 = the second length reading, L_3 = the third length reading, C_f = correction factor.

Three specimens for each paving site were made for CTE test. Among them, one specimen was randomly selected for CTE measurement in increasing temperature from 10 ± 1 °C to 50 ± 1 °C and in decreasing temperature from 50 ± 1 °C to 10 ± 1 °C. However, the CTE values obtained for this particular specimen from the two different temperature protocols are not much different (difference of the CTE values in the two different temperature protocols for two different sites are 7.64×10^{-7} ε/°C for US-34 near Burlington and 1.11×10^{-7} ε/°C for US-30 near Marshalltown.), so the CTE measurements of other two specimens were made only in the increasing temperature range (from 10 ± 1 °C to 50 ± 1 °C). The CTE measurements of all the three specimens in each paving site are provided in Appendix 1.

3.3 Field Monitoring

The temperature and humidity sensors installed within the test sections detected the temperature and moisture variations inside the slab corresponding to the weather conditions and these measurements were monitored by ISU's PCC mobile laboratory parked near the test section. In order to measure the slab deformations corresponding to environmental loads, LVDTs were installed at strategic locations within the slab and also

the surface profiles were measured along the diagonal and transverse directions on the slab using an inclinometer-profiler. In addition, the surface profiling was continuously conducted in the future traffic direction (longitudinal direction) on different locations of test section pavements.

3.3.1 Slab Temperature and Moisture Gradient

Temperature and humidity sensors installed within the test sections recorded the slab temperature and moisture data at five- minute intervals throughout the field evaluation periods. Temperature instrumentation consisted of over seven Thermochron I-buttons[®] (Maxim/Dallas, 2006) attached to a stake at different depths and placed at 0.9m (3 ft) from the pavement edge before the paving as shown in Figure 3-5 (a). All the results from this instrumentation in each test section during the evaluation periods are provided in Appendix 2. After obtaining temperature profiles during the evaluation periods, Thermochron I-buttons[®] were reset to log data at 3-hour interval then extended the leadwires beyond the shoulder in a buried pipe to facilitate future research as shown in Figure 3-5 (b).
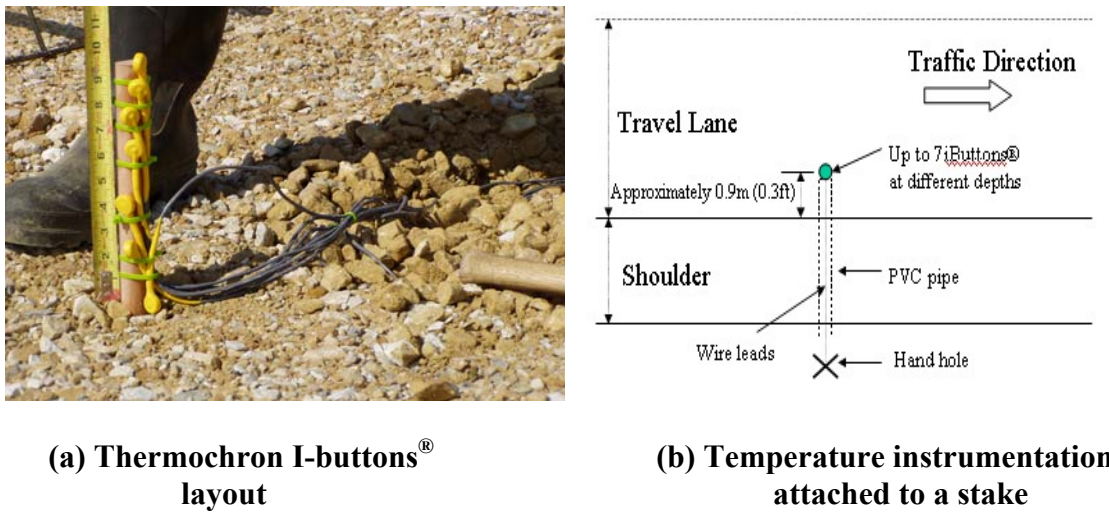
| (a) Thermochron I-buttons® layout | (b) Temperature instrumentation attached to a stake |

Figure 3-5 Typical temperature instrumentation in this study

Humidity instrumentation consisted of four Hygrochron I-Buttons® (Maxim/Dallas, 2006). The installation process was facilitated with Air Void Analyzer (AVA) sampling on fresh concrete slab as shown in Figure 3-6 (a) and then each Hygrochron I-Buttons® were inserted into each of the small Poly Vinyl Chloride (PVC) pipes which were placed side by side at different depths from pavement surface as shown in Figure 3-6 (b). The results from this instrumentation in test sections are provided in Appendix 3.

| (a) AVA sampling | (b) PVC pipes Hygrochron I-Buttons® inserted |

Figure 3-6 Typical humidity instrumentation in this study

3.3.2 Vertical Slab Movement

Two slabs which were paved in the afternoon were selected as representative

slabs to study the pavement vertical movements entirely due to environmental loads.

LVDT used in this study is LD 400-5 by Omega. Inc. that has 1.55 μm resolution and ±5

mm measurement range (Omega, 2006). LVDTs were installed in special locations such

as corners, the mid-slab edges and the center of the slab on each slab to capture the

vertical movements of the slab. All the sensors were placed only after the concrete

hardened (one day after paving). As shown in Figure 3-7, LVDTs were held by a bracket

fastened to the steel rod inserted in subgrade and placed on a smooth glass attached on

the concrete slab. The LVDTs were connected to data loggers, which collected data at ten

minute interval throughout the field evaluation periods. All the LVDTs results on each

installed slab are provided in Appendix 4.

Figure 3-7 Typical LVDT installation in this study

3.3.3 Pavement Surface Profile

The pavement surface profile measurements were undertaken to collect the slab curvature profiles and the roughness index during the morning and afternoon diurnal cycles. The maximum upward curling condition of a slab generally occurs during early morning hours, just before sunrise when the bottom of the slab is warmer than the top, while the maximum downward curling condition generally occurs around noon or in the very early afternoon when the surface of the slab is heated by the sun. These "maximum" conditions of the slab deformations responding environmental loads, of course, couldn't depend only temperature gradient condition but also several environmental factors such as moisture and shrinkage. But in general, these should follow the timeframes for the maximum and minimum ambient temperature conditions. Therefore, the diurnal cycle measurement of profiles for the same location in each section could provide a better understanding of the changes in the slab curl that occur on a daily basis.

An International Cybernetics Corporation (ICC) Rollingprofiler (SurPRO 2000$^®$) as shown in Figure 3-8 with system features was used for surface profile measurements. A Rollingprofiler, an inclinometer-based device, can measure true unfiltered elevation profile of surface along the line being profiled for the slab curvature profile and the roughness index (ICC., 2006). Many researchers have used the inclinometer profiler measurements to quantify the slab curvature (Rao et. al., 2001; Vandenbossche et. al., 2005)

- Word bank class 1 profiling performance (the interval of sampling is less than or equal to 25 mm)
- Fully automatic data collection for longitudinal and transverse profiles
- Produce accurate, repeatable data for 250 mm – 300mm (12 in.) interval
- Provides unfiltered true elevation profiles measured by two inclinometers
- Report multiple roughness indexes (IRI , RN)
- Prints profile and roughness information on site without a notebook computer
- Rolling inclinometer with loaded suspension to ensure stability and accuracy for all speeds and surface conditions
- Permanent factory calibration

Figure 3-8 ICC Rollingprofiler (SurPRO 2000®) (adopted from ICC., 2006)

Several profile patterns as shown in Figure 3-9 were used to accommodate the data collection. Rollingprofiler measurements made as following future traffic direction (longitudinal direction) on different locations of each test section pavements, as shown in Figure 3-9 (a) and (b), could be transformed to roughness index such as IRI and RN as provided in Appendix 7. Profile measurements done in the transverse and diagonal traces, on four selected slabs in each test section (shown in Figure 3-9 (c)), were utilized for identifying the slab curvature profile due to environmental loads at different measurement times. These slab curvature profiles are presented in Appendix 5.

48

(a) Profiling at outside edge and tied centerline

(b) Profiling at 0.3 m(1 ft) and 0.9 m(3 ft) from tied centerline & at 0.6m (2ft) and 0.9 m(3ft) from outside edge

(c) Profiling at diagonal and transverse direction
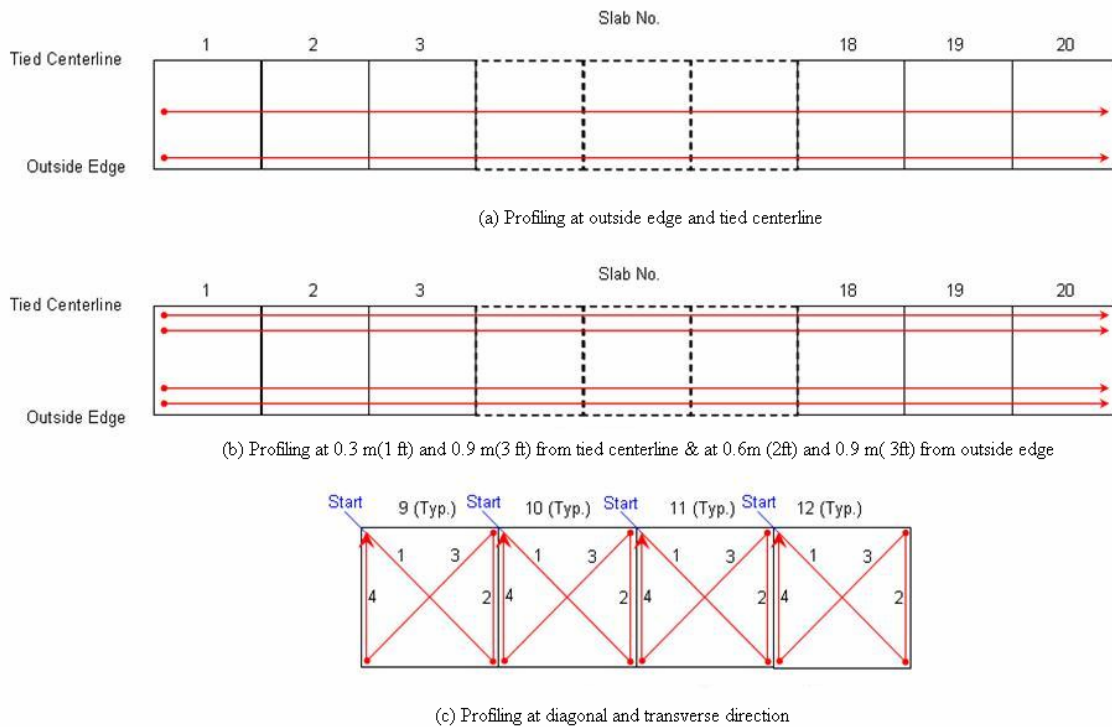
Figure 3-9 Typical profile patterns

3.4 References

AASHTO. TP60-00: Standard test method for coefficient of thermal expansion of hydraulic cement concrete, *AASHOTO'S Standard Specification for Transportation Materials and Methods of Sample and Testing,* 2000.

ASTM. C39-01: Standard Test Method for Compressive Strength of Cylindrical Concrete Specimens, *Annual Book of ASTM stand*ards, Vol. 04. 02, ASTM International, West Conshohocken, PA, 2001.

ASTM. C192-00: Standard practice for making and curing concrete test specimens in the laboratory, *Annual Book of ASTM stand*ards, Vol. 04. 02, ASTM International, West Conshohocken, PA, 2001.

ASTM. C469-94: Standard test method for static modulus of elasticity and poisson's ratio of concrete in compression, *Annual Book of ASTM stand*ards, Vol. 04. 02, ASTM International, West Conshohocken, PA, 2001.

ASTM. C496-96: Standard test method for splitting tensile strength of cylindrical concrete specimens, *Annual Book of ASTM stand*ards, Vol. 04. 02, ASTM International, West Conshohocken, PA, 2001.

International Cybernetics Corporation (ICC.), 2006, http://www. internationalcybernetics.com/ rollprofile.htm, accessed May, 2006.

Maxim/Dallas, Inc., 2006, http://www.maxim-ic.com/ appnotes.cfm/ appnote_number/3808, accessed May, 2006.

Omega Engineering, Inc., 2006, http: //www. Omega.com. accessed May, 2006.

Rao, C., Barenberg, E. J., Snyder, M. B., and Schmidt, S., 2001, "Effects of Temperature and Moisture on the Response of Jointed Concrete Pavements," *Proceedings of 7th International Conference on Concrete Pavements*, Orlando, Florida.

Vandenbossche, J. M. and Snyder, M. B., 2005, "Comparison between Measured Slab Profiles of Curled Pavements and Profile Generated Using the Finite Element method," *Proceedings of 8th International Conference on Concrete Pavements*, Colorado Springs, Colorado.

CHAPTER 4. EARLY AGE RESPONSE OF JOINTETD PLAIN CONCRETE PAVEMENTS TO TEMPERATURE AND MOISTURE VARIATIONS

A paper submitted to *The Journal of Testing and Evaluation*

Sunghwan Kim,[1] Halil Ceylan,[2] Kasthurirangan Gopalakrishnan,[3] and Kejin Wang[4]

4.1 Abstract

In this paper, a study of early age behavior of Jointed Plain Concrete Pavement(JPCP) to temperature and moisture variations at the time of paving and immediately following construction is presented. A newly constructed JPCP on US-30 near Marshalltown, Iowa was instrumented and monitored during the critical time immediately following construction to identify its early age behavior with respect to pavement deformation due to temperature and moisture variations. The instrumentation consisted of Linear Variable Differential Transducers (LVDTs) at the slab corner, center, and edges, thermocouples and humidity sensors installed within the slab depth. The slab deformation associated with temperature and moisture variations were quantified using field-measured vertical displacements and pavement surface profiles. The positive temperature gradients during setting times and the negative moisture difference after setting times caused permanent upward curling and warping in the instrumented

---

1Graduate Research Assistant, Iowa State University, Ames, IA

2 Assistant Professor, Iowa State University, Ames, IA

3 Post-Doctoral Research Associate, Iowa State University, Ames, IA

4 Associate Professor, Iowa State University, Ames, IA

pavement. The relative corner deflection of the slab to center or mid-edge calculated using the profile and LVDT measurements show similar trends.

4.2 Introduction

The temperature and moisture variations across the depth of the Portland Cement Concrete (PCC) pavements due to changes in the climate result in a unique deflection behavior which has been recognized as curling and warping of the pavements since mid 1920 (Westergaard, 1926; Harr, 1958). In general, temperature differences across the depth of the concrete pavement result in curling while moisture differences result in warping behavior (Janssen, 1987; Jeong and Zollinger, 2005). Both temperature and moisture gradients can cause either upward or downward distortion of pavement slabs, and pavement slabs are not necessarily flat at rest (i.e., under no external forces that cause slab distortion) (Yu, et al., 2004).

Curling and warping of PCC slab influences the degree of support by subgrade and the stiffness along the joint (Armaghani et al., 1986; Armaghani et al., 1987). The weight of the slab tends to hinder the curling and warping deformation from taking place and as a result restraint stresses are induced within the concrete slab (Huang, 1993). Creep in tension, develops with early-age curling and warping behavior and tends to reduce the level of tensile related restraint stresses (Jeong and Zollinger, 2005).

The early age behavior of PCC is significantly influenced by temperature, moisture, and creep of concrete (Rao et al., 2001). Based on profilograph records of concrete pavements in California, Hveem (1951) concluded that slab curling was due to the combined effect of temperature and moisture, both of which change non-uniformly

through the depth of the slab. Many significant research efforts in the past have tried to address the combined effects of temperature, moisture, and creep on the early-aged slab behavior (Westergaard, 1926; Westergaard, 1927; Bradbury, 1938; Thomlinson, 1940(a) and (b); Yoder and Witczack, 1975; Korovesis, 1990; Jeong and Zollinger, 2005).

A positive temperature difference between the top and the bottom surfaces of the concrete slab in daytime causes the slab corners to curl downwards, while a negative temperature difference during night time results in the upward curling of PCC. The moisture difference through the slab depth because of weather condition results in non-uniform concrete shrinkage and non-uniform volume changing through depth (Rao et al., 2001). However, curling and warping behavior of early aged concrete is affected by not only temperature and moisture differences due to weather conditions but also early age curing conditions and temperature conditions during pavement construction (Janssen, 1987; Yu et. al., 1998; Rao et al., 2001; Rao and Roesler, 2005).

A significantly irreversible drying shrinkage of concrete near the top of the slab and a positive temperature gradient at the time of concrete setting can cause permanent upward curling and warping at zero temperature gradient (Yu et al., 1998; Yu et al., 2004). This permanent curling and warping (built-in curling and warping) is partially recovered by the creep of the slab after hardening of the concrete over time (Yu et al., 1998; Yu et al., 2004; Rao and Roesler, 2005). Once the pavement attains permanent curling and warping after setting, the upward curling of the slab for the first few nights after the placement of concrete is the critical condition for early age cracking because the tensile stresses at the top due to upward curling and slab weight are greater than incompletely developed concrete strength (Lim and Tayabji, 2005).

Several field studies have been undertaken to better understand the actual behavior of the concrete under pure environmental loading. Armaghani et al. (1987) studied vertical and horizontal slab displacements associated with temperature variations in a specially designed test section constructed to simulate actual design features of Florida highways. They analyzed temperature data obtained from 229 mm (9-in.) concrete slab over a period of three years.

Studies by Rao et al. (2001) and Yu et al. (1998) showed evidence of permanent curling and warping condition in instrumented pavement sections in Minnesota and Colorado, respectively. Jeong and Zollinger (2004; 2005) evaluated the environmental effects on the behavior of fully instrumented JPCP test slab. In this study, it was shown that the zero-stress condition observed from the instrumented test slab was related to the final setting times of concrete mixture obtained from the laboratory tests. They reported that the trends in the slab displacements were clearly dependent upon the changes in ambient temperature and slab temperature gradients, while the drying shrinkage and creep strains cause an overall shift in slab movements (Jeong and Zollinger, 2004; Jeong and Zollinger, 2005). Recently, Vandenbossche et al. (2006) and Jeong et al. (2006) has shown the earliest days after construction (early age) is the important periods for the developing permanent curling and warping. In addition, the new Mechanistic-Empirical Pavement Design Guide (MEPDG) for the design of new and rehabilitated pavement structures require quantifying the permanent curling and warping in terms of temperature difference (NCHRP, 2004).

In spite of many research efforts, the early-age curling and warping behavior of PCC pavements under environmental conditions has not been fully understood. In

addition, the early-age behavior of concrete pavements have drawn attention because of the growing need to expedite construction without compromising in pavement quality to minimize traffic delay and user cost (Rasmussen, 1996).

The current study was conducted as a part of an ongoing research effort to assess the impact of curling, warping and other early-age behavior on concrete pavement smoothness during the critical time immediately following construction. For this study, a newly constructed JPCP slab on US-30 near Marshalltown, Iowa was instrumented to monitor the pavement response to temperature and moisture variations during the first seven days after the construction in the summer of 2005. A series of laboratory tests were undertaken to characterize the properties of paving material during the controlled field evaluation. The instrumentation installed within the pavement is described. The procedure and the results of data analysis using the collected data from the instrumented pavement are discussed in this paper highlighting the important findings regarding the early-age curling and warping behavior of JPCP slabs.

4.3 Objective

The primary objective of this study was to measure and evaluate the early-age JPCP behavior in terms of changes in pavement deflections to temperature and moisture variations. To achieve this objective, a newly constructed 267 mm (10.5-in.) thick JPCP pavement on US-30 near Marshalltown, Iowa was instrumented to monitor temperature, relative humidity, and deflections.

Temperature instrumentation consisted of Thermochron I-Buttons® attached to a stake at different depths within the PCC. LVDTs installed at the corner and mid-slab free

edge recorded the vertical slab movements. Relative humidity instrumentation consisted of Hygrochron I-Buttons[®] inserted into small Poly Vinyl Chloride (PVC) pipes which were placed side by side at different depths from pavement surface. In addition, pavement surface profile was measured twice (morning and afternoon) in a day using a Rollingprofiler (SurPRO 2000[®]) manufactured by a International Cybernetics Corporation (ICC., 2006) to detect the change in pavement curvature during the field evaluation periods.

4.4 Project Description

The test JCPC pavement was constructed on an open-graded granular base. The transverse joint spacing was approximately 6 m (20 ft). The passing lane was approximately 3.7 m (12 ft) in width, and the travel lane was approximately 4.3 m (14 ft) in width. A Hot-Mix Asphalt (HMA) shoulder was added approximately two months after initial construction.

Tie-bars of 914 mm (36-in) length and 12.7 mm (0.5-in) diameter were inserted approximately every 76 mm (30-in) across the longitudinal joints. Dowel bars of 457 mm (18-in) length and 38 mm (1.5-in) diameter were inserted approximately every 305 mm (12-in) across the transverse joints.

As shown in Figure 4-1, two test sections, one corresponding to late morning (11:00 AM CST) construction conditions and the other representative of afternoon (3:30 PM CST) construction, were selected for Rollingprofiler (SurPRO 2000[®]) measurements. Temperature sensors, relative humidity sensors, and LVDTs were placed in each section to observe the environmental effects on the slab behavior during early age (seven day

after construction) without traffic loading. Iowa State University's (ISU's) PCC mobile

laboratory parked near the test section monitored the weather conditions such as ambient

temperature, ambient relative humidity, wind direction and rainfall on special days.

During the field evaluation periods, sky was clear and sunny.
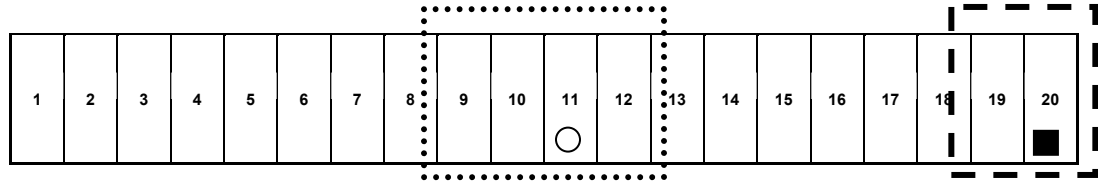
(a) Test section 1 : paving during afternoon hours (7/13/05, 3:30PM CST)
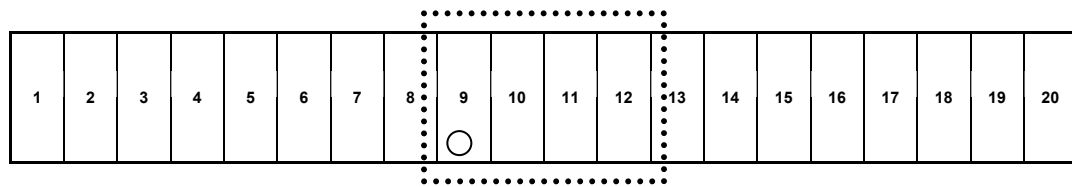
(b) Test section 2 : paving during late morning hours (7/14/05, 11:00PM CST)

Legend : ◯ - Temperature instrumentation location
■ - Relative humidity instrumentation location
⌐ - LVDT instrumentation location
⋮⋮ - Butterfly profiling –Diagonal and Transverse –location

Figure 4-1 Instrumentation layout in JPCP test sections

4.4.1 PCC Laboratory Testing

To obtain the fundamental physical properties of the paving material, a series of

laboratory tests at various ages were conducted in ISU's PCC mobile laboratory and

ISU's PCC laboratory using in-situ samples obtained from the paving site. The split

tensile test (ASTM C 496, 1996), the compressive strength test (ASTM C 39, 2001), and

the elastic modulus test (ASTM C 469, 1994) was performed on PCC samples obtained

during construction. The results of laboratory tests are summarized in Table 4-1. In

addition, the coefficient of thermal expansion (CTE, AASHTO TP 60, 2000) was

measured to be 9.63×10^{-6} ε / °C (5.35×10^{-6} ε /°F).

Table 4-1 Summary of laboratory test results

Age, Hours	Splitting Tensile Strength, MPa	Compression Strength, MPa	Modulus of Elasticity, MPa
0	0.0	0.0	0.0
12	2.7	22.5	28,143
24	2.3	25.9	28,390
72	3.0	32.9	30,680
120	2.3	34.7	32,971
168	2.4	36.6	30,086
672	2.8	45.4	34,641
1,344	2.8	49.5	33,646

4.4.2 Pavement Temperature and Relative Humidity Instrumentation

Temperature and humidity sensors installed within the test sections recorded the

slab temperature and moisture data at five- minute intervals throughout the field

evaluation periods.

Temperature instrumentation as shown in Figure 4-2 consisted of Thermochron I-

buttons® attached to a stake at different depths and placed at 0.9 m (3 ft) from the

pavement edge before the paving. The location of each I-button® attached to a stake is

listed in Table 4- 2. As shown in Figure 4-3, humidity instrumentation consisted of

Hygrochron I-Buttons® inserted into small PVC pipes which were placed side by side at

different depths from pavement surface (38.1 mm, 88.9 mm, 127 mm, and 165.1 mm).

Figure 4-2 Temperature instrumentation

Table 4-2 Pavement temperature instrumentation (I-button[®] locations)

Sensor	Depth below top slab in test section 1, mm	Depth below top slab in test section 2, mm
Sensor 6	63.5	63.5
Sensor 5	88.9	114.3
Sensor 4	114.3	139.7
Sensor 3	165.1	190.5
Sensor 2	190.5	215.9
Sensor 1	266.7	266.7
Sensor 0	419.1	419.1

Figure 4-3 Humidity instrumentation

4.4.3 Measurement of Vertical Slab Movements Using LVDT

Two slabs which were paved in the afternoon (slab19 and slab20 in Test section 1) were selected as representative slabs to study the pavement vertical movements entirely due to environmental loads. As shown in Figure 4-4, LVDTs were installed in special locations on each slab to capture the vertical movements of the slab. In the test slab19, nine LVDTs were installed at corners, the mid-slab edges and the center of the slab. In the test slab20, seven LVDTs were installed at the corners, the mid-slab edges near longitudinal joints and transverse joints. All the sensors were placed only after the concrete hardened (1 day after paving). LVDTs were held by a bracket fastened to the steel rod inserted in subgrade and placed on a smooth glass on the PCC pavement. The LVDTs were connected to data loggers, which collected data at ten minute interval throughout the field evaluation periods.

(a) Slab19 in test section 1   (b) Slab20 in test section 1
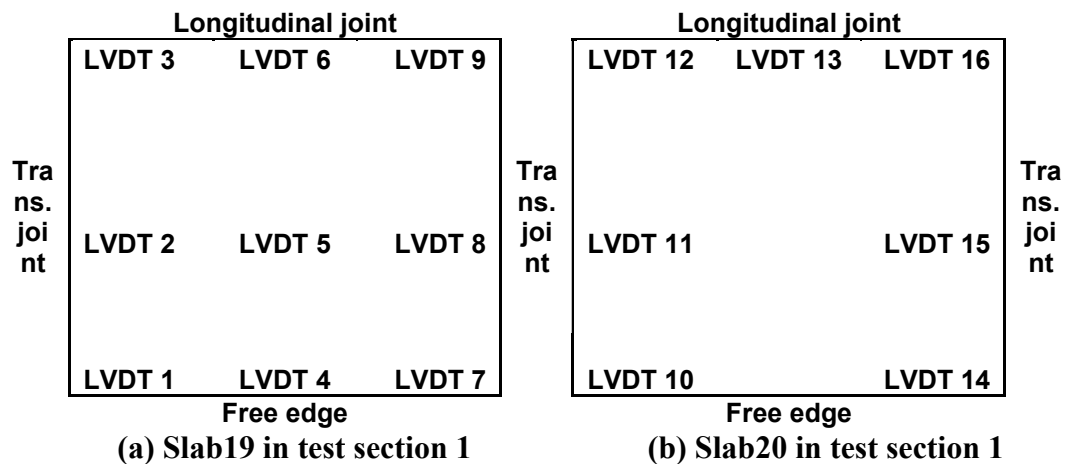
Figure 4-4 LVDT instrumentation layout

4.4.4 Pavement Surface Profile Measurement

Rollingprofiler (SurPRO 2000$^®$) by a International Cybernetics Corporation as shown in Figure 4-5 was used for surface profile measurements at different times (morning and the afternoon) in both test sections. Rollingprofiler, a kind of inclinometer profiler, can measure true unfiltered elevation profile of surface along the line being profiled (ICC., 2006). Many researchers have used the inclinometer profiler measurements to quantify slab curvature (Rao et al., 2001; Vandenbossche and Snyder, 2005). Rollingprofiler measurements in this study followed transverse and diagonal traces as shown in Figure 4-6, to capture the slab curvature. Measurements were made on four individual slabs in both test sections at different times. Each profiling segment was measured independently

Figure 4-5 Rollingprofiler (SurPRO 2000®)
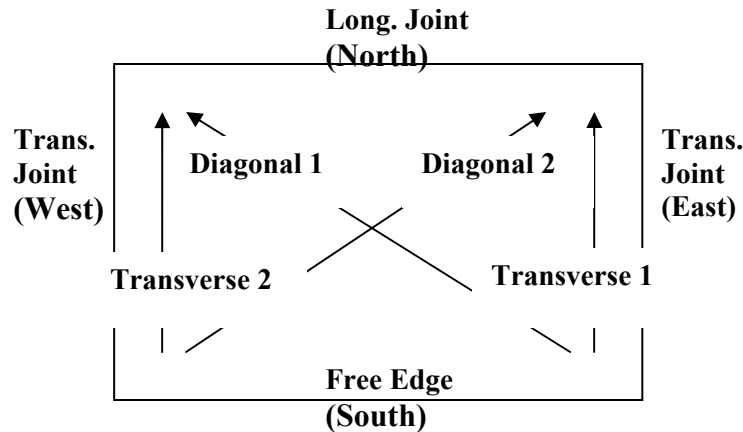
Figure 4-6 Rollingprofiler profiling pattern

4.5 Analysis of Temperature and Moisture Data

The temperature and moisture variations within the PCC pavement during early-age (seven days after construction) could be obtained from the installed temperature and moisture sensors. In addition, average pavement temperatures, differences in temperature and moisture between the top and bottom of the pavement, and temperature distributions with depth could be obtained from the measured temperature data.

Average pavement temperatures were calculated from temperature readings of six temperature I-button® sensors (Sensor 1, 2, 3, 4, 5, and 6). Temperature differences were calculated by subtracting the temperature sensor reading at 266.7 mm below the slab surface (Sensor 1) from the sensor reading at 63.5 mm below the slab surface (Sensor 6). Note that the closest temperature sensor to the top of the pavement surface was located at 63.5mm below the slab surface. Moisture differences were computed by subtracting the moisture sensor reading at 165.1 mm below the slab surface (Sensor 1) from the sensor reading at 38.1mm below the slab surface (Sensor 4).

Air temperature, average pavement temperature and subgrade temperature variations during the initial day (day zero after paving) and during the early aged days (six and seven days after paving) are compared in Figures 4-7 and 4-8. Weather conditions were clear and sunny during both days.
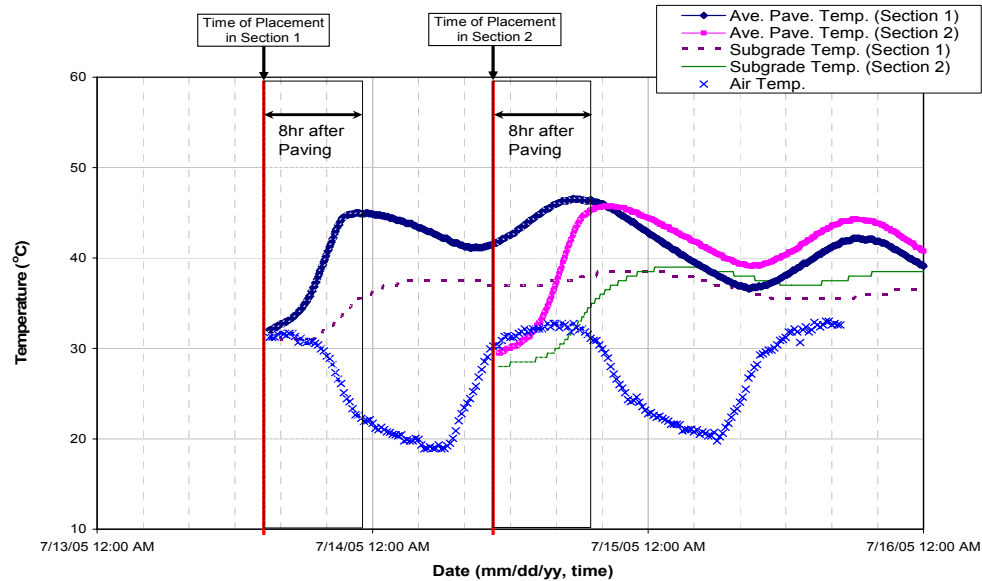
Figure 4-7 Temperature variation with time during paving
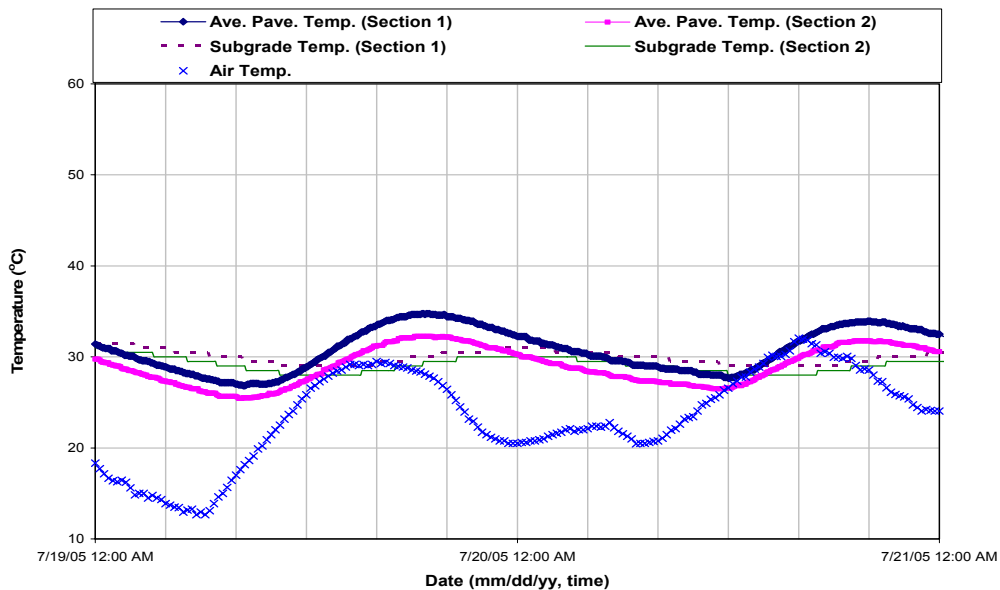
Figure 4-8 Temperature variation with time during early aged days (day 6 and day 7)

In both Figure 4-7 and 4-8, average pavement temperatures are higher than ambient temperature. From Figure 4-7, it can be observed that the average pavement temperature within 8hrs of paving increases and reaches a maximum value, while air temperature decreases. The same trend is observed during the first 8hrs of paving for both the test sections. After 8hrs of paving, the pavement temperature follows a pattern that is similar to that of air temperature as reported by previous research studies (Armaghani et al., 1987). This increase in pavement temperature within the first 8 hrs of paving may be due to the heat of concrete hydration at the time of setting. Note that after eight hrs of paving, the maximum and minimum pavement temperatures occurred normally one to two hr after air temperature reached their maxima and minima. Armaghani et al. (1987) reported that this trend was observed in the majority of the samples that were randomly selected from the collected temperature data obtained over a period of three years in Florida. Both from Figure 4-7 and 4-8, the subgrade temperature variation is not high and usually follows the pattern of pavement temperature.

To better investigate the pavement temperature variations, the pavement temperature variations for test section 1 and test section 2 are plotted in Figures 4-9 and 4-10, respectively.
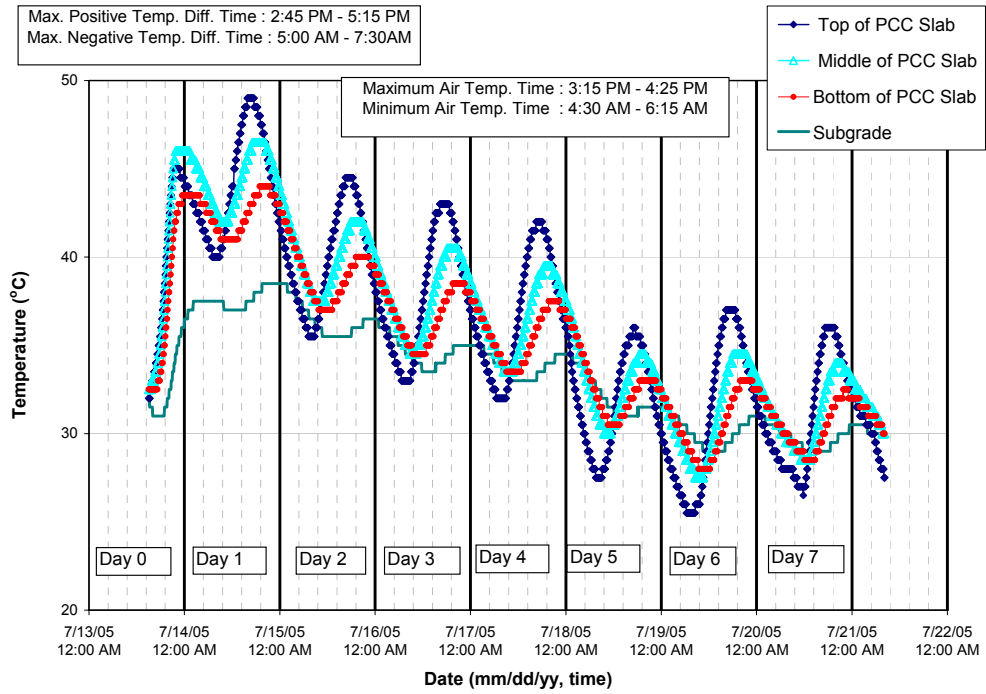
Figure 4-9 Pavement temperature variation with time in test section 1
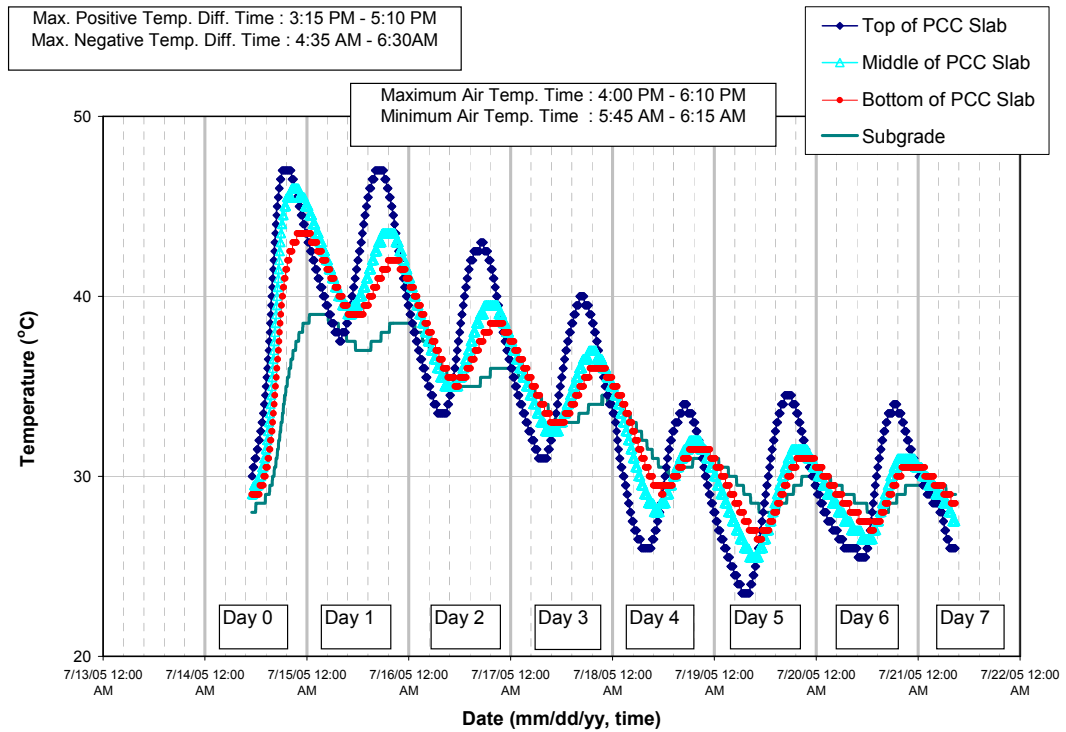
Figure 4-10 Pavement temperature variation with time in test section 2

Pavement temperatures at 63.5 mm below the slab surface reached the maximum and minimum values at approximately two hours after the maximum and minimum in air temperature occurred. The rate at which the maximum and minimum temperatures occurred with depth in this PCC pavement is 75.6 sec./mm (32 min./in.) and 99.2 sec./min(42 min./in), respectively. Maximum subgrade temperature occurred only six hrs after the air temperature reached its maximum and minimum subgrade temperature occurred only eight hrs after the minimum occurred in air temperature.

In-depth temperature distributions within 12hrs and seven days of paving in test section 1 are plotted in Figures 4-11 and 4-12, respectively. It can be observed from Figure 4-11 that within 12hrs of paving, temperature distributions shifted towards the right. This means that the pavement temperatures at night time were higher than those of day time without increase in air temperature. Also the mitigation of temperature due to heat of hydration of concrete occurred through the thickness. From Figure 4-12, the maximum positive temperature difference decreased with depth whereas the maximum negative temperature difference increased with depth with the air temperatures changing. Within 12hrs of paving, the concrete hardened at the positive temperature difference condition (78 %) rather than the negative temperature difference condition (11 %). The laboratory test results showed that within 12 hrs, the PCC achieved 50 % of the 28-day compressive strength. Thus, if 12hrs.after paving is assumed to be sufficient for the PCC to acquire a certain degree of hardening, a flat slab condition (zero-stress condition) in this test section could be associated with a positive temperature gradient rather than a zero temperature gradient (Yu et al., 1998; Jeong and Zollinger, 2005).
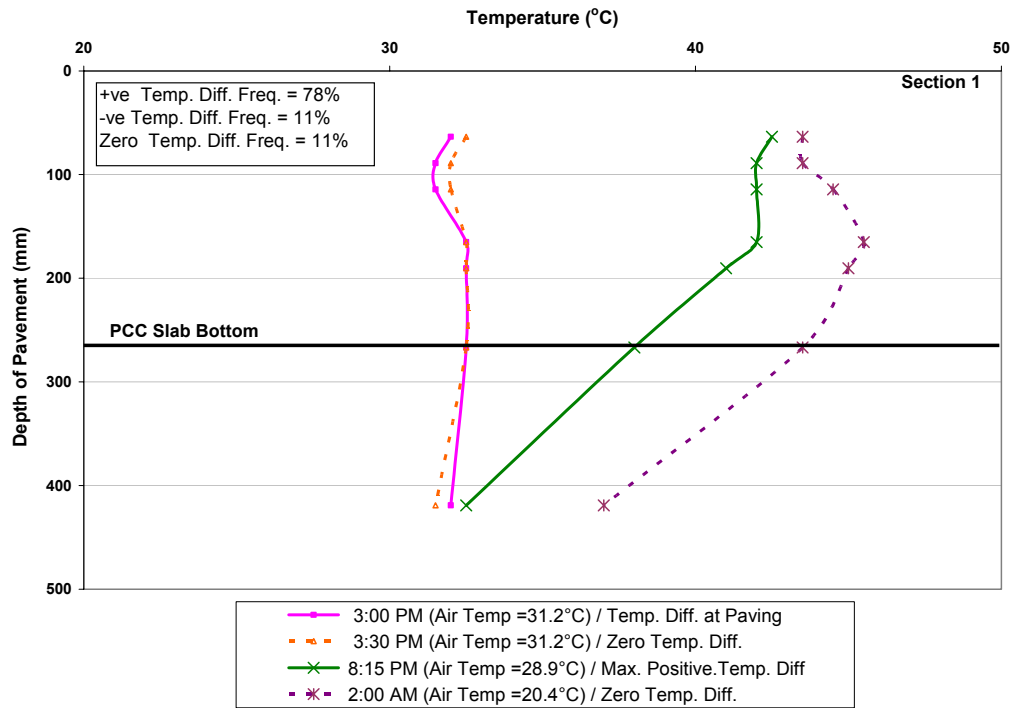
Figure 4-11 Pavement temperature distributions with depth in 12hr. after paving
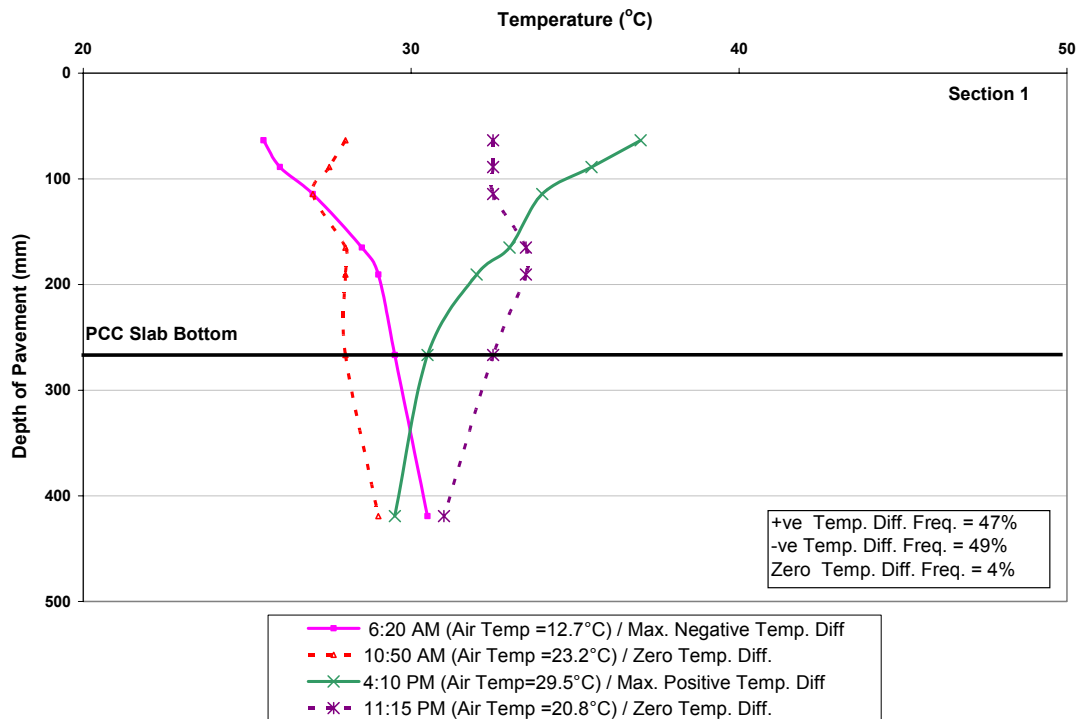
Figure 4-12 Pavement temperature distribution with depth in 7days after paving

The variations in PCC slab curvature were influenced not only by temperature difference but also moisture difference between the top and the bottom of the slab surface. The variations in temperature and moisture differences with time are plotted in Figure 4-13. In general, temperature differences are positive during daytime and early night time and negative during late night time and early morning. In contrast, moisture differences presented as "RH. Diff" in Figure 4-13 show the reverse trend. Especially during day 0 and day 1 of paving, moisture differences are negative for most part, i.e., higher moisture at the bottom of the slab compared to the top. This indicates higher drying shrinkage of concrete near the top of the slab causing the slab corner to warp upward during the day 0 and day 1 of paving.
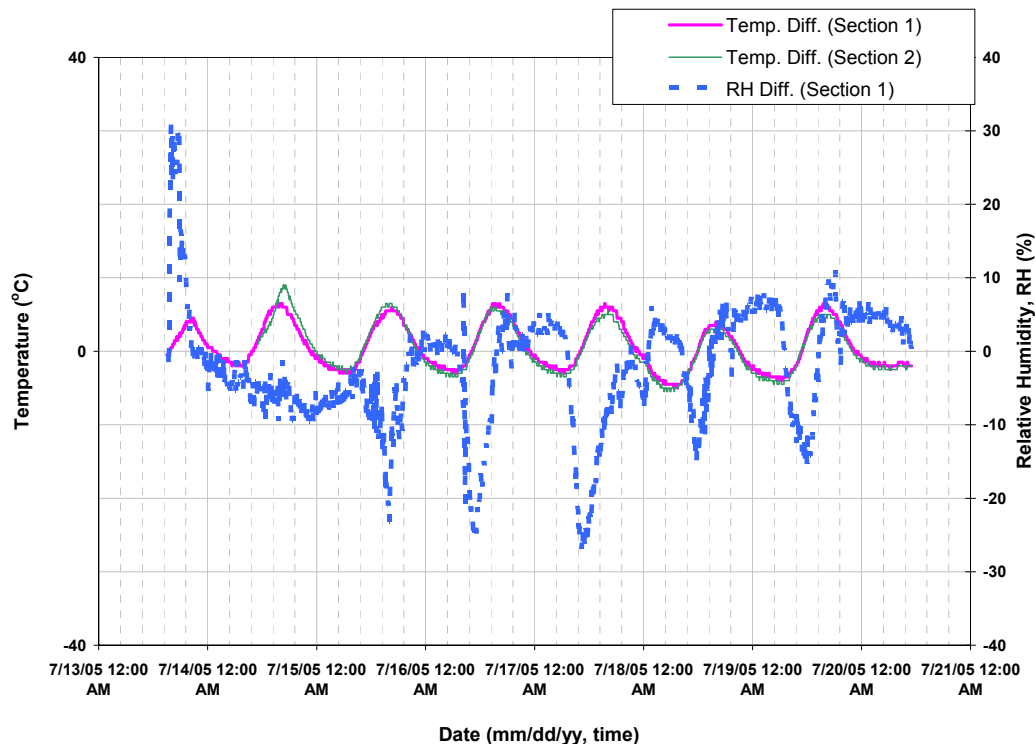
Figure 4-13 Pavement temperature and moisture difference between the top and the bottom of slab with time

4.6 Changes in LVDT Measurements Response to Temperature and Moisture Variations

The collected data from the LVDTs were voltage variations corresponding to the slab vertical displacement. To get the relative slab vertical displacement, each LVDT voltage reading was subtracted from the reference voltage reading which represents the flat slab condition. However, it's quite difficult to ascertain the time of occurrence of flat slab condition. So the LVDT voltage reading corresponding to first zero-temperature gradient during the evaluation periods was selected as the reference reading. Thus, the actual pavement behavior could be studied based on the shape of the PCC slab at zero temperature difference. The subtracted voltage readings were then converted to displacement values based on the equation provided by the LVDT manufacturer (Omega, 2006). The calculated vertical displacements were then calibrated considering the temperature movement of the steel rods holding the LVDTs.

The vertical displacements for different slab locations (corner, edge, and center) were obtained from the corresponding LVDTs, averaged and then compared. Table 4-3 shows the vertical displacements for each slab location at maximum positive temperature difference and at maximum negative temperature difference during each day of the field evaluation period. In this table, a negative displacement value indicates downward movement of the slab while a positive value indicates upward movement of the slab.

Table 4-3 Vertical displacement of slab at maximum temperature difference

| Condition | Day (Date / Temp Diff.) | Corner,μm | | Edge,μm | | Center,μm |
		Slab 19	Slab 20	Slab 19	Slab 20	Slab19
Max. Positive Temp. Diff.	Day1 (7/14/05 / 6 °C)	-54.3	-44.6	-37.2	-20.6	-25.3
	Day2 (7/15/05 / 6 °C)	-57.3	-90.0	-58.3	-66.1	-34.1
	Day3 (7/16/05 / 6.5 °C)	-72.9	-87.5	-60.3	-62.9	-29.6
	Day4 (7/17/05 / 6.5 °C)	-55.9	-83.8	-57.7	-61.4	-27.3
	Day5 (7/18/05 /4 °C)	-8.3	-47.9	-25.3	-11.9	19.6
	Day6 (7/19/05 /6 °C)	-25.0	-55.4	-36.0	2.7	11.0
Max. Negative Temp. Diff.	Day1 (7/14/05 /-1.0 °C)	8.6	6.3	5.4	2.0	1.1
	Day2 (7/15/05 /-3.0 °C)	48.4	32.0	27.3	16.8	34.4
	Day3 (7/16/05 /-3.0 °C)	75.8	41.7	37.1	22.9	36.2
	Day4 (7/17/05 /-3.0 °C)	113.7	67.0	53.4	37.9	36.6
	Day5 (7/18/05 /-5.0 °C)	126.0	90.2	63.3	48.3	52.0
	Day6 (7/19/05 /-4.0 °C)	104.6	77.9	67.0	39.6	70.8
	Day7 (7/20/05 /-2.5 °C)	81.7	55.6	43.5	25.3	56.4

The measured vertical displacements by the high-quality LVDTs (Omega, 2006) used in this study varied within a narrow range of ± 130 μm. Since there has been no reported study, to the best of authors' knowledge, on response of PCC to pure environmental loading immediately after construction (very early age), it is not possible to ascertain whether the LVDT measured values in this study correspond to the actual vertical displacement magnitudes of the slabs. Thus, attention is given to the trends in LVDT measurements rather than the magnitude of the measurements.

In general, the vertical displacement at the slab corner is higher than at other locations. Note that the vertical displacement of slab corner relative to center displacement could be obtained only for slab 19 as slab 20 does not include an LVDT at the center (see Figure 4-4). The relative vertical displacements of corner to center in slab

19 are plotted in Figure 4-14. From the relative vertical displacement of corner to center, an upward movement of the slab is observed for negative temperature gradients (slab curls upward) while a positive temperature difference results in downward movement of the slab (slab curls downward).

However, considering that the average maximum positive and negative temperature differences during field evaluation period were 5.8 $^{\circ}$C and -3.0 $^{\circ}$C, respectively, the relative vertical displacement at the maximum positive temperature difference should be higher than at the maximum negative temperature difference. However, this could not be observed in this study. Therefore, the upward curling of the slab associated with negative temperature gradient appears to be more obvious in this study compared to the downward curl of the slab which is associated with a positive temperature gradient. This phenomenon may be related to a certain positive temperature gradient which results in flat slab condition.

A positive temperature gradient occurred between the top and the bottom of the pavement due to daytime construction and heat of hydration. Due to rapid drying of moisture in the exposed slab top, there might have been drying shrinkage of concrete near the slab top and a higher saturated condition at the slab bottom. This in combination with slower moisture movement through slab depth compared to temperature led to a flat slab condition at positive temperature gradient. This phenomenon has been commonly observed in previous research studies on PCC early age behavior and is referred (Yu et al., 1998; Rao et al., 2001; Rao, S., and Roesler, 2005). In addition, the concrete is still plastic and hence it is quite difficult to support the whole weight just by the slab corners

(Byrum, 2001). Therefore, when a zero temperature gradient occurs, the slab tends to curl upwards (Yu et al., 1998; Rao et al., 2001; Rao, S. and Roesler, 2005).
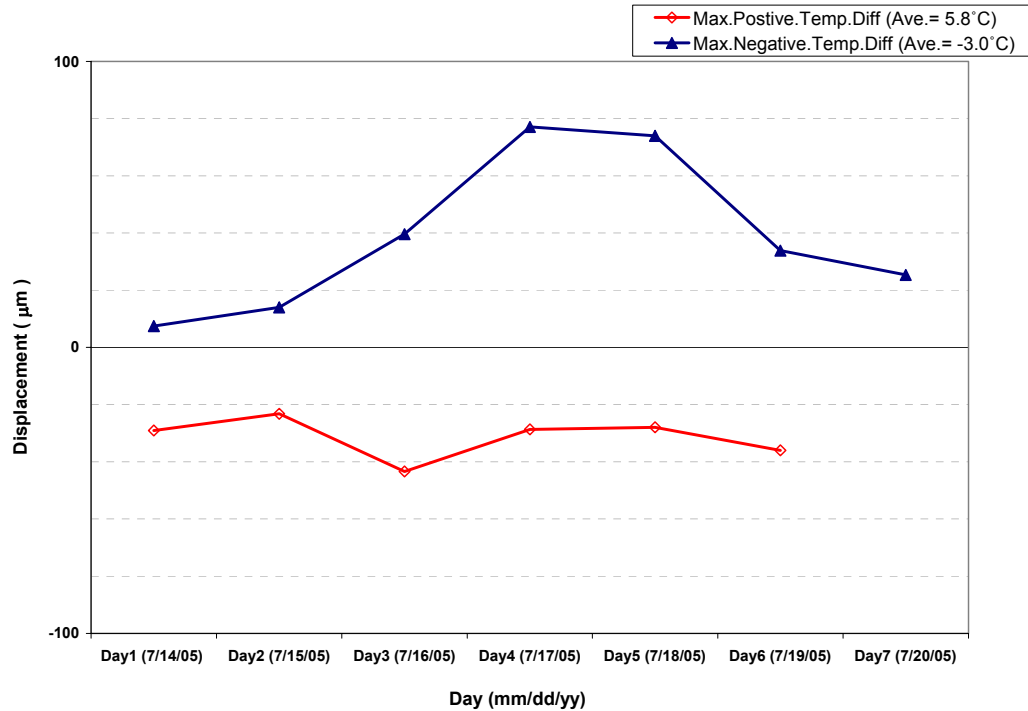
Figure 4-14 Relative vertical displacement of slab at maximum temperature difference

4.7 Profile Measurements Response to Temperature and Moisture Changing

The Rollingprofiler profile measurements were analyzed to confirm the trend in LVDT vertical displacements. The curvature of the slab measured by the Rollingprofiler, called as slab curvature profile in this study, was confounded with the construction slope and surface irregularities in the raw data of surface profile measurements. Currently, there does not seem to be a standard method to identify the curvature of the slab due to curling and warping from the raw surface profiling data. However, several procedures

have been proposed to detect the slab curvature profile (Byrum, 2000; Sixbey et al., 2001; Marsey and Dong, 2004; Vandenbossche, J.M. and Snyder, 2005) from raw surface profiling data. Among them, the similar procedure suggested by Sixbey et al. (2001) and Vandenbossche (2003) was used in this study.

A straight line from the first reading to the end reading of the raw surface profile curve was plotted. Each raw surface profile data point was subtracted from this linear line to remove the construction slope, and then normalized to the first measured profile data point to eliminate the effect of surface irregularities. In this manner, the slab curvature profiles were zeroed to first reading and end reading in a measured trace. The slab curvature profiles in each test section were the average of diagonal and transverse measurements to represent the slab curvature behavior in each test section.

The diagonal slab curvature profile in test section 1 constructed using this procedure is displayed in Figure 4-15 for illustration. The slab curvature profile measured in test section 1 clearly showed upward curling for the morning measurements and almost flat shape for the afternoon measurements. This behavior could be attributed to the permanent upward curling and warping resulting from the positive temperature gradients during setting time and to the negative moisture differences after setting time. The profile results for test section 2 could not be discussed here due to space constraints.
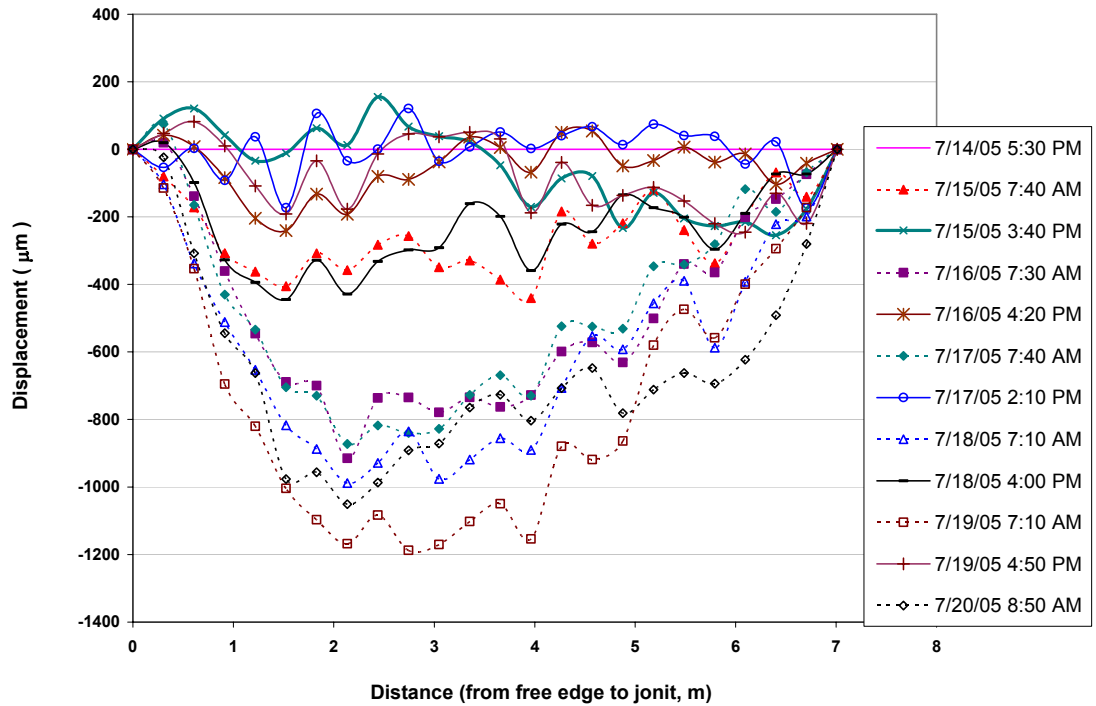
Figure 4-15 Diagonal slab curvature profile

Comparisons between LVDT readings and slab curvature profile readings in test section 1 were conducted. The relative displacements of the corner to the center or the mid-edge in measured direction (Rc) were calculated as following similar procedure by previous researchers (Marsey and Dong, 2004) and plotted with time as shown in Figure 4-16.The upward movement at the slab corner is positive in Figure 4-16.

Diagonal Direction
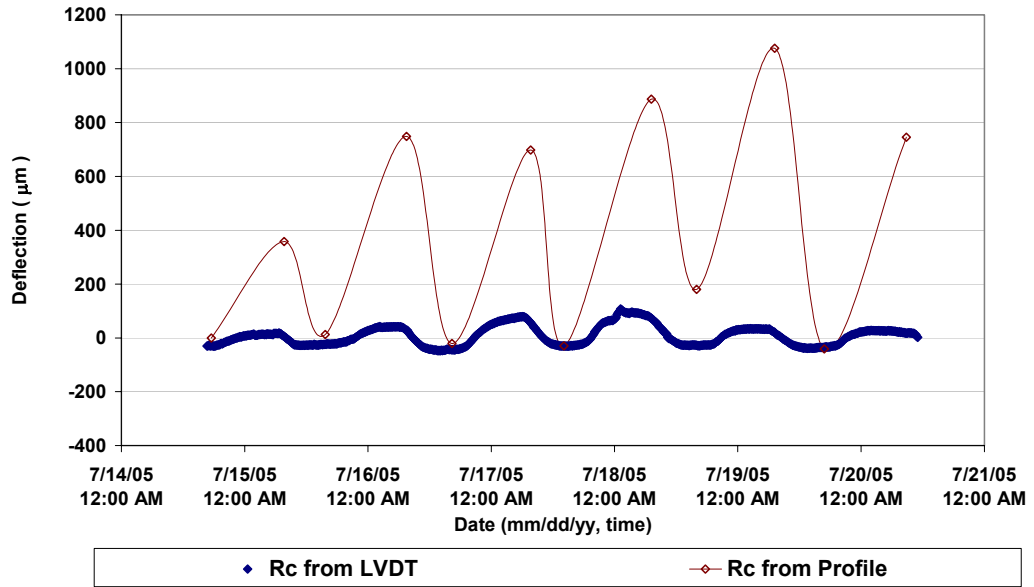
Transverse Direction
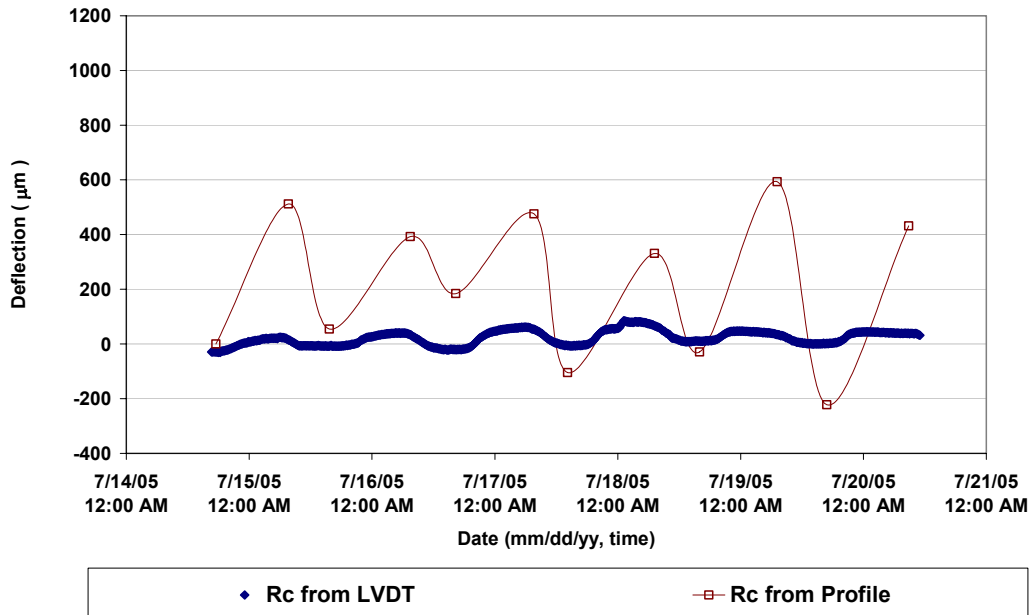
Figure 4-16 The comparison of relative displacement of the corner (Rc) with time between LVDT measurement and slab curvature profile

The Rc trends with time are similar for both LVDT measurements and slab curvature profiles. Especially, the upward curling of the slab is evident in both measured directions, indicative of the presence of permanent upward curling and warping during the field evaluation periods. It is interesting to note that the magnitudes of Rc calculated from slab curvature profile are higher compared to the LVDT measurements. However, this trend has been indirectly observed from previous research studies (Armaghani et al., 1987; Yu et al., 1998; Rao et al., 2001; Yu and Khazanovich, 2001; Rao and Roesler, 2005), which estimated temperature difference associating flat slab condition with different slab curvature measurement techniques (using either LVDT or surface profile data).

In general, research studies have reported higher temperature difference associating flat slab condition based on surface profile measurements compared to those estimated from the LVDT measurements. Using the LVDT measurements, Armaghani et al. (1987) reported the temperature difference associating flat slab condition to be 5 ^{o}C (9 °F) for a 229 mm (9- in.) thickness slab in Florida. Beckemeyer et al. (2002) calculated this value to be 8.8 ^{o}C (16 °F) and 6.7 ^{o}C (12 °F) for a 330 mm (13-in) PCC slab on open-graded granular bases and asphalt treated permeable base in Pennsylvania using ISLAB 2000 software. Byrum (2000) reported the positive temperature difference which makes slab flat at 35 ^{o}C (63 °F) for a 203.2 mm (8-in.) slab by analyzing high speed profile data. Rao et al. (2001) estimated this value to be 22.2 ^{o}C (40 °F) for a 216mm (8.5-in.) thickness slab at three days after construction using dipstick measurement data in Minnesota. In general, the trends observed in this study are in agreement with the findings from previous research studies.

It is also noted that the slab curvature data in this study were extracted from the processed raw surface profile data. And the LVDTs were installed a day after paving by which time the slab had already acquired some curvature. It is suspected that these might have led to the observed differences in magnitude between the LVDT measurements and slab curvature profiles.

4.8 Conclusions

The newly constructed JPCP on US-30 near Marshalltown, Iowa was instrumented to evaluate and identify the early aged JPCP behavior in terms of pavement deflection to temperature and moisture variations. Temperature data and moisture data obtained were analyzed. The slab deformation associated with temperature and moisture were measured and analyzed through vertical displacement and pavement surface profiles. The following are the findings of this study:

- During the first 8 hours of paving, the average pavement temperature trends do not follow the air temperature trends. Although the air temperature decreases, the pavement temperature increases possibly due to the heat of concrete hydration. After the first 8 hours of paving, the pavement temperature follows the air temperature with some phase lag.

- Pavement temperatures at 63.5 mm (2.5-in.) below the slab reached the maximum and minimum at approximately two hours after the maximum and minimum occurred in air temperature. The rates at which the maximum and minimum temperatures occurred with depth in the PCC pavement were 75.6 sec/mm (32 min/in) and 99.2 sec/mm (42 min/in), respectively.

- The maximum and minimum temperature occurred in the subgrade about 6 to 8 hours after the maximum and minimum occurred in air temperature.

- The temperature differences usually are positive at daytime and early night time and negative at late night time and early morning while moisture differences show the reverse trend. Especially, at day 0 and day 1 after paving, the moisture differences (between the top and bottom of the slab) are negative for most of the times resulting in a higher drying shrinkage near the top slab and then causing the corner of the slab to warp upward.

- The magnitude of LVDT measurements varied within a small range of $\pm$ 130 μm. Nonetheless, the influence of temperature variations on the LVDT measured vertical displacements could be observed. Especially, the upward slab curling associated with a negative temperature gradient was more evident compared to the downward slab curling.

- The diagonal and transverse slab curvature profiles measured in test section 1 showed clearly upward curling for the measurements made in the morning and almost flat shape for the afternoon measurements. This behavior can be attributed to the permanent upward curling and warping resulting from positive temperature gradients during setting time and negative moisture differences after setting time.

- The relative corner displacements from center or mid-edge (Rc) calculated from both slab curvature profile measurements and the LVDT measurements show similar trend. Both measurements show that the slab behavior during field evaluation periods tend to be mostly upward at the corner. This indicates

that the corner curl-up was built in the LVDT instrumented pavement during
the concrete hardening.

- The Rc magnitudes calculated from the slab curvature profiles are higher
compared to those estimated from LVDT measurements.

4.9 Acknowledgments

4.10 References

AASHTO. TP60-00: Standard test method for coefficient of thermal expansion of
hydraulic cement concrete, *AASHOTO'S Standard Specification for
Transportation Materials and Methods of Sample and Testing,* 2000.

Armaghani, J. M., Lybas, J. M., Tia, M., and Ruth, B. E., 1986, "Concrete Pavement
Joint Stiffness Evaluation," *Transportation Research Record*, Vol. 1099,
Transportation Research Board, Washington, D.C., pp. 22-36.

Armaghani, J. M., Larsen, T. J., and Smith, L. L., 1987, "Temperature Response of
Concrete Pavements," *Transportation Research Record*, Vol. 1121,
Transportation Research Board, Washington, D.C., pp. 23-33.

ASTM. C39-01: Standard Test Method for Compressive Strength of Cylindrical Concrete Specimens, *Annual Book of ASTM stand*ards, Vol. 04. 02, ASTM International, West Conshohocken, PA, 2001.

ASTM. C469-94: Standard test method for static modulus of elasticity and poisson's ratio of concrete in compression, *Annual Book of ASTM stand*ards, Vol. 04. 02, ASTM International, West Conshohocken, PA, 2001.

ASTM. C496-96: Standard test method for splitting tensile strength of cylindrical concrete specimens, *Annual Book of ASTM stand*ards, Vol. 04. 02, ASTM International, West Conshohocken, PA, 2001.

Beckemeyer, C. A., Khazanovich, L., and Yu, H. T., 2002, "Determining Amount of Built-in Curling in Jointed Plain Concrete Pavement: Case Study of Pennsylvania I-80," *Transportation Research Record*, Vol. 1809, Transportation Research Board, Washington, D.C., pp 85-92.

Bradbury, R. D., 1938, *Reinforced Concrete Pavements*, Wire Reinforcement Institute, Washington, D.C.

Byrum, C. R., 2000, "Analysis by High-Speed profile of Jointed Concrete Pavement Slab Curvatures," *Transportation Research Record*, Vol. 1730, Transportation Research Board, Washington, D.C., pp.1-9.

Byrum, C. R., 2001, *A High Speed Profile Based Slab Curvature Index for Jointed Concrete Pavement Curling and Warping Analysis*, Ph.D. Thesis, University of Michigan, Ann Arbor, Michigan.

Harr, M. E., 1958, *Warping stress and Deflections in Concrete Slabs*, Ph.D. Thesis, Purdue University, Lafayette, Indiana.

Huang, Y. H., 1993, *Pavement Design and Analysis*, 1st edition, Prentice Hall, Englewood Cliffs, NJ.

Hveem, F. N., 1951, "Slap Warping affects Pavement Joint Performance," *Proceedings of American Concrete Institute*, Vol. 47, pp. 797-808.

International Cybernetics Corporation (ICC.), 2006, http://www. internationalcybernetics.com/ rollprofile.htm, accessed May, 2006.

Janssen, D. J., 1987, "Moisture in Portland Cement Concrete," *Transportation Research Record*, Vol. 1121, Transportation Research Board, Washington, D.C., pp. 40-44.

Jeong, J. H. and Zollinger, D. G., 2004, "Insights on Early Age Curling and Warping behavior from Fully Instrumented Test Slab System," *CD-ROM Proceedings of the 83rd Annual Meeting of the Transportation Research Board*, Transportation Research Board, Washington, D.C.

Jeong, J. H. and Zollinger, D. G., 2005, "Environmental Effects on the Behavior of Jointed Plain Concrete," *Journal of Transportation Engineering*, Vol. 131, No. 2, American Society of Civil Engineering, pp.140-148.

Jeong, J. H., Lee, J. H., Suh, Y. C., and Zollinger, D.G., 2006, "Effect of SLAB Curling on Movement and Load Transfer Capacity of Saw-Cut Joints," *CD-ROM Proceedings of the 85th Annual Meeting of the Transportation Research Board*, Transportation Research Board, Washington, D.C.

Korovesis, G. T., 1990, *Analysis of SLAB on Grade Pavement Systems Subjected to Wheel and Temperature Loadings*, Ph.D. Thesis, University of Illinois, Urbana Champaign, Illinois.

Lim, S. W. and Tayabji, S. D., 2005, "Analytical Technique to Mitigate Early-Age
Longitudinal Cracking in Jointed Concrete Pavements," *Proceedings of 8th
International Conference on Concrete Pavements*, Colorado Springs, Colorado.

Marsey, W and Dong, M., 2004, "Profile Measurements of Portland Cement Concrete
Test Slab at National Airport Pavement Test Facility," The 2004 FAA
Worldwide Airport Technology Transfer Conference, Atlantic City, New Jersey.

National Cooperative Highway Research Program (NCHRP), 2004, *Guide for
Mechanistic- Empirical Design of New and Rehabilitated Pavement Structures –
Final Report*, http://www.trb.org/mepdg, National Cooperative Highway
Research Program 1-37 A, Transportation Research Board, National Research
Council, 2004.

Omega Engineering inc., 2006, http: //www. Omega.com., accessed March 2006.

Rao, C., Barenberg, E. J., Snyder, M. B., and Schmidt, S., 2001, "Effects of Temperature
and Moisture on the Response of Jointed Concrete Pavements," *Proceedings of
7th International Conference on Concrete Pavements*, Orlando, Florida.

Rao, S. and Roesler, J. R., 2005, "Characterizing Effective Built in Curling from
Concrete pavement Field Measurements," *Journal of Transportation Engineering*,
Vol. 131, No. 4, American Society of Civil Engineering, pp.320-327.

Rasmussen. R. O., 1996, *Development of an Early Age Behavior Model for Portland
Cement Concrete Pavements*, Ph.D. Thesis, University of Texas at Austin, Austin,
Texas.

Sixbey, D., Swanlund, M., Gagarin, N. and Mekemson, J. R., 2001, "Measurement and
Analysis of Slab Curvature in JPC Pavements Using Profiling Technology,"

Proceedings of 7th International Conference on Concrete Pavements, Orlando, Florida.

Thomlinson, J., 1940a, "Temperature Variations and Consequent Stresses Produced by Daily and Seasonal Temperature Cycle in Concrete Slabs," *Concrete and Constructional Engineering*, Vol. 36, No. 6, pp. 298-307.

Thomlinson, J., 1940b, "Temperature Variations and Consequent Stresses Produced by Daily and Seasonal Temperature Cycle in Concrete Slabs," *Concrete and Constructional Engineering*, Vol. 36, No. 7, pp. 352-360.

Vandenbossche, J. M., 2003, *Interpreting Falling Weight Deflectometer Results for Curled and Warped Portland Cement Concrete Pavements*, Ph.D. Thesis, University of Minnesota, Minneapolis, Minnesota.

Vandenbossche, J. M. and Snyder, M. B., 2005, "Comparison between Measured Slab Profiles of Curled Pavements and Profile Generated Using the Finite Element Method," *Proceedings of 8th International Conference on Concrete Pavements*, Colorado Springs, Colorado.

Vandenbossche, J. M., Wells, S. A., and Phillips, B.M., 2006, "Quantifying Built-in Construction Gradients and Early-Age Slab Shape to Environmental Loads for Jointed Plain Concrete Pavements," *CD-ROM Proceedings of the 85th Annual Meeting of the Transportation Research Board*, Transportation Research Board, Washington, D.C.

Westergaard, H. M., 1926, "Analysis of Stresses in Concrete Pavements Due to Variations of Temperature," *Proceedings of Highway Research Board*, Vol. 6, National Research Council, Washington, D.C., pp.201-217.

Westergaard, H. M., 1927, "Theory of Concrete Pavement Design," *Proceedings of Highway Research Board*, Part I, pp. 175-181.

Yoder, E. J. and Witczack, M. W., 1975, *Principle of Pavement Design*, 2nd edition, Wiley, New York.

Yu, H. T., Khazanovich, L. Darter, M. I, and Ardani, A., 1998, "Analysis of Concrete Pavement Response to Temperature and Wheel Loads Measured from Instrumented Slab," *Transportation Research Record*, Vol. 1639, Transportation Research Board, Washington, D.C., pp. 94-101.

Yu, T. H., Khazanovich, L., and Darter, M. I., 2004, "Consideration of JPCP Curling and Warping in the 2002 Design Guide," CD-ROM Proceedings of the 83rd Annual Meeting of the Transportation Research Board, Transportation Research Board, Washington, D.C.

Yu, H. T., Khazanovich, L., 2001, "Effects of Construction on Concrete Pavement Behavior," *Proceedings of 7th International Conference on Concrete Pavements*, Orlando, Florida.

CHAPTER 5. CHARACTERIZATION OF THE EARLY AGE JOINTED PLAIN CONCRETE PAVEMENTS DEFORMATION UNDER ENVIRONMENTAL LOADS USING EQUIVALENT TEMPERATURE DIFFERENCE CONCEPT

Sunghwan Kim,[1] Kasthurirangan Gopalakrishnan,[2] Halil Ceylan,[3] and Kejin Wang[4]

5.1 Abstract

Studies on deformation characteristics of early-age Jointed Plan Concrete Pavements (JPCP) subjected to pure environmental loading has drawn significant interest as it is believed that the early-age deformation of Portland Cement Concrete (PCC) slab could result in the loss of pavement smoothness and the tensile stresses induced by these deformations could result in early-age cracking. However, the complex nature of the problem arising from interacting environmental factors has resulted in difficulties in predicting the JPCP deformation characteristics under environmental loading.

This study proposes a simplified approach for predicting the early-age deformation of JPCP under environmental loading using an equivalent temperature difference concept. A newly constructed JPCP section on highway US-30 near

[1]Graduate Research Assistant, Iowa State University, Ames, IA
[2] Post-Doctoral Research Associate, Iowa State University, Ames, IA
[3] Assistant Professor, Iowa State University, Ames, IA
[4] Associate Professor, Iowa State University, Ames, IA

Marshalltown, Iowa was instrumented to monitor the pavement response to variations in temperature and moisture during first seven days after construction. Based on the collected field data, the equivalent temperature difference (ΔT_{etd}) corresponding to the actual deformation under environmental loads was quantified using two Finite Element (FE) based approaches: ISLAB 2000 (two-dimensional) and EverFE 2.24 (three-dimensional). The FE-based calculations were compared with the field measured slab deformation properties. Better comparisons were obtained when the equivalent temperature difference accounted for variability in PCC displacement due to actual moisture gradient variations which made the FE simulations more accurate.

5.2 Introduction

The early-age deformations of PCC slab due to pure environmental loading (i.e., without traffic loading) have been noticeable recently (Siddique and Hossain, 2005; Rao et al., 2001). It is believed that this early-age slab deformation could result in the loss of pavement smoothness (Siddique and Hossain, 2005) and the tensile stress induced by these deformations could result in early-age cracking (Lim and Tayabji, 2005). Even though the deformation of slab due to environmental loading has long been recognized as curling and warping primarily due to temperature and moisture variations, many other factors such as the curing condition, influence of climatic conditions on paving, and the creep of slab (Janssen, 1987; Rao et al., 2001; Rao and Roesler, 2005) may also be involved. Especially, the complex interactions of different factors involved results in "locked-in" curvature such that the slab shape at zero-temperature gradient did not

remain plain (Byrum, 2000). This permanent deformation makes the prediction of PCC deformation under environmental loads difficult.

The Finite Element Method (FEM) is believed to provide analytical solution for predicting the PCC deformation under environmental loads because FEM can solve a broad class of boundary value problems (Hammons and Ioannides, 1997). And, the FE-programs specifically developed for rigid pavement analysis such as ISLAB 2000 (Khazanovich et al., 2000) and EverFE 2.24 (Davids, 2003; Davids, 2006) include the analysis of pavement response due to temperature changes as well. However, these FE-programs can't account for slab deformation due to moisture variations and permanent deformation at zero temperature difference which can be obvious during early age of the PCC. To overcome this and to provide prediction of deformation under environmental loads, recently researchers have attempted to convert the effect of environmental loading into an "equivalent temperature difference" (Rao et al., 2001; Yu and Khazanovich, 2001; Jeong and Zollinger, 2004; Yu et al., 2004; Rao and Roesler, 2005).

This study focuses on predicting the early-age deformation of JPCP due to environmental loads using the equivalent temperature difference (ΔT_{etd}) concept with two FE-based primary response models, namely ISLAB 2000 and EverFE 2.24. These models were primarily selected because of some special advantages over other FE programs: ISLAB 2000 as representing two dimensional (2-D) FE program was used as the main structural model for generating pavement responses in the new Mechanistic-Empirical Pavement Design Guide (MEPDG) under National Cooperative Highway Research Program (NCHRP) 1-37 A project (2004) and EverFE 2.24 is the only 3-D FE program

among the FE programs specifically designed for modeling and analyzing rigid pavements (Davids, 2003).

For this study, a newly constructed JPCP section on highway US-30 near Marshalltown, Iowa was instrumented to monitor the pavement response to variations in temperature and moisture during first seven days after construction. Based on collected field data, the equivalent temperature difference corresponding actual deformation due to environmental effects were quantified with two different approaches. The procedures and the results of FE models based on the collected data and the quantified equivalent temperature differences are discussed. Comparisons between the field measured and the FE computed slab deformations are presented in this paper.

5.3 Equivalent Temperature Difference Concept

The temperature and moisture variations across the depth of rigid pavements result in pavement displacement. In addition, a higher unrecoverable drying shrinkage of concrete near the top of the slab, a positive temperature gradient during the concrete hardening and settlement of the foundation can cause permanent displacement at zero-temperature gradient (Yu et al., 2004). There is also the weight of the slab contributing to the creep of the slab. Therefore, the displacement caused by each of these factors must be taken into consideration. The total environmental effect resulting in PCC slab displacement has been represented as a temperature difference – the total equivalent linear temperature difference (TELTD), ΔT_{etd} (Yu et al., 2004; Rao and Roesler, 2005):

$$\Delta T_{etd} = \Delta T_{transient} + \Delta T_{permanent} \qquad \text{(Equation 5-1)}$$

Where:

ΔT_{etd} = Total equivalent linear temperature difference

$\Delta T_{transient}$ = Transient component of total equivalent linear temperature difference

$\Delta T_{permanent}$ = Permanent component of total equivalent linear temperature difference

The transient component caused by daily or seasonal weather condition change can result in slab deflection variation while the permanent component caused by the combination of several environmental effects induce the deflection of slab at zero-temperature and zero-moisture gradient. The transient and the permanent component can be further decomposed with respect to individual environmental effect as follows:

$$\Delta T_{transient} = \Delta T_{trans\text{-}temp\text{-}diff} + \Delta T_{trans\text{-}mois\text{-}diff} \qquad \text{(Equation 5- 2)}$$

$$= \Delta T_{trans\text{-}linear\text{-}temp\text{-}diff} + \Delta T_{trans\text{-}nonliner\text{-}temp\text{-}diff} + \Delta T_{trans\text{-}linear\text{-}mois\text{-}diff} + \Delta T_{trans\text{-}nonliner\text{-}mois\text{-}diff} \qquad \text{(Equation 5-3)}$$

$$\Delta T_{permanent} = \Delta T_{perm\text{-}temp\text{-}diff} + \Delta T_{perm\text{-}moi\text{-}diff} + \Delta T_{perm\text{-}settle} + \Delta T_{perm\text{-}creep} \qquad \text{(Equation 5- 4)}$$

Where:

$\Delta T_{trans\text{-}temp\text{-}diff}$ = Transient component due to actual temperature gradient decomposed into linear and non-linear component between top and bottom

$\Delta T_{trans\text{-}mois\text{-}diff}$ = Transient component due to actual moisture gradient decomposed into linear and non-linear component between top and bottom

$\Delta T_{trans\text{-}linear\text{-}temp\text{-}diff}$ = Transient linear temperature difference component between top and bottom of slab

$\Delta T_{trans\text{-}nonliner\text{-}temp\text{-}diff}$ = Transient non-linear temperature difference component between top and bottom of slab

$\Delta T_{trans\text{-}linear\text{-}mois\text{-}diff}$ = Temperature difference between top and bottom of a slab equivalent to (producing similar response to) transient linear moisture difference component between top and bottom of slab

$\Delta T_{trans\text{-}nonlinear\text{-}mois\text{-}diff}$ = Temperature difference between top and bottom of a slab equivalent to (producing similar response to) transient non-linear moisture difference component between top and bottom of slab

$\Delta T_{perm\text{-}temp\text{-}diff}$ = locked (or built-in) temperature difference component between top and bottom of slab during the time of PCC hardening.

$\Delta T_{perm\text{-}moi\text{-}diff}$ = Temperature difference between top and bottom of slab equivalent to (producing similar response to) irreversible differential dry shrinkage component between top and bottom of slab

$\Delta T_{perm\text{-}settle}$ = Temperature difference between top and bottom of a slab equivalent to (producing similar response to) settlement of foundation

$\Delta T_{perm\text{-}creep}$ = Temperature difference between top and bottom of a slab equivalent to (producing similar response to) creep behavior of slab.

Although the total environmental effect resulting in slab displacements could be theoretically decomposed as shown in these equations, the concept of an equivalent temperature difference to combine all the active effects has been more often used by researchers (Rao et al., 2001; Rao and Roesler, 2005; Jeong and Zollinger, 2004) since the environmental effects are highly correlated with each other and some effects such as non–uniform moisture distribution are difficult to quantify in terms of temperature difference. Especially, Rao and Roesler (2005) modified Equation 5-1 and quantified

ΔT_{etd} (TELTD) using a combination of a transient temperature difference, $\Delta T_{trans-temp-diff}$ and an effective built-in temperature difference (EBITD), ΔT_{ebi}, as shown in Equation 5-5.

$$\Delta T_{etd} = \Delta T_{trans-temp-diff} + \Delta T_{ebi} \qquad \text{(Equation 5-5)}$$

Where:

ΔT_{ebi} = Effective built-in temperature difference = $\Delta T_{trans-mois-diff} + \Delta T_{permanent}$

Based on the assumption that reversible moisture difference in slab has more influence on seasonal weather variation rather than daily weather variation, ΔT_{ebi} (EBITD) as a constant value includes $\Delta T_{trans-mois-diff}$ in Equation 5-4 so that ΔT_{ebi} (EBITD) can be that temperature difference producing curling and warping at zero-temperature difference with any moisture gradient. Therefore, the concept of ΔT_{ebi} (EBITD) is little different from $\Delta T_{permanent}$ used in MEDPG to indicate that temperature difference which produces curling and warping at a zero-temperature and a zero-moisture gradient. However, many researchers (Armaghani et al, 1987; Poblete et al, 1988; Yu, et al., 1998; Byrum, 2000; Rao et al.,2001; Yu and Khazanovich, 2001; Rao and Roesler, 2003; Rufino and Roesler, 2006) have reported ΔT_{ebi} (EBITD) rather than $\Delta T_{permanent,}$ since ΔT_{ebi} can easily be quantified (from observing the temperature difference for maintaining a flat-slab condition). The ΔT_{ebi} or $\Delta T_{permanent}$ values reported by previous researchers are summarized in Table 5-1 which was originally reported by Hiller and Roesler (2005).

Table 5-1 Effective built-in temperature difference (ΔT_{ebi}) and permanent component of equivalent temperature difference ($\Delta T_{permanent}$) (after Hiller and Roesler (2005))

Location	ΔT_{ebi} or $\Delta T_{permanent}$ (^{O}C)	Comment	Reference
Florida[a]	ΔT_{ebi} = -5.0	Undoweled / slab thickness = 229 mm	Armaghani et al. (1987)
I-70 in Colorado[a]	ΔT_{ebi} =-11.1	Dowels/ tied shoulder/ bituminous base/ slab thickness = 292 mm	Yu et al.(1998)
I-80 in Pennsylvania[a]	ΔT_{ebi} =-8.9	Dowels / aggregate base/ slab thickness= 330 mm	Yu et al.(2001)
	ΔT_{ebi} =-6.7	Dowels / bituminous base / slab thickness = 330 mm	
Chile[b]	ΔT_{ebi} =-19.2	Multiple sections	Poblete et al.(1998)
Palmdale, California[b]	ΔT_{ebi} =-22.7	Undoweled / bituminous base	Rao and Roesler(2003)
	ΔT_{ebi} =-9.8	Dowels / tied shoulder	
	ΔT_{ebi} =-17.2	Widened lane/ bituminous shoulder	
Ukiah, California[b]	ΔT_{ebi} =-10.0	Undoweled / bituminous shoulder	
Denver[c]	ΔT_{ebi} =-5 to -8.3	Air field slabs/cemmentitious base / slab thickness = 432 mm	Ruffino and Roesler (2006)
Mankato, Minnesota[d]	ΔT_{ebi} =-22.2	Undoweled / aggregate base / slab thickness =216 mm / 3day after paving	Rao et al. (2001)
LTPP GPS3 site 55-3009[e]	ΔT_{ebi} =-37.2 to -48.3	Slab thickness =218 mm	Byrum (2000)
National average	$\Delta T_{permanent}$ = -5.6	The recommended value at Mechanistic-Empirical Pavement Design Guide (MEPDG)	Yu et al.(2004)

[a] Using fixed surface gage for deflections.

[b] Using falling –weight or heavy –weight deflectometer deflection measurements.

[c] Using multidepth deflectometers.

[d] Using inclometer profiler.

[e] Using high speed profiling device.

5.4 Test Sections and Data Collection

A newly constructed JPCP section on an open-graded granular base on US-30 near Marshalltown, Iowa was selected for this study. The transverse joint spacing was approximately 6 m (20 ft). The passing lane was approximately 3.7 m (12 ft) in width, and the travel lane was approximately 4.3 m (14 ft) in width. Tie-bars of 914-mm (36-in) length and 12.7-mm (0.5-in) diameter were inserted approximately every 762 mm (30-in) across the longitudinal joints. Dowel bars of 457 mm (18-in) length and 38 mm (1.5-in) diameter were inserted approximately every 305 mm (12-in) across the transverse joints. A bituminous shoulder was added about 2 months after construction. Iowa State PCC mobile laboratory parked in the test section monitored and recorded the weather condition information such as the ambient temperature, ambient relative humidity, wind direction, and rainfall during seven days after construction. During the field evaluation periods, the weather was clear and sunny.

As shown in Figure 5-1, two test sections in the JPCP travel lane, one corresponding to late morning (11:00 AM CST) construction conditions and the other representative of afternoon (3:30 PM CST) construction, were selected for data collections in this study.

Thermochron I-Buttons® were placed throughout the depth of the pavement on each section and Hygrochron I-Buttons® were installed at various depths on test section 1 during construction to observe the temperature and moisture effect on the slab behavior during early age (7 day after construction). Slab temperature and moisture data were collected at five–minute intervals throughout the field evaluation periods. Linear Variable

Differential Transducers (LVDTs) were installed at the slab corner, center, and edges on two adjacent slabs in test section 1.

Surface profiling was conducted with a Rollingprofiler (SurPRO 2000[®]) following diagonal and transverse directions on four individual slabs in each test section at different times (morning and the afternoon) representing negative/positive pavement temperature difference conditions to study the slab deformation behavior. A rollingprofiler can measure true unfiltered elevation profile of the slab surface (ICC, 2006). The raw elevation profile of surface was filtered using a procedure suggested by Sixbey et al. (2001) and Vandenbossches (2003) to obtain slab deformation pattern called as "slab curvature profile". Each profiling segment was measured independently.

(a)

(b)
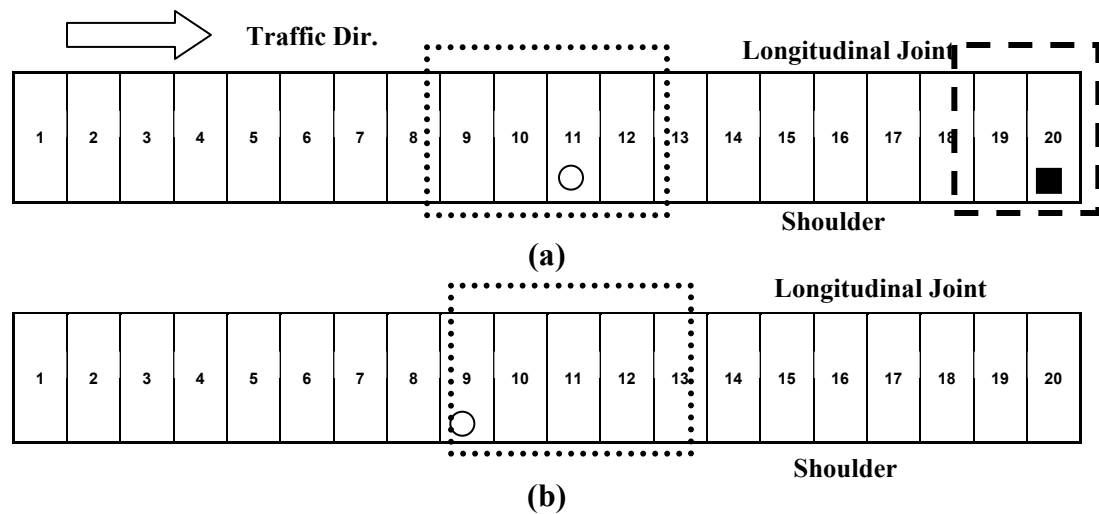
Legend : ◯ - Thermochron I-Buttons[®] instrumentation location
■ - Hygrochron I-Buttons[®] instrumentation location
⌐⌐ - LVDT instrumentation location
⋯ - Rollingprofiler measurement (diagonal and transverse trace) location

Figure 5-1 Instrumentation layout in JPCP test sections: (a) test section 1 - paving during afternoon hours (7/13/05, 3:30PM CST); (b)test section 2 - paving during late morning hours (7/14/05, 11:00PM CST)

5.5 Field Data Results

Slab temperature, moisture and deflection measurements were taken over a seven-day period after construction on these test sections. The results from these test sections provide an excellent source of information for understanding the early age slab displacement behavior under environmental loading. The results are summarized in the following sections.

5.5.1 Temperature and Moisture

Temperature differences were calculated by subtracting the temperature sensor reading at the bottom of slab (267 mm below the slab surface) from the sensor reading at the closest temperature sensors to the top of the pavement surface (64 mm below the slab surface). Moisture differences were computed by subtracting the moisture sensor reading at the middle of slab (165mm below the slab surface) from the moisture sensor reading at 38mm below the slab surface (closest moisture sensor to the slab surface). The variations in temperature and moisture differences with time are plotted in Figure 5-2. In general, temperature differences are positive during daytime and early night time and negative during late night time and early morning. In contrast, moisture differences presented as "RH Diff." in Figure 5-2 show the reverse trend. Especially during day 0 and day 1 of paving, moisture differences are negative for most part, i.e., higher moisture at the bottom of the slab compared to the top. This indicates higher drying shrinkage of concrete near the top of the slab causing the slab corner to warp upward during day 0 and day 1 of paving.

Since the top and bottom temperature sensors were not equidistant from the top and bottom of slab, extrapolated temperature differences between top and bottom of the slab, assuming a linear temperature distribution, were utilized in this study.
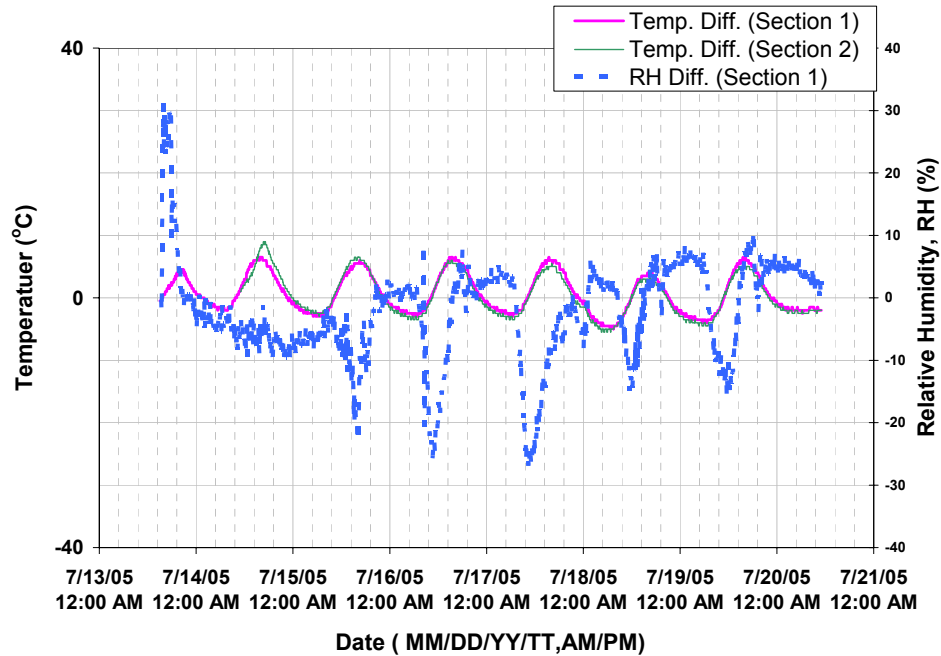
Figure 5-2 Pavement temperature and moisture difference between the top and the bottom of slab with time

5.5.2 Changes in Measured LVDT Responses to Environmental Effects

To identify the slab curling behavior of LVDT instrumented slabs, the relative vertical displacement to center were needed. Even though LVDTs were installed on two slabs (slab 19 and slab 20), slab 19 was selected as the representative slab for this study because the LVDTs on slab 20 were not installed in some positions (the center of slab and the mid-slab edge near shoulder) due to limitations imposed by the data logger. The

relative vertical displacements of corner to center in slab 19 are plotted in Figure 5-3. An upward movement of the slab is observed for negative temperature gradients (upward slab curling) while a positive temperature difference results in downward movement of the slab (downward slab curling).

However, considering that the average maximum positive and negative temperature differences during the LVDT measurement periods were 7.6 $^{\circ}$C and -4.0 $^{\circ}$C, respectively, the relative vertical displacement at the maximum positive temperature difference should be higher than at the maximum negative temperature difference. However, this was not observed in this study. Therefore, the upward curling of the slab appeared to be more obvious in this study compared to the downward curl of the slab.

This phenomenon may be related to a certain positive temperature gradient which results in flat slab condition. A positive temperature gradient occurred due to daytime construction and heat of hydration. Due to rapid drying of moisture in the exposed slab surface, there might have been drying shrinkage of concrete near the slab top and a higher saturated condition at the slab bottom. This in combination with slower moisture movement through slab depth compared to temperature led to a flat slab condition at positive temperature gradient. This phenomenon has been commonly observed in previous research studies focusing on the early age behavior of PCC (Yu, et al., 1998; Rao et al., 2001; Rao and Roesler, 2005; Vandenbossche et al, 2006). In addition, the concrete is still plastic immediately after construction and hence it is quite difficult to support the whole weight just by the slab corners (Byrum, 2001). Therefore, when a zero-temperature gradient occurs, the slab tends to curl upwards (Yu, et al., 1998; Rao et al., 2001; Rao and Roesler, 2005; Vandenbossche et al, 2006).
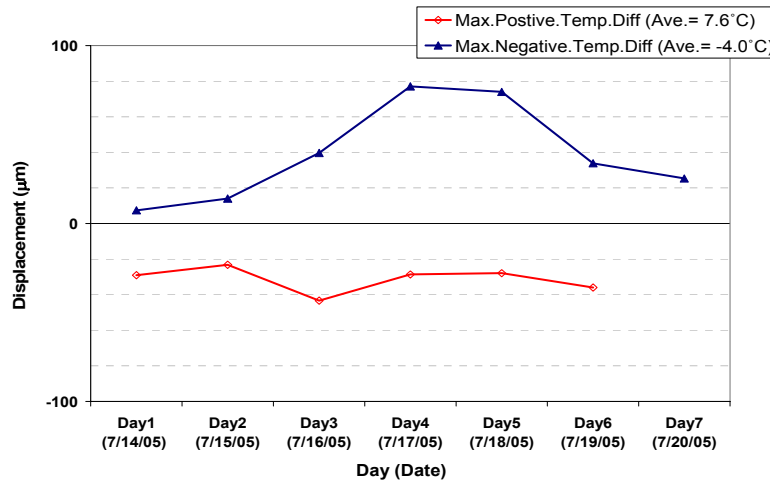
Figure 5-3 Relative vertical displacement of slab at maximum temperature difference

5.5.3 Profile Measurements Response to Environmental Effects

The slab curvature profiles obtained from Rollingprofiler surface profile measurements were analyzed to confirm the trend in LVDT vertical displacements. The typical slab curvature profile in this study is displayed in Figure 5-4 for illustration. The slab curvature profile measured in test sections clearly showed upward curling for the morning measurements corresponding to negative temperature difference and almost flat shape for the afternoon measurements corresponding to positive temperature difference. This behavior is in agreement with the LVDT observations and could be attributed to the permanent upward curling and warping resulting from the positive temperature gradients (during PCC hardening) and the negative moisture differences (after PCC hardening). Therefore, both the LVDT measurements and slab curvature profiles clearly demonstrate that the early-age JPCP slab curling behavior can not only account for temperature variations but also other environmental effects such as moisture and temperature conditions during PCC hardening.
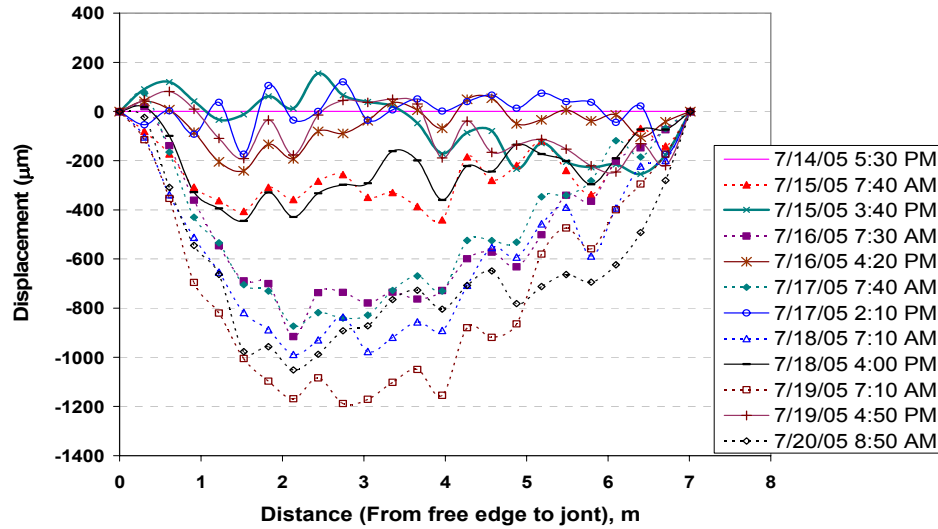
Figure 5-4 Typical slab curvature profile

5.6 Simulation of Deformation under Environmental Loads with Finite Element Method (FEM)

Finite element simulations using ISLAB 2000 and EverFE 2.24 were conducted to understand the early age deformation behavior of concrete pavement systems under environmental loads in more detail.

Both ISLAB 2000 and EverFE 2.24 can only simulate the slab deformations due to temperature changes but cannot directly simulate the slab deformations due to moisture variation and permanent deformation at zero-temperature difference which can be quite obvious during the early age. Therefore, FE simulations conducted based on the actual material inputs and the linear/ non-linear temperature distributions cannot entirely reflect the deflection of the slabs due to environmental effects (Rao et al., 2001). However, the concept of an equivalent temperature difference (ΔT_{etd}) combining all of the active effects

in terms of temperature difference could possibly circumvent this limitation of these FE programs. The equivalent temperature differences (ΔT_{etd}) can be quantified in two ways:

1. Quantifying equivalent temperature difference (ΔT_{etd}) based on the observation of temperature difference for maintaining a flat-slab condition from LVDT measurements

2. Establishing the relation between the actual measured temperature differences ($\Delta T_{trans-temp-diff}$) and the equivalent temperature differences (ΔT_{etd}) through back-estimating temperature difference to generate the relative corner deflection to center of the measured slab curvature profiles from FE programs

5.6.1 FE Modeling of Instrumented Pavements

Based on the actual geometric proportions and the collected material properties from the test sections, those input parameters which were required in FE simulations, but could not be collected, were assigned reasonable values based on the results of the parametric study. For instance, it was observed that the slab deformation increased for increasing modulus of subgrade reaction (k) from 8.1 kPa/mm (30 psi/in) to 35.3 kPa/mm (130 psi/in), but after 35.3 kPa/mm (130 psi/in) the slab deformation did not increase much. The k-value, 35.3 kPa/mm (130 psi/in), is a typical minimum value for Iowa conditions and therefore, 62.4 kPa/mm (230 psi/in) was assumed as the k-value for the FE simulations.

The values of input parameters used in this modeling are summarized in Table 5-2. Three-consecutive slabs in each test lane, as shown in Figure 5-5, were used and middle slab in the travel lane was selected for representing field measurements. Although the

slab temperature profiles with depth have been recognized as non-linear distributions by previous studies (Thomlinson, 1940; Choubane and Tia, 1992), the observed temperature profiles under which the pavement profile data were collected in this study showed nearly a linear temperature distribution. Additionally, the non-linear component of the slab temperature distribution causing zero-moment but causing stress didn't influence the deflections very much (Yu et al, 2004). So, the linear temperature distributions were used in this simulation.

Table 5-2 Values of input parameters used in FE-modeling

Geometry Properties					
Layer	Lane	No. of segm.	Width (m) in a segm.	Length (m) in a segm.	Depth (mm)
Concrete	Passing	3	3.7	6	267
	Traveling	3	4.3	6	267
Material Properties					
Material		Property			Value
Concrete		Modulus of elasticity (MPa)			30,483
		Unit weight (kg/m^3)[a]			2,400
		Poisson's ratio			0.2
		Coefficient of thermal expansion (/^{o}C)			9.63×10^{-6}
Dowel Bar		Diameter (mm)			38
		Length (mm)			457
		Spacing (mm)			305
		Modulus of elasticity (MPa)[a]			20×10^4
		Poisson's ratio[a]			0.3
Tie Bar		Diameter (mm)			13
		Length (mm)			914
		Spacing (mm)			762
		Modulus of elasticity (MPa)[a]			20×10^4
		Poisson's ratio[a]			0.3
Subgrade		Modulus of subgrade reaction (kPa/mm)[a]			62.4

[a] assumed value as typical value

Figure 5-5 Three-consecutive slab systems in each lane used in FE simulation

5.6.2 Method 1: Quantifying Equivalent Temperature Difference (ΔT$_{etd}$) Using LVDT Measurements

Based on the LVDT measurements displayed in Figure 5-3, a value of 8.5 ^{o}C (15.3 ^{o}F) was assumed as the temperature difference to maintain a flat-slab condition for a 267 mm (10.5-in) thick slab in this study. This means that -8.5 ^{o}C (-15.3 ^{o}F) was defined as the effective built-in temperature difference (ΔT$_{ebi}$) which produces the same amount of deformation resulting from a combination of environmental effects such as moisture and temperature conditions during PCC hardening, creep, and settlement.

Thus, an equivalent temperature difference (ΔT$_{etd}$) can be defined as the sum of the measured temperature difference (ΔT$_{trans-temp-diff}$) and the effective built-in temperature difference (ΔT$_{ebi}$) as presented in Equation 5-5. The equivalent temperature differences (ΔT$_{etd}$) at both the positive and negative temperatures under which pavement profile data were collected were calculated and used as input values for both the FE programs.

5.6.3 Method 2: Quantifying Equivalent Temperature Difference (ΔT$_{etd}$) Using Profile Measurements

Since all the environmental effects are highly correlated with each other, it is quite difficult to quantify each of these effects in terms of temperature differences and therefore the concept of combining all of the active effects into an equivalent temperature difference (ΔT_{etd}) has been used by previous researchers (Rao et al., 2001; Yu and Khazanovich, 2001 ; Jeong and Zollinger, 2004; Rao and Roesler, 2005). Following this concept, the relation between actual measured temperature difference ($\Delta T_{trans-temp-diff}$) and equivalent temperature difference associated with actual pavement behavior could be established. Similar to the approach used by previous researchers (Rao et al., 2001; Yu and Khazanovich, 2001; Jeong and Zollinger, 2004), equivalent temperature differences of both FEM programs were back-estimated to generate the relative corner deflection to center of the measured slab curvature profiles from diagonal direction because these profiles are the longest segment along the slab and include the internal center in slab. Once the ΔT_{etd} on given measured temperature difference was estimated, the ΔT_{etd} values were plotted with measured temperature differences ($\Delta T_{trans-temp-diff}$) as shown in Figure 5-6. From Figure 5-6, the equivalent temperature differences and the measured temperature differences show a linear relation. This linear relation can be also observed in data collected in US-34 near Burlington, Iowa (Ceylan et al, 2006) as shown in Figure 5-7.

Linear regression equations from Figures 5-6 and 5-7 show the difference between ISLAB 2000 and EverFE 2.24 approaches since the basic elements constituting the meshes in these programs (thin plate element for ISLAB 2000 and solid element for

EverFE 2.24) have different nodes and degrees of freedom. It is interesting to note that the coefficient of linear regression equation is less than unity. It is possible to relate the coefficient and the independent variable of the linear regression equation to the transient component of equivalent temperature difference ($\Delta T_{transient}$) and the intercept of the regression equation to the permanent component of equivalent temperature difference ($\Delta T_{permanent}$).

It is interesting to note that approximately -4 ^{o}C (-8 ^{o}F) for ISLAB 2000 and -6 ^{o}C (-11 ^{o}F) for EverFE 2.24 were obtained as intercepts for the linear regression equations in this study which is similar to -5.6 ^{o}C (-10 ^{o}F) defined as $\Delta T_{permanent}$ in the MEPDG through national calibration results. Additionally, those values are smaller than -8.5 ^{o}C (-15.3 ^{o}F) obtained as ΔT_{ebi} from LVDT measurements.

Based on linear regression equations from Figure 5-6, equivalent temperature differences during pavement profile data collection were calculated and used as inputs for both FEM programs.
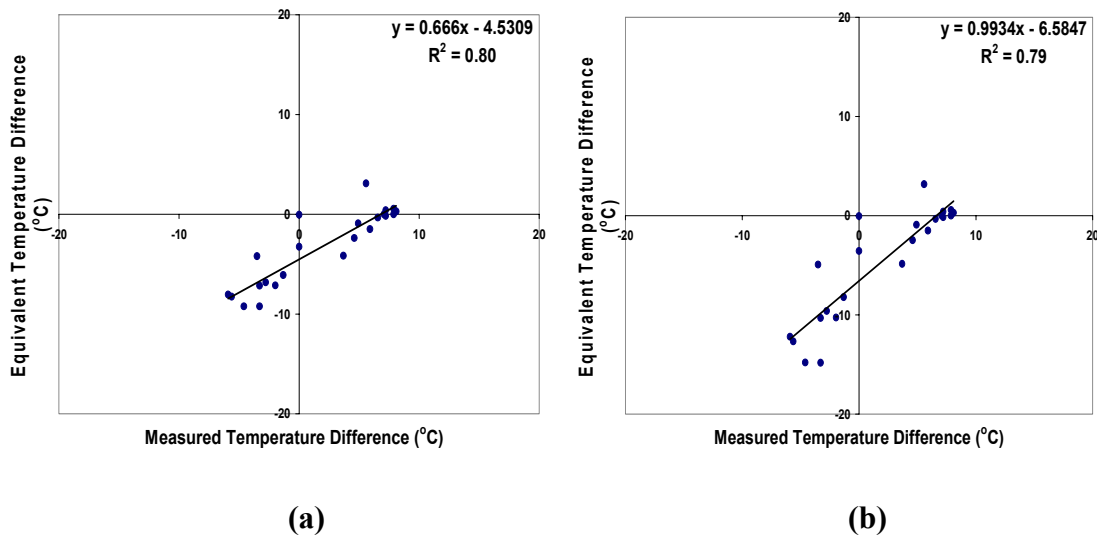
(a)   **(b)**

Figure 5-6 Equivalent temperature differences versus measured temperature differences in US-30 near Marshalltown, Iowa: (a) ISLAB2000; (b) EverFE 2.24

(a)   (b)
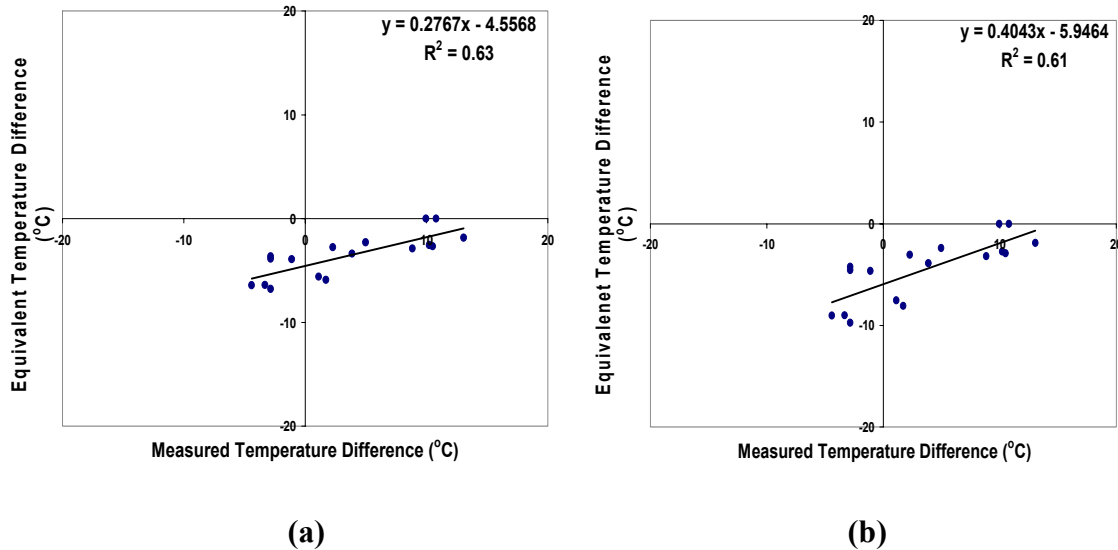
Figure 5-7 Equivalent temperature differences versus measured temperature differences in US-34 near Burlington, Iowa: (a) ISLAB 2000; (b) EverFE 2.24

5.7 Verification of FE Simulations on Field Measurements

FE-based simulation results were required to quantify the slab curvature profile and characterize the differences between the measured and FE – simulated slab curvature profiles. If the slab behavior could be characterized in terms of total amount of deflection and the slab shape, the total amount of slab deflection could be quantified using the relative deflection of corner to center in the measured direction (Rc) and the slab shape could be quantified by the curvature of slab profile (k). The relative deflection of corner to center (Rc) in the defined direction could easily be calculated by subtracting the elevation of center in the defined direction from that of corner in the same direction. The curvature of slab profile (k) was calculated using a methodology proposed by Vandenbossche (2005). A second-order polynomial curve was fit to FE-calculated slab deformation profile and then the curvature was calculated using Equation 5-6 as follows:

$$k = \frac{\dfrac{d^2 y}{dx^2}}{\left[1 + \left(\dfrac{dy}{dx}\right)^2\right]^{\frac{3}{2}}}$$

(Equation 5-6)

Where:

$y = Ax^2 + Bx + C$

k = Curvature

y = Measured displacement

x = Location along the profile traverse

A, B, and C = Coefficients

Since profile measurements were conducted on diagonal and transverse direction in test sections, Rc and k were calculated in same direction on slab simulated.

5.7.1 Verification of FE Simulations Based on Method 1

Comparisons between the field-measured slab curvature profiles and the FE-computed slab curvature profiles using method 1 in terms of Rc and k were undertaken. The quantitative comparisons between the measured profiles and the FE-computed profiles using method1 for both test sections are presented in Figures 5- 8, 5-9, 5-10 and 5-11. In these figures, a positive value indicates the upward movement of the slab and a negative value indicates the down ward movement of the slab.

(a) Diagonal Direction @Negative Temperature Difference

(b) Transverse Direction @Negative Temperature Difference

(c) Diagonal Direction @Positive Temperature Difference

(d) Transverse Direction @Positive Temperature Difference

Figure 5-8 Comparisons of relative corner deflection (Rc) between measured and FE-predicted slab curvature profiles using method 1 in test section 1: (a) diagonal direction at negative temperature difference condition; (b) transverse direction at negative temperature difference condition; (c) diagonal direction at positive temperature difference condition; (d) transverse direction at positive temperature difference condition
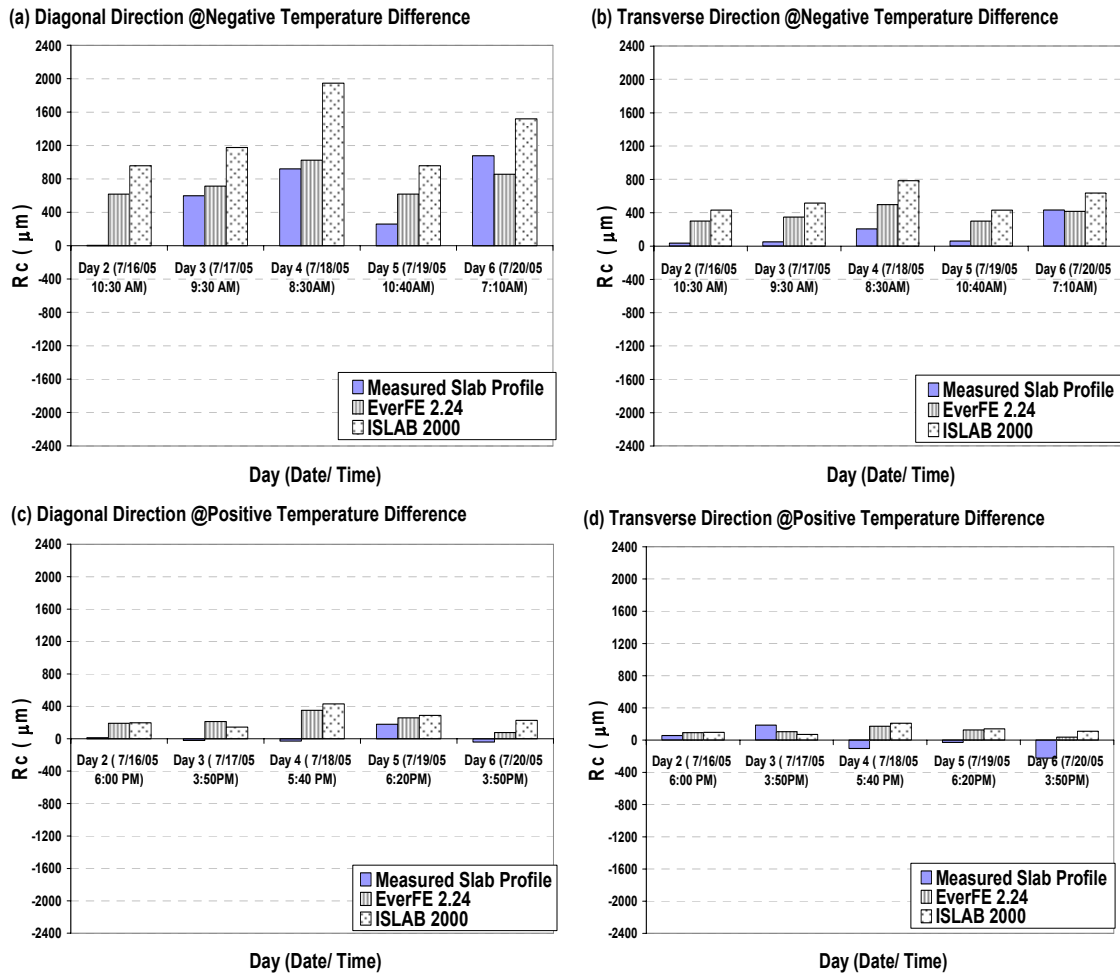
Figure 5-9 Comparisons of relative corner deflection (Rc) between measured and FE-predicted slab curvature profiles using method 1 in test section 2:(a) diagonal direction at negative temperature difference condition; (b) transverse direction at negative temperature difference condition; (c) diagonal direction at positive temperature difference condition; (d) transverse direction at positive temperature difference condition

(a) Diagonal Direction @Negative Temperature Difference

(b) Transverse Direction @Negative Temperature Difference

(c) Diagonal Direction @Positive Temperature Difference

(d) Transverse Direction @Positive Temperature Difference
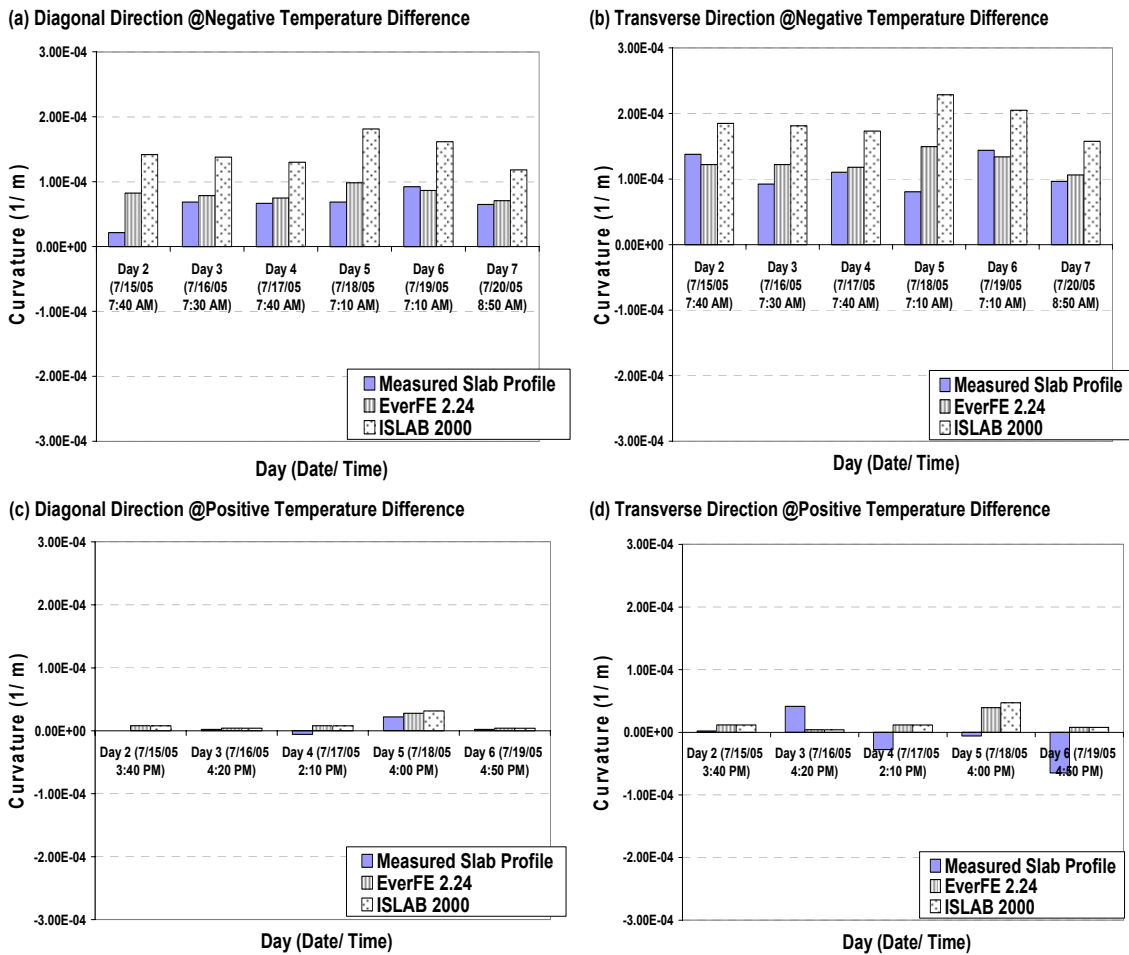
Figure 5-10 Comparisons of curvature (*k*) between measured and FE-predicted slab curvature profiles using method 1 in test section 1:(a) diagonal direction at negative temperature difference condition; (b) transverse direction at negative temperature difference condition; (c) diagonal direction at positive temperature difference condition; (d) transverse direction at positive temperature difference condition
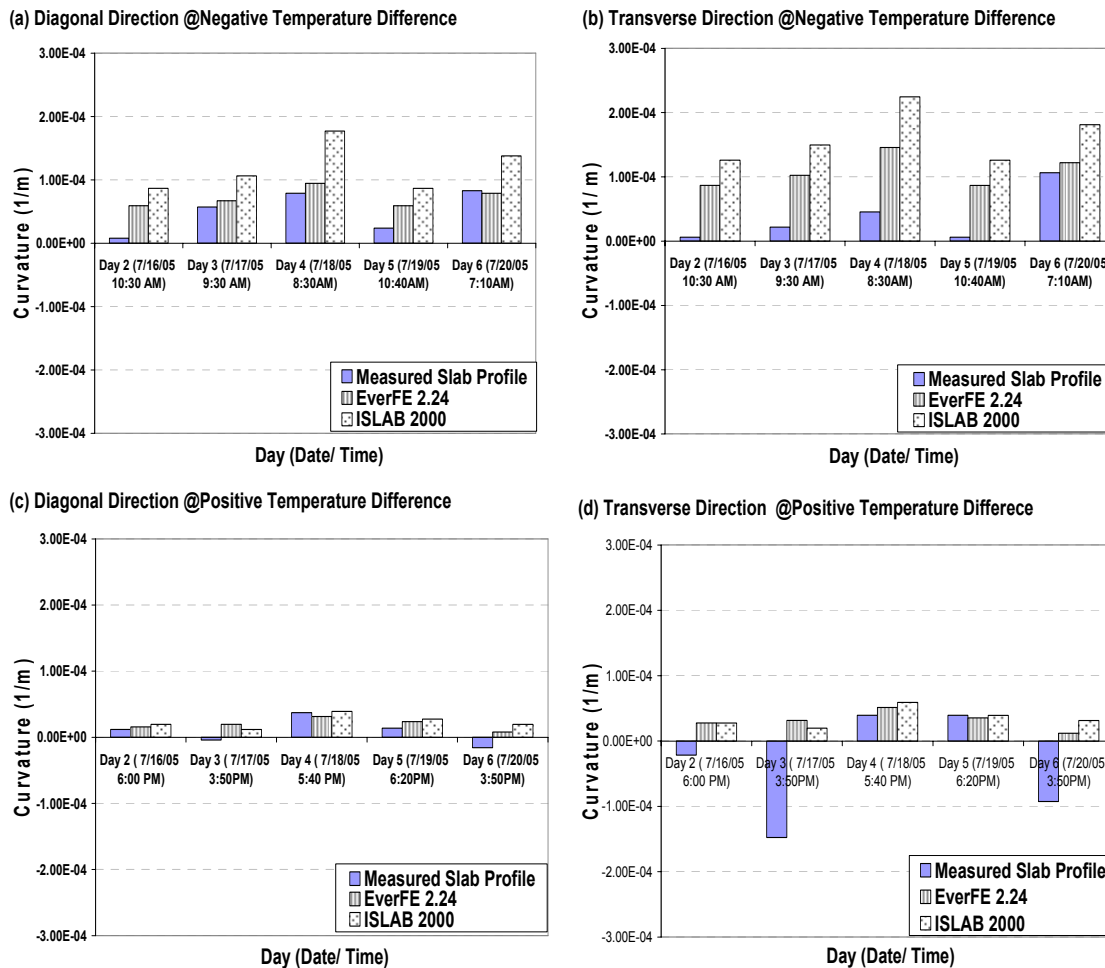
Figure 5-11 Comparisons of curvature (*k*) between measured and FE-predicted slab curvature profiles using method 1 in test section 2: (a) diagonal direction at negative temperature difference condition; (b) transverse direction at negative temperature difference condition; (c) diagonal direction at positive temperature difference condition; (d) transverse direction at positive temperature difference condition

From these observations, it is clearly noted that the measured slab curvature profiles show upward curl at negative temperature differences and maintain almost a flat shape at positive temperature differences. FE models based on method 1 could also simulate these observed trends of the measured slab curvature. The comparisons indicated that the 3-D FE model, EverFE 2.24, provided better estimations of the

curvature (k) and the relative corner deflection (Rc) with the slab profile compared to ISLAB 2000 (2-D FE software) in test section 1. But, both FE programs seem to overestimate the curvature (k) and the relative corner deflection (Rc) with the slab profile in test section 2. It is not too surprising to observe inaccuracy of predicting k and Rc in test section 2 since the effective built-in temperature difference (ΔT_{ebi}) used in method 1 was estimated from LVDTs measurements of slabs in test section 1. However, this inaccuracy in test section 2 indicated that the effective built-in temperature difference (ΔT_{ebi}) may be lower than -8.5 ^{o}C (-15.3 ^{o}F) which was obtained from LVDT measurements in test section 1 and used as the effective built-in temperature difference (ΔT_{ebi}) to calculate the equivalent temperature difference (ΔT_{etd}) in Method 1.

To evaluate the statistical accuracy of FE models based on method 1, a statistical test, Analysis of Variance (ANOVA), was used. ANOVA results can be expressed in terms of a p-value, which represents the weight of evidence for rejecting the null hypothesis (Ott and Longnecker, 2001). The null hypothesis of sample equality cannot be rejected if p-value is greater than the selected significant level. Tables 5-3 and 5-4 present the ANOVA results for Rc and k in terms of p-value. For the significance level (α) of 0.05, the ANOVA results from Table 5-3 and 5-4 confirmed that the FE-predictions based on method 1 provide good estimates of slab curvature properties in term of Rc and k in test section 1 but couldn't estimate slab properties in test section 2 since the equivalent temperature difference (ΔT_{etd}) of method 1 was quantified from the observation of LVDT measurements in test section1.

Table 5-3 ANOVA results for Rc and *k* of slab curvature profiles measured and predicted from ISLAB 2000

Test Section	Temperature Different Condition	Response	Direction			
			Diagonal		Transverse	
			p-value	Different ?	p-value	Different ?
Section 1	Positive	Rc	0.1284	NO	0.5398	NO
		k	0.1598	NO	0.3806	NO
	Negative	Rc	0.0001	Yes	0.1136	NO
		k	0.0001	Yes	0.026	Yes
Section 2	Positive	Rc	0.0008	Yes	0.2321	NO
		k	0.0428	Yes	0.0128	Yes
	Negative	Rc	0.001	Yes	0.0001	Yes
		k	0.0003	Yes	0.0001	Yes

Table 5-4 ANOVA results for Rc and *k* of slab curvature profiles measured and predicted from EverFE 2.24

Test Section	Temperature Different Condition	Response	Direction			
			Diagonal		Transverse	
			p-value	Different ?	p-value	Different ?
Section 1	Positive	Rc	0.14	NO	0.5576	NO
		k	0.1765	NO	0.4055	NO
	Negative	Rc	0.2417	NO	0.8269	NO
		k	0.0502	NO	0.6442	NO
Section 2	Positive	Rc	0.0028	Yes	0.2968	NO
		k	0.1152	NO	0.0175	Yes
	Negative	Rc	0.2071	NO	0.0028	Yes
		k	0.0693	NO	0.0003	Yes

5.7.2 Verification of FE Simulations Based on Method 2

Similar to the previous section, the quantitative comparisons between the measured slab curvature profiles and the FE-computed slab curvature profiles using method 2 for both test section were conducted and presented in Figures 5-12, 5-13, 5-14 and 5-15.

112
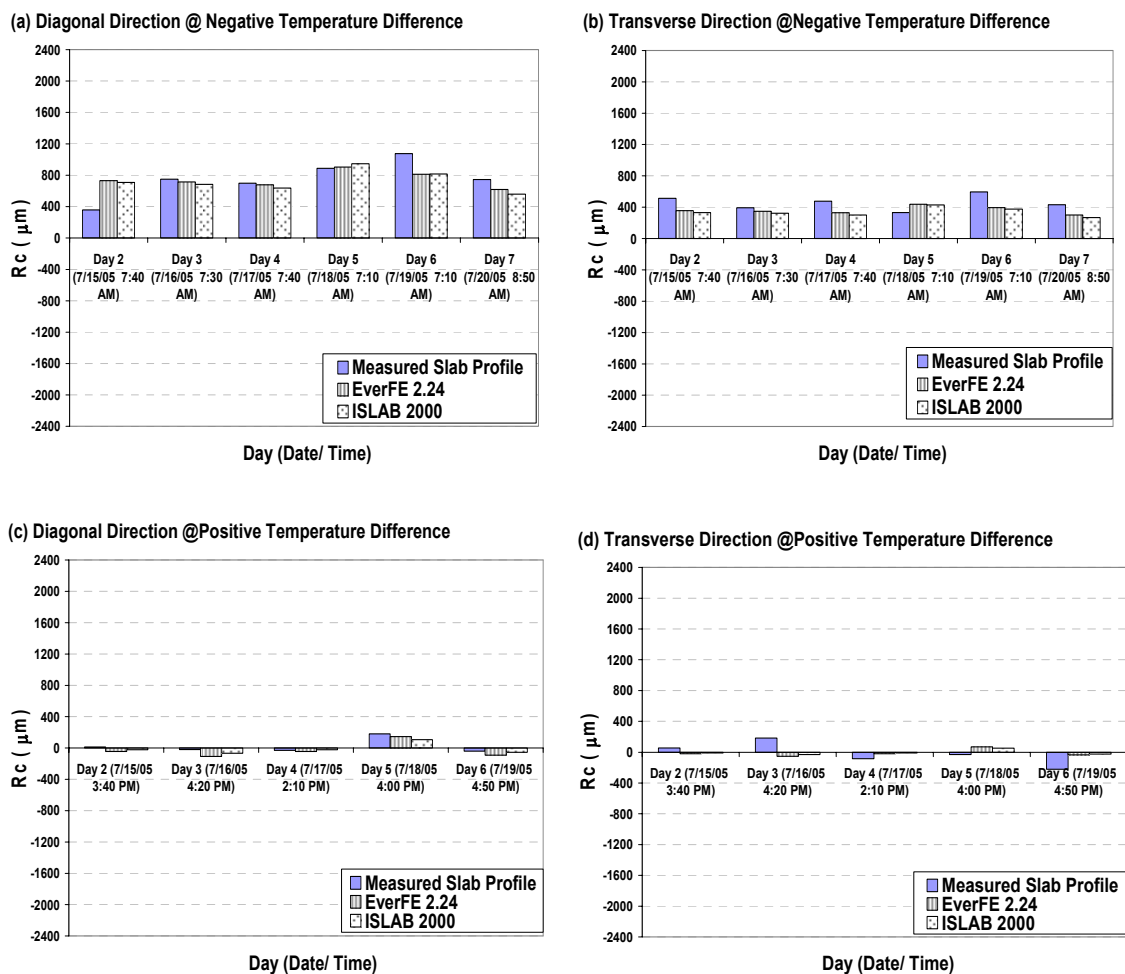
Figure 5-12 Comparisons of relative corner deflection (Rc) between measured and FE-predicted slab curvature profiles using method 2 in test section 1: (a) diagonal direction at negative temperature difference condition; (b) transverse direction at negative temperature difference condition; (c) diagonal direction at positive temperature difference condition; (d) transverse direction at positive temperature difference condition

114

Figure 5-14 Comparisons of curvature (*k*) between measured and FE-predicted slab curvature profiles using method 2 in test section 1:(a) diagonal direction at negative temperature difference condition; (b) transverse direction at negative temperature difference condition; (c) diagonal direction at positive temperature difference condition; (d) transverse direction at positive temperature difference condition

(a) Diagonal Direction @Negative Temperature Difference

(b) Transverse Direction @Negative Temperature Difference

(c) Diagonal Direction @Positive Temperature Difference
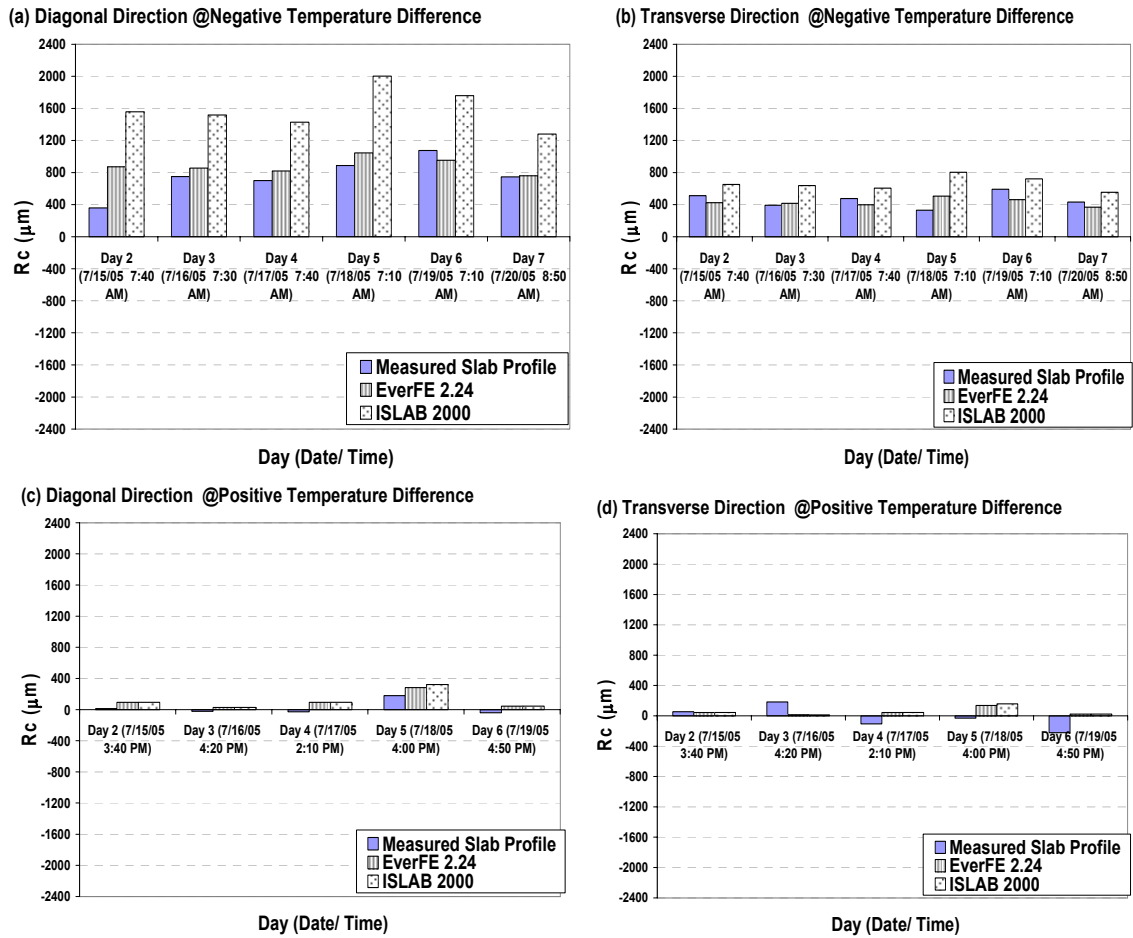
(d) Transverse Direction @Positive Temperature Difference

Figure 5-15 Comparisons of curvature (*k*) between measured and FE-predicted slab curvature profiles using method 2 in test section 2:(a) diagonal direction at negative temperature difference condition; (b) transverse direction at negative temperature difference condition; (c) diagonal direction at positive temperature difference condition; (d) transverse direction at positive temperature difference condition

From a cursory examination of the comparison charts, it can be observed that the FE-predicted slab curvature properties agree well with the measured slab curvature properties such as Rc and *k*.

ANOVA statistical test was conducted to evaluate if the measured slab curvature properties (Rc and *k*) were statistically different from the measured properties. It is important to note that the relation between the measured temperatures ($\Delta T_{\text{trans-temp-diff}}$) and

equivalent temperature differences (ΔT_{etd}) was established from the measured slab curvature profile of diagonal direction in both test sections as presented in Figure 5-6. Table 5-5 presents the ANOVA results for Rc and k in terms of p-value (based on method 2).

Since the equivalent temperature differences (ΔT_{etd}) were computed based on the diagonal slab curvature profile, it is only expected that the FE-predicted diagonal slab curvature profiles will match the actual slab curvature profile reasonably well. However, for the significance level of 0.05, the null hypothesis of equality between the measured slab curvature profiles properties and the FE-predicted slab curvature profiles properties using method 2 cannot be rejected under different conditions, which indicated that FE-models based on method 2 to quantify equivalent temperature difference (ΔT_{etd}) could estimate the slab deformation statistically well at a level of significance of 0.05.

Table 5-5 ANOVA results for Rc and k of slab curvature profiles measured and predicted from FE-programs

Temperature Difference Condition	Response	Direction			
		Diagonal		Transverse	
		p-value	Different ?	p-value	Different ?
Positive	Rc	0.9378	No	0.8201	No
	k	0.4385	No	0.1455	No
Negative	Rc	0.9276	No	0.9286	No
	k	0.6114	No	0.4758	No

5.7.3 Comparisons of FE–models Based on Method 1 and Method 2

The main difference in approach between the FE-based method 1 and method 2 utilized to quantify the equivalent temperature difference (ΔT_{etd}) is the consideration of variability of transient displacement behavior due to actual moisture gradient.

The equivalent temperature difference (ΔT_{etd}) in method 1 is a function of the measured temperature difference ($\Delta T_{trans\text{-}temp\text{-}diff}$) and the effective built-in temperature difference (ΔT_{ebi}) considering transient component due to actual moisture gradient ($\Delta T_{trans\text{-}mois\text{-}diff}$) as constant value. However, the equivalent temperature difference (ΔT_{etd}) in method 2 is a function of the transient component of equivalent temperature difference ($\Delta T_{transient}$) including effect of actual moisture gradient variability as coefficient of $\Delta T_{trans\text{-}temp\text{-}diff}$ and the permanent component of equivalent temperature difference ($\Delta T_{permanent}$). Therefore, the equivalent temperature difference (ΔT_{etd}) in method 2 would better reflect the effect of moisture variation due to weather conditions and provide better predictions. This indicates that the effect of moisture change is significant in displacement behavior due to environmental loads at early aged JPCP, which is in agreement with the results reported by Hayhoe from the observation of curling behavior at rigid pavement test items of the Federal Aviation Administration's National Airport Pavement Test Facility (NAPTF) (2004).

5.8 Conclusions

This study characterized the early age JPCP deformation due to environmental effects in terms of equivalent temperature difference by employing two FE-based primary response models, namely ISLAB 2000 and EverFE 2.24. The concept of equivalent linear temperature difference (ΔT_{etd}) was reviewed and presented. Based on field data collected from instrumented JPCP on highway US-30 near Marshalltown, Iowa, the equivalent temperature difference corresponding to actual deformation under environmental loads was quantified using two different approaches. The procedures and

the results of the FE analyses based on the collected data and the quantified equivalent temperature differences were presented. Comparisons between the field measured and the FE computed slab deformations due to environmental effects were reported in this paper. Based on this study, the following conclusions were drawn;

- A linear relation was observed between the actual measured temperature difference ($\Delta T_{\text{trans-temp-diff}}$) and equivalent temperature difference (ΔT_{etd}) associated with actual slab displacement under pure environmental loading.

- The coefficient and the independent variable of the linear regression equation could be related to the transient component of equivalent temperature difference ($\Delta T_{\text{transient}}$) and the intercept of the regression equation could be related to the permanent component of equivalent temperature difference ($\Delta T_{\text{permanent}}$).

- Better comparisons were obtained when the equivalent temperature difference accounted for variability in PCC displacement due to actual moisture gradient variations which made the FE simulations more accurate.

5.9 Acknowledgments

5.10 References

Armaghani, J. M., Larsen, T. J., and Smith, L. L., 1987, "Temperature Response of Concrete Pavements," *Transportation Research Record*, Vol. 1121, Transportation Research Board, Washington, D.C., pp. 23-33.

Byrum, C. R., 2000, "Analysis by High-Speed profile of Jointed Concrete Pavement Slab Curvatures," *Transportation Research Record*, Vol. 1730, Transportation Research Board, Washington, D.C., pp.1-9.

Byrum, C. R., 2001, *A High Speed Profile Based Slab Curvature Index for Jointed Concrete Pavement Curling and Warping Analysis*, Ph.D. Thesis, University of Michigan, Ann Arbor, Michigan.

Ceylan, H., Kim, S, Gospalakrishnan, K., and Wang, K., 2006, "Environmental Effects on Deformation and Smoothness Behavior of Early Age Jointed Plain Concrete Pavements," *Paper Submitted to the Transportation Research Board for Publication and Presentation at the 86th Annual meeting to be held on January 21-25, 2007 in Washington, D.C.*

Choubane, B. and Tia, M., 1992, "Nonlinear Temperature Gradient Effect on Maximum Warping Stresses in Rigid Pavements," *Transportation Research Board*, Vol. 1370, Washington, D.C., pp. 14-24.

Davids, W.G., 2003, *EverFE Theory Manual*, University of Maine, Civil Engineering Department, Orono, Main, pp.1-18.

Davids, W.G., 2006, *EverFE : Software for the 3D Finite Element Analysis of Jointed Plain Concrete Pavements*, University of Maine, Civil Engineering Department, Orono, Main, http://www.civil.umaine.edu/EverFE/, Accessed May, 2006.

Hammons, M. I. and Ioannides, A. M., 1997, *Advanced Pavement Design:Finite Element Modeling for Rigid Pavement Joints Report I: Background Investigation*, Technical Report DOT- FAA- AR-95-85, Federal Aviation Administration, U.S. Department of Transportation.

Hayhole, G. F., 2004, "Traffic Testing Results from the FAA's National Airport Pavement Test Facility," *Proceedings of 2nd International Conference on Accelerated Pavement Testing*, Minneapolis, Minnesota.

Hiller, J. E. and Roesler, J. R., 2005, "Determination of Critical Concrete Pavement Fatigue Damage Locations Using Influence Lines," *Journal of Transportation Engineering*, Vol. 131, No. 8, American Society of Civil Engineering, pp.599-607.

International Cybernetics Corporation (ICC.), 2006, http://www. internationalcybernetics.com/ rollprofile.htm, accessed May, 2006.

Janssen, D. J., 1987, "Moisture in Portland Cement Concrete," *Transportation Research Record*, Vol. 1121, Transportation Research Board, Washington, D.C., pp. 40-44.

Jeong, J. H. and Zollinger, D. G., 2004, "Insights on Early Age Curling and Warping behavior from Fully Instrumented Test Slab System," *CD-ROM Proceedings of the 83rd Annual Meeting of the Transportation Research Board* , Transportation Research Board, Washington, D.C.

Khazanovich, L., Yu, H. T., Rao, S., Galasova, K., Shats, E., and Jones, R., 2000, *ISLAB2000-Finite Element Analysis Program for Rigid and Composite Pavements*, User's Guide, ERES Consultant, Champaign, Illinois.

Lim, S. W. and Tayabji, S. D., 2005, "Analytical Technique to Mitigate Early-Age Longitudinal Cracking in Jointed Concrete Pavements," *Proceedings of 8th International Conference on Concrete Pavements*, Colorado Springs, Colorado.

National Cooperative Highway Research Program (NCHRP), 2004, *Guide for Mechanistic-Empirical Design of New and Rehabilitated Pavement Structures*, http://trb.org/mepdg, National Cooperative Highway Research Program 1-37A, Transportation Research Board, Washington, D.C.

Ott, L.R. and Longnecker, M., 2001, *An introduction to Statistical Methods and Data Analysis*, 5th edition, Duxbury, Pacific Grove, California.

Poblete, M., Salsili, R., Valenzuela, R., Bull, A., and Spratz, P., 1988, "Field Evaluation of Thermal Deformations in Undoweled PCC Pavement Slabs," *Transportation Research Record,* Vol. 1207, Transportation Research Board, Washington, D.C., pp. 217-228.

Rao, C., Barenberg, E. J., Snyder, M. B., and Schmidt, S., 2001, "Effects of Temperature and Moisture on the Response of Jointed Concrete Pavements," *Proceedings of 7th International Conference on Concrete Pavements*, Orlando, Florida.

Rao. S. and Roesler, J. R., 2003, *Analysis and Estimation of Effective Built –in Temperature Difference for North Tangent Slabs*, Draft Report, University of California –Berkeley Pavement Research Center, University of Illinois, Urbana Champaign.

Rao, S. and Roesler, J. R., 2005, "Characterizing Effective Built in Curling from Concrete pavement Field Measurements," *Journal of Transportation Engineering*, Vol. 131, No. 4, American Society of Civil Engineering, pp.320-327.

Rufino, D. and Roesler, J. R., 2006, "Effect of Slab-Base Interaction on Measured
Concrete Pavement Responses," *Journal of Transportation Engineering*, Vol. 132,
No. 5, American Society of Civil Engineering, pp.425-434.

Sixbey, D., Swanlund, M., Gagarin, N. and Mekemson, J. R., 2001,"Measurement and
Analysis of Slab Curvature in JPC Pavements Using Profiling Technology,"
Proceedings of 7th International Conference on Concrete Pavements, Orlando,
Florida.

Siddique, Z. and Hossain. M.,2005, "Finite Element Analysis of PCCP Curling and
Roughness," *Proceedings of 8th International Conference on Concrete
Pavements*, Colorado Springs, Colorado.

Thomlison, J., 1940, "Temperature Variations and Consequence Stress Produced by
Daily and Seasonal Temperature Cycles in Concrete Slabs," *Concrete
Constructional Engineering*, Vol. 36, No. 6, pp.298-307 and No.7, pp.352-360.

Vandenbossche, J. M., 2003, *Interpreting Falling Weight Deflectometer Results for
Curled and Warped Portland Cement Concrete Pavements*, Ph.D. Thesis,
University of Minnesota, Minneapolis, Minnesota.

Vandenbossche, J. M. and Snyder, M. B., 2005, "Comparison between Measured Slab
Profiles of Curled Pavements and Profile Generated Using the Finite Element
Method," *Proceedings of 8th International Conference on Concrete Pavements*,
Colorado Springs, Colorado.

Vandenbossche, J. M., Wells, S. A., and Phillips, B.M., 2006, "Quantifying Built-in
Construction Gradients and Early-Age Slab Shape to Environmental Loads for
Jointed Plain Concrete Pavements," *CD-ROM Proceedings of the 85th Annual*

Meeting of the Transportation Research Board, Transportation Research Board, Washington, D.C.

Yu, H. T., Khazanovich, L. Darter, M. I, and Ardani, A., 1998, "Analysis of Concrete Pavement Response to Temperature and Wheel Loads Measured from Instrumented Slab," *Transportation Research Record*, Vol. 1639, Transportation Research Board, Washington, D.C., pp. 94-101.

Yu, H. T. and Khazanovich, L., 2001, "Effects of Construction on Concrete Pavement Behavior," *Proceedings of 7th International Conference on Concrete Pavements*, Orlando, Florida.

Yu, H. T., Khazanovich, L., and Darter, M. I., 2004, "Consideration of JPCP Curling and Warping in the 2002 Design Guide," *CD-ROM Proceedings of the 83rd Annual Meeting of the Transportation Research Board*, Washington, D.C.

CHAPTER 6. THE EFFECT OF SLAB CURVATURE DUE TO ENVIRONMENTAL LOADING ON INITIAL SMOOTHNESS OF JOINTED PLAIN CONCRETE PAVEMENTS

A paper to be presented and published at *the 6th International Workshop on Fundamental Modeling of Design and Performance of Concrete Pavements, at Delft University of Technology in Belgium*

Sunghwan Kim,[1] Halil Ceylan,[2] Kasthurirangan Gopalakrishnan,[3] and Kejin Wang[4]

6.1 Abstract

In this paper, the effect of early-age slab curvature, caused by environmental loading, on the initial smoothness of concrete pavements is discussed. Surface profile measurements were made during the early morning and late afternoon hours on an instrumented Jointed Plain Concrete Pavement (JPCP) on highway US-30 near Marshalltown, Iowa. Measurements were made at frequent intervals during the first seven days after the construction in the summer of 2005. Variations in temperature and moisture during this critical period were monitored using the temperature and relative humidity sensors installed within the test sections at the time of construction. Based on the measured surface profile data, it was observed that the initial pavement smoothness,

---
[1] Graduate Research Assistant, Iowa State University, Ames, IA
[2] Assistant Professor, Iowa State University, Ames, IA
[3] Post-Doctoral Research Associate, Iowa State University, Ames, IA
[4] Associate Professor, Iowa State University, Ames, IA

in terms of International Roughness Index (IRI) and the Ride Number (RN), was not influenced by JPCP's early-age curling and warping behavior (during the first seven days after paving). Using Finite Element Modeling (FEM), sensitivity studies were conducted to investigate the influence of slab curvature on initial pavement smoothness for a range of equivalent temperature differences between the top and bottom of the slab. The results showed that the initial JPCP smoothness is sensitive to changes in slab curvature resulting from environmental loading only at higher magnitudes. Although the FEM-based IRI predictions were higher than the surface profile-based IRI values, the differences were not significant.

6.2 Introduction

Pavement smoothness can de defined as a lack of noticeable roughness and a more optimistic view of the road condition (Akhter et al., 2002; Sayers and Karamihas, 1998). Pavement smoothness has been recognized as an important measurement in evaluating pavement performance because it is directly related to the serviceability of road for the traveling public (Ksaibatti et al., 1995). Smooth roads provide comfortable ride, resulting in lower dynamic loads, reduced vehicle operation cost, increased safety, and longer pavement life (Hajek et al., 1998; Ma et al., 1995; Perera et al., 2002; Rawool et al., 2005). In addition, smoother roads will have a positive effect on noise reduction due to the motor vehicles. Especially, the initial smoothness immediately after construction can significantly affect the pavement service life (Janoff, 1990). Smith et al. (1997) reported that pavements constructed smoother stayed smoother over time provided all other things affecting smoothness remained the same. Many agencies have established

and implemented smoothness specifications for newly constructed pavements. Using these specifications, the agencies determine the bonuses or penalties to the contractor thereby encouraging the contractor to construct pavements with smoothness levels higher than a specified value (Chou et al., 2005).

Even though it has been recognized that higher initial smoothness can provide longer pavement life (Ma et al., 1995; Perera et al., 2002), the factors influencing the initial smoothness of a concrete pavement are not very well discussed in literature. However, it is believed that several factors are related to the initial smoothness of a concrete pavement. These include elements related to the pavement design, material selection, concrete uniformity, climate, and construction practices (Rasmussen et al., 2002; Rasmussen et al., 2004). Among them, the temperature and moisture variation in climate could result in change in curvature of slab known as curling and warping. Hveem (1951) is one of the first researchers to notice the effect of curling and warping on pavement smoothness measurements. Based on analysis of data collected from the Long Term Pavement Performance (LTPP) study, Byrum (2001) reported that the construction condition and the complex interactions of temperature, moisture and material creep during early pavement life could result in built-in slab curling. The results of National Cooperative Highway Research Program (NCHRP) Project 10-47 also showed upward curvature in pavement profile during a period when the temperature difference between top and bottom of slab was low (Karamihas et al.,1999).

Previous studies (Bradbury,1938; Korovesis, 1990; Thomlinson, 1940a; Thomlinson, 1940b; Westergaard, 1926; Westergaard, 1927; Yoder and Witczack, 1975), have linked slab curling to stresses in concrete pavements. However, there is very little

discussion on the effects of slab curling on smoothness and subsequently pavement life (Karamihas et al., 2001). Based on a number of smoothness measurements in eleven test pavements starting early morning to late afternoon, Karamihas (2001) suggested that changes in slab curvature due to temperature variations can influence the smoothness of a concrete pavement. However, the pavements selected in this study were at least a few years old, and therefore his findings may not apply with respect to the smoothness of a newly constructed pavement, which is an important quality control factor for deciding the payment for contractor. For instance, Perera et al. (2005) observed that there was no noticeable effect of slab curvature changes affecting the smoothness in five newly constructed pavements.

The current study discussed in this paper was conducted to investigate the effect of slab curvature resulting from environmental loading on the initial smoothness of concrete pavements. In this study, surface profile measurements were conducted during the early morning and late afternoon hours in 267-mm (10.5-in) thick JPCPs near Marshalltown, Iowa during the first seven days after construction in the summer of 2005. Temperature and humidity variations in the pavement sections were monitored during the same times. Based on FEM-generated slab curvature profiles, sensitivity analysis were conducted to investigate the influence of temperature variations on initial smoothness over a wide range of temperature differences which could not be observed in the tested pavements. The procedure and the results of data analysis are discussed in this paper highlighting the important findings regarding the effect of slab curvature resulting from environmental loadings on the smoothness of newly constructed pavements at the critical time immediately following construction.

6.3 Smoothness Index

Since pavement smoothness is related to a lack of roughness, the severity of roughness in pavements has been used to characterize the smoothness. Several smoothness indices representing the severity of roughness have been developed. Among them, the three most common roughness indices currently used in many agencies are the IRI, RN, and Profile Index (PI) (Perera et al., 2002; Smith et al., 2002).

The world bank initiated the development of IRI based on the findings of a correlation experiment conducted in Brazil so that that all roughness–measuring instruments in use throughout the world could produce measures on a common scale, and then establish IRI as that scale (Sayers, 1995). The computation of IRI is based on a mathematical model simulating the vehicle dynamic response to measured pavement profile (Sayers, 1995). Considering the complications involved in modeling the IRI, the IRI is typically computed in specially designed computer programs based on the measured pavement profiles.

RN was developed to simulate the subjective rating of expert panel members about the road roughness based on the pavement profile data (Janoff, 1985; Janoff, 1988). A true pavement profile filtered using specific procedures is summarized as a statistic value such as the Root–Mean-Square (RMS). This statistic value (RMS) is transformed to RN ranging from 5 (perfectly smooth) to 0 (the maximum possible roughness) with a nonlinear statistical equation as shown in Equation 6-1 (Sayers and Karamihas, 1998).

$$RN = 5e^{-160(RMS)}$$

(Equation 6-1)

Where, RN = Ride Number, RMS = Root – Mean- Square of filtered pavement profile

Like IRI, computation of RN can be conducted by a computer program (Sayers and Karamihas, 1998). RN is more sensitive to shorter wave lengths in pavement profile than the IRI. Thus, RN is correlated to IRI but the two are not interchangeable and each parameter provides unique information about the roughness of the pavement (Sayers and Karamihas, 1998).

Since the time California type profilograph has been used for measuring the smoothness of newly constructed pavements, many agencies have used a parameter known as PI. The PI is the accumulated deviations beyond some specific blanking bands drawn on a recorded pavement trace with profilogragh. It should be noted that each agency follows its own standard procedure for determining the PI because of the absence of universal standard for the application of specific blanking band such as 0, 2.5 and 5 mm (Perera et al., 2002).

Currently, most state agencies use the PI for judging the quality of new pavements and a profile statistic such as IRI for monitoring the condition of their pavement network (Perera et al., 2002; Smith et al., 2002). In this case, it is difficult to relate the smoothness of the pavement at some point in time with its initial smoothness. The newly released Mechanistic-Empirical Pavement Design Guide (MEPDG) under NCHRP Project 1-37A incorporates IRI prediction models which include the initial IRI as an input parameter (NCHRP, 2004). Thus, many agencies are trying to establish IRI as the future smoothness index for the acceptance of new pavements (Smith et al., 2002).

6.4 Test Section and Data Collection

Profile measurements were conducted on 267-mm (10.5-in) thick JPCP slabs in highway US-30 near Marshalltown, Iowa. The pavement was constructed on an open-graded granular base. The transverse joint spacing was approximately 6 m (20 ft). The passing lane was approximately 3.7 m (12 ft) in width, and the travel lane was approximately 4.3 m (14 ft) in width. A Hot-Mix Asphalt (HMA) shoulder was added approximately two months after initial construction. Tie-bars of 914-mm (36-in) length and 12.7-mm (0.5-in) diameter were inserted approximately every 76-mm (30-in) across the longitudinal joints. Dowel bars of 457-mm (18-in) length and 38-mm (1.5-in) diameter were inserted approximately every 305-mm (12-in) across the transverse joints.

The travel lanes in two test section as shown in Figure 6-1 correspond to morning and afternoon construction selected for profile measurements. An International Cybernetics Corporation Rollingprofiler® (ICC., 2006) was used for surface profile measurements at different times (morning and the afternoon) along the different traces of longitudinal direction in test sections to obtain a roughness index such as IRI or RN. The temperature and humidity variations were monitored during profiling measurements. These profile measurements in a diurnal cycle for the same location could provide a better understanding of the effect of the slab curling and warping on the smoothness. In addition, four individual slabs in each test section were selected for identifying the slab deformation due to environmental loading with the Rollingprofiler®. The Rollingprofiler® measured surface profiles following the diagonal and transverse traces in each slab. The slab curvature profiles as shown in Figure 6-2 were obtained from the measured surface

profiles after removing the noise based on a similar procedure suggested by Sixbey et al.
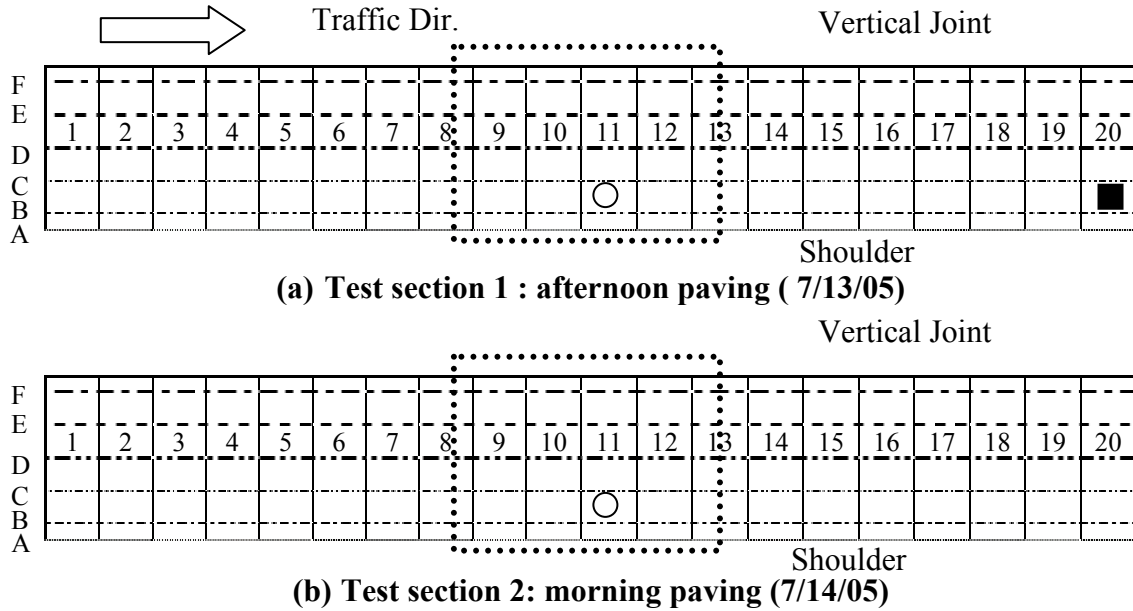
(2001) and Vandenbossche (2003).

(a) Test section 1 : afternoon paving (7/13/05)

(b) Test section 2: morning paving (7/14/05)

Legend: ○ - Temperature instrumentation location
■ - Relative humidity instrumentation location
⋮⋮ - Diagonal and Transverse profiling trace locations
A - Profiling at edge
B - Profiling at 0.6 m (2 ft) from shoulder
C - Profiling at 0.9 m (3 ft) from shoulder
D - Profiling at center
E - Profiling at 0.9 m (3 ft) from vertical joint
F - Profiling at 0.3 m (1 ft) from vertical joint

Figure 6-1 Test section instrumentation and profile measurement layout
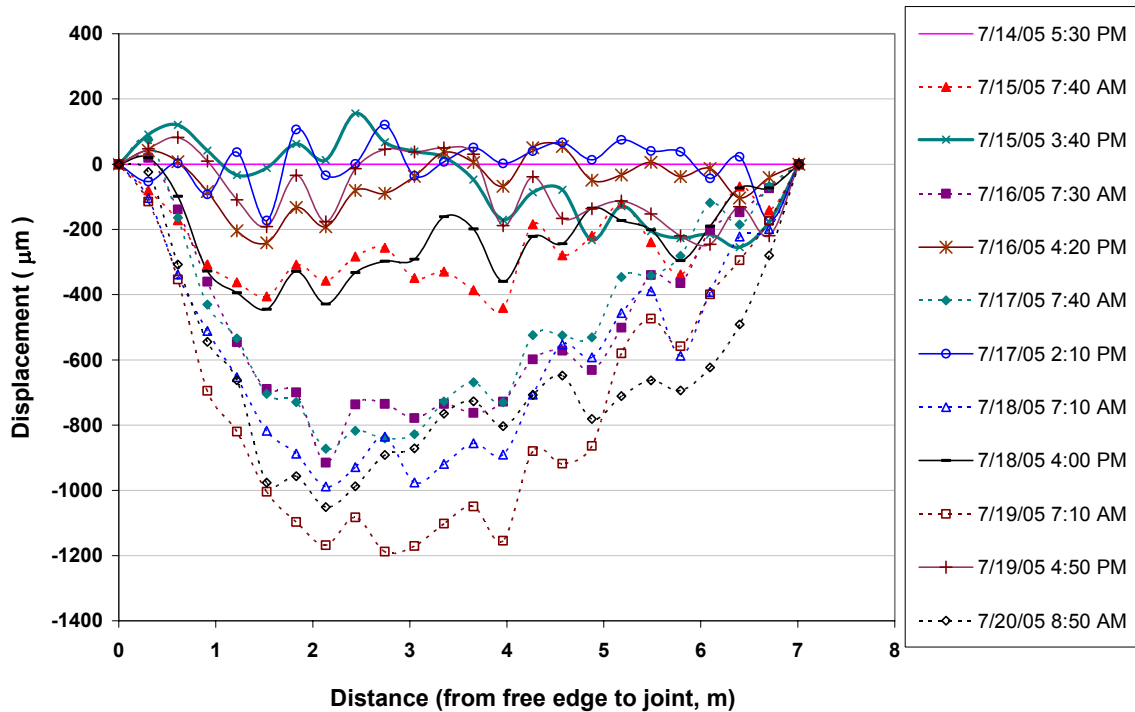
Figure 6-2 JPCP slab curvature profile

The variations in slab deformation were influenced not only by temperature differences but also by moisture differences between the top and the bottom of the PCC slab. The temperature and humidity sensors installed within the test sections detected the temperature and moisture variations. Slab temperature and moisture data were collected at five–minute intervals throughout the field evaluation periods. Temperature instrumentation consisted of seven Thermochron I-buttons® attached to a stake at different depths below surface and placed 0.9-m (3-ft) from the pavement edge before the paving started. Six Thermochron I-buttons® measured the slab temperature and one Thermochron I-button® measured the subgrade temperature. Humidity instrumentation consisted of four moisture sensors inserted into small Poly Vinyl Chloride (PVC) pipes

which were placed side by side at different depths from the pavement surface to measure the humidity variation in the slab.

Temperature differences were calculated by subtracting the temperature sensor reading at 267-mm (10.5-in) below the slab surface (Sensor 1) from the sensor reading at 63.5-mm (2.5-in) below the slab surface (Sensor 6). Note that the closest temperature sensor to the top of the pavement surface was located at 63.5-mm (2.5-in) below the slab surface. Moisture differences were computed by subtracting the moisture sensor reading at 165 mm (6.5 in) below the slab surface (Sensor 1) from the sensor reading at 38 mm (1.5 in) below the slab surface (Sensor 4).

The variations in temperature and moisture differences with time are plotted in Figure 6-3. In general, temperature differences are positive during daytime and early night time and negative during late night time and early morning. In contrast, moisture differences presented as "RH Diff" in Figure 6-3 show the reverse trend. Especially during day 0 and day 1 of paving, moisture differences are negative for most part, i.e., higher moisture at the bottom of the slab compared to the top. This indicates higher drying shrinkage of concrete near the top of the slab causing the slab corner to warp upward during the day 0 and day 1 of paving.
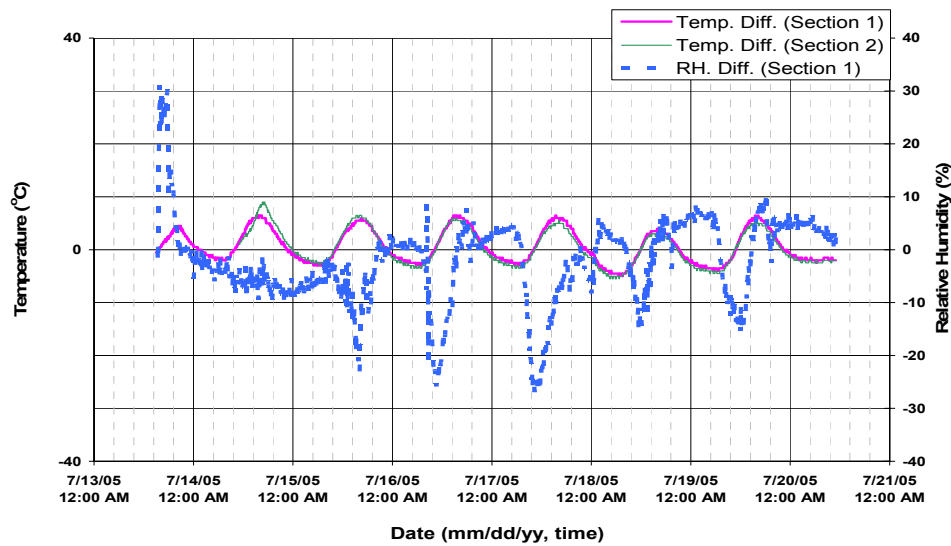
Figure 6-3 Temperature and moisture differences between top and bottom of JPCP slab with time

6.5 Profile Data Analysis

The raw data measured with Rollingprofiler[®] indicated the differences in elevation between the supports along the line being profiled (ICC., 2006). Even though the raw data itself can give some indication of the pavement roughness based on the measured elevation differences on the pavement surface, it is necessary to transform these data to a roughness index such as IRI or RN. The Pavement Profile Viewing and Analysis (ProVAL) software (version 2.5) was used to compute IRI and RN from the measured raw data. This software is a product of Federal Highway Administration (FHWA) research efforts and it allows the user to view and analyze pavement profile in many different ways (FHWA, 2004; Proval, 2006).

Figure 6-4 shows the variation in IRI and temperature differences of two test sections during the days on which profile measurements were conducted. Since RN ranges from 5 (perfectly smooth) to 0 (the maximum possible roughness), the variations

in RN values are separately presented in Figure 6-5. The temperature differences varied from -6.5 $^{\circ}$C (-11.8 $^{\circ}$F) to 8.5 $^{\circ}$C (15.3 $^{\circ}$F) during the experimental periods.

Test section 2 paved in the morning shows higher smoothness values compared to test section 1 paved in the afternoon. The differences in IRI and RN between the two sections are nearly 528 mm/km (33.5 in/mile) and 0.4, respectively. In addition, there are variations with respect to measurement locations in test sections 1 and 2. The maximum differences in IRI and RN values considering different measurement locations are 466 mm/km (29.6 in/mile) and 0.7 for test section 1, and 432 mm/km (27.4 in/mile) and 0.5 in test section 2. However, the measured IRI and RN in both the test sections were not considerably influenced by variations in temperature differences as seen in Figures 6-4 and 6-5. These observations strongly suggest that the slab deflection caused by temperature variations in these test sections did not influence the pavement smoothness. This is in agreement with the results reported by previous research studies (Perera et al., 2005)
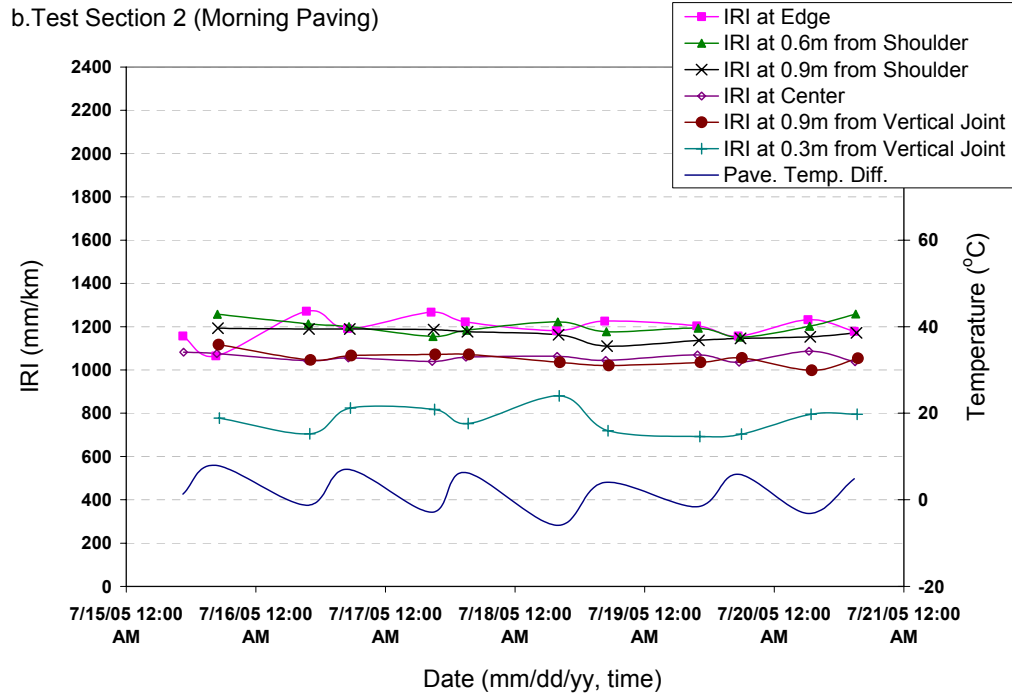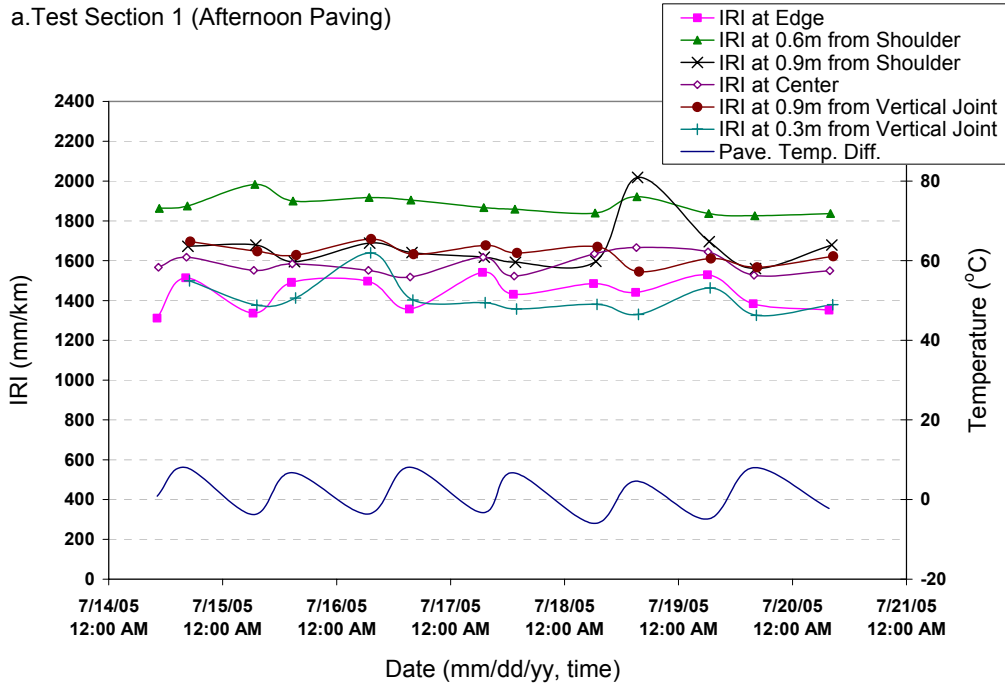
Figure 6-4 Variations in IRI during first seven days after paving: (a) Test section 1, (b) Test section 2
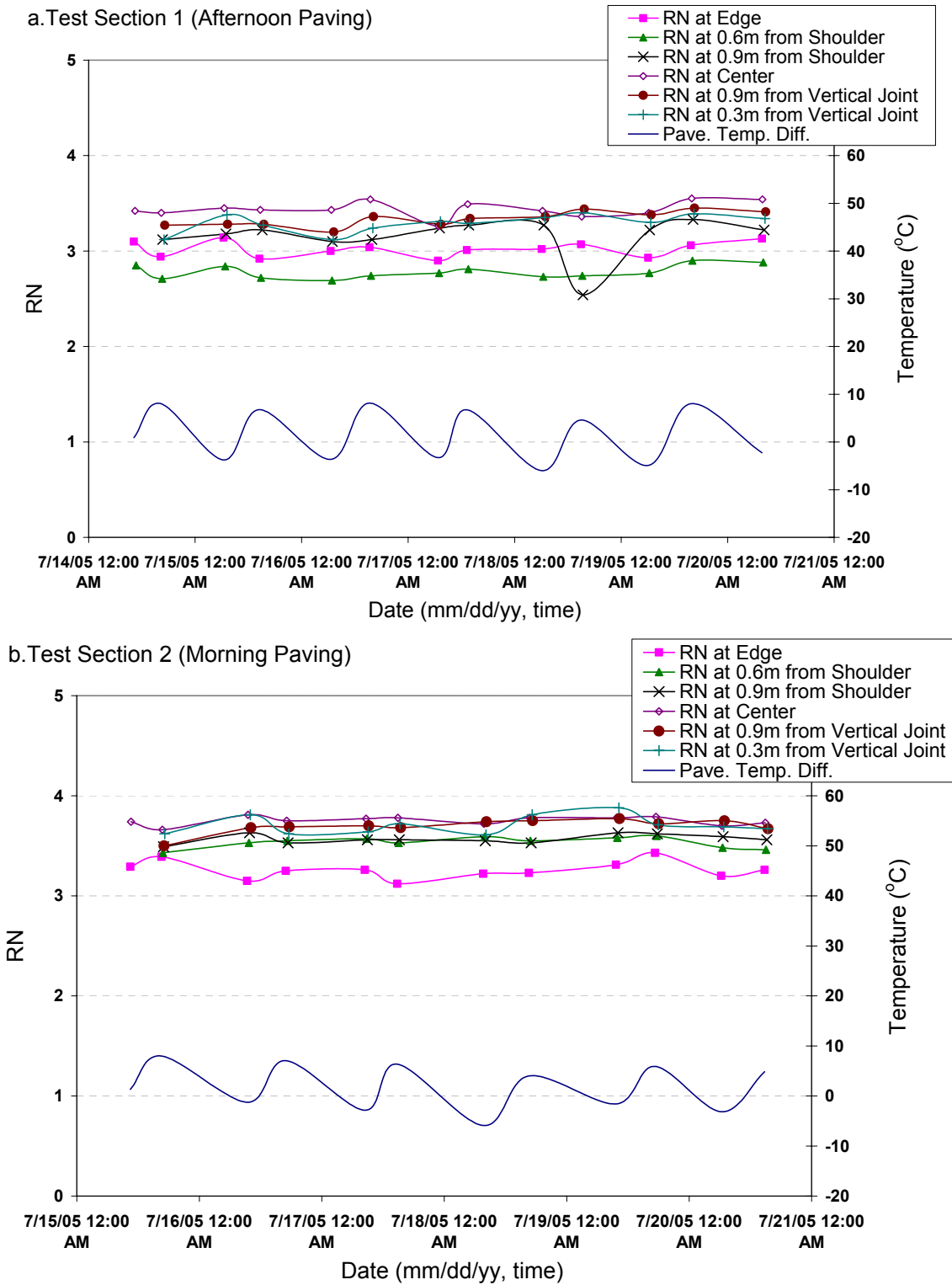
Figure 6-5 Variations in Ride Number during first seven days after paving: (a) Test section 1, (b) Test section 2

6.6 FE Simulation for Deflection Response to Environmental Loads

Even though the field-measured IRI and RN did not seem to have much influence on the slab deformation due to environmental loads, still it cannot be concluded that the slab curvature has no influence on the initial smoothness because the range of measured temperature differences is quite narrow. Finite Element (FE) models using ISLAB 2000 (two-dimensional FEM model) and Ever FE 2.24 (three-dimensional FEM model) were built for modeling the test sections in this study to investigate the effect of environmental loading on smoothness. The models were built with the actual geometric proportions and material properties from the test sections. Even though the slab temperature profiles with depth have long been characterized as non-linear distributions, the observed temperature profile in this study showed nearly a linear temperature distribution. Additionally, it has been reported that the non-linear component of the slab temperature distribution doesn't influence the deflections very much (Yu et al. 2004). Therefore, a linear temperature distribution was used in the FE modeling to investigate slab deflections in this study. Although this assumption is not strictly valid, it makes the design conservative and simple (Silfwerbrand et al., 2004).

Preliminary analyses of the pavement systems using the ISLAB 2000 and Ever FE 2.24 software with appropriate material properties inputs and nonlinear temperature distributions indicated that the FEM results could not generate the effect of permanent upward curling and warping measured in the field, i.e., the field-measured slab shape at maximum positive temperature difference in seven days was almost flat while the FEM-

generated slab shape showed downward curling at the same temperature difference. This may be because of the permanent curling and warping at zero temperature difference due to differential irrecoverable shrinkage or a positive temperature difference during setting of the concrete (Beckemeyer et al., 2002; Rao et al., 2001; Rao et al., 2005; Yu et al., 1998; Yu et al., 2004). When the pavement temperature difference reaches some amount of positive value after the hardening of concrete, this permanent curling and warping are removed so that the slab tends to flatten. Thus, the permanent curling and warping could be considered as the deformation associated with the negative value of a positive temperature difference making slab flat. This is defined in the MEPDG (NCHRP, 2004) as the effective permanent curling and warping temperature difference (Yu et al., 2004).

In this study, a maximum positive temperature difference of 8.5 ^{o}C (15.3 ^{o}F) during evaluation periods was assumed for maintaining a flat-slab condition (for a 267-mm (10.5-in) thick slab) since the measured slab curvature profiles show upward curl at negative temperature differences and maintain almost a flat shape at positive temperature differences. This temperature difference is similar in magnitude to those reported by other researchers in the past. Armaghani et al. (1986) reported a value of 5 ^{o}C (9 ^{o}F) for a 229-mm (9-in.) thick slab in Florida. Beckemeyer et al. (2002) observed positive temperature difference magnitudes of 8.8 ^{o}C (16 ^{o}F) and 6.7 ^{o}C (12 ^{o}F) for a 330-mm (13-in.) thick slab on an open-graded granular base and an asphalt-treated permeable base, respectively, in Pennsylvania. In addition, the MEPDG (NCHRP, 2004) specifies -5.6 ^{o}C (-10 ^{o}F) as the effective permanent curling and warping temperature difference producing permanent curling and warping at zero temperature difference without considering slab thickness. In this study, the equivalent temperature difference,

associated with the actual pavement behavior, was defined as the sum of the measured temperature difference and the effective permanent curling and warping temperature difference.

Comparisons between the field-measured slab curvature profiles and the FE-computed slab curvature profiles were undertaken. The measured slab curvature profiles following diagonal and transverse traces were obtained from four individual slabs in each test section (see Figure 6-1 for slab locations). The predicted slab curvature profiles at the equivalent (positive and negative) temperature differences at which pavement profiles were measured were computed by the FE programs. The FE-generated profiles used in making comparisons were zeroed to the center elevation along each direction because the measured slab curvature profiles were normalized at the center in each measured direction to remove the construction slope and surface irregularity components.

A total of forty-four field profiling measurements and the corresponding FE-predicted profiles were obtained during the field evaluation periods. The measured and predicted slab curvature profiles along the diagonal direction at the equivalent temperature difference three days after paving are compared in Figures 6-6 and 6-7 for the sake of illustration. In general, the comparisons showed that the FE-predicted slab curvature profiles are in good agreement with the measured slab deflection profiles. Although not elaborated here, the upward curling of the slab at negative temperature difference as shown in Figure 6-6 could provide the critical condition for early age cracking because the tensile stress at the top due to upward curling and slab weight is greater than incompletely developed concrete strength (Lim et al., 2005; Nam et al., 2006).
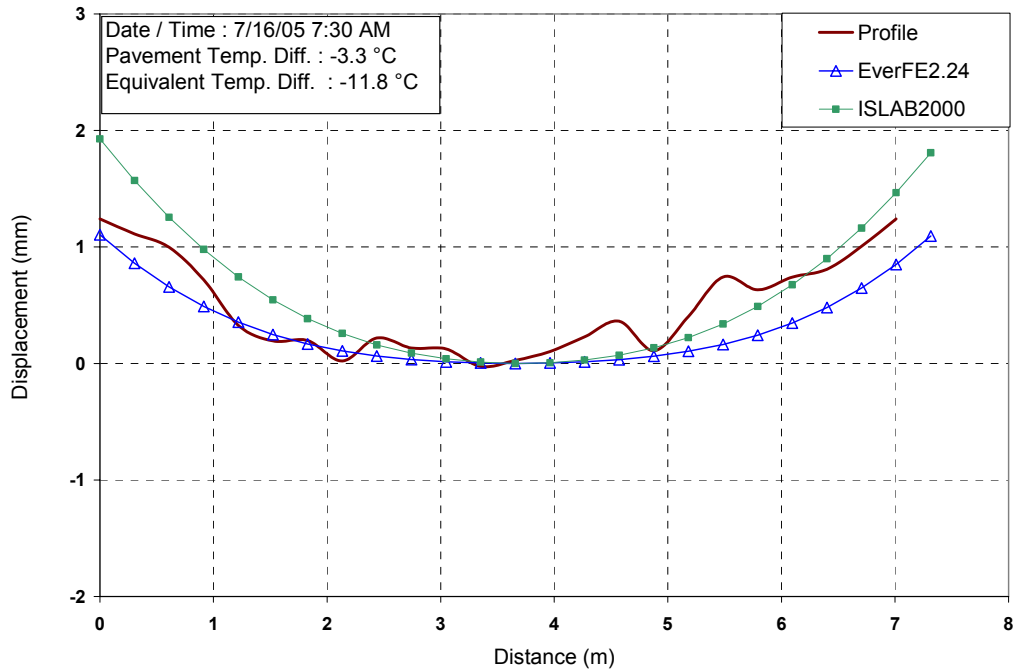
Figure 6-6 Comparison between measured and FEM-predicted slab curvature profiles at a negative temperature difference three days after paving
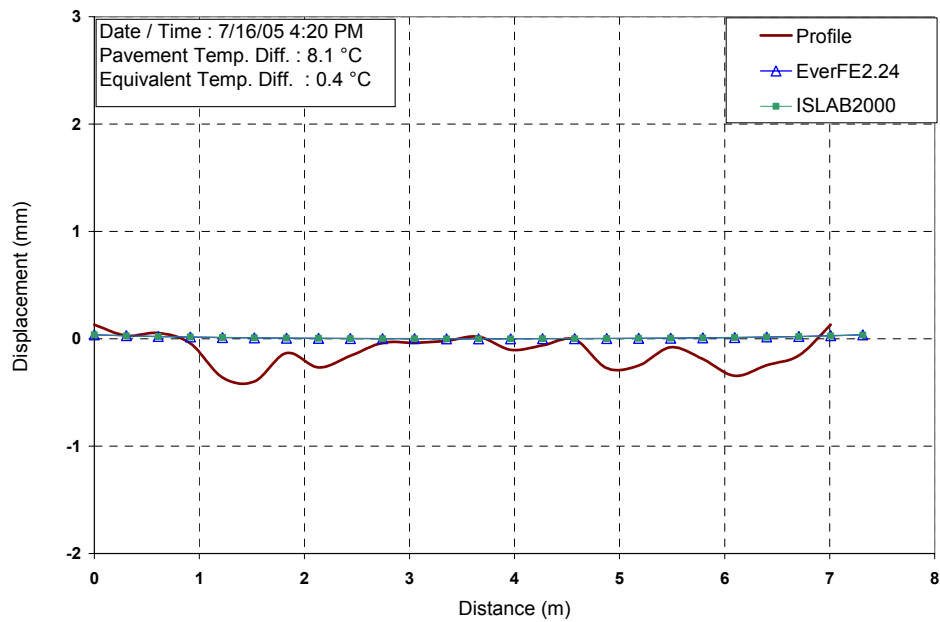
Figure 6-7 Comparison between measured and FEM-predicted slab curvature profiles at a positive temperature difference three days after paving

6.7 Sensitivity Analysis of Smoothness Index for Equivalent Temperature Variation Using FEM

Using the FEM models, sensitivity analyses of IRI and RN values were conducted at different equivalent temperature differences in each measured location. This approach has been previously used by Siddique et al. (2005). Since the JPCP is a combination of several slabs, the same slab deflection profile could be repeated in each slab to form a continuous deflection profile provided all of material properties, geometry, and applied environmental loading of these slabs are same (Siddique et al., 2005). Figure 6-8 displays such continuous slab deflection profiles for the test sections resulting from different equivalent temperature differences.
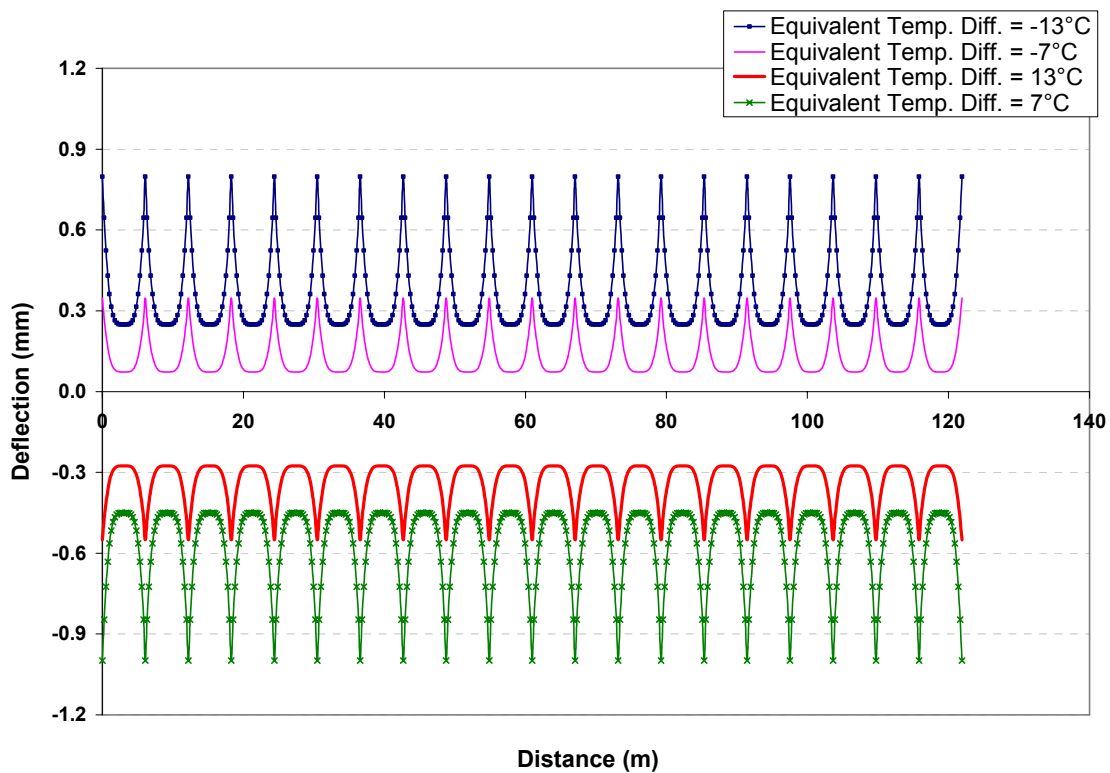
Figure 6-8 Deflection profile for 20 continuous slabs

The IRI and RN values were calculated from these continuous deflection profiles generated by EverFE2.24 and ISLAB 2000 at different equivalent temperature differences. The IRI and RN values were calculated for each measured location, respectively, and were found to be very similar. Therefore, the average IRI and average RN values for all measured locations are displayed in Figures 6-9 and 6-10.

Since the FE-generated slab deflection profiles were influenced by only the equivalent temperature differences, the computed IRI and RN values will reflect the effect of environmental loading. The computed IRI values increased with respect to changes in equivalent temperature differences while the calculated RN values decreased. The IRI values obtained using EverFE2.24 were similar for both positive and negative equivalent temperature differences. Using ISLAB 2000, the IRI values associated with the negative equivalent temperature differences were higher than those obtained at the positive equivalent temperature differences. The maximum IRI values associated with the maximum equivalent temperature differences (-13 ^{o}C and 13 ^{o}C) were 216 mm/km for EverFE 2.24. Using ISLAB 2000, the IRI was 334 mm/km for the maximum positive equivalent temperature difference condition (13 ^{o}C) and 448 mm/km for the maximum negative temperature difference condition (-13 ^{o}C). The RN values varied with a narrow range of 4.6 to 5.0 for the range of equivalent temperature differences considered in this study.

The IRI and RN values were calculated from these continuous deflection profiles generated by EverFE2.24 and ISLAB 2000 at different equivalent temperature differences. The IRI and RN values were calculated for each measured location,

respectively, and were found to be very similar. Therefore, the average IRI and average

RN values for all measured locations are displayed in Figures 6-9 and 6-10.
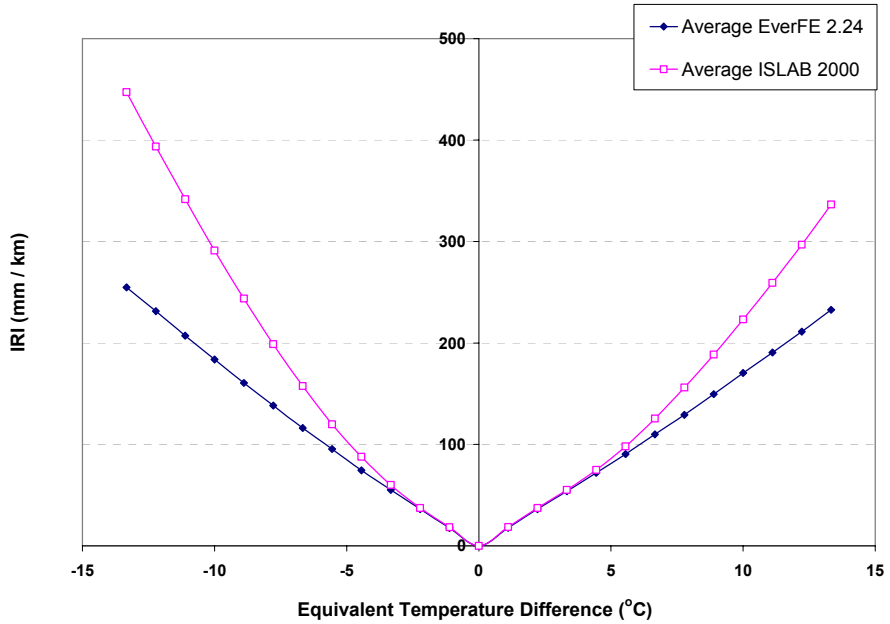
Figure 6-9 FEM-predicted IRI versus equivalent temperature difference
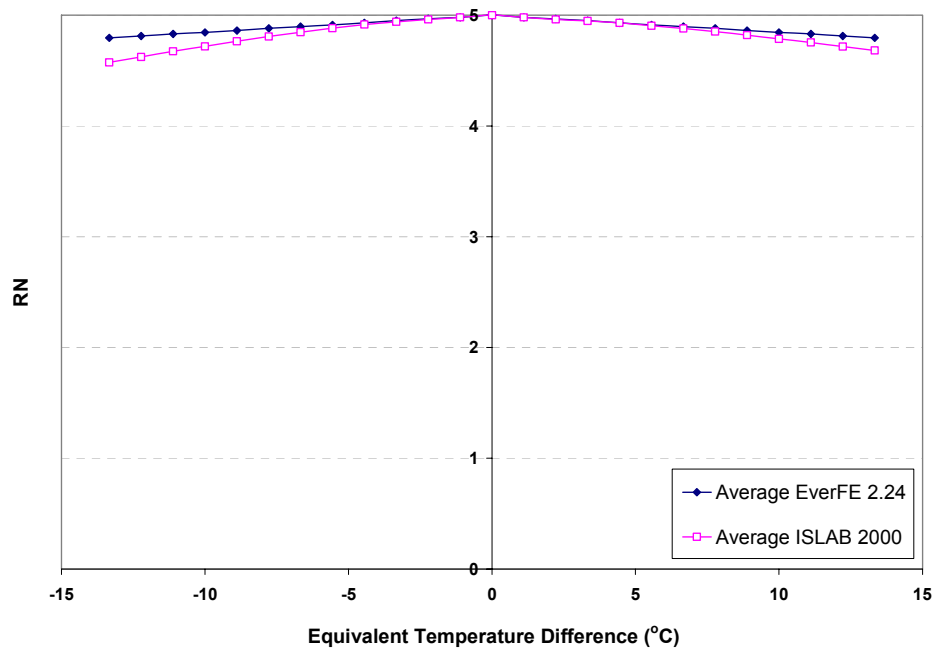
Figure 6-10 FEM-predicted RN versus equivalent temperature difference

Although it can be observed that the deflection resulting from environmental loading can influence the JPCP smoothness in terms of IRI and RN in limited equivalent temperature difference ranges, it is necessary to compare these results with the smoothness specification of new concrete pavements used by state highway agencies to investigate if this smoothness variation is significant. Unfortunately, most state highway agencies in the USA use PI as initial smoothness specification; the IRI specification for new concrete pavements used by some states can be found in the literature (Smith et al., 2002). According to typical IRI specifications, the difference in IRI value from the bonus range to correction range is approximately 631 mm/km.

6.8 Comparison of Measured Smoothness Index and FEM Predicted Smoothness Index

The field measured smoothness index included all of surface behavior such as surface irregularities, constructed slopes and slab deflections while the FEM predicted smoothness index included only slab deformation due to environmental loading. In this study, the change in smoothness index value between positive temperature difference and negative temperature difference was selected for making comparisons. Because the profile measurements were made during diurnal cycles for the same location, the change in field-measured IRI values between the positive and negative temperature conditions could only be influenced by slab deflection due to environmental loading.

As mentioned previously, it is also necessary to consider the permanent curling and warping slab behavior in the field resulting from the construction conditions and irrecoverable shrinkage. Thus, the measured IRI value at a certain temperature difference

should correspond to the FEM-predicted IRI value at an equivalent temperature difference. Note that the equivalent temperature difference was defined as the sum of the measured temperature difference and the effective permanent curling and warping temperature difference. The FEM predicted IRI values and RN values can be obtained from Figures 6-9 and 6-10, respectively, for each measured location. The results are compared and summarized in Tables 6-1 and 6-2.

From Tables 6-1 and 6-2, the differences in IRI and RN values predicted by both the FEM programs are higher than the field-measured values. The differences between the field-measured values and FE-predicted values may be due to a number of reasons. The assumptions used in FE model for simplifying actual field condition could be ascribed to this difference. Apart from the environmental loading, the field measurements are also influenced by interactions of environmental loading such as the moisture variation and creep behavior to temperature loading. Although the FEM-predicted IRI was calibrated to reflect the effect of the permanent built-in curling and warping, it cannot include all the effects resulting from the moisture variation and creep behavior. The moisture variation due to daily weather variation and the creep behavior of slab can lead to recovery of slab deformation resulting from temperature loading thus reducing the difference in IRI between positive and negative temperature conditions. In addition, poor construction practices will lead to having a rough pavement surface and thus having a high IRI and RN and this factor not considered during the finite element modeling of the slabs. The movement of the pavement foundation (any differential heave and differential settlement of the pavement subgrade) is also something that was not included in the FE modeling of the rigid pavement systems analyzed in this study.

However, in a study conducted by Smith et al. (2002), which established the equivalent IRI value corresponding to PI based smoothness specifications, it was shown that the standard error of the equivalent IRI values ranged from 264 mm/km to 316 mm/km considering the PI based specifications used by different agencies. Thus, in the context of findings reported by Smith et al. (2002), the differences between FEM-predicted and measured IRI values in this study are not significant. In the future, statistical analyses using paired t-tests, etc. will be conducted to quantify the actual differences between the field-measured and FEM-predicted values.

Table 6-1 Comparison between measured and FEM-predicted IRI values for different temperature conditions

Test Sect.	Location	Neg. Temp. Diff. Condition			Pos. Temp. Diff. Condition			Comparison		
		Pave. Temp. Diff.	Equiv alent Temp. Diff.	Measu red IRI	Pave. Temp. Diff.	Equiv alent Temp. Diff.	Measu red IRI	Measu red IRI diff.	Predicte d IRI diff. with EverFE	Predicte d IRI diff. with ISLAB
		(^{o}C)	(^{o}C)	(mm/ km)	(^{o}C)	(^{o}C)	(mm/ km)	(mm/ km)	(mm/ km)	(mm/ km)
1	Edge	-3.4	-11.9	1435.9	7.0	-1.5	1435.9	0.0	160.7	365.9
	0.6m from shoulder	-3.3	-11.8	1877.4	6.9	-1.6	1880.5	3.2	164.7	355.0
	0.9m from shoulder	-3.9	-12.4	1659.2	7.1	-1.4	1679.7	20.5	181.7	381.5
	Center	-3.2	-11.7	1585.9	7.0	-1.5	1572.4	13.5	171.0	329.6
	3ft from vertical joint	-3.8	-12.3	1655.7	7.1	-1.4	1617.9	37.9	197.8	423.4
	1ft from vertical joint	-4.0	-12.5	1437.5	7.1	-1.4	1387.5	50.0	181.0	387.3
2	Edge	-2.5	-11.0	1218.7	6.1	-2.4	1173.2	45.5	132.9	308.3
	0.6m from shoulder	-3.0	-11.5	1197.1	6.1	-2.4	1204.8	7.7	145.1	324.4
	0.9m from shoulder	-2.9	-11.4	1165.9	6.0	-2.5	1164.6	1.3	135.1	285.2
	Center	-2.6	-11.1	1064.1	6.0	-2.5	1051.2	12.9	143.0	280.7
	0.9m from vertical joint	-2.6	-11.1	1037.1	6.0	-2.5	1064.1	27.0	122.1	242.6
	0.3m from vertical joint	-2.6	-11.1	778.1	6.0	-2.5	762.0	16.1	121.0	248.5

Table 6-2 Comparison between measured and FEM-predicted RN values for different temperature conditions

Test Sect.	Location	Neg. Temp. Diff. Condition			Pos. Temp. Diff. Condition			Comparison		
		Pave. Temp. Diff.	Equivalent Temp. Diff.	Measured RN	Pave. Temp. Diff.	Equivalent Temp. Diff.	Measured RN	Measured RN Diff.	Predicted RN Diff. with EverFe	Predicted RN Diff. with ISLAB
		(°C)	(°C)		(°C)	(°C)				
1	Edge	-3.4	-11.9	3.031	7.0	-1.5	3.007	0.025	0.151	0.352
	0.6m from shoulder	-3.3	-11.8	2.790	6.9	-1.6	2.770	0.020	0.158	0.332
	0.9m from shoulder	-3.9	-12.4	3.205	7.1	-1.4	3.100	0.105	0.169	0.365
	Center	-3.2	-11.7	3.430	7.0	-1.5	3.462	0.032	0.166	0.311
	3ft from vertical joint	-3.8	-12.3	3.318	7.1	-1.4	3.357	0.038	0.187	0.400
	1ft from vertical joint	-4.0	-12.5	3.300	7.1	-1.4	3.285	0.015	0.173	0.368
2	Edge	-2.5	-11.0	3.238	6.1	-2.4	3.280	0.042	0.126	0.301
	0.6m from shoulder	-3.0	-11.5	3.550	6.1	-2.4	3.520	0.030	0.143	0.302
	0.9m from shoulder	-2.9	-11.4	3.592	6.0	-2.5	3.548	0.044	0.125	0.272
	Center	-2.6	-11.1	3.753	6.0	-2.5	3.748	0.005	0.152	0.263
	0.9m from vertical joint	-2.6	-11.1	3.728	6.0	-2.5	3.668	0.060	0.117	0.234
	0.3m from vertical joint	-2.6	-11.1	3.726	6.0	-2.5	3.692	0.034	0.114	0.234

6.9 Conclusions

This study investigated the effect of slab curvature due to environmental loading on the concrete pavement initial smoothness. In this study, surface profile measurements were conducted during the early morning and late afternoon hours on 267-mm (10.5-in) thick JPCP on US-30 near Marshalltown, Iowa during first seven days after construction in the summer of 2005. Temperature and humidity variations for the pavement sections were monitored at the same times. The differences in initial pavement smoothness index, in terms of IRI and RN between different measurement times, were studied considering limited temperature difference conditions. A wider range of temperature differences was

used in conducting sensitivity analysis to study its effect on smoothness using FEM technique. Two different FE programs were used to generate slab curvature profiles and subsequently compute the IRI values. The field-measured IRI values were compared with the FEM-predicted IRI values. Based on the results of this study, the following observations were drawn:

- The measured IRI and RN values were different at different measurement locations within a test section.

- The measured IRI and RN were not considerably influenced by the limited range of temperature differences considered in this study.

- The IRI and RN differences (between the positive and negative temperature conditions) predicted by both the 2-D and 3-D FEM programs overestimate the field-measured counterparts. However, the difference between the FEM predicted IRI and measured IRI may not be significant considering the range of specifications used by different transportation agencies.

6.10 Acknowledgments

6.11 References

Akhter, M., Hussain, M., Boyer, J., and Parcells, W. J., 2002, "Factors Affecting Rapid Roughness Progression on Portland Cement Concrete Pavements in Kansas," *Transportation Research Record*, Vol. 1809, Transportation Research Board, Washington, D.C., pp 74-84.

Armaghani, J. M., Lybas, J. M., Tia, M., and Ruth, B. E., 1986, "Concrete Pavement Joint Stiffness Evaluation," *Transportation Research Record*, Vol.1099, Transportation Research Board, Washington, D.C., pp. 22-36.

Beckemeyer, C. A., Khazanovich, L., and Yu, H. T., 2002, "Determining Amount of Built-in Curling in Jointed Plain Concrete Pavement: Case Study of Pennsylvania I-80," *Transportation Research Record*, Vol. 1809, Transportation Research Board, Washington, D.C., pp. 85-92.

Bradbury, R. D., 1938, *Reinforced Concrete Pavements*, Wire Reinforcement Institute, Washington, D.C.

Byrum, C.R., 2000, *A High Speed Profile Based Slab Curvature Index for Jointed Concrete Pavement Curling and Warping Analysis*, Ph.D. Thesis, University of Michigan, Ann Arbor, Michigan.

Chou, S. F. and Pellinen, T. K., 2005, "Assessment of Constriction Smoothness Specification Pay Factor Limits Using Artificial Neural Network Modeling," *Journal of Transportation Engineering*, Vol. 131, No.7, American Society of Civil Engineering, pp.563-570.

.

Federal Highway Administration (FHWA), 2004, *Introducing Proval 2.0*, Product Brief, FHWA Publication No. FHWA-HRT-04-154, Federal Highway Administration Washington, D.C., pp1-2.

Hajek, J, J., Kazmierowski, T. J. and Musgrove, G., 1998, "Switching to International Roughness Index," *Transportation Research Record*, Vol. 1643, Transportation Research Board, Washington, D.C., pp. 116-124.

Hveem, F. N., 1951, "Slap Warping affects Pavement Joint Performance," *Proceedings of American Concrete Institute*, Vol. 47, pp. 797-808.

International Cybernetics Corporation (ICC.), 2006, http://www. internationalcybernetics.com/ rollprofile.htm, accessed May, 2006.

Janoff, M. S., 1985, *Pavement Roughness and Reliability*, National Cooperative Highway Research Program Report 275, Transportation Research Board, Washington, D.C.

Janoff, M. S., 1990, "The Prediction of Pavement Ride Quality from Profile Measurements of Pavement Roughness," *Surface Characteristic of Roadways: International Research Technologies*, ASTM STP 1031, American Society of Testing and Materials, Philadelphia, Pennsylvania, pp.259-267.

Karamihas, S. M., Gillespie, T. D., Perera, R. W., and Kohn, S. D., 1999, *Guidelines for Longitudinal Pavement Profile Measurement*, National Cooperative Highway Research Program Report 434, Transportation Research Board, Washington. D.C.

Karamihas, S. M., Perera, R. W., Gillespie, T. D., and Kohn, S.D., 2001,"Diurnal Changes in Profile of Eleven Jointed PCC Pavement," *Proceedings of 7th International Conference on Concrete Pavements*, Orlando, Florida.

Korovesis, G. T., 1990, *Analysis of SLAB on Grade Pavement Systems Subjected to Wheel and Temperature Loadings*, Ph.D. Thesis, University of Illinois, Urbana Champaign, Illinois.

Ksaibati, K., Staigle, R. and Adkins, T. M., 1995, "Pavement Construction Smoothness Specification in the United States," *Transportation Research Record*, Vol.1491, Transportation Research Board, Washington, D.C., pp.27-32.

Lim, S. W. and Tayabji, S. D., 2005, "Analytical Technique to Mitigate Early-Age Longitudinal Cracking in Jointed Concrete Pavements," *Proceedings of 8th International Conference on Concrete Pavements*, Colorado Springs, Colorado.

Ma, S. and Caprez, M., 1995, " The Pavement Roughness Requirement for WIM," *First European Conference on Weight –in –motion of Road Vehicle*, Switzerland.

National Cooperative Highway Research Program (NCHRP), 2004, *Guide for Mechanistic- Empirical Design of New and Rehabilitated Pavement Structures – Final Report*, http://www.trb.org/mepdg, National Cooperative Highway Research Program 1-37 A, Transportation Research Board, National Research Council, 2004.

Nam, J. H., Kim, S. M., and Won, M. C., 2006, "Measurement and Analysis of Early-Age Concrete Strains and Stresses in Continuously Reinforced Concrete Pavement Under Environmental Loading," *CD-ROM Proceedings of the 85th Annual Meeting of the Transportation Research Board*, Washington, D.C.

Perera. R. W and Kohn. S. D., 2002, *Issues in Pavement Smoothness*, National Cooperative Highway Research Program Web Document No. 42, Transportation Research Board, Washington, D.C.

Perera, R. W., Kohn, S. D. and Tayabji, S. D., 2005, *Achieving a High level of Smoothness in Concrete Pavement without Sacrificing Long-Term Performance*, Tech Brief, Federal Highway Administration Publication No. FHWA-HRT-05-068, Federal Highway Administration, Washington, D.C., pp1-4.

Proval. The Transtec Group, Inc., 2006, http://www.roadprofile.com, accessed January, 2006

Rasmussen, R. O., Karamihas, S. K. and Chang, C. K., 2002, *Inertial Profile Data for Pavement Performance Analysis : Project Overview*, Tech Brief Number 1, Federal Highway Administration Contact DTFH 61-02-C-00077, Washington, D.C.

Rasmussen, R. O., Karamihas, S. K., Cape, W. R., Chang, C. K. and Guntert, R. M., 2004, "Stringline Effects on Concrete Pavement Construction," *Transportation Research Record*, Vol. 1900, Transportation Research Board, Washington, D.C., pp 3-11.

Rao, C., Barenberg, E. J., Snyder, M. B., and Schmidt, S., 2001, "Effects of Temperature and Moisture on the Response of Jointed Concrete Pavements," *Proceedings of 7th International Conference on Concrete Pavements*, Orlando, Florida.

Rao, S. and Roesler, J. R., 2005, "Characterizing Effective Built in Curling from Concrete pavement Field Measurements," *Journal of Transportation Engineering*, Vol. 131, No. 4, American Society of Civil Engineering, pp.320-327.

Rawool, S. and Fernando, E., 2005, "Methodology of Detection of Defect Locations in Pavement Profile," *CD-ROM Proceedings of the 84th Annual Meeting of the Transportation Research Board*, Washington, D.C.

Sayers, M. W., 1995, "On the Calculation of International Roughness Index from Longitudinal Road Profile," *Transportation Research Record*, Vol. 1501, Transportation Research Board, Washington, D.C., pp. 1-18.

Sayers, M. W. and Karamihas, S. M., 1998, *The Little Book of Profiling*. University of Michigan, Ann Arbor, Michigan.

Smith, K. L., Smith, K. D. Evans, L. D., Hoerner, T. E., Darter, M. I., and Woodstrom, J. H., 1997, *Smoothness Specifications for Pavements*. National Cooperative Highway Research Program Web. Document No. 1, Transportation Research Board, Washington, D.C.

Siddique, Z. and Hossain. M.,2005, "Finite Element Analysis of PCCP Curling and Roughness," *Proceedings of 8th International Conference on Concrete Pavements*, Colorado Springs, Colorado, 2005.

Silfwerbrand. J and Soderqvist. J., 2004, "Curling and Warping of New-Cast Concrete Pavements – A Theoretical Discussion," *Proceedings of the 5th International Crow – Workshop on Fundamental Modeling of Design and Performance of Concrete Pavements*, Istanbul, Turkey.

Sixbey, D., Swanlund, M., Gagarin, N. and Mekemson, J. R., 2001, "Measurement and Analysis of Slab Curvature in JPC Pavements Using Profiling Technology," *Proceedings of 7th International Conference on Concrete Pavements*, Orlando, Florida.

Smith, K. L., and Clover, L. T., Evans, L. D., 2002, *Pavement Smoothness Index Relationships*, Technical Report FHWA- RD- 02-057, Federal Highway Administration, U.S. Department of Transportation.

Thomlinson, J., 1940a. Temperature Variations and Consequent Stresses Produced by

Daily and Seasonal Temperature Cycle in Concrete Slabs. Concrete and

Constructional Engineering, Vol.36, No.6, pp.298-307.

Thomlinson, J. 1940b. Temperature Variations and Consequent Stresses Produced by

Daily and Seasonal Temperature Cycle in Concrete Slabs, Concrete and

Constructional Engineering, Vol.36, No.7, pp. 352-360.

Vandenbossche, J. M., 2003, *Interpreting Falling Weight Deflectometer Results for

Curled and Warped Portland Cement Concrete Pavements*, Ph.D. Thesis,

University of Minnesota, Minneapolis, Minnesota.

Westergaard, H. M., 1926, "Analysis of Stresses in Concrete Pavements Due to

Variations of Temperature," *Proceedings of Highway Research Board*, Vol. 6,

National Research Council, Washington, D.C., pp.201-217.

Westergaard, H. M., 1927, "Theory of Concrete Pavement Design," *Proceedings of

Highway Research Board*, Part I, pp. 175-181.

Yoder, E. J. and Witczack, M. W., 1975, *Principle of Pavement Design*, 2nd edition,

Wiley, New York.

Yu, H. T., Khazanovich, L. Darter, M. I, and Ardani, A., 1998, "Analysis of Concrete

Pavement Response to Temperature and Wheel Loads Measured from

Instrumented Slab," *Transportation Research Record*, Vol. 1639, Transportation

Research Board, Washington, D.C., pp.94-101.

Yu, H. T., Khazanovich, L., and Darter, M. I., 2004, "Consideration of JPCP Curling and

Warping in the 2002 Design Guide," *CD-ROM Proceedings of the 83rd Annual

Meeting of the Transportation Research Board*, Washington, D. C.

CHAPTER 7. EVALUATION OF FINITE ELEMENT MODELS FOR STUDYING EARLY-AGE DEFORMATION OF JOINTED PLAIN CONCRETE PAVEMENTS UNDER ENVIRONMENTAL LODING

A paper to be submitted to *The International Journal of Pavement Engineering*

Sunghwan Kim,[1] Halil Ceylan,[2] Kasthurirangan Gopalakrishnan,[3] and Kejin Wang[4]

7.1 Abstract

In this study, the use of Finite Element (FE) based primary response model is investigated for the early-age deformation characteristics of Jointed Plain Concrete Pavements (JPCP) under environmental loading. The FE-based ISLAB 2000 (two-dimensional) and EverFE 2.24 (three-dimensional) softwares were used for this study. Analytical solutions by Westergaard and numerical models used in both FE programs for the computation of slab deflection under pure environmental loading are briefly reviewed and discussed. Sensitivity analyses of input parameters used in ISLAB 2000 and EverFE 2.24 were conducted based on field and laboratory test data collected from instrumented pavements on US-34 near Burlington, Iowa. Based on input parameter combination and equivalent temperature established from the preliminary studies, FE analyses were performed and compared with the field measurements.

1Graduate Research Assistant, Iowa State University, Ames, IA

2 Assistant Professor, Iowa State University, Ames, IA

3 Post-Doctoral Research Associate, Iowa State University, Ames, IA

4 Associate Professor, Iowa State University, Ames, IA

FE-based sensitivity analyses indicated that temperature difference between top and bottom of slab and Coefficient of Thermal Expansion (CTE) were the most sensitive parameters to computed slab deformations for typical JPCP cross-sections used in Iowa. Sensitivity analyses also showed that the estimated deflection resulting from temperature differences using ISLAB 2000 is 26 % and 38 % higher for positive and negative temperature differences respectively, compared to EverFE 2.24. Comparisons between field measured and computed deformations showed that both FE programs using the equivalent temperature difference concept could statistically estimate the actual slab deformation due to environmental effects well.

7.2 Introduction

Studies on deformation characteristics of early-age JPCP subjected to pure environmental loading has drawn significant interest (Siddique and Hossain, 2005; Rao, et al., 2001) as it is believed that the early-age deformation of Portland Cement Concrete (PCC) slab could result in the loss of pavement smoothness (Siddique and Hossain, 2005) and the tensile stresses induced by these deformations could result in early-age cracking (Lim and Tayabji, 2005). However, the complex nature of the problem arising from interactions of multiple environmental factors has resulted in difficulties in predicting the JPCP deformation characteristics under environmental loading.

In the recent Mechanistic-Empirical Pavement Design Guide (MEPDG) developed under the National Cooperative Highway Research Program (NCHRP) 1-37A project, FE-based structural analysis models using a neural networks approach were employed for rigid pavement analysis and design. The application of FE modeling

techniques has significantly increased over the past decade in understanding and characterizing rigid pavement behavior in special situations where it is difficult to conduct laboratory and field testing (Armaghani, et al., 1986; Ioannides and Salsili-Murua, 1989; Ioannides and Korovesis, 1990; Ioannides and Korovesis, 1992; Chatti et al., 1994; Hammons and Ioannides, 1997; Vepa and George, 1997; Davids, 2001; Beckemeyer et al., 2002; Rao and Roesler, 2005).

This study focuses on evaluation of two FE-based primary response models, namely ISLAB 2000 (Khazanovich et al, 2000) and EverFE 2.24(Davids, 2006), for characterizing the deformation of early-age JPCP under environmental loading. These models were primarily selected because of some special advantages over other FE programs. The ISLAB 2000 2-D FE program was used as the main structural model for generating rigid pavement responses in the new MEPDG under the NCHRP 1-37 A project (2004) and EverFE 2.24 is the only 3-D FE program among the FE programs specifically designed for modeling and analyzing rigid pavements (Davids, 2003).

Analytical solutions proposed by Westergaard (1926) and the numerical models used in both the FE programs for computing slab deflection under environmental loading are briefly reviewed. Sensitivity analyses of input parameters used in ISLAB 2000 and EverFE 2.24 were conducted based on field and laboratory test data collected from instrumented pavements on US-34 near Burlington, Iowa. Comparisons between the field measured and the FE computed slab deformations are also discussed in this paper.

7.3 Review of Rigid Pavement Displacement Models Subjected to Environmental Loading

The temperature and moisture variations across the depth of rigid pavements result in pavement displacement. In addition, a higher unrecoverable drying shrinkage of concrete near the top of the slab, a positive temperature gradient during the concrete hardening and settlement of the foundation can cause permanent displacement at zero-temperature gradient (Yu et al, 1998; Yu et al., 2004). There is also the weight of the slab contributing to the creep of the slab. Therefore, the displacement caused by each of these factors must be taken into consideration. Although analytical or numerical solutions have been proposed in the past to predict the rigid pavement responses, such as stress, strain or displacement under environmental loading without conducting laboratory or field experiment, these methods have their own limitations and have not successful in fully characterizing the environmental effects.

7.3.1 Analytical Solutions

Based on plate bending theory, Westergaard (1926) developed analytical solutions of displacement due to temperature for different slab conditions (a semi-infinite and an infinitely long strip) assuming a linear temperature differential for a concrete slab over a Winkler foundation. Since actual slab condition is finite and the other environmental effects resulting in slab displacement are not considered in these analytical solutions, it is an approximation of reality. For the case of a semi-infinite slab and the case of an infinitely long strip, the deflection along the infinite–axis is given as follows:

7.3.1.1 Semi-infinite slab condition

The semi-infinite slab condition has a semi–infinite width along the Y–axis and an infinite length along the X-axis. The deflection along the y-axis due to temperature under semi-infinite slab condition is derived as follows (Westergaard, 1926):

$$\Delta_y = -\Delta_o \sqrt{2} \cos\left(\frac{y}{l\sqrt{2}}\right) e^{-\frac{y}{l\sqrt{2}}} \qquad \text{(Equation 7-1)}$$

Where:

Δ_y = Deflection in y-axis

$$\Delta_O = \frac{(1+v)\alpha_t \Delta T}{h} l^2$$

l = Radius of relative stiffness = $\sqrt[4]{\dfrac{Eh^3}{12(1-v^2)k}}$

v = Poisson's ratio

α_t = Coefficient of thermal expansion of concrete

ΔT = Linear temperature differential through the thickness of the slab

h = Thickness of the slab

E = Modulus of elastic of concrete

k = Modulus of subgrade reaction

7.3.1.2 Infinitely long strip slab condition

The infinitely long strip slab has a finite width (4.2*l*) along Y-axis and infinite length along the X–axis. The deflection along the Y-axis due to temperature under infinitely long strip slab is derived from (Westergaard, 1926):

$$\Delta_y = -\Delta_b \left\{ \frac{2\cos\lambda_b \cosh\lambda_b}{\sin 2\lambda_b + \sinh 2\lambda_b} \left[(-\tan\lambda_b + \tanh\lambda_b)\cos\frac{y}{l\sqrt{2}}\cosh\frac{y}{l\sqrt{2}} + (\tan\lambda_b + \tanh\lambda_b)\sin\frac{y}{l\sqrt{2}}\sinh\frac{y}{l\sqrt{2}} \right] \right\} \quad \text{(Equation 7-2)}$$

Where;

$$\lambda_b = \frac{b}{l\sqrt{8}}$$

b = Slab width

7.3.2 ISLAB 2000

ISLAB 2000 is a 2-D FE program for the analysis of rigid pavements developed by ERES Division of Applied Research Association (ARA) with support from the Michigan Department of Transportation and the Minnesota Department of Transportation (Khazanovich et al, 2000). The ISLAB 2000 is the most recent version of an evolving ILLI-SLAB developed in 1977 at University of Illinois at Urbana-Champaign and the primary structural model for generating pavement responses in the new MEDPG (NCHRP, 2004). During the improvement and extension of ILLI-SLAB over the years, a curling analysis was incorporated in 1989 by Korovesis (1990).

To calculate the displacement due to temperature, thin plate element (Kirchhoff plate element) having three displacement components at each node – a vertical deflection in Z-direction, a rotation (Өx) about the X-axis, and a rotation (Өy) about the Y-axis is

used for concrete slab on Winkler foundation. The equilibrium matrix equation of element assemblage as shown in Equation 7-3 is formulated using the principle of virtual work and is used to calculate the stress, strain and displacement incorporating the element boundary condition (Korovesis, 1990). Temperature effect is considered through the load vector in Equation 7-3. The stress–strain–temperature relation shown in Equation 7-4 is used to derive this load vector due to temperature.

$$P=KU \qquad \text{(Equation 7-3)}$$

Where;

P = Load vector = $P_B+P_S-P_I+P_C$

P_B = Load vector due to element body forces

P_S = Load vectors due to element surface forces

P_I = Load vector due to element initial stresses

P_c = Concentrated Loads

K = Structure stiffness matrix

U = Displacement vector

$$\sigma = \alpha_t \Delta T E = \varepsilon E \qquad \text{(Equation 7-4)}$$

Where;

σ = Stress due to temperature

ε = Strain due to temperature = $\alpha_t \Delta T$

Since the load vector in Equation 7-3 includes the self–weight of layer and temperature distribution, the calculated displacement as shown in Figure 7-1 is more

realistic than analytical solution but still do not include the displacement due to moisture changes and the permanent displacement at zero gradient temperature.

(a)   (b)

Figure 7-1 Deformed slab shape generated from ISLAB 2000: (a) positive temperature difference condition; (b) negative temperature difference condition

7.3.3 EverFE 2.24

EverFE is a 3-D FE analysis tool for simulating the response of JPCP to traffic loads and temperature effects. The original software, EverFE 1.02, was developed at the University of Washington and has been continuously upgraded. The most recent version, EverFE2.24, was used in this study. EverFE 2.24 can easily be obtained from the public domain (Davids, 2006).

EverFE uses five elements to simulate JPCP systems; 20-noded quadratic element having three deflection components at each node are used for the slab, elastic base, and sub-base layer; 8-noded planar quadratic elements simulate the dense liquid foundation below the bottom-most elastic layer; 16-noded quadratic interface element implement both aggregate interlock joint and shear transfer at the slab-base interface; and 3-noded embedded flexural elements coupled with conventional 2-noded shear beam are used to model the dowel bar and tie bar (Davids, 2003). Similar to ISLAB 2000, the equilibrium

matrix equation of element assemblage is formulated and is used to compute the stress, strain and displacements incorporating boundary condition of element. The formulation of structural stiffness, K, is required to solve the equilibrium equation. However, 3D models of rigid pavement systems need large combination of memory and computational requirements if using the direct matrix factorization for K. To circumvent this problem, EverFE employs multi-grid methods to solve the equilibrium equation, which are the most efficient iterative techniques available (Davids et al, 1998; Davids and Turkiyyah, 1999).

Like ISLAB 2000, the temperature changes are converted to equivalent element pre-strain via the slab coefficient, and these strains are numerically integrated over the element to generate equivalent nodal forces (Davids et al, 2003). The computed displacements from EverFE 2.24 can be provided in the form of 3-D deformed shapes as shown in Figure 7-2 or in terms of numerical values depending on user's choice. Like ISLAB 200, EverFE also has limitations with respect to environmental loading analysis, i.e., it can't directly calculate the displacement due to moisture change and the permanent displacement at zero-gradient temperatures.

(a)   (b)
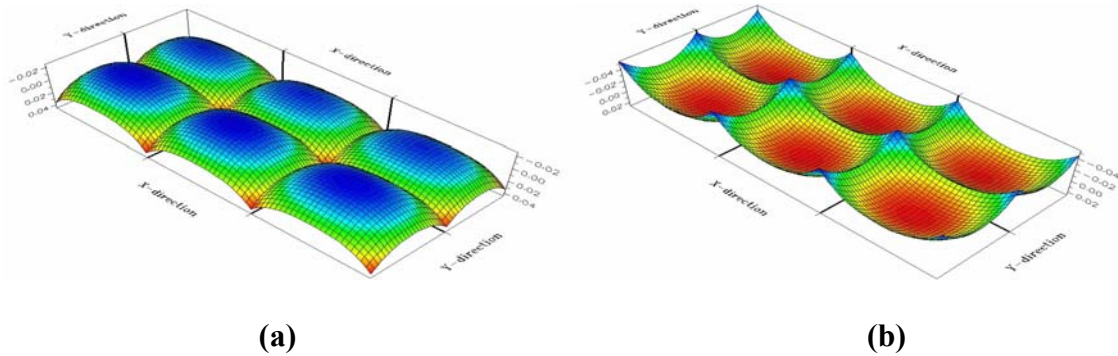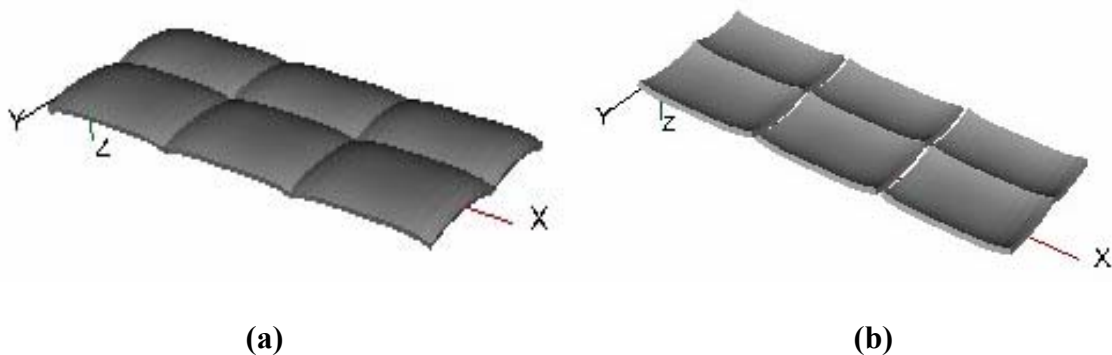
Figure 7-2 Deformed slab shape generated from EverFE 2.24:(a) positive temperature difference condition; (b) negative temperature difference condition

7.4 Sensitivity Analyses of FE- based Input Parameters to Slab Displacements under Environmental Loading

The MEPDG developed under NCHRP 1-37A employs FE-based models to compute pavement primary response for predicting rigid pavement performance. Although ISLAB 2000 and Ever FE 2.24 have their limitations in calculating slab displacements under environmental loading, it is important to evaluate these programs and establish the numerical relation between field measurements and predicted responses to improve the accuracy of prediction. To do this, it is desirable that the input parameters used in the simulations be as close as possible to the actual situation. However, it is not realistic to collect all input parameters in the field or from lab testing and then simulate the actual behavior. In such situations, sensitivity analyses could be performed to identify the critical input parameters which have the most effect on slab displacement under environmental loading. Based on the results of sensitivity analyses, a realistic combination of input parameters to simulate the actual field behavior could be established.

A total of eight key inputs related to material properties and climate were selected for sensitivity analyses using both ISLAB 2000 and EverFE 2.24. The concrete pavement was modeled as a 6–slab assembly over dense liquid foundation. Based on typical rigid pavement geometry used for highway pavements in Iowa (IDOT, 2005), each slab was modeled as shown in Table 7-1. When one input parameter was varied over the typical range of values, the value of the other input parameter assigned as standard value kept constant during the analyses. Table 7-2 summarizes the input parameters and ranges used in this study.

Table 7-1 Concrete slab geometry properties used in sensitivity analyses study

Lane	No. of Segment	Width (m) in a segment	Length (m) in a segment	Depth (mm)
Passing	3	3.7	6	267
Traveling	3	4.3	6	267

Table 7-2 Summary of input parameters

Parameter	Standard Value	Ranges of value
Unit weight (kg/m^3)	2400	2240, 2400, 2560
Poisson's ratio	0.2	0.1,0.2,0.3
Coefficient Thermal Expansion (CTE, / ^{o}C)	9.63×10^{-6}	$6.3, 9.63, 13.5, 17.1 \times 10^{-6}$
Elastic modulus (MPa)	30483	13790, 30483, 41370
Load Transfer Efficiency (LTE,%)	90	0.1, 50, 90
Modulus of subgrade reaction (k,kPa /mm)	62.4	8.1, 35.3, 62.4, 89.6
FE Mesh size (mm × mm)	254 × 178	76 × 76, 152 × 152, 254 × 178, 305 × 305
Temp difference between top and bottom of slab (^{o}C)	1. 8.5 ^{o}C – Positive temperature difference 2. -6.6 ^{o}C -Negative temperature difference	-13.3 ^{o}C to 13.3 ^{o}C with increasing 2.2 ^{o}C

Simulated results were necessary to quantify the numerical values in order to identify the difference. If the slab behavior could be characterized in terms of total amount of deflection and the slab shape, the total amount of deflection could be quantified using the relative deflection of corner to center in the measured direction (Rc) and the slab shape could be quantified by the curvature of slab profile (k). The relative deflection of corner to center (Rc) in the defined direction could easily be calculated by subtracting the elevation of center in the defined direction from that of corner in same direction. The curvature of slab profile (k) was calculated using a methodology similar to that proposed by Vandenbossche (2005). A second-order polynomial curve was fit to FE-

calculated slab deformation profile and then the curvature was calculated by using Equation 7-5 shown below:

$$k = \frac{\dfrac{d^2 y}{dx^2}}{\left[1 + \left(\dfrac{dy}{dx}\right)^2\right]^{\frac{3}{2}}}$$ (Equation 7-5)

Where;

$y = Ax^2 + Bx + C$

k = Curvature

y = Measured displacement

x = Location along the profile traverse

A, B, and C = Coefficients

Even though Rc and k could be calculated in transverse, longitudinal and diagonal direction on simulated concrete pavements, diagonal direction on middle slab of traveling lane was selected in this study. The Rc and k in simulated concrete pavement are summarized in Tables 7-3, 7- 4, 7-5, and 7- 6

Based the observation of absolute difference (ABD) of Rc and k between two adjacent input values in one parameter, most input parameters except LTE and mesh size used in this study influenced the calculated Rc and k. This finding is quite reasonable considering the parameters composing the inside algorism of these two FE programs. Especially, small changes in CTE and temperature difference between top and bottom of slab resulted in relatively large difference of Rc and k. Even though other parameters,

such as unit weight, poisson's ratio, elastic modulus and modulus of subgarde reaction, could affect the computed Rc and k, the changes in Rc and k were relatively small with respect to unit weight and poisson's ratio ranges normally observed in reality or are only large in the large change of elastic modulus and modulus of subgrade reaction value.

The differences in deflections calculated in two FE programs were also investigated. The estimated deflection using ISLAB 2000 was 26 % higher at positive temperature difference conditions and 38 % higher at negative temperature difference condition than EverFE 2.24 in terms of %-average difference of Rc and k. Especially, this difference was more higher when the estimated deflections became higher. The differences in deflections between the two FE programs could be mainly due to the type of element used for slab and joint model by the respective FE programs. The elements in 3-D FE program, EverFE 2.24, have more nodes, thus increasing the accuracy of deflection calculations compared to the 2-D ISLAB 2000 FE program. The deflection evaluated in this study was due to temperature change. However, the study by Wang et al. (2006) showed EverFE more highly estimated than ISLAB for deflection calculated from axial loading simulation.

Table 7-3 Relative corner deflections (Rc) for different input values in input parameters of ISLAB2000 and EverFE2.24 on positive temperature different condition

Input Parameter	Input Value	Rc (μM)		ABD of Rc in Input values (μM) [a]		% Difference of Rc in FE-programs[b]
		ISLAB2000	EverFE2.24	ISLAB2000	EverFE2.24	
Unit weight	2,240	-1,035	-792	0	0	30.8
(kg/m^3)	2,400	-1,007	-792	28	0	27.2
	2,560	-983	-792	25	0	24.1
Poisson's Ratio	0.1	-954	-758	0	0	25.9
	0.2	-1,008	-792	53	33	27.3
	0.3	-1,066	-830	58	38	28.4
CTE	6.3	-564	-518	0	0	8.9
($\times 10^{-6}$ / ^{o}C)	9.63	-1,008	-792	444	274	27.3
	13.5	-1,599	-1,110	591	318	44.0
	17.1	-2,193	-1,406	594	296	55.9
Elastic modulus	13,790	-540	-504	0	0	7.2
(MPa)	30,483	-1,007	-792	467	288	27.2
	41,370	-1,189	-921	182	129	29.1
LTE	0.1	-1,018	-794	0	0	28.2
(%)	50	-1,012	-791	6	4	27.9
	90	-1,008	-786	4	5	28.3
k	8.1	-1,660	-1,614	0	0	2.8
(kPa/mm)	35.3	-1,149	-1,032	510	583	11.4
	62.4	-1,007	-792	142	240	27.2
	89.6	-932	-653	75	138	42.6
Mesh size	76 $\times$ 76	-1,007	N/A	0	N/A	N/A
(mm $\times$ mm)	152 $\times$ 152	-1,007	-793	0	0	27.0
	254 $\times$ 178	-1,007	-792	0	1	27.2
	305 $\times$ 305	-1,006	-791	1	1	27.2
Temp Diff	2.2	-211	-207	0	0	2.3
(^{o}C)	4.4	-427	-414	215	207	3.1
	6.7	-721	-621	294	207	16.1
	8.9	-1,072	-828	351	207	29.5
	11.1	-1,455	-1,035	383	207	40.5
	13.3	-1,861	-1,242	406	207	49.8

[a] Absolute difference (ABD) of Rc between two adjacent input values in one parameter

[b] % Difference of Rc in FE-programs $= \left(\dfrac{Rc \ of \ ISLAB\,2000 - Rc \ of \ EverFE\,2.24}{Rc \ of \ EverFE\,2.24} \right) \times 100$

Table 7-4 Relative corner deflections (Rc) for different input values in input parameters of ISLAB2000 and EverFE2.24 on negative temperature different condition

Input Parameter	Input Value	Rc (μM)		ABD of Rc in Input values (μM)		% Difference of Rc in FE-programs
		ISLAB2000	EverFE2.24	ISLAB2000	EverFE2.24	
Unit weight	2,240	851	611	0	0	39.2
(kg/m^3)	2,400	828	611	23	0	35.4
	2,560	807	611	21	0	31.9
Poisson's Ratio	0.1	790	585	0	0	34.9
	0.2	828	611	38	26	35.5
	0.3	870	641	42	30	35.7
CTE	6.3	466	400	0	0	16.4
($\times 10^{-6}$ / $^{\circ}$C)	9.63	828	611	363	211	35.5
	13.5	1,326	857	498	246	54.7
	17.1	1,838	1,085	512	228	69.4
Elastic modulus	13,790	486	390	0	0	24.7
(MPa)	30,483	828	611	342	222	35.4
	41,370	970	711	143	100	36.5
LTE	0.1	843	613	0	0	37.5
(%)	50	830	611	14	3	35.9
	90	828	607	1	4	36.5
k	8.1	1,276	1,247	0	0	2.4
(kPa/mm)	35.3	923	797	353	450	15.9
	62.4	828	611	95	185	35.5
	89.6	778	504	50	107	54.3
Mesh size	76 $\times$ 76	830	N/A	0	N/A	N/A
(mm $\times$ mm)	152 $\times$ 152	829	612	1	0	35.4
	254 $\times$ 178	828	611	1	1	35.5
	305 $\times$ 305	825	611	3	1	35.0
Temp Diff	-2.2	212	208	0	0	2.0
($^{\circ}$C)	-4.4	488	415	276	207	17.7
	-6.7	847	621	359	206	36.5
	-8.9	1,266	829	419	208	52.7
	-11.1	1,724	1,036	459	207	66.5
	-13.3	2,208	1,243	484	207	77.7

Table 7-5 Curvature (*k*) for different input values in input parameters of ISLAB2000 and EverFE2.24 on positive temperature different condition

Input Parameter	Input Value	k ($\times10^{-5}$/m)		ABD of k in Input values ($\times10^{-5}$/m) [a]		% Difference of k in FE-programs [b]
		ISLAB2000	EverFE2.24	ISLAB2000	EverFE2.24	
Unit weight	2,240	-7.48	-5.91	0	0	26.7
(kg/m^3)	2,400	-7.48	-5.91	0	0	26.7
	2,560	-7.09	-5.91	0.39	0	20.0
Poisson's Ratio	0.1	-7.09	-5.51	0	0	28.6
	0.2	-7.48	-5.91	0.39	0.39	26.7
	0.3	-7.87	-5.91	0.39	0	33.3
CTE	6.3	-3.94	-3.94	0	0	0.0
($\times10^{-6}$ / ^{o}C)	9.63	-7.48	-5.91	3.5	2.0	26.7
	13.5	-11.8	-7.87	4.3	2.0	50.0
	17.1	-16.1	-10.2	4.3	2.4	57.7
Elastic modulus	13,790	-3.94	-3.54	0	0	11.1
(MPa)	30,483	-7.48	-5.91	3.5	2.4	26.7
	41,370	-8.66	-6.69	1.2	0.79	29.4
LTE	0.1	-7.48	-5.91	0	0	26.7
(%)	50	-7.48	-5.91	0	0	26.7
	90	-7.48	-5.51	0	0.39	35.7
k	8.1	-12.2	-11.8	0	0	3.3
(kPa/mm)	35.3	-8.27	-7.48	3.9	4.3	10.5
	62.4	-7.48	-5.91	0.79	1.6	26.7
	89.6	-6.69	-4.72	0.79	1.2	41.7
Mesh size	76 × 76	-7.09	N/A	0	N/A	N/A
(mm × mm)	152 × 152	-7.09	-5.51	0	0	28.6
	254 × 178	-7.09	-5.51	0	0	28.6
	305 × 305	-7.09	-5.51	0	0	28.6
Temp Diff	2.2	-1.57	-1.57	0	0	0.0
(^{o}C)	4.4	-3.15	-3.15	1.6	1.6	0.0
	6.7	-5.12	-4.33	2.0	1.2	18.2
	8.9	-7.87	-5.91	2.8	1.6	33.3
	11.1	-10.6	-7.48	2.8	1.6	42.1
	13.3	-13.8	-9.06	3.1	1.6	52.2

[a] Absolute difference (ABD) of k between two adjacent input values in one parameter

[b] % Difference of k in FE-programs $= \left(\dfrac{k \ of \ ISLAB\,2000 - k \ of \ EverFE\,2.24}{k \ of \ EverFE\,2.24} \right) \times 100$

Table 7-6 Curvature (*k*) for different input values in input parameters of ISLAB2000 and EverFE2.24 on negative temperature different condition

Input Parameter	Input Value	k ($\times 10^{-5}$/m)		ABD of k in Input values ($\times 10^{-5}$/m)		% Difference of k in FE-programs
		ISLAB2000	EverFE2.24	ISLAB2000	EverFE2.24	
Unit weight	2,240	6.30	4.33	0	0	45.5
(kg/m^3)	2,400	5.91	4.33	0.39	0	36.4
	2,560	5.91	4.33	0	0	36.4
Poisson's Ratio	0.1	5.91	4.33	0	0	36.4
	0.2	5.91	4.33	0	0	36.4
	0.3	6.30	4.72	0.39	0.39	33.3
CTE	6.3	3.54	2.76	0	0	28.6
($\times 10^{-6}$ / $^{\circ}$C)	9.63	5.91	4.33	2.4	1.6	36.4
	13.5	9.84	6.30	3.9	2.0	56.3
	17.1	13.8	7.87	3.9	1.6	75.0
Elastic modulus	13,790	3.54	2.76	0	0	28.6
(MPa)	30,483	5.91	4.33	2.4	1.6	36.4
	41,370	7.09	5.12	1.2	0.79	38.5
LTE	0.1	6.30	4.33	0	0	45.5
(%)	50	5.91	4.33	0.39	0	36.4
	90	5.91	4.33	0	0	36.4
k	8.1	9.45	9.45	0	0	0.0
(kPa/mm)	35.3	6.69	5.91	2.8	3.5	13.3
	62.4	5.91	4.33	0.79	1.6	36.4
	89.6	5.51	3.54	0.39	0.79	55.6
Mesh size	76 × 76	5.91	N/A	0	N/A	N/A
(mm × mm)	152 × 152	5.91	4.33	0	0	36.4
	254 × 178	5.91	4.33	0	0	36.4
	305 × 305	5.91	4.33	0	0	36.4
Temp Diff	-2.2	1.57	1.57	0	0	0.0
($^{\circ}$C)	-4.4	3.54	3.15	2.0	1.6	12.5
	-6.7	6.30	4.33	2.8	1.2	45.5
	-8.9	9.45	5.91	3.1	1.6	60.0
	-11.1	12.6	7.48	3.1	1.6	68.4
	-13.3	16.5	9.06	3.9	1.6	82.6

7.5 Modeling Instrumented Pavement for ISLAB 2000 and EverFE 2.24

Comparison of FE-based simulation results against field measurements is necessary to verify the FE-based model. The instrumented pavements on highway US-34 near Burlington, Iowa were modeled with ISLAB 2000 and EverFE 2.24 for this comparison.

## 7.5.1 Instrumented Pavement on US-34 near Burlington

A newly constructed JPCP section on an open-graded granular base on US-34 near Burlington, Iowa was selected for this study. The transverse joint spacing was approximately 6 m (20 ft). The passing lane was approximately 3.7 m (12 ft) in width, and the travel lane was approximately 4.3 m (14 ft) in width. Tie-bars of 914-mm (36-in) length and 12.7-mm (0.5-in) diameter were inserted approximately every 762 mm (30-in) across the longitudinal joints. Dowel bars of 457 mm (18-in) length and 38 mm (1.5-in) diameter were inserted approximately every 305 mm (12-in) across the transverse joints.

As shown in Figure 7-3, two test sections in the JPCP travel lane, one corresponding to afternoon (June 7, 2005, 5:30 PM CST) construction conditions and the other representative of late morning (June 8, 2005, 10:45 AM CST) construction, were selected for field data collection.

Thermochron I-Buttons[R] were placed throughout the depth of the pavement on each section during construction to observe the temperature effect on the slab behavior during early age (7 day after construction). Surface profiling was conducted with a Rollingprofiler (SurPRO 2000[R]) following diagonal and transverse directions on four

individual slabs in each test section at different times (morning and the afternoon)

representing negative/positive pavement temperature difference conditions to study the

slab deformation behavior. A Rollingprofiler can measure true unfiltered elevation profile

of the slab surface (ICC, 2006). The raw elevation profile of surface was filtered using a

procedure suggested by Sixbey et al. (2001) and Vandenbossches (2003) to obtain slab

deformation pattern called as "slab curvature profile". Each profiling segment was

measured independently.

A series of laboratory tests were undertaken during the controlled field evaluation

periods to provide material input parameters values of FE-based models.
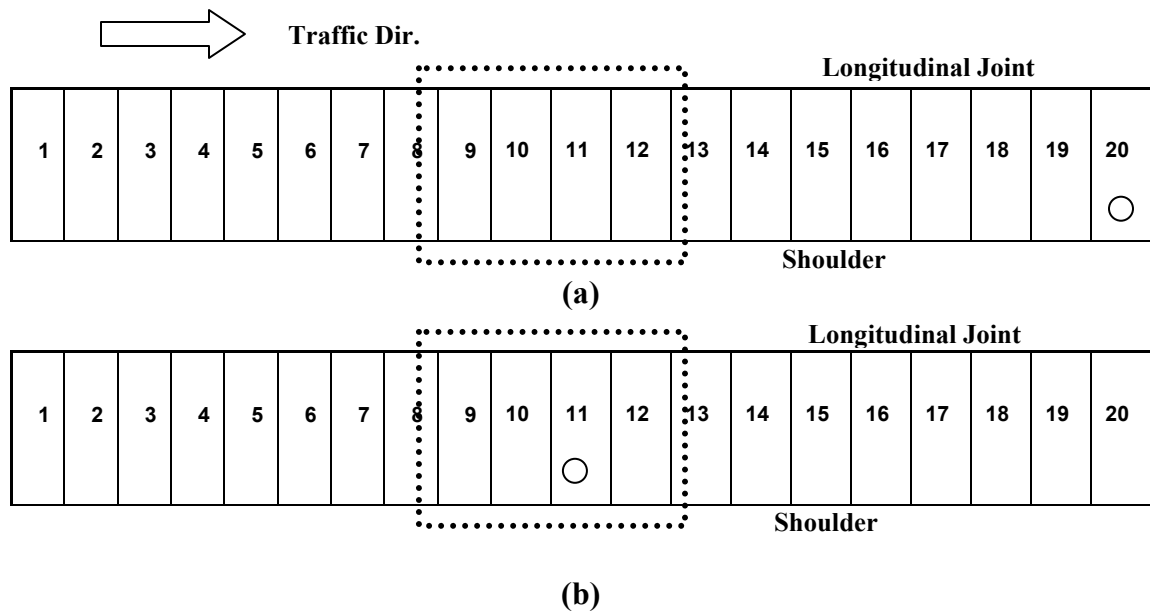
Legend : ◯ - Thermochron I-Buttons® instrumentation location
⋰⋱ - Rollingprofiler measurement (diagonal and transverse trace) location

Figure 7-3 Instrumentation and profile measurement layout in two test section: (a) test section 1 - paving on afternoon hours (6/7/05 5:30PM); (b) test section 2 - paving on morning hours (6/8/05 10:45AM)
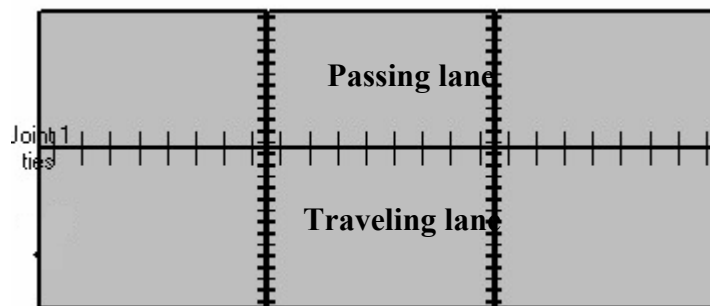
7.5.2 Simulation Methods

Based on the actual geometric proportions and the collected material properties from the test sections, the FE simulations were conducted. Note the actual geometric proportions in US-34 near Burlington, Iowa are same as ones used for sensitivity analyses in this study. The uncollected input parameters but required in FE simulations were assumed as reasonable values based on the results of previous sensitivity runs. For instance, it was observed that the slab deformation increased for increasing modulus of subgrade reaction (k) from 8.1 kPa/mm (30 psi/in) to 35.3 kPa/mm (130 psi/in), but after 35.3 kPa/mm (130 psi/in) the slab deformation did not increase much. The k-value, 35.3 kPa/mm (130 psi/in), is a typical minimum value for Iowa conditions and therefore, 62.4 kPa/mm (230 psi/in) was assumed as the k-value for the FE simulations.

The values of input parameters used in this simulation were summarized in Table 7-7. Three-consecutive slab system in each lane as show in Figure 7-4 was used and middle slab in travel lane was selected for the slab representing field measurement because the measured slabs in test sections were surrounded by other slabs. Even though the slab temperature profile with depth has been recognized as a non-linear distribution, the observed temperature profiles under which pavement profile data were collected in this study showed nearly a linear temperature distribution so that a linear temperature distribution was used in this simulation.

Table 7-7 Values of input parameters used in FE-simulation

Geometry Properties					
Layer	Lane	No. of segm.	Width (m) in a segm.	Length (m) in a segm.	Depth (mm)
Concrete	Passing	3	3.7	6	267
	Traveling	3	4.3	6	267
Material Properties					
Material		Property			Value
Concrete		Modulus of elasticity (MPa)			22,195
		Unit weight (kg/m^3)^a			2400
		Poisson's ratio			0.2
		Coefficient of thermal expansion (/^{o}C)			11.25×10^{-6}
Dowel Bar		Diameter (mm)			38
		Length (mm)			457
		Spacing (mm)			305
		Modulus of elasticity (MPa)^a			20×10^4
		Poisson's ratio^a			0.3
Tie Bar		Diameter (mm)			13
		Length (mm)			914
		Spacing (mm)			762
		Modulus of elasticity (MPa)^a			20×10^4
		Poisson's ratio^a			0.3
Subgrade		Modulus of subgrade reaction (kPa/mm)^a			62.4

^{a} assumed value as typical value

Figure 7-4 Three-consecutive slab systems in each lane used in FE simulation

7.5.3 Equivalent Temperature Difference

Even though ISLAB 2000 and EverFE 2.24 can simulate the slab deformation due

to temperature changes, it can't directly simulate the slab deformation due to moisture

variations and permanent deformation at zero temperature difference and zero moisture

difference which can be obvious at early age concrete pavement. Therefore, if FE simulation was conducted by the actual material inputs and the linear / non-linear temperature distribution, the calculated deflection couldn't estimate the actual deflection due to environmental effects (Rao et al, 2001). However, it has been believed that this limitation of these FE programs could circumvent if the effects of other environmental loadings could be converted to equivalent temperature difference (Korovesis, 1990; Davids, 2003).

Since all the environmental effects are highly correlated with each other, it is quite difficult to quantify each of these effects in terms of temperature differences and therefore the concept of combining all of the active effects into an equivalent temperature difference has been used by previous researchers (Rao et al., 2001; Yu and Khazanovich, 2001; Jeong and Zollinger, 2004; Rao and Roesler, 2005). Following this concept, the relation between actual measured temperature difference and equivalent temperature difference associated with actual pavement behavior could be established. Similar to the approach used by previous researchers (Rao et al., 2001; Yu and Khazanovich, 2001; Jeong and Zollinger, 2004), equivalent temperature differences of both FE-programs were back-estimated to generate the relative corner deflection to center of the measured slab curvature profiles from diagonal direction because these profiles are the longest segment along the slab and include the internal center in slab. Once the equivalent temperature difference on given measured temperature difference was estimated, the equivalent temperature difference values were plotted with measured temperature differences as shown in Figure 7-5. From Figure 7-5, the equivalent temperature differences and the measured temperature differences show a linear relation. This linear

relation can be also observed in data collected in US-30 near Marshalltown, Iowa as shown in Figure 7-6. Based on linear regression equations from Figure 7-5, equivalent temperature differences during pavement profile data collection were calculated and used as inputs for both FE-programs.
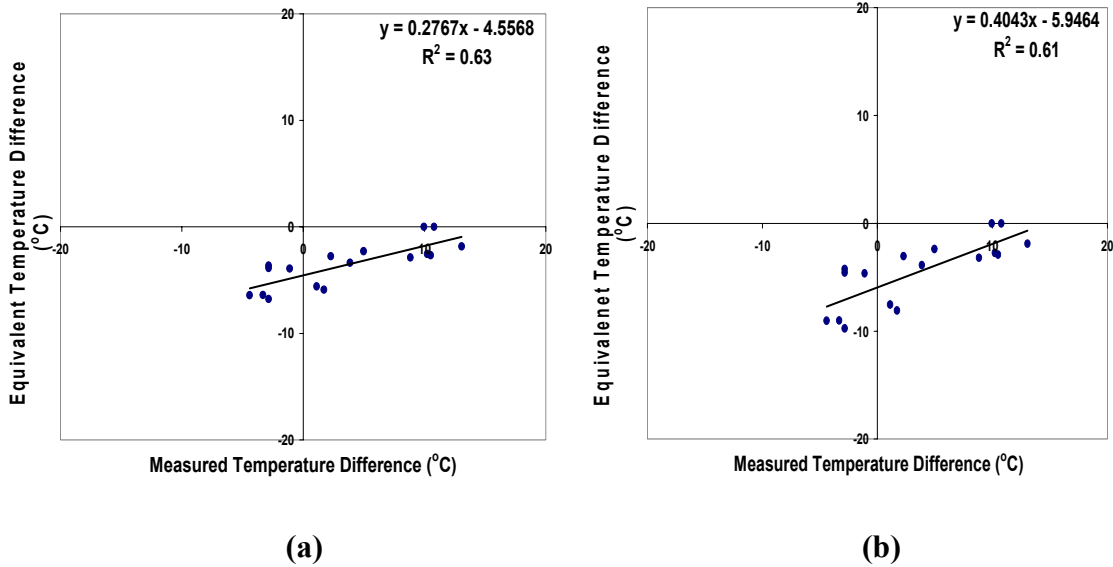

(a)   (b)

Figure 7-5 Equivalent temperature differences versus measured temperature differences in US-34 near Burlington, Iowa: (a) ISLAB 2000; (b) EverFE 2.24

(a)   (b)
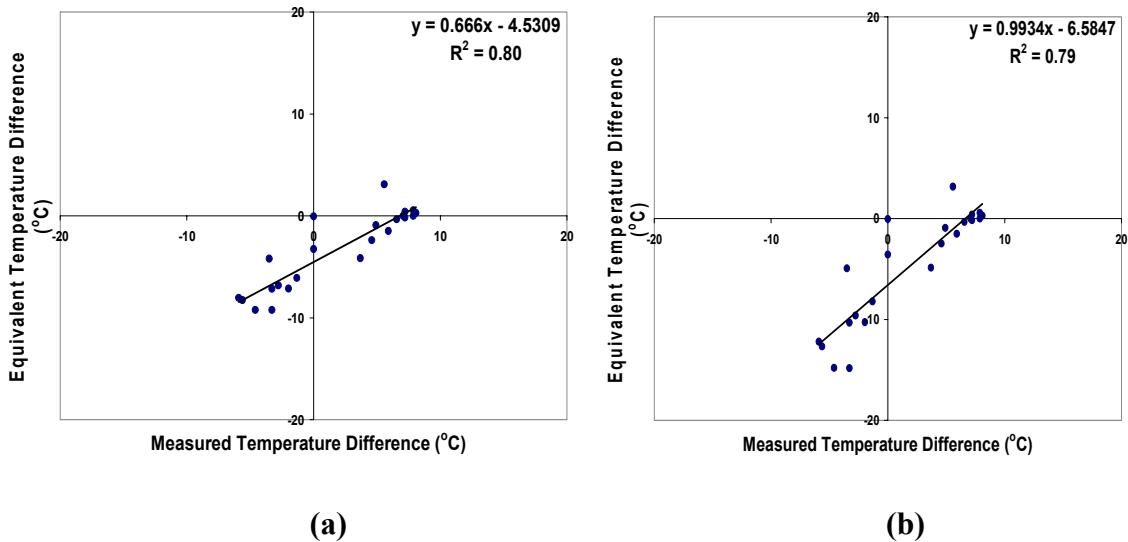
Figure 7-6 Equivalent temperature differences versus measured temperature differences in US-30 near Marshalltown, Iowa: (a) ISLAB2000; (b) EverFE 2.24

7.6 Verification of FE models Based on Field Measurement

Comparisons between the field-measured slab curvature profiles and the FE-computed slab curvature profiles in terms of Rc and *k* were undertaken to verify the FE-based model. The quantitative comparisons between the measured profiles and the FE simulated profiles for test section 1 and test section 2 are presented in Figures 7-7, 7-8, 7-9 and 7-10.

From these figures, it is clearly noted that the measured slab curvature profiles at negative temperature differences show more obviously upward curl rather than at positive temperature differences except transverse direction measurements on test section 1. The different behavior of transverse direction measurement on test section 1 is quite difficult to explain. Even though deflection due to temperature changes could be confounded by other environmental effects, it has been believed that temperature change could be a main dominating factor for slab deformation due to environmental effects. At this time, the only plausible explanation for this behavior is that built in construction slope at transverse direction could be higher than at diagonal direction so it still influenced the slab curvature profile and the relative corner displacement to edge used in transverse slab curvature profile could be less obvious rather than the relative corner displacement to center.

Analysis of Variance (ANOVA) statistical test was conducted to evaluate if the measured slab curvature properties (Rc and *k*) were statistically different from the measured properties. ANOVA results can be expressed in terms of a p-value, which represents the weight of evidence for rejecting the null hypothesis (Ott and Longnecker, 2001). The null hypothesis of sample equality cannot be rejected if p-value is greater than

the selected significant level. Table 7-8 present the ANOVA results for Rc and *k* in terms of p-value. For the significance level (α) of 0.05, the ANOVA results from Table 7-8 confirmed that the FE-predictions provide good estimates of slab curvature properties in term of Rc and *k* under different conditions except the positive temperature different condition of transverse direction measurement. Considering the transverse direction measurements on test section 1 as discussed previously, the inaccuracy of FE-predictions for the positive temperature difference condition of transverse direction measurements should be not unexpected.
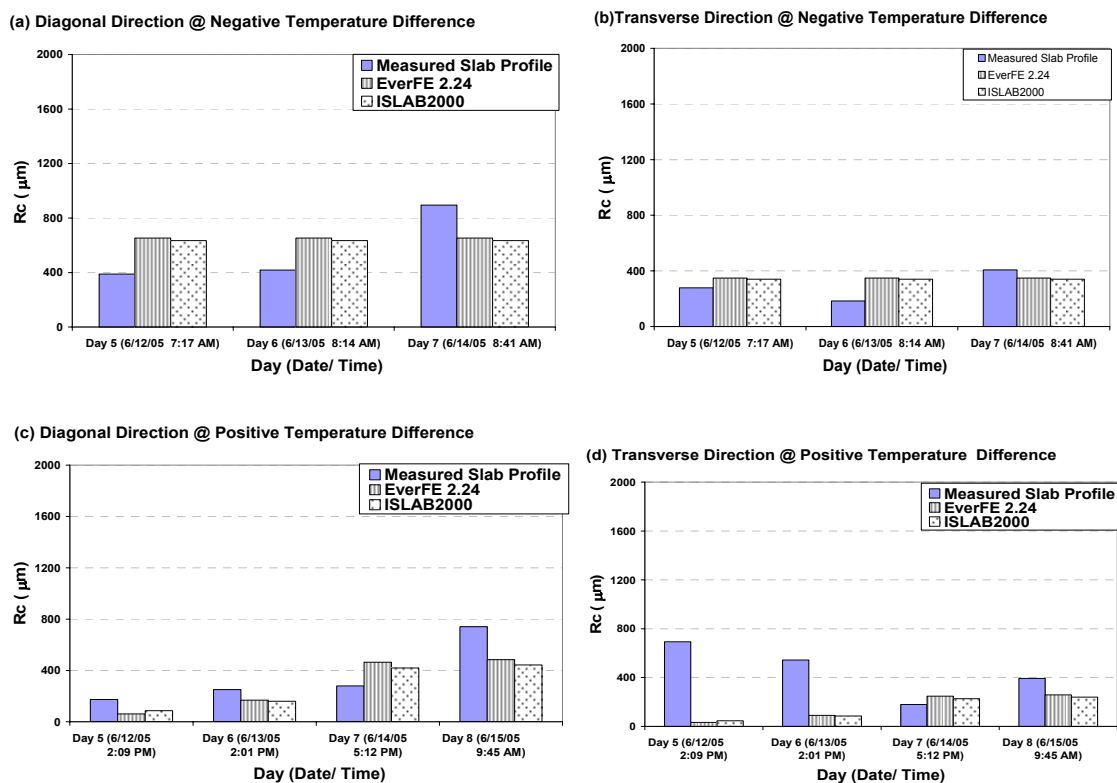

Figure 7-7 Comparisons of relative corner deflection (Rc) between measured and FE-predicted slab curvature profiles in test section 1: (a) diagonal direction at negative temperature difference condition; (b) transverse direction at negative temperature difference condition; (c) diagonal direction at positive temperature difference condition; (d) transverse direction at positive temperature difference condition
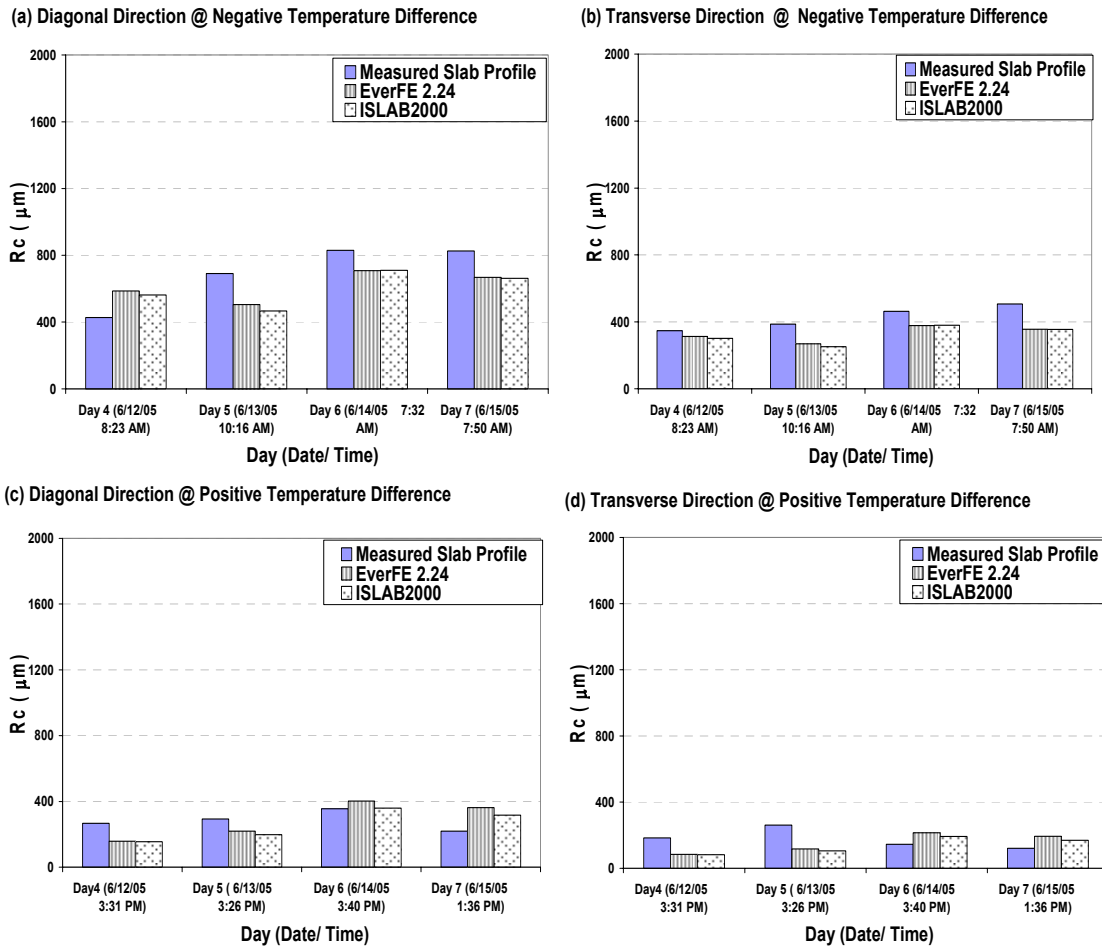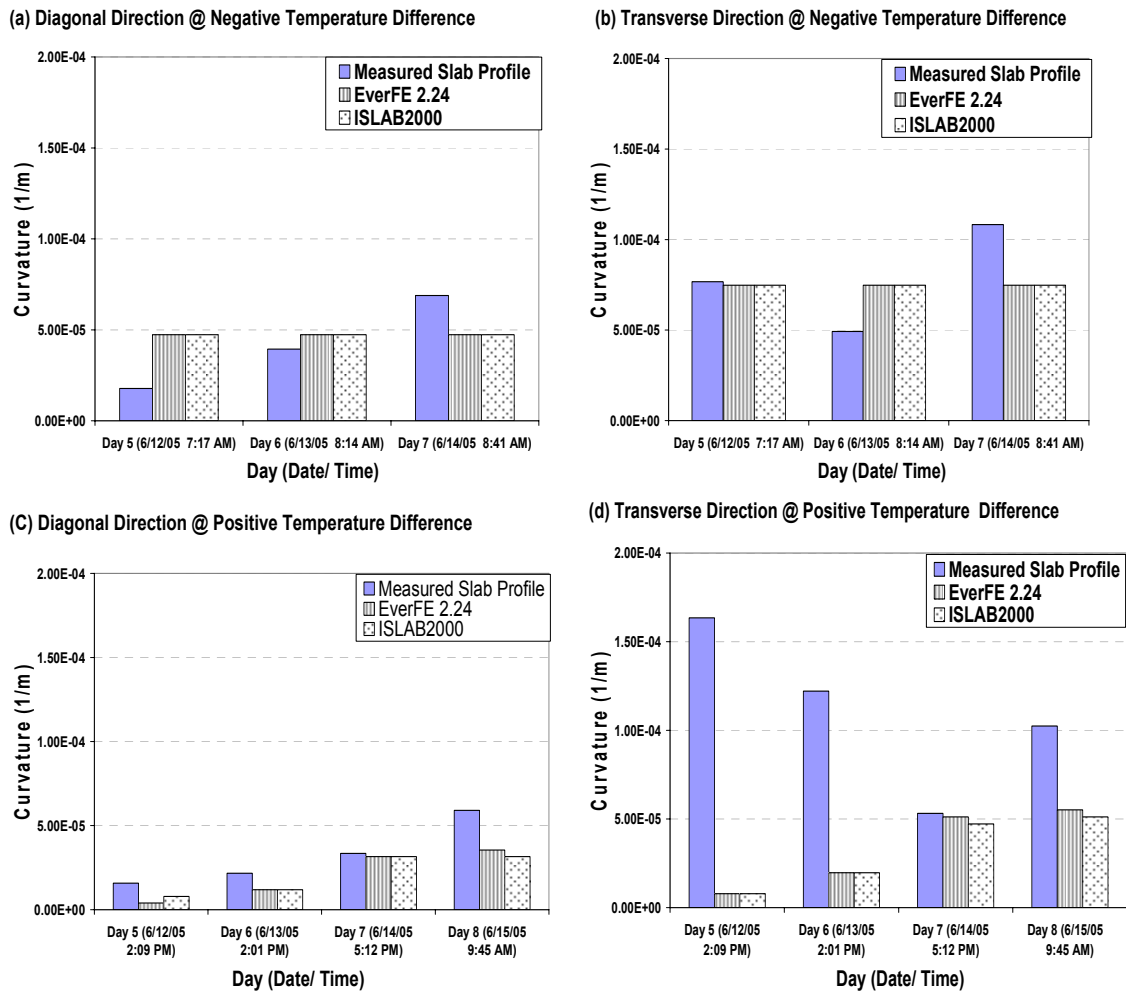
(a) Diagonal Direction @ Negative Temperature Difference

(b) Transverse Direction @ Negative Temperature Difference

(c) Diagonal Direction @ Positive Temperature Difference

(d) Transverse Direction @ Positive Temperature Difference

Figure 7-8 Comparisons of relative corner deflection (Rc) between measured and FE-predicted slab curvature profiles in test section 2:(a) diagonal direction at negative temperature difference condition; (b) transverse direction at negative temperature difference condition; (c) diagonal direction at positive temperature difference condition; (d) transverse direction at positive temperature difference condition
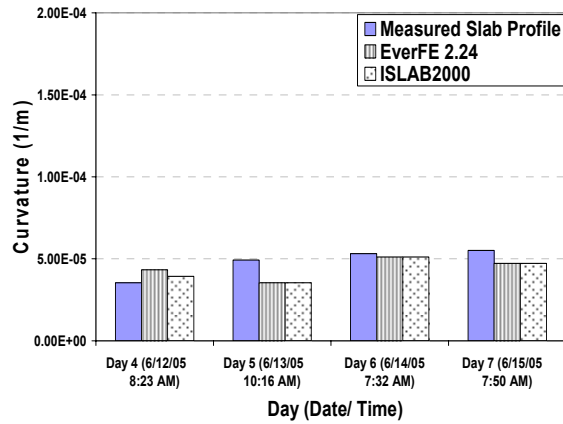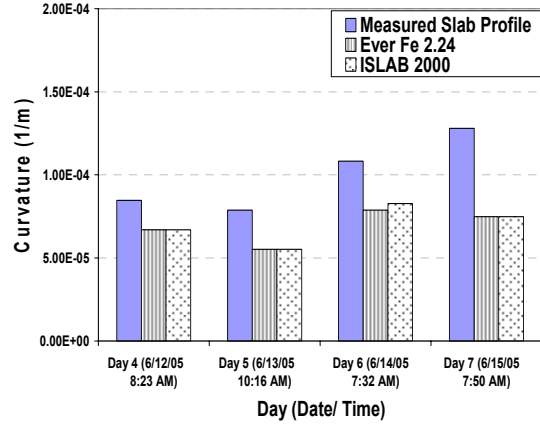
(a) Diagonal Direction @ Negative Temperature Difference

(b) Transverse Direction @ Negative Temperature Difference

(C) Diagonal Direction @ Positive Temperature Difference

(d) Transverse Direction @ Positive Temperature Difference

Figure 7-9 Comparisons of curvature (*k*) between measured and FE-predicted slab curvature profiles in test section 1:(a) diagonal direction at negative temperature difference condition; (b) transverse direction at negative temperature difference condition; (c) diagonal direction at positive temperature difference condition; (d) transverse direction at positive temperature difference condition
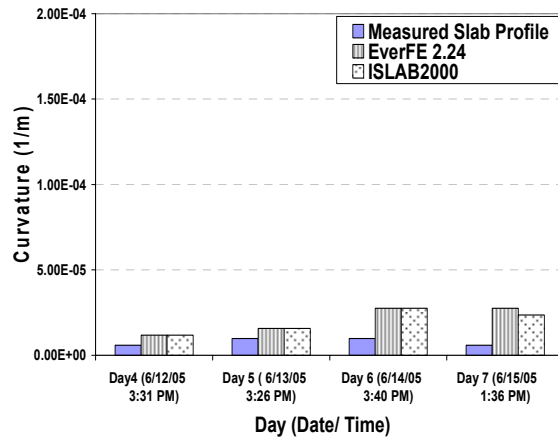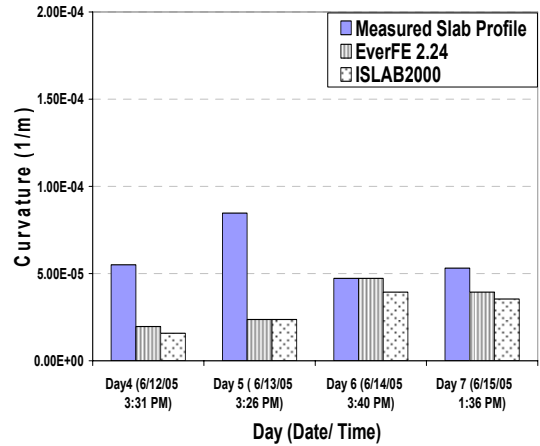
Figure 7-10 Comparisons of curvature (*k*) between measured and FE-predicted slab curvature profiles in test section 2:(a) diagonal direction at negative temperature difference condition; (b) transverse direction at negative temperature difference condition; (c) diagonal direction at positive temperature difference condition; (d) transverse direction at positive temperature difference condition

Table 7-8 ANOVA results for Rc and *k* of slab curvature profiles

Temperature Difference Condition	Response	Direction			
		Diagonal		Transverse	
		p-value	Different ?	p-value	Different ?
Positive	Rc	0.6717	No	0.004	Yes
	k	0.9937	No	0.001	Yes
Negative	Rc	0.9095	No	0.6978	No
	k	0.9911	No	0.1837	No

7.7 Conclusions

This study evaluated two FE-based primary response models, namely ISLAB 2000 and EverFE 2.24, used in characterizing the deformation of early aged JPCP under environmental loading. Analytical solutions and numerical models used in both FE programs for computing the slab displacement under environmental loading were briefly reviewed. Based on typical rigid pavement geometry used in Iowa highway pavements, sensitivity analyses were conducted using ISLAB 2000 and EverFE 2.24 for identifying the critical input parameters that have the most influence on PCC slab deflection due to environmental effects. The procedure and the results of the FE analyses based on established input parameter combination and equivalent temperature difference were presented. Comparisons between the field measured and the FE computed slab deformations due to environmental effects were performed. Based on the results of this study, the following conclusions were drawn;

- Temperature difference and CTE are the most sensitive parameters to calculated slab deformations due to temperature based on ISLAB 2000 and EverFE2.24 FE- analyses for typical rigid pavement geometry used in Iowa.

- The estimated deflection resulting from temperature by ISLAB 2000 is 26 % higher for positive temperature difference conditions and 38 % higher for negative temperature difference conditions compared to EverFE 2.24 predictions.

- The actual field-measured temperature difference and the equivalent temperature difference based on FE simulations (associated with the actual field slab displacement) showed a linear relation.

- The computed slab deformations from both FE programs based on established input parameter combination and equivalent temperature difference have good agreement with the field measured deformations.

7.8 Acknowledgments

7.9 References

Armaghani, J. M., Lybas, J. M., Tia, M., and Ruth, B. E., 1986, "Concrete Pavement Joint Stiffness Evaluation," *Transportation Research Record*, Vol.1099, Transportation Research Board, Washington, D.C., pp. 22-36.

Beckemeyer, C. A., Khazanovich, L., and Yu, H. T., 2002, "Determining Amount of Built-in Curling in Jointed Plain Concrete Pavement: Case Study of Pennsylvania I-80," *Transportation Research Record*, Vol. 1809, Transportation Research Board, Washington, D.C., pp 85-92.

Chatti, K., Lysmer, J., and Monismith, C. L., 1994, "Dynamic Finite Element Analysis of Jointed Concrete Pavement," *Transportation Research Record*, Vol. 1449, Transportation Research Board, Washington, D.C., pp. 79-90.

Davids, W. G., Turkiyyah, G. M., and Mahoney, J. P., 1998, "EverFE: Rigid Pavement Three –Dimensional Finite Element Analysis Tool," *Transportation Research Record*, Vol. 1629, Transportation Research Board, Washington, D.C., pp. 41-49.

Davids, W. G. and Turkiyyah, G. M., 1999, "Multigrid Preconditioner for Unstructured Nonlinear 3D FE Models," *Journal of Engineering Mechanics*, Vol. 125, No. 2, American Society of Civil Engineering, 1999, pp.186-196.

Davids, W. G., 2001, "3D Finite Element Study on Load Transfer at Doweled Joints in Flat and Curled Rigid Pavements," *The International Journal of Geomechanics*, American Society of Civil Engineering, Vol.1, No.3, pp. 309-323.

Davids, W.G., Wang, Z., Turkiyyah, G. M., Mahoney, J. P., and Bush, D., 2003, "Three-Dimensional Finite Element Analysis of Jointed Plan Concrete Pavement with EverFE2.2," *Transportation Research Record*, Vol. 1853, Transportation Research Board, Washington, D.C., pp. 92-99.

Davids, W.G., 2003, *EverFE Theory Manual*, University of Maine, Civil Engineering Department, Orono, Main, pp.1-18.

Davids, W.G., 2006, *EverFE : Software for the 3D Finite Element Analysis of Jointed Plain Concrete Pavements*, University of Maine, Civil Engineering Department, Orono, Main, http://www.civil.umaine.edu/EverFE/, Accessed May, 2006.

Hammons, M. I. and Ioannides, A. M., 1997, *Advanced Pavement Design:Finite Element Modeling for Rigid Pavement Joints Report I: Background Investigation*,

Technical Report DOT- FAA- AR-95-85, Federal Aviation Administration, U.S. Department of Transportation.

Ioannides, A. M. and Salsili-Murua, R. A., 1989, "Temperature Curling in Rigid Pavements: An Application of Dimensional Analysis," *Transportation Research Record*, Vol. 1227, Transportation Research Board, Washington, D.C., pp. 1-10.

Ioannides, A. M. and Korovesis, G. T., 1990, "Aggregate Interlock: A Pure-Shear Load Transfer Mechanism," *Transportation Research Record*, Vol.1286, Transportation Research Board, Washington, D.C., pp. 14-24.

Ioannides, A. M. and Korovesis, G. T., 1992, "Analysis and Design of Doweled Slab-on-grade Pavement Systems" *Journal of Transportation Engineering*, Vol. 118, No. 6, American Society of Civil Engineering, pp. 745-768.

International Cybernetics Corporation (ICC.), 2006, http://www. internationalcybernetics.com/ rollprofile.htm, accessed May, 2006.

Iowa Department of Transportation (IDOT), 2005, *Standard Road Plans*, Electronic Reference Library, http://165.206.203.37/Oct_2005/RS/frames.htm, Accessed May, 2006.

Jeong, J. H. and Zollinger, D. G., 2004, "Insights on Early Age Curling and Warping behavior from Fully Instrumented Test Slab System," *CD-ROM Proceedings of the 83rd Annual Meeting of the Transportation Research Board* , Transportation Research Board, Washington, D.C.

Khazanovich, L., Yu, H. T., Rao, S., Galasova, K., Shats, E., and Jones, R., 2000, *ISLAB2000-Finite Element Analysis Program for Rigid and Composite Pavements*, User's Guide, ERES Consultant, Champaign, Illinois.

Korovesis, G. T., 1990, *Analysis of SLAB on Grade Pavement Systems Subjected to Wheel and Temperature Loadings*, Ph.D. Thesis, University of Illinois, Urbana Champaign, Illinois.

Lim, S. W. and Tayabji, S. D., 2005, "Analytical Technique to Mitigate Early-Age Longitudinal Cracking in Jointed Concrete Pavements," *Proceedings of 8th International Conference on Concrete Pavements*, Colorado Springs, Colorado.

National Cooperative Highway Research Program (NCHRP), 2004, *Guide for Mechanistic-Empirical Design of New and Rehabilitated Pavement Structures*, http://trb.org/mepdg, National Cooperative Highway Research Program 1-37A, Transportation Research Board, Washington, D.C.

Ott, L.R. and Longnecker, M., 2001, *An introduction to Statistical Methods and Data Analysis*, 5th edition, Duxbury, Pacific Grove, California.

Rao, C., Barenberg, E. J., Snyder, M. B., and Schmidt, S., 2001, "Effects of Temperature and Moisture on the Response of Jointed Concrete Pavements," *Proceedings of 7th International Conference on Concrete Pavements*, Orlando, Florida.

Rao, S. and Roesler, J. R., 2005, "Characterizing Effective Built in Curling from Concrete pavement Field Measurements," *Journal of Transportation Engineering*, Vol. 131, No. 4, American Society of Civil Engineering, pp.320-327.

Siddique, Z. and Hossain. M., 2005, "Finite Element Analysis of PCCP Curling and Roughness," *Proceedings of 8th International Conference on Concrete Pavements*, Colorado Springs, Colorado.

Sixbey, D., Swanlund, M., Gagarin, N. and Mekemson, J. R., 2001, "Measurement and Analysis of Slab Curvature in JPC Pavements Using Profiling Technology,"

189

Proceedings of 7th International Conference on Concrete Pavements, Orlando, Florida.

Vepa, T. S. and George, K. P.,1997, "Deflection Response Model for Cracked Rigid Pavements," *Journal of Transportation Engineering*, Vol. 123, No. 5, American Society of Civil Engineering, pp.377-384.

Vandenbossche, J. M., 2003, *Interpreting Falling Weight Deflectometer Results for Curled and Warped Portland Cement Concrete Pavements*, Ph.D. Thesis, University of Minnesota, Minneapolis, Minnesota.

Vandenbossche, J. M. and Snyder, M. B., 2005, "Comparison between Measured Slab Profiles of Curled Pavements and Profile Generated Using the Finite Element Method," *Proceedings of 8th International Conference on Concrete Pavements*, Colorado Springs, Colorado.

Wang, W., Basheer, I., and Petros, K., 2006, "Jointed Plain Concrete Pavement Models Evaluation," *CD-ROM Proceedings of the 85rd Annual Meeting of the Transportation Research Board*, Washington, D.C.

Westergaard, H. M.,1926, "Analysis of Stressed in Concrete Pavements Due to Variations of Temperature," *Proceedings of Highway Research Board*, Vol. 6, National Research Council, Washington, D.C., pp.201-217.

Yu, H. T., Khazanovich, L. Darter, M. I, and Ardani, A., 1998, "Analysis of Concrete Pavement Response to Temperature and Wheel Loads Measured from Instrumented Slab," *Transportation Research Record*, Vol. 1639, Transportation Research Board, Washington, D.C., pp. 94-101.

Yu, H. T., Khazanovich, L., 2001, "Effects of Construction on Concrete Pavement Behavior," *Proceedings of 7th International Conference on Concrete Pavements*, Orlando, Florida.

Yu, H. T., Khazanovich, L., and Darter, M. I., 2004, "Consideration of JPCP Curling and Warping in the 2002 Design Guide," *CD-ROM Proceedings of the 83rd Annual Meeting of the Transportation Research Board*, Washington, D.C.

CHAPTER 8. ENVIRONMENTAL EFFECTS ON DEFORMATION AND SMOOTHNESS BEHAVIOR OF EARLY AGE JOINTED PLAIN CONCRETE PAVEMENTS

A paper presented *the 86th Annual Meeting of the Transportation Research Board*

Halil Ceylan,[1] Sunghwan Kim,[2] Kasthurirangan Gopalakrishnan,[3] and Kejin Wang[4]

8.1 Abstract

In this paper, a study of environmental effects on the deformation and smoothness behavior of Jointed Plain Concrete Pavement (JPCP) during its early age is presented. A newly constructed JPCP on highway US-34 near Burlington, Iowa was instrumented and monitored during the critical time immediately following construction to identify its early age behavior with respect to temperature variations. The surface profiles were measured in diurnal cycles. The primary objective of this research was to investigate the effect of the early-age curling and warping behavior on the initial smoothness of newly constructed JPC pavements.

Variations in temperature during these critical periods were monitored using the temperature sensors installed within the pavement test sections at the time of construction. The slab deformations associated with environmental loading were quantified and the smoothness indices, in terms of International Roughness Index (IRI) and the Ride

---

1 Assistant Professor, Iowa State University, Ames, IA
2 Graduate Research Assistant, Iowa State University, Ames, IA
3 Post-Doctoral Research Associate, Iowa State University, Ames, IA
4 Associate Professor, Iowa State University, Ames, IA

Number (RN), were computed using the measured pavement surface profiles. The changes in smoothness indices at different measurement times were investigated and compared with those obtained using Finite Element (FE) simulations.

Based on the variations in measured and predicted smoothness indices, it was observed that the initial pavement smoothness was not significantly influenced by JPCP's curling and warping behavior (during the first seven days after paving).

8.2 Background and Introduction

The temperature and moisture variations across the depth of the Portland Cement Concrete (PCC) pavements due to changes in the climate result in a unique deflection behavior which has been recognized as curling and warping of the pavements since the mid 1920s (Westergaard, 1926; Westergaard, 1927). In general, temperature differences across the depth of the concrete pavement result in curling while moisture differences result in warping behavior (Janssen, 1987; Jeong and Zollinger, 2005). A positive temperature difference between the top and the bottom surfaces of the concrete slab in daytime causes the slab corners to curl downwards, while a negative temperature difference during night time results in the upward curling of PCC slab. The moisture difference through the slab depth because of weather condition results in non-uniform concrete shrinkage and non-uniform volume change through depth (Rao et al., 2001). However, curling and warping behavior of early-age concrete is affected not only by temperature and moisture differences due to weather conditions, but also by early-age curing conditions and temperature conditions during pavement construction (Janssen, 1987; Rao et al., 2001; Yu et al., 1998; Rao and Roesler, 2005; Byrum, 2001).

High unrecoverable drying shrinkage of concrete near the top of the slab and a positive temperature gradient at the time of concrete setting can cause permanent upward curling and warping at zero-temperature and zero-moisture gradient (Yu et al., 1998; Yu et al., 2004). This permanent upward curling and warping is partially recovered by the creep of the slab after hardening of the concrete over time (Rao and Roesler, 2005). Once the pavement attains permanent upward curling and warping after setting, the upward curling of the slab for the first few nights after the placement of concrete is the critical condition for early-age cracking. This is especially so since the tensile stress at the top of the slab due to upward curling and slab weight is greater than the incompletely developed concrete strength (Lim and Tayabji, 2005).

Pavement smoothness can de defined as a lack of noticeable roughness and a more optimistic view of the road condition (Sayers and Karamihas, 1998; Akhter et al., 2002). Pavement smoothness has been characterized as the transformed numbers from roughness in pavement profiles measured by various equipments. Pavement smoothness has been recognized as the major measurement in evaluating the pavement performance because it is directly related to the serviceability of road for the traveling user (Ksaibati et al., 1995). Especially, the initial smoothness immediately after construction has been reported to affect the pavement service life significantly (Janoff, 1990). Smith et al. (1997) reported that a pavement constructed smoother stayed smoother over time if all other things affecting smoothness remain the same. Recognizing the importance of achieving smoothness in newly constructed pavements, many agencies have established and implemented the smoothness specifications for newly constructed pavement systems. In these specifications, many agencies determine the bonus or penalties to the contractor for

constructed pavements to encourage the contractor to construct pavements with smoothness indices (or roughness indices) lower than a certain threshold value (Chou and Pellinen, 2005).

It is believed that several factors are related to the initial smoothness of a concrete pavement. These include elements related to the pavement design, material selection, and concrete uniformity, climate, and construction practices (Rasmussen et al., 2002; Rasmussen et al., 2004). Among these, the temperature and moisture variations could result in changes in slab curvature known as curling and warping. Based on profilograph records of concrete pavements in California, Hveem (1951) noticed that curling and warping of PCC slab could influence the pavement smoothness measurements. Based on the analysis of data collected during the Long Term Pavement Performance (LTPP) study, Byrum (2000, 2001) reported that the construction condition and the complex interactions of temperature, moisture and material creep during early pavement life could result in permanent curling and warping of PCC slabs. Analysis of data collected for the National Cooperative Highway Research Program (NCHRP) Project 10-47 *Guidelines for Longitudinal Pavement Profile Measurement* also showed upward curvature in pavement profile during a period when the temperature difference between top and bottom of slab was low (1999).

Several research studies reported in the literature have linked slab curling to concrete pavement stresses (Westergaard, 1926; Westergaard, 1927; Bradbury, 1938; Thomlinson, 1940; Korovesis, 1990). However, there is very little discussion on the effects of slab curling on smoothness and the pavement age at which slab curling can significantly affect smoothness (Karamihas, 2001). Based on a number of smoothness

measurements made in eleven pavement test sections from early morning to late afternoon, Karamihas et al. (2001) suggested that the slab curvature due to temperature can possibly influence the smoothness of a concrete pavement. However, the pavements selected in his study were several years old at the time the measurements were taken, and therefore his findings may not necessarily apply for newly constructed pavements. Note that the smoothness of a newly constructed concrete pavement is an important quality control factor to decide the payment for the contractor. In a recent study, Perera et al. (2005) observed that there was no noticeable effect of slab curvature changes affecting the smoothness of five newly constructed pavements.

In spite of many research efforts (Jeong and Zollinger, 2005; Rao et al., 2001; Yu et al., 1998; Rao and Roesler, 2005; Armaghani et al., 1987), the early-age curling and warping behavior of PCC pavements under pure environmental loading and the effect of this behavior on the initial smoothness of concrete pavement have not been fully understood. The current study was primarily conducted to fulfill this research need. In this study, a newly constructed JPCP on US 34 near Burlington, Iowa was instrumented to monitor the pavement response to environmental loading during the first seven days after construction in the summer of 2005. A series of laboratory tests were undertaken to characterize the properties of paving material during the controlled field evaluation. In addition, the surface profile measurements were made during early morning and late afternoon to identify the slab deflection and to compute smoothness indices in terms of IRI and RN. The changes in smoothness indices at different measurement times were investigated and compared with results obtained using FE simulations.

8.3 Site Description and Data Collection

The 267 mm (10.5 in) test JPC pavement was constructed on a 152 mm (6 in) well-graded crushed limestone granular base. The transverse joint spacing was approximately 6 m (20 ft). The passing lane was 3.7 m (12 ft) in width, and the travel lane was 4.3 m (14 ft) in width.

As shown in Figure 8-1, two 122 m (400 ft) length test sections on the travel lane of the JPCP, one corresponding to afternoon (June 7, 2005, 5:30 PM CST) construction conditions and the other representative of morning (June 8, 2005, 10:45 AM CST) construction, were selected for surface profile measurements. Temperature sensors were placed in each test section to observe the temperature effect on the slab behavior during early age (seven days after construction). In additional, Linear Variable Distance Transducers (LVDTs) installed at the corner, mid-slab on free edge and slab center to record the vertical slab displacements. Iowa State University's (ISU's) PCC mobile laboratory parked near the test section monitored the weather conditions such as ambient temperature, ambient relative humidity, wind speed and rainfall during the evaluation periods.
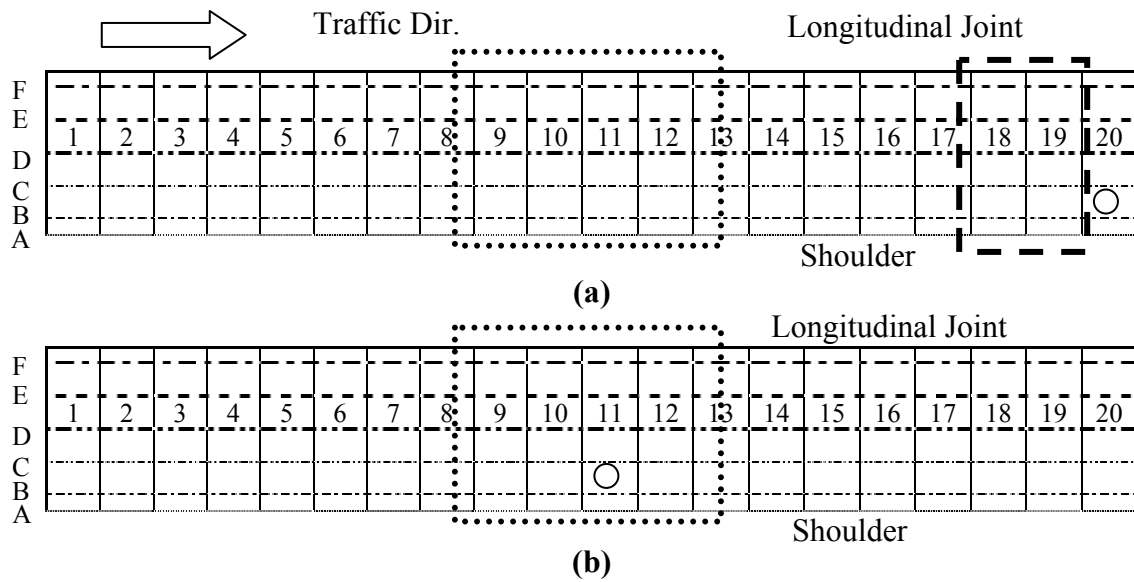
Legend : ○ - Temperature instrumentation location
⌐⌐ - LVDT instrumentation location
⫶⫶ - Diagonal and transverse trace profiling location
A - Profiling at edge
B - Profiling at 0.6m(2ft) from shoulder
C - Profiling at 0.9m(3ft) from shoulder
D - Profiling at center
E - Profiling at 0.9m(3ft) from longitudinal joint
F - Profiling at 0.3m (1ft) from longitudinal joint

Figure 8-1 Instrumentation and profile measurement layout: (a) test section 1 on the travel lane - paving during afternoon hours (6/7/05 5:30PM); (b) test section 2 on the travel lane - paving during morning hours (6/8/05 10:45AM)

8.3.1 PCC Laboratory Testing

To obtain the fundamental physical properties of the paving material, a series of laboratory tests were conducted in ISU's PCC mobile laboratory and ISU's PCC laboratory at different times using in-situ samples obtained from the paving site. The split tensile test (ASTM C 496), compressive strength test (ASTM C 39), and the elastic modulus test (ASTM C 469) were performed on PCC samples obtained during

construction. In addition, the PCC Coefficient of Thermal Expansion (CTE) (AASHTO TP 60) was measured to be 1.13×10^{-5} / ^{o}C.

8.3.2 Pavement Temperature Instrumentation

Temperature sensors installed within the test sections recorded the slab temperature data at five-minute intervals throughout the field evaluation periods. Temperature instrumentation consisted of Thermochron I-buttons[®] attached to a stake at different depths and placed at 0.9-m (3-ft) from the pavement edge before the paving.

8.3.3 Measurement of Vertical Slab Movements Using LVDTs

Two slabs, paved in the afternoon (slabs 18 and 19 in test section 1, see Figure 8-1), were selected as representative slabs to study the pavement vertical movements entirely due to environmental loads. LVDTs were installed in special locations on each slab to capture the vertical movements of the slab. Nine LVDTs in test slab 18 and seven LVDTs in test slab 19 were installed at corners, mid-slab edges and slab center. LVDTs were held by a bracket fastened to a steel rod inserted in subgrade and placed on a smooth glass on the PCC pavement. The LVDTs were connected to data loggers, which collected data at 10-minute intervals throughout the field evaluation periods.

All the sensors were placed only after the concrete hardened (1 day after paving) but unexpected weather conditions (strong thunderstorms) resulted in the damage of installed LVDTs and therefore all LVDTs were re-installed on the second day after paving. However, the re-installed LVDTs could not provide the desired level of reliable information due to some malfunctioning.

8.3.4 Pavement Surface Profile Measurement

An International Cybernetics Corporation Rollingprofiler (SurPRO 2000®) (ICC., 2006), as shown in Figure 8-2(a), was used for surface profile measurements in morning and afternoon along different traces in the test sections. Rollingprofiler (SurPRO 2000®), a kind of inclinometer profiler, can measure true unfiltered elevation profile of surface to compute smoothness index (ICC., 2006). The diurnal cycle measurement of profile for the same location could provide a better understanding of the effect of the slab curling and warping to the smoothness. Four individual slabs in each test section were selected for identifying the deformation of the slab due to environmental loading using the Rollingprofiler. The Rollingprofiler measured surface profiles in each slab along the diagonal and transverse traces as shown in Figure 8-2(b).
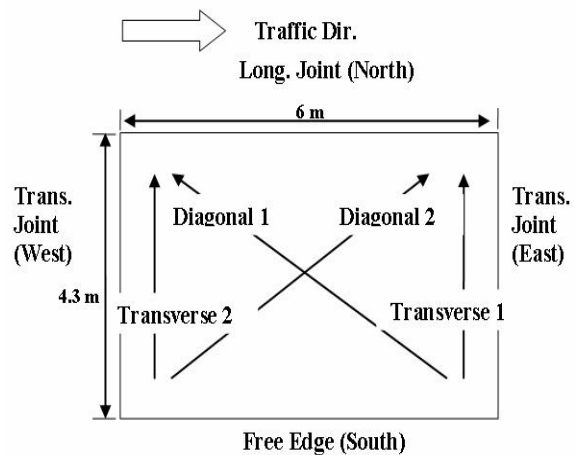
(a)   (b)

Figure 8-2 International Cybernetic Corporation Rollingprofiler (SurPRO 2000®): (a) equipment in operation; (b) profiling pattern
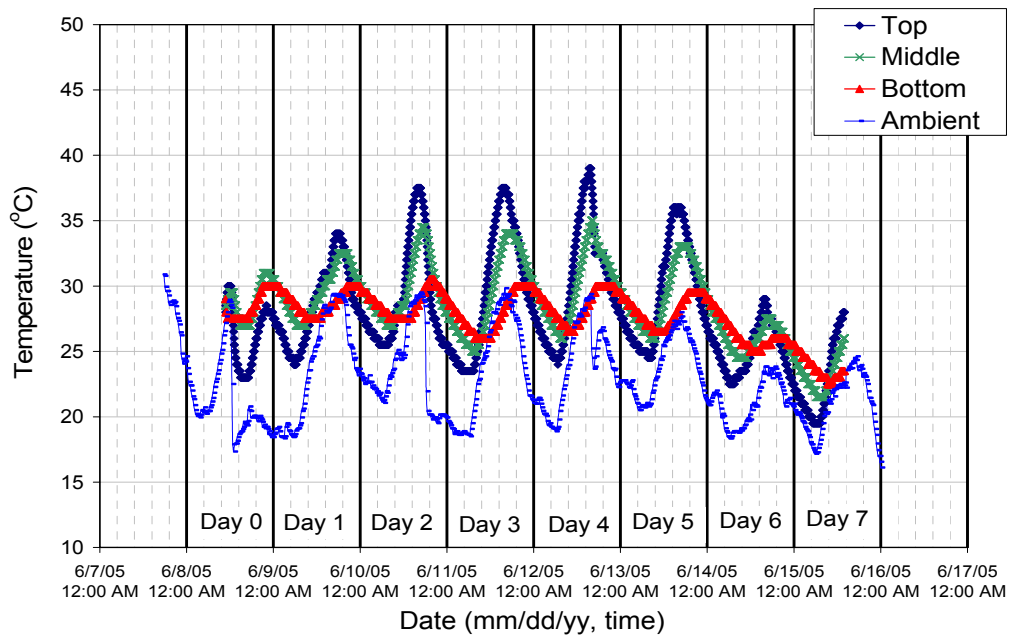
8.4 Pavement Temperature

The temperature variations within the PCC pavement during the early age (7 days after construction) could be obtained from the installed temperature sensors. In addition, weather data such as ambient temperature, ambient relative humidity, wind speed and rainfall could be collected from the weather station housed within the ISU PCC mobile laboratory. The PCC pavement temperature and ambient temperature variations in test sections 1 and 2 are together illustrated in Figure 8-3.

From Figure 8-3, pavement temperature is generally higher than ambient temperature. Over the first seven days after construction, ambient temperature ranged from a low in the mid 10s $^{\circ}$C (60s $^{\circ}$F) in the morning to a high in the 30s $^{\circ}$C (80s $^{\circ}$F) in the afternoon. The pavement temperature ranged from a low in the 20s $^{\circ}$C (70s $^{\circ}$F) in the morning and to a high about 40s $^{\circ}$C (100s $^{\circ}$F). Except for the first day of paving (day 0), the pavement temperature followed a pattern that is similar to that of ambient temperature, as reported by previous research studies (Armaghani et. al., 1987). During day 0 of paving, it is suspected that the concrete's heat of hydration might have influenced the pavement temperature. It is also observed that the ambient temperature on June 8th between 12:30 pm to 3:30 pm suddenly drops down from 29 $^{\circ}$C (84 $^{\circ}$F) to 17 $^{\circ}$C (63 $^{\circ}$F) because of the strong thunderstorms.
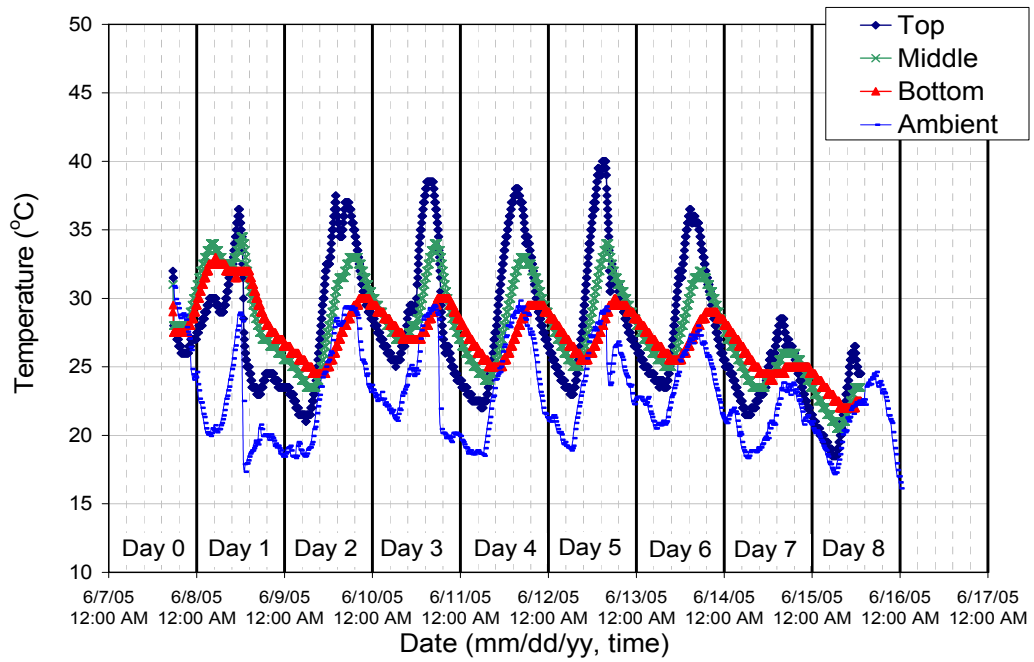
(a)

(b)

Figure 8-3 Field temperature variations: (a) test section 1; (b) test section 2

8.5 Environmental Effects on Pavement Behavior

In the original plan, it was expected that the collected data from both the LVDTs and the Rollingprofiler in each test section would be used to study the slab deformation due to environmental loads. However, unexpected weather conditions (strong thunderstorms) resulted in the damage of the installed LVDTs and therefore the data collected from the LVDTs could not provide reliable information although the LVDTs were re-installed after the thunderstorm. Thus, the profile measurements following diagonal and transverse traces were used to identify the slab deformation. Previous researchers have utilized the surface profiles measured by inclinometer profiler for identifying the slab curvature profile due to environmental loads (Rao et al., 2001; Vandenbossche and Snyder, 2005). The raw data of surface profile measurements include not only slab deformation pattern referred to as slab curvature profile, but also the built-in construction slope and the surface irregularities. Currently, there does not seem to be a standard method to identify the slab curvature due to curling and warping from the raw surface profiling data. However, several indirect procedures have been proposed to detect the slab curvature profile from the raw surface profiling data (Byrum, 2000; Vandenbossche, 2003; Sixbey et al., 2001; Siddique et al., 2003; Sondag and Snyder, 2006). Among them, the procedures suggested by Sixbey et al (2001), Vandenbossche (2003) and Sondag and Snyder (2006) were used in this study since this method has been successfully employed by many researchers in the past and also the method is simple.

The diagonal slab curvature profile measurements averaging diagonal 1 and 2 in test sections 1 and 2 are illustrated in Figure 8-4. The diagonal slab curvature profile measured in both test sections clearly showed upward curling for the morning

measurements and almost flat shape for the afternoon measurements. This behavior could be attributed to the permanent curling and warping resulting from unrecoverable shrinkage due to non-uniform moisture distribution, early age curing conditions and temperature conditions during pavement construction. However, the transverse slab curvature profiles, not presented here due to space limitations, did not show any clear difference between morning and afternoon measurements.
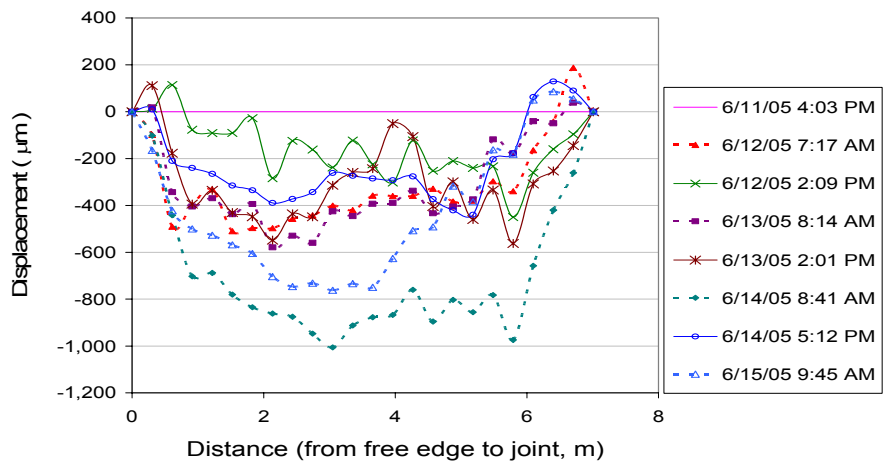
(a)
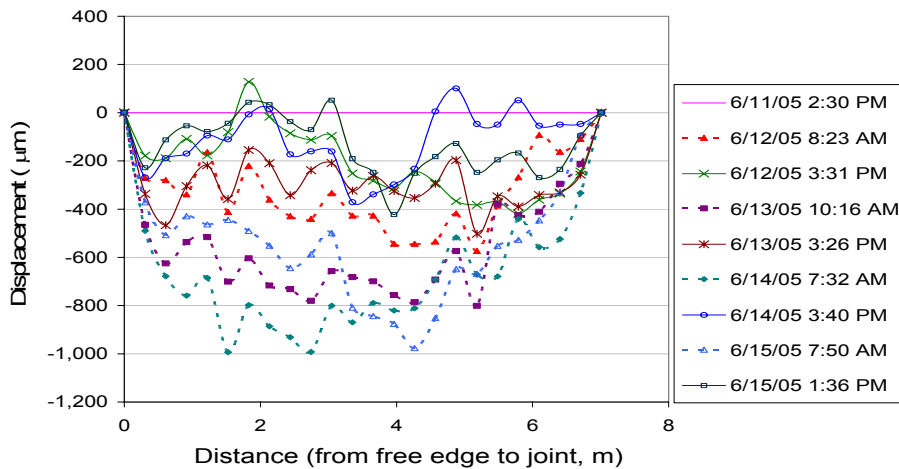
(b)

Figure 8-4 Diagonal slab curvature profile: (a) test section 1; (b) test section 2

8.6 Smoothness Index Variations Due to Environmental Effects

The raw data measured with Rollingprofiler indicates the difference in height between the supports along the line being profiled (ICC., 2006). Even though the raw data can indirectly reflect the roughness of pavement, it is necessary to transform these data into a roughness index (or smoothness index) such as IRI or RN to identify the effect of deformation due to environmental loading on smoothness. The Pavement Profile Viewing and Analysis program (ProVAL) 2.5 was used to compute IRI and RN from the measured raw data. This software is a product of Federal Highway Administration (FHWA) research efforts and allows user to view and analyze pavement profile in many different ways (FHWA., 2004; Proval, 2006).

Figure 8-5 shows the variations in IRI and temperature differences between top and bottom of the slab for the two test sections. Since RN varies over a narrow range of 0 (the maximum possible roughness) to 5 (perfectly smooth), the variations in RN are separately presented in Figure 8-6. The temperature differences between slab top and bottom varied from -5.1 ^{o}C (-9.2 ^{o}F) to 13.5 ^{o}C (24.3 ^{o}F) during the experimental periods.
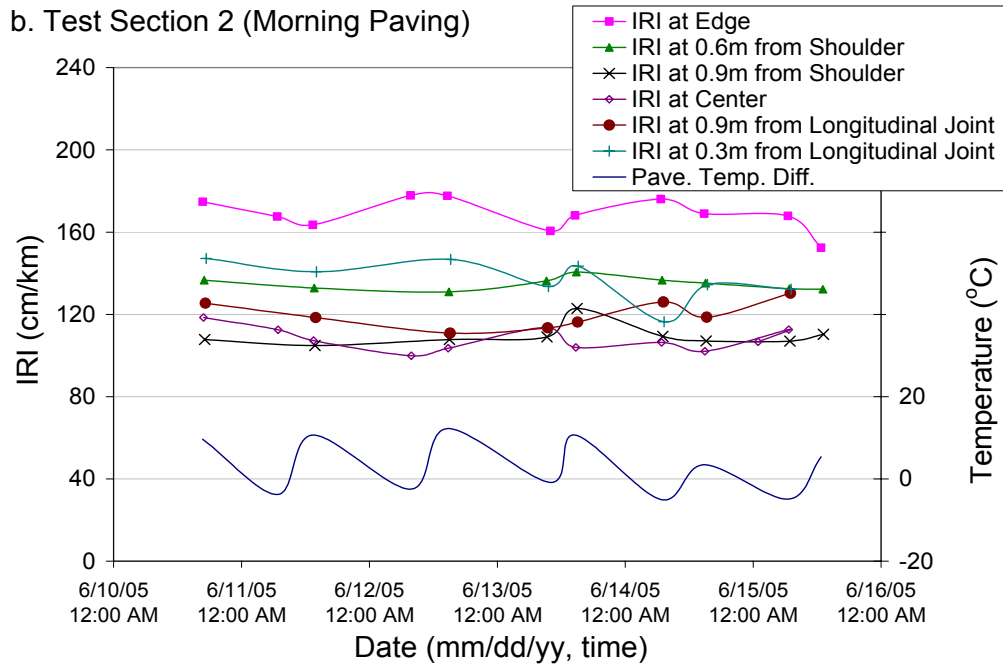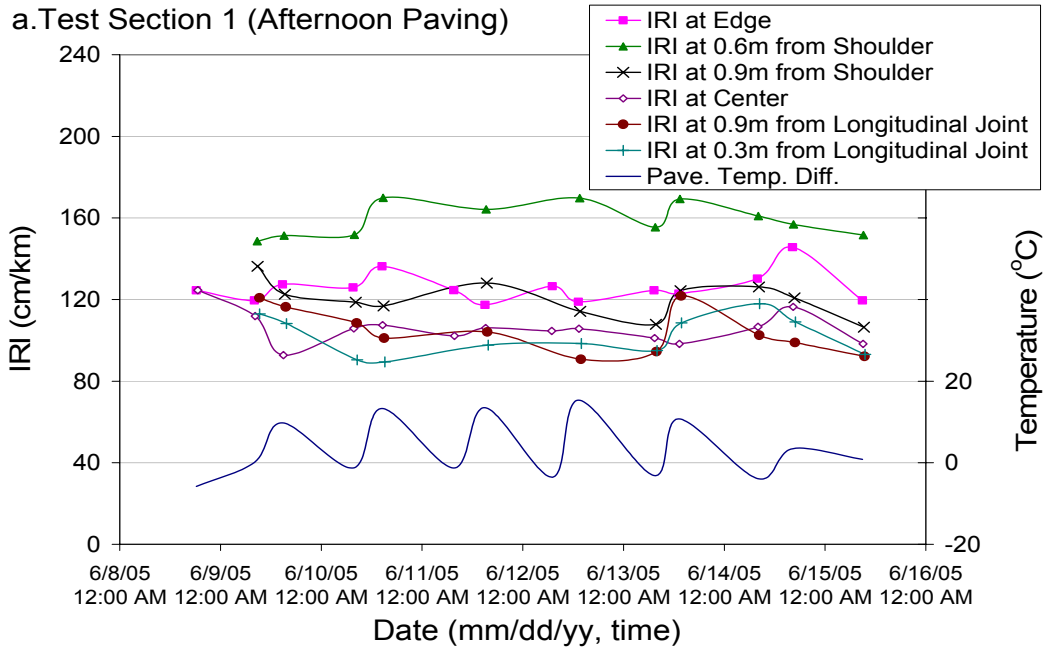
Figure 8-5 IRI and temperature difference variations during experiment periods: (a) test section 1; (b) test section 2
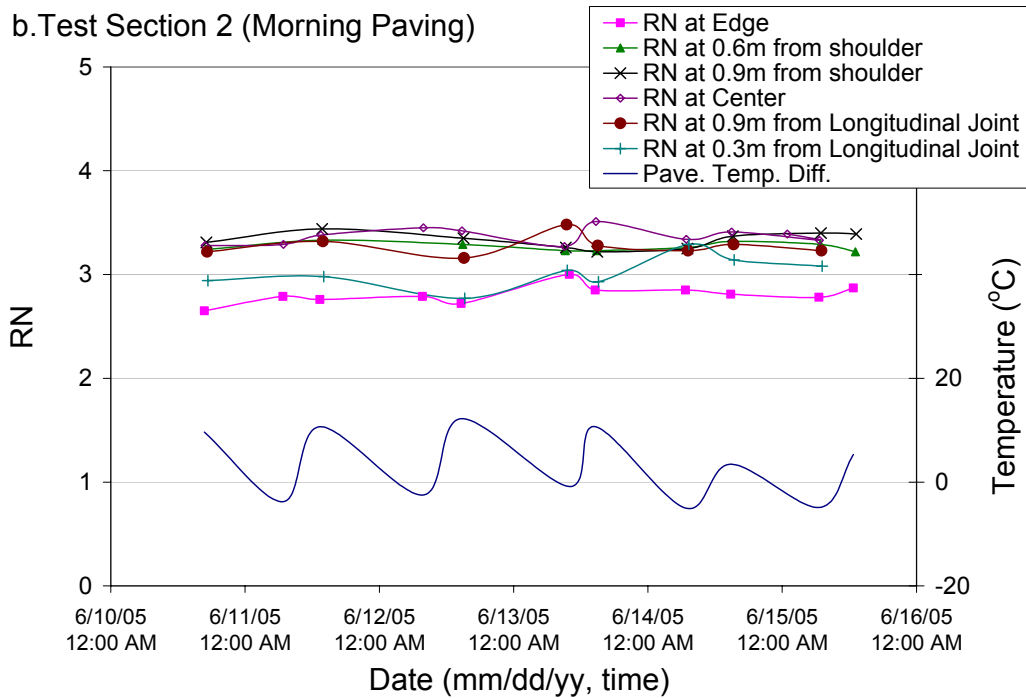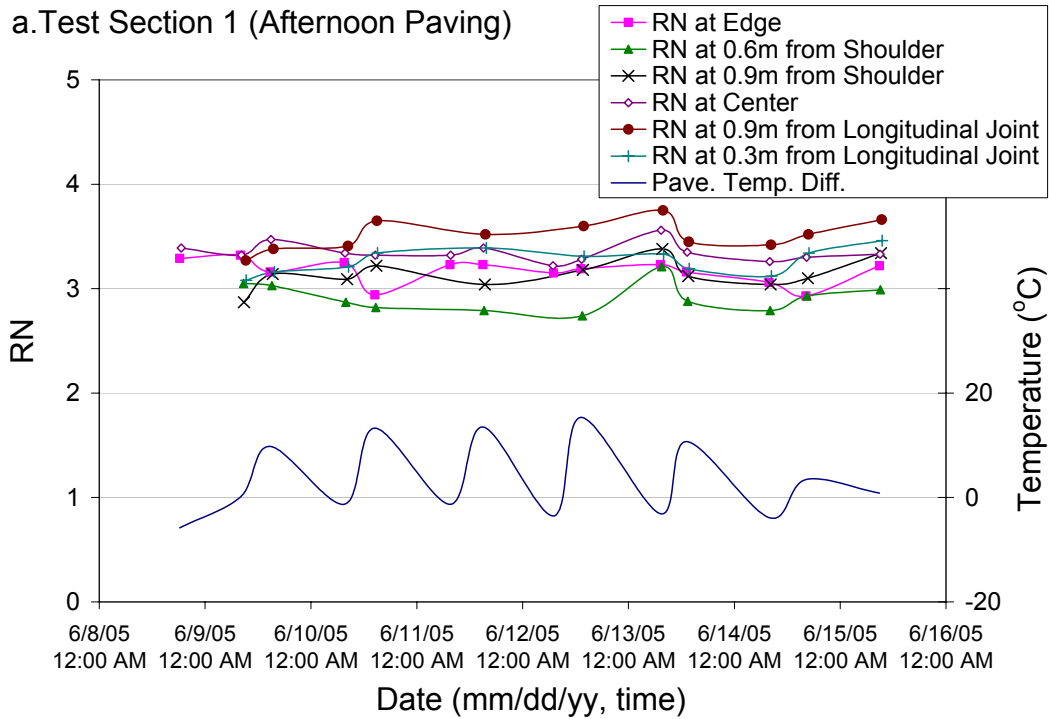
Figure 8-6 RN and temperature difference variations during experiment periods: (a) test section 1; (b) test section 2

There are variations with respect to measurement locations in both test sections 1 and 2 as reported by Karamihas et al. (1999). These results indicate that profiling measurement for quality control should be conducted along the actual traffic wheel-path of pavement to obtain consistent measurements. Although the measured IRI and RN showed some apparent variations with respect to measurement times (morning and afternoon), they may not be significant. To verify if these variations were statistically significant, a statistical test, Analysis of Variance (ANOVA), was conducted and the results are summarized in Table 8-1.

Table 8-1 ANOVA for the measured IRI and RN at different times

Test section number	IRI (cm/km)			RN		
	Mean @ morning measurement (negative temp. diff.)	Mean @ afternoon measurement (positive temp. diff.)	p-value	Mean @ morning measurement (Negative temp. diff.)	Mean @ afternoon measurement (Positive temp. diff.)	p-value
1	117.5	120.9	0.51	3.24	3.21	0.55
2	130.8	130.6	0.98	3.18	3.16	0.81

ANOVA results can be expressed in terms of p-value, which represent the weight of evidence for rejecting the null hypothesis (Ott and Longnecker, 2001). The null hypothesis of sample equality cannot be rejected if the p-value is greater than the selected significant level. From Table 8-1, all p-values are higher than 0.05 (95% significance level) which indicate that there is no significant difference in measured IRI and RN values with respect to measurement times.

8.7 FE Simulation of the Effect of Environmental Loadings on Pavement Smoothness

FE analyses were conducted to verify the findings based on field measurements. ISLAB 2000 and Ever FE 2.24 were chosen as the 2.5-D FE and 3-D FE models for this study. These two programs have evolved from earlier versions with validation using field data and can simulate field observed response very well (Wang, et al., 2006). In addition, these two FE- programs have some special advantages over other FE programs.

ISLAB 2000 was used as the main structural model for generating pavement responses in the new Mechanistic-Empirical Pavement Design Guide (MEPDG) under NCHRP 1-37 A project (2004). Even though basic element in this program is two-dimensional thin plate element, it can provide the pavement response on slab top and bottom. Thus, it can be classified as a 2.5-D FE program. EverFE 2.24 employs three-dimensional continuum elements for modeling the slab behavior. EverFE 2.24 is the only 3-D FE program among the FE programs specifically designed for modeling and analyzing rigid pavements (Davids, 2003).

The FE models were built with the actual geometric proportions and material properties from the test sections. Because both of these programs can simulate the slab deformation resulting from environmental loading in terms of temperature changes, it is required to establish the relation between actual measured temperature difference and equivalent temperature difference associated with the actual pavement behavior. Similar to the methodology adopted by previous researchers (Rao et al., 2001; Jeong and Zollinger, 2004; Beckemeyer et al., 2002), equivalent temperature differences for both

FE programs were back-calculated to generate the relative corner deflection to center profile measurements. Figure 8-7 shows that there is a linear relation between the equivalent temperature difference and the measured temperature difference. Although not presented in this paper due to space restrictions, this linear relation can be also observed in data collected in US 30 near Marshalltown, Iowa.
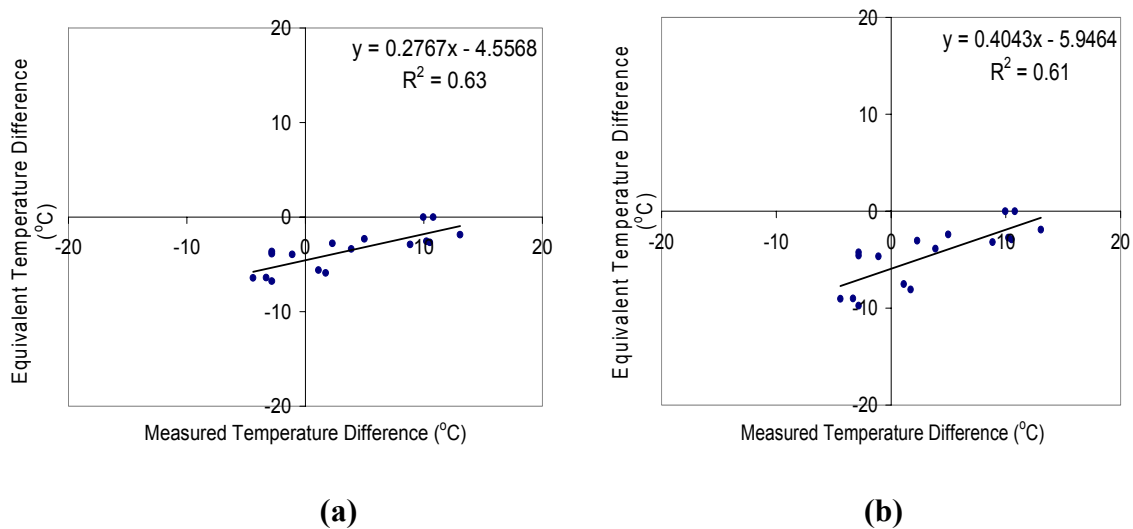

(a)   **(b)**

Figure 8-7 Equivalent temperature difference versus measured temperature difference in US-34 near Burlington, Iowa: (a) ISLAB 2000 results; (b) EverFE 2.24 results

Using the relation between equivalent and measured temperature differences, the predicted slab curvature profiles were generated using equivalent temperature difference as input parameter at different measurement times (morning and the afternoon). This predicted slab curvature profile by EverFE 2.24 and ISLAB 2000 can be used as input data into ProVAL 2.5 software to compute the IRI and RN values, as described by Kim et al. (2006).

The changes in field measured smoothness indices (IRI and RN) between afternoon measurements (positive temperature difference condition) and morning

measurements (negative temperature difference condition) are compared with the FE-based results in Table 8-2.

The changes in smoothness indices predicted by both of the FE programs provide good estimation of the measured values and suggest that the measurement times (morning versus afternoon) may have some influence over the predicted values. But, these variations with respect to measurement times may not be significant considering the smoothness criteria used in several states. Note that the range of IRI value from the bonus range to correction range is approximately 63.1 cm/km (40 in./mile) to 173.5 cm/km (110 in./mile) in several states (Smith et al., 2002; FHWA., 1999). These results have good agreement with the observations reported by Karamihas et al (2001) in which nine out of eleven pavements showed changes in IRI from early morning to late afternoon ranging from 9.5 cm/km (6 in./mile) to 39.4 cm/km (25 in./mile).

Although not discussed in this paper, it was interesting to observe that the JPCP smoothness indices were more sensitive to the deflection resulting from environmental loads at higher magnitudes of slab deflection as shown by FE simulation results (2006). Especially, considering the IRI criteria from the bonus range to correction range as approximately 60 cm/km (38 in./mile), slab deflections higher than 1.5 mm resulting from environmental loads could have significant influence on IRI.

Table 8-2 Comparison of measured and FE-predicted smoothness index changes

Sec.	Location	IRI changes between morning and afternoon			RN changes between morning and afternoon		
		Measured	Predicted with EverFe 2.24	Predicted with ISLAB2000	Measured	Predicted with EverFe 2.24	Predicted with ISLAB2000
		(cm/km)	(cm/km)	(cm/km)			
1	Edge	3.67	8.50	9.24	0.107	0.085	0.094
	0.6m from shoulder	9.89	8.14	8.49	0.117	0.079	0.082
	0.9m from shoulder	2.05	7.89	7.70	0.011	0.075	0.067
	Center	0.07	9.10	8.05	0.016	0.087	0.074
	0.9m from longi. joint	1.80	7.71	7.15	0.018	0.074	0.063
	0.3m from longi. joint	0.01	7.37	7.27	0.048	0.072	0.069
2	Edge	2.38	7.36	9.02	0.065	0.075	0.093
	0.6m from shoulder	0.42	7.92	9.35	0.012	0.075	0.088
	0.9m from shoulder	1.68	7.15	8.87	0.043	0.069	0.078
	Center	1.92	8.78	8.27	0.064	0.082	0.074
	0.9m from longi. joint	5.32	8.53	8.74	0.059	0.084	0.079
	0.3m from longi. joint	15.07	8.14	9.03	0.185	0.079	0.087

8.8 Conclusions

The newly constructed JPCP on US34 near Burlington, Iowa was instrumented to identify the early-age JPCP behavior in terms of pavement deflection due to environmental loads. In addition, the surface profile measurements in early morning and late afternoon were conducted to investigate the effect of the early-age curling and warping behavior on the initial smoothness of newly constructed concrete pavements. Temperature data obtained were analyzed. The slab deformations associated with

environmental loading were measured and analyzed through pavement surface profiles. The changes in smoothness indices (IRI and RN) at different measurement times were investigated and compared with FE-based predictions. Based on the observations of the measured data and the results of FE analyses, the following conclusions were drawn:

- Pavement temperatures were usually higher than ambient temperature. Except the day 0 of paving periods, the pavement temperature followed a pattern that is similar to that of ambient temperature.

- The diagonal slab curvature profiles measured in both test sections showed clearly upward curling for the measurements made in the morning and almost flat shape for the afternoon measurements. This behavior can be attributed to permanent curling and warping resulting from irrecoverable shrinkage due to non-uniform moisture distribution, early age curing conditions and temperature conditions during pavement construction.

- The measured IRI and RN values between morning and afternoon in both test sections showed some apparent variations, but these variations are not statistically significant.

- The changes in IRI and RN at different measurement times predicted by both the 2.5-D and 3-D FE programs provide good estimation of the measured values.

8.9 Acknowledgments

are responsible for the facts and accuracy of the data presented within. The contents do not necessarily reflect the official views and policies of the Federal Highway Administration. This paper does not constitute a standard, specification, or regulation.

8.10 References

AASHTO. TP60-00: Standard test method for coefficient of thermal expansion of hydraulic cement concrete, *AASHOTO'S Standard Specification for Transportation Materials and Methods of Sample and Testing,* 2000.

ASTM. C39-01: Standard Test Method for Compressive Strength of Cylindrical Concrete Specimens, *Annual Book of ASTM stand*ards, Vol. 04. 02, ASTM International, West Conshohocken, PA, 2001.

ASTM. C469-94: Standard test method for static modulus of elasticity and poisson's ratio of concrete in compression, *Annual Book of ASTM stand*ards, Vol. 04. 02, ASTM International, West Conshohocken, PA, 2001.

ASTM. C496-96: Standard test method for splitting tensile strength of cylindrical concrete specimens, *Annual Book of ASTM stand*ards, Vol. 04. 02, ASTM International, West Conshohocken, PA, 2001.

Akhter, M., Hussain, M., Boyer, J., and Parcells, W. J., 2002, "Factors Affecting Rapid Roughness Progression on Portland Cement Concrete Pavements in Kansas," *Transportation Research Record*, Vol. 1809, Transportation Research Board, Washington, D.C., pp 74-84.

Armaghani, J. M., Larsen, T. J., and Smith, L. L., 1987, "Temperature Response of Concrete Pavements," *Transportation Research Record*, Vol. 1121, Transportation Research Board, Washington, D.C., pp. 23-33.

Beckemeyer, C. A., Khazanovich, L., and Yu, H. T., 2002, "Determining Amount of Built-in Curling in Jointed Plain Concrete Pavement: Case Study of Pennsylvania I-80," *Transportation Research Record*, Vol. 1809, Transportation Research Board, Washington, D.C., pp 85-92.

Bradbury, R. D., 1938, *Reinforced Concrete Pavements*, Wire Reinforcement Institute, Washington, D.C.

Byrum, C. R., 2001, *A High Speed Profile Based Slab Curvature Index for Jointed Concrete Pavement Curling and Warping Analysis*, Ph.D. Thesis, University of Michigan, Ann Arbor, Michigan.

Byrum, C. R., 2000, "Analysis by High-Speed profile of Jointed Concrete Pavement Slab Curvatures," *Transportation Research Record*, Vol. 1730, Transportation Research Board, Washington, D.C., pp.1-9.

Chou, S. F. and Pellinen, T. K., 2005, "Assessment of Constriction Smoothness Specification Pay Factor Limits Using Artificial Neural Network Modeling," *Journal of Transportation Engineering*, Vol. 131, No.7, American Society of Civil Engineering, pp.563-570.

Davids, W.G., 2003, *EverFE Theory Manual*, University of Maine, Civil Engineering Department, Orono, Main, pp.1-18.

Federal Highway Administration (FHWA.), 1999, *Status of the Nation's Highways, Bridges, and Transit : Conditions and Performance Report*, Federal Highway Administration., Washington, D.C.

Federal Highway Administration (FHWA.), 2004, *Introducing Proval 2.0*, Product Brief, Federal Highway Administration Publication No. FHWA-HRT-04-154, Federal Highway Administration, Washington, D.C., pp1-2.

Hveem, F. N., 1951, "Slap Warping affects Pavement Joint Performance," *Proceedings of American Concrete Institute*, Vol. 47, pp. 797-808.

International Cybernetics Corporation (ICC.), 2006, http://www.internationalcybernetics.com/ rollprofile.htm, accessed May, 2006.

Janssen, D. J., 1987, "Moisture in Portland Cement Concrete," *Transportation Research Record*, Vol. 1121, Transportation Research Board, Washington, D.C., pp. 40-44.

Janoff, M. S., 1990, "The Prediction of Pavement Ride Quality from Profile Measurements of Pavement Roughness," *Surface Characteristic of Roadways: International Research Technologies*, ASTM STP 1031, American Society of Testing and Materials, Philadelphia, Pennsylvania, pp.259-267.

Jeong, J. H. and Zollinger, D. G., 2004, "Insights on Early Age Curling and Warping behavior from Fully Instrumented Test Slab System," *CD-ROM Proceedings of the 83rd Annual Meeting of the Transportation Research Board*, Transportation Research Board, Washington, D.C.

Jeong, J. H. and Zollinger, D. G., 2005, "Environmental Effects on the Behavior of Jointed Plain Concrete," *Journal of Transportation Engineering*, Vol. 131, No. 2, American Society of Civil Engineering, pp.140-148.

Karamihas, S. M., Gillespie, T. D., Perera, R. W., and Kohn, S. D., 1999, *Guidelines for Longitudinal Pavement Profile Measurement*, National Cooperative Highway Research Program Report 434, Transportation Research Board, Washington. D.C.

Karamihas, S. M., Perera, R. W., Gillespie, T. D., and Kohn, S. D., 2001,"Diurnal Changes in Profile of Eleven Jointed PCC Pavement," *Proceedings of 7th International Conference on Concrete Pavements*, Orlando, Florida.

Ksaibati, K., Staigle, R. and Adkins, T. M., 1995, "Pavement Construction Smoothness Specification in the United States," *Transportation Research Record*, Vol.1491, Transportation Research Board, Washington, D.C., pp.27-32.

Korovesis, G. T., 1990, *Analysis of SLAB on Grade Pavement Systems Subjected to Wheel and Temperature Loadings*, Ph.D. Thesis, University of Illinois, Urbana Champaign, Illinois.

Kim, S. H., Ceylan, H., Gospalakrishnan, K., and Wang, K., 2006, "The Effect of Slab Curvature due to Environmental Loading on Initial Smoothness of Jointed Plain Concrete Pavements," *Proceedings of the 6th International DUT-Workshop on Fundamental Modeling of Design and Performance of Concrete Pavements*, Old-Turnout, Belgium.

Lim, S. W. and Tayabji, S. D., 2005, "Analytical Technique to Mitigate Early-Age Longitudinal Cracking in Jointed Concrete Pavements," *Proceedings of 8th International Conference on Concrete Pavements*, Colorado Springs, Colorado.

National Cooperative Highway Research Program (NCHRP), 2004, *Guide for Mechanistic-Empirical Design of New and Rehabilitated Pavement Structures*,

http://trb.org/mepdg, National Cooperative Highway Research Program 1-37A,

Transportation Research Board, Washington, D.C.

Ott, L.R. and Longnecker, M., 2001, *An introduction to Statistical Methods and Data Analysis*, 5th edition, Duxbury, Pacific Grove, California.

Perera, R. W., Kohn, S. D. and Tayabji, S. D., 2005, *Achieving a High level of Smoothness in Concrete Pavement without Sacrificing Long-Term Performance*, Tech Brief, Feral Highway Administration Publication No. FHWA-HRT-05-068, Federal Highway Administration, Washington, D.C., pp1-4.

Proval. The Transtec Group, Inc., 2006, http://www.roadprofile.com, accessed January, 2006

Rao, C., Barenberg, E. J., Snyder, M. B., and Schmidt, S., 2001, "Effects of Temperature and Moisture on the Response of Jointed Concrete Pavements," *Proceedings of 7th International Conference on Concrete Pavements*, Orlando, Florida.

Rao, S. and Roesler, J. R., 2005, "Characterizing Effective Built in Curling from Concrete pavement Field Measurements," *Journal of Transportation Engineering*, Vol. 131, No. 4, American Society of Civil Engineering, pp.320-327.

Rasmussen, R. O., Karamihas, S. K. and Chang, C. K., 2002, *Inertial Profile Data for Pavement Performance Analysis : Project Overview*, Tech Brief Number 1, Federal Highway Administration Contact DTFH 61-02-C-00077, Federal Highway Administration, Washington, D.C.

Rasmussen, R. O., Karamihas, S. K., Cape, W. R., Chang, C. K. and Guntert, R. M., 2004, "Stringline Effects on Concrete Pavement Construction," *Transportation*

Research Record, Vol. 1900, Transportation Research Board, Washington, D.C., pp 3-11.

Sayers, M. W. and Karamihas, S. M., 1998, *The Little Book of Profiling*. University of Michigan, Ann Arbor, Michigan.

Siddique, Z. Q., Hossain, M., Devore, J., and Parcells, W. H., 2003, "Effect of Curling on As-constructed and Early Life Smoothness of PCC Pavements," *Proceedings of 2003 Mid-Continent Transportation Research Symposium*, Ames, Iowa.

Sixbey, D., Swanlund, M., Gagarin, N. and Mekemson, J. R., 2001, "Measurement and Analysis of Slab Curvature in JPC Pavements Using Profiling Technology," *Proceedings of 7th International Conference on Concrete Pavements*, Orlando, Florida.

Smith, K. L., Clover, L. T., and Evans, L. D., 2002, *Pavement Smoothness Index Relationships*. Technical Report FHWA- RD- 02-057, Federal Highway Administration, Washington, D.C.

Smith, K. L., Smith, K. D. Evans, L. D., Hoerner, T. E., Darter, M. I., and Woodstrom, J. H., 1997, *Smoothness Specifications for Pavements*. National Cooperative Highway Research Program Web Document No. 1, Transportation Research Board, Washington, D.C.

Sondag, S. K. and Snyder, M. B., 2006, "Analysis of "built-in" Curling and Warping of PCC Pavements," *Proceedings of the 6th International DUT-Workshop on Fundamental Modeling of Design and Performance of Concrete Pavements*, Old-Turnout, Belgium, September 2006.

Thomlinson, J., 1940, "Temperature Variations and Consequent Stresses Produced by Daily and Seasonal Temperature Cycle in Concrete Slabs," *Concrete and Constructional Engineering*, Vol. 36, No. 6, pp. 298-307 and No. 7, pp. 352-360.

Vandenbossche, J. M. and Snyder, M. B., 2005, "Comparison between Measured Slab Profiles of Curled Pavements and Profile Generated Using the Finite Element Method," *Proceedings of 8th International Conference on Concrete Pavements*, Colorado Springs, Colorado.

Vandenbossche, J. M., 2003, *Interpreting Falling Weight Deflectometer Results for Curled and Warped Portland Cement Concrete Pavements*, Ph.D. Thesis, University of Minnesota, Minneapolis, Minnesota.

Wang, W., Basheer, I. and Petros, K. "Jointed Plain Concrete Pavement Models Evaluation," CD-ROM, *Presented at 85th Annual Transportation Research Board Meeting, Transportation Research Board*, Transportation Research Board, Washington, D.C., 2006.

Westergaard, H. M.,1926, "Analysis of Stressed in Concrete Pavements Due to Variations of Temperature," *Proceedings of Highway Research Board*, Vol. 6, National Research Council, Washington, D.C., pp.201-217.

Westergaard, H. M., 1927, "Theory of Concrete Pavement Design," *Proceedings of Highway Research Board*, Part I, pp. 175-181.

Yu, H. T., Khazanovich, L. Darter, M. I, and Ardani, A., 1998, "Analysis of Concrete Pavement Response to Temperature and Wheel Loads Measured from Instrumented Slab," *Transportation Research Record*, Vol. 1639, Transportation Research Board, Washington, D.C., pp. 94-101.

Yu, H. T., Khazanovich, L., and Darter, M. I., 2004, "Consideration of JPCP Curling and Warping in the 2002 Design Guide," CD-ROM Proceedings of the 83rd Annual Meeting of the Transportation Research Board, Transportation Research Board, Washington, D.C.

CHAPTER 9. GENERAL CONCLUSIONS

9.1 Summary

In this study, the early-age deformation characteristics of Jointed Plain Concrete Pavements (JPCP) subjected to environmental loads was investigated. Two newly constructed JPCP test sections; one on highway US-34 near Burlington and the other on US-30 near Marshalltown, Iowa were instrumented and monitored during the critical time (seven days) immediately following construction on summer of 2005. A series of laboratory tests were conducted at various times to characterize the fundamental physical properties of the in-situ paving materials.

Temperature data and moisture data obtained from both sites were analyzed and presented. The slab deformations associated with temperature and moisture were analyzed through vertical displacement or pavement surface profiles. The relation between the temperature and moisture variations and the measured slab deflection was discussed.

The early-age deformation behavior of instrumented JPCP under environmental loading was simulated using ISLAB 2000 (2-D) and EverFE 2.24 (3-D) Finite Element (FE) programs and response analysis was performed. Sensitivity analyses of input parameters used in ISLAB 2000 and EverFE 2.24 were conducted to identify the critical inputs having the most influence on slab deflection under environmental loading. In order to combine all the active environmental effects in terms of temperature differences, the equivalent temperature difference concept (which is the temperature difference

corresponding to actual slab deformation under environmental loading) was quantified using the LVDT measurements and the measured slab curvature profiles, and utilized as inputs for both the FE-programs. A total of 228 comparisons between the field measured and the FE computed slab curvature profiles were conducted and discussed.

Using surface profile measurements following future traffic direction (longitudinal direction) on different locations of the test section during the morning and afternoon diurnal cycles, the smoothness index (or roughness index) such as IRI and RN were computed using ProVAL 2.5. The differences in pavement smoothness index between different measurement times corresponding to positive/negative temperature differences were studied. The slab curvature profiles generated using ISLAB2000 and EverFE software were also used to compute the smoothness index produced by slab deformation under environmental loading. The measured changes in smoothness indices with respect to measurement times were compared with their FE predicted counterparts.

The major study findings corresponding to each study objective are as follows:

1. Understand the early-age behavior of JPCP subjected to environmental loads

- Pavement temperatures were usually higher than ambient temperature. Except the day zero of paving periods, the pavement temperature followed a pattern that is similar to that of ambient temperature.

- The temperature differences usually are positive at daytime and early nighttime and negative at late nighttime and early morning while moisture differences show the reverse trend. Especially, at day 0 and day 1 after paving, the moisture differences (between the top and bottom of the slab) observed in test section of US-30 Marshalltown are negative for most of the times

resulting in a higher drying shrinkage near the top slab and then causing the corner of the slab to warp upward.

- The magnitude of LVDT measurements observed in test section of US-30 Marshalltown varied within a small range of ± 130 μm (± 5 mils). Nonetheless, the influence of temperature variations on the LVDT measured vertical displacements could be observed. Especially, the upward slab curling associated with a negative temperature gradient was more evident compared to the downward slab curling.

- The diagonal slab curvature profiles measured in both test sites showed clearly upward curling for the measurements made in the morning and almost flat shape for the afternoon measurements. This behavior can be attributed to permanent curling and warping resulting from irrecoverable shrinkage due to non uniform moisture distribution, early age curing conditions and temperature conditions during pavement construction.

- Slab curvature behavior measured from the profile testing and the LVDT readings show similar trends.

2. Examine and develop Finite Element based models for studying JPCP subjected to pure environmental loading at critical periods immediately after construction

- Temperature difference and Coefficient of Thermal Expansion (CTE) are the most sensitive parameters to calculated slab deformations due to temperature based on ISLAB 2000 and EverFE2.24 FE analyses for typical rigid pavement geometry used in Iowa.

- The estimated deflection resulting from temperature by ISLAB 2000 is 26 % higher for positive temperature difference conditions and 38 % higher for negative temperature difference conditions compared to EverFE 2.24 predictions.

- A linear relation was observed between the actual measured temperature difference ($\Delta T_{\text{trans-temp-diff}}$) and equivalent temperature difference (ΔT_{etd}) associated with actual slab displacement under pure environmental loading.

- The coefficient and the independent variable of the linear regression equation could be related to the transient component of equivalent temperature difference ($\Delta T_{\text{transient}}$) and the intercept of the regression equation could be related to the permanent component of equivalent temperature difference ($\Delta T_{\text{permanent}}$).

- Better comparisons were obtained when the equivalent temperature difference accounted for variability in PCC displacement due to actual moisture gradient variations which made the FE simulations more accurate.

- The permanent curling and warping temperature difference identified from this study ranged approximately from -4 $^{\circ}$C (-8 $^{\circ}$F) to -8.5 $^{\circ}$C (-15.3 $^{\circ}$F) on different sites, using measurement methods and FE-programs.

3. Investigate the effect of slab curvature resulting from environmental loading on the initial smoothness of concrete pavements.

- The measured IRI and RN values were different at different measurement locations within a test section.

- The measured IRI and RN were not considerably influenced by the limited range of temperature differences considered in this study.

9.2 Significance of Research Findings

The findings of this research can provide the following benefits to the pavement researchers and practitioners;

- Document pavement temperature variation and moisture variation for seven days after paving which are the important quality control periods for agencies and contractors.

- Document the slab curvature behavior without traffic loading for seven days after paving.

- Verify the environmental loading factors resulting in permanent curling and warping which will be an important contribution to advance the state-of-the art in mechanistic-empirical rigid pavement analysis and design.

- Examine different test techniques for measuring the early age slab deformation.

- Use of 2-D and 3-D FEM models for studying the early slab behavior due to environmental loads.

- Simulate the actual slab curvature behavior considering the permanent curling and warping with 3-D FEM models (EverFE 2.24).

- Investigate the effect of environmental loads on initial smoothness.

- Simulate initial smoothness variations in diurnal cycles due to environmental loads.

- Provide insight into PCC thermal properties input for the implementation of Mechanistic-Empirical Pavement Design Guide (MEPDG) by State Department of Transportations (DOTs).

9.3 Recommendations

It is important that the pavement engineers should understand the early–age JPCP behavior to apply the best construction method for the improvement of long–term JPCP performance. In addition, agencies should consider the factors resulting in the variation of profile measurements to obtain the accurate smoothness condition of pavement.

Based on the findings of this research, the followings recommendations are proposed for JPCP construction, smoothness evaluation, and future research.

9.3.1 Recommendations for JPCP Construction

The followings recommendation is suggested for JPCP construction to reduce JPCP deformation due to environmental loads.

- Schedule the paving time to maintain minimal temperature gradient change during the concrete hardening. JPCP placed during the daytime shows positive temperature gradient prior to hardening and experiences cooling at top surface after hardening, usually during the nighttime. This changing temperature gradient before and after hardening of concrete could result in permanent curling and warping, which can influence the JPCP performance. Since nighttime paving seems to reduce the permanent curling and warping by preventing the temperature gradient change before and after concrete

hardening, nighttime paving could be considered as an alternative in view of JPCP performance. However, nighttime paving can increase construction cost (productivity tends to be lower) and cause safety issues. To decide upon the paving time, a pavement engineer should strike a balance between the JPCP performance and construction issues by considering the pros and cons.

- Avoid the use of aggregates having high CTE value. Aggregate type is the one of most significant factors influencing the PCC curling behavior. Aggregates with higher CTE values can increase slab curling. In general, the CTE value of quartz and gravel (11.9×10^{-6} ε/ °C to 10.8×10^{-6} ε/ °C) is approximately twice that compared to limestone (6.8×10^{-6} ε/ °C), and therefore limestone aggregate may be more preferable for JPCP construction in this context.

- Apply curing method with uniform and adequate coverage over entire surface to prevent the loss of mixing water from the surface of concrete. The rapid drying of moisture in an exposed slab surface can result in the drying shrinkage of concrete near the top of a slab and a higher saturated condition at the bottom of a slab. This moisture difference through the slab depth can cause non-uniform concrete shrinkage and non-uniform volume changing as function of depth. Caution is necessary when curing is being done.

9.3.2 Recommendations for JPCP Smoothness Evaluation

Agencies should understand the following items to judge and monitor JPCP smoothness condition.

- Conduct profile measurements along the actual traffic wheel-path of pavement to obtain consistent measurements.

- Pay attention to that the slab curvature behavior due to environmental loads can possibly influence the profile measurement.

9.3.3 Recommendations for Future Research

The followings recommendations are proposed for the future research;

- Develop more accurate and reliable test protocol to measure slab movement such as installing multi-depth deflection (MDD) gages underneath slab.

- Develop the laboratory or field test protocol for determining the shrinkage gradient in early-age PCC.

- Implement studies of the effects of parameters such as material properties (aggregate type, cementitious materials, etc), different curing techniques and compounds, slab thickness and geometry, and base type on permanent curling and warping.

- Verify/validate the proposed methodology of quantifying equivalent temperature difference by studying more sites and collecting long-term field test data.

- Investigate the rigid pavement response and curling and warping behavior associated with simultaneous traffic and environmental loading with experimental research.

- Identify the significance of internal stresses induced from slab deflection under environmental loading on early-age cracking.

- Exam the effects of seasonal and climatic changes on smoothness of rigid pavement and identify the periods when climate changes can significantly influence the smoothness.

APPENDIX 1 LABORATORY RESULTS

Split Tensile Strength with Time
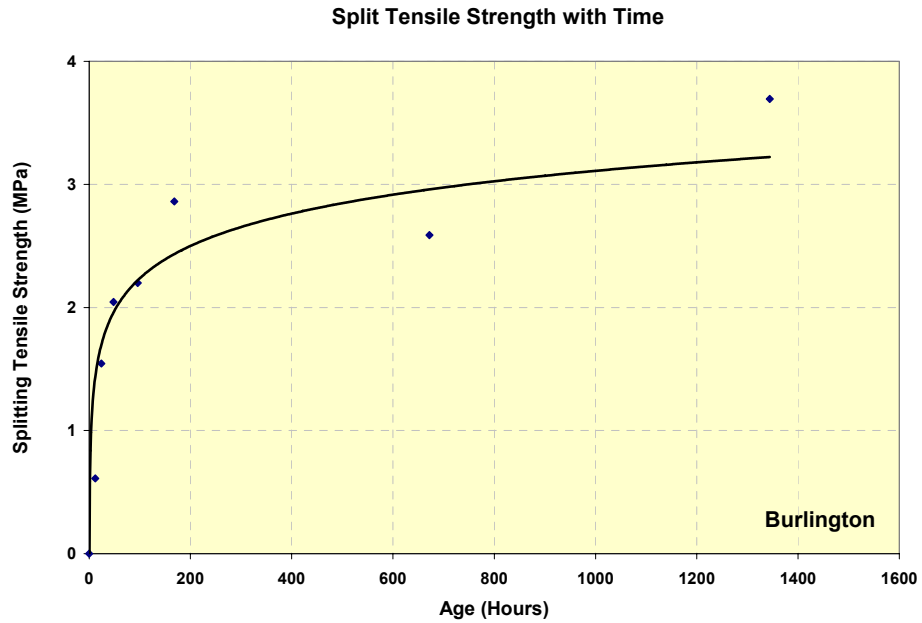
Figure A1-1 Split tensile strength with time for specimens in US-34, Burlington

Split Tensile Strength with Time
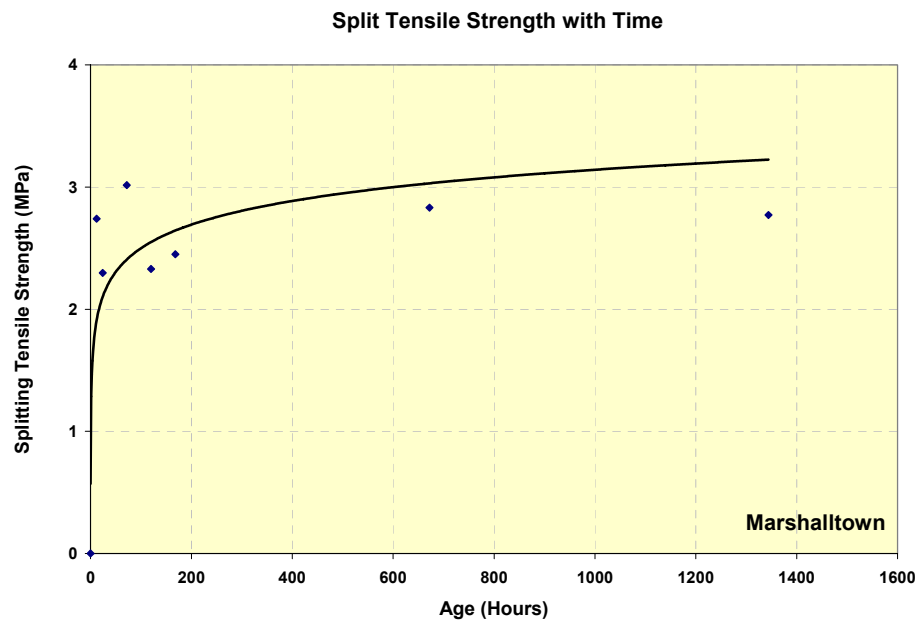
Figure A1-2 Split tensile strength with time for specimens in US-30, Marshalltown
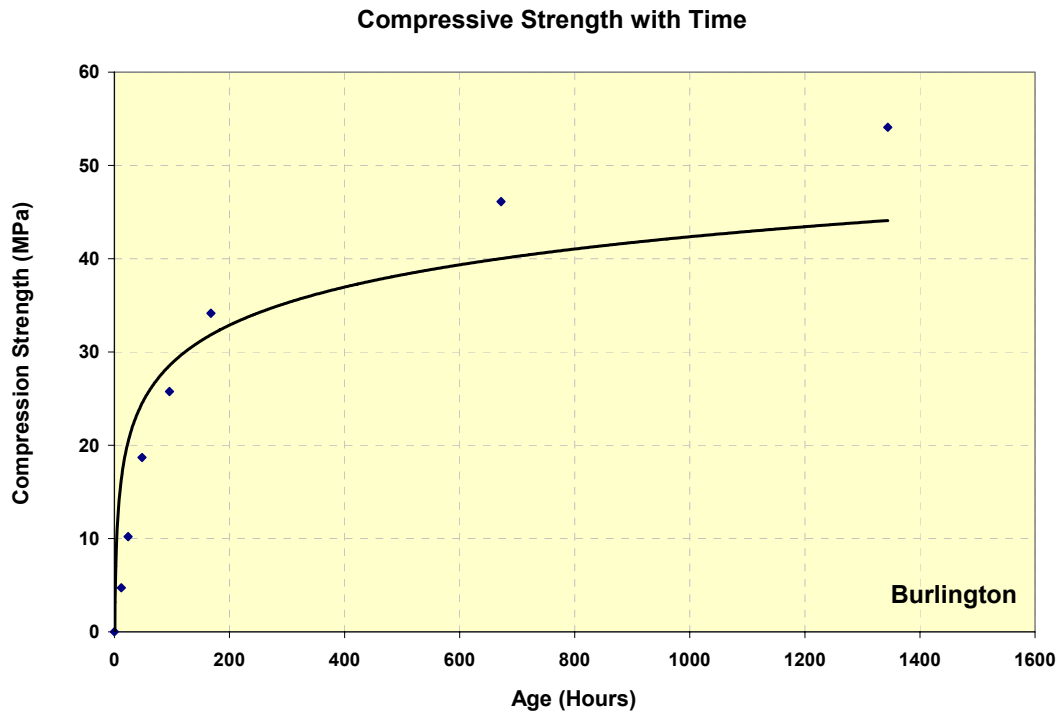
Figure A1-3 Compressive strength with time for specimens in US-34, Burlington
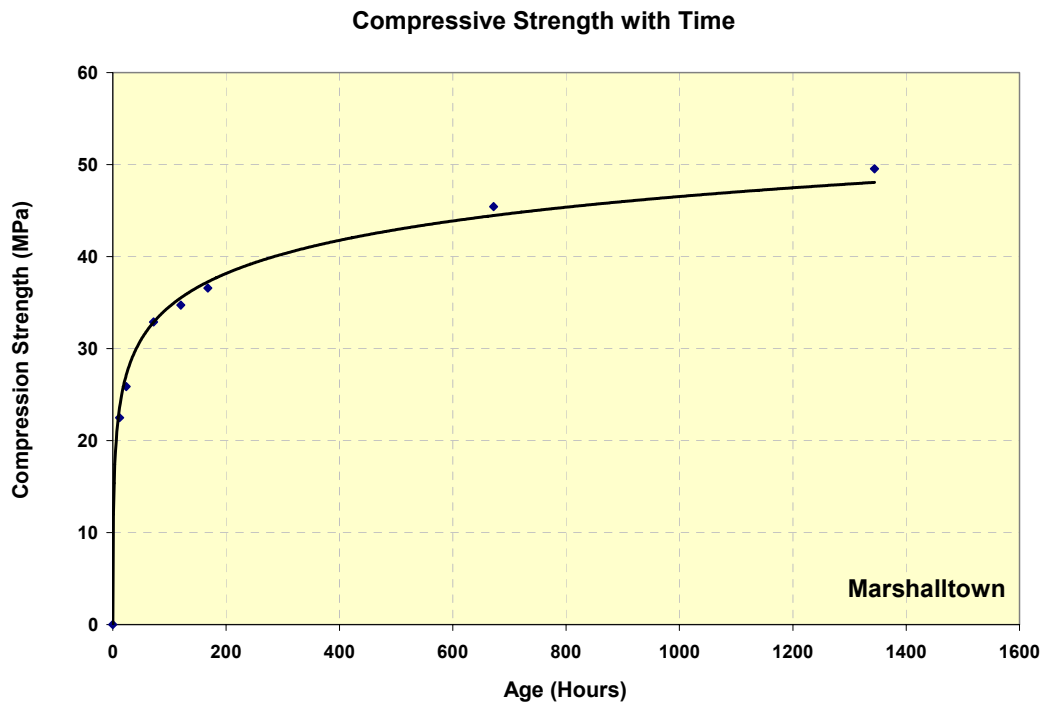
Figure A1-4 Compressive strength with time for specimens in US-30, Marshalltown

Modulus of Elasticity with Time
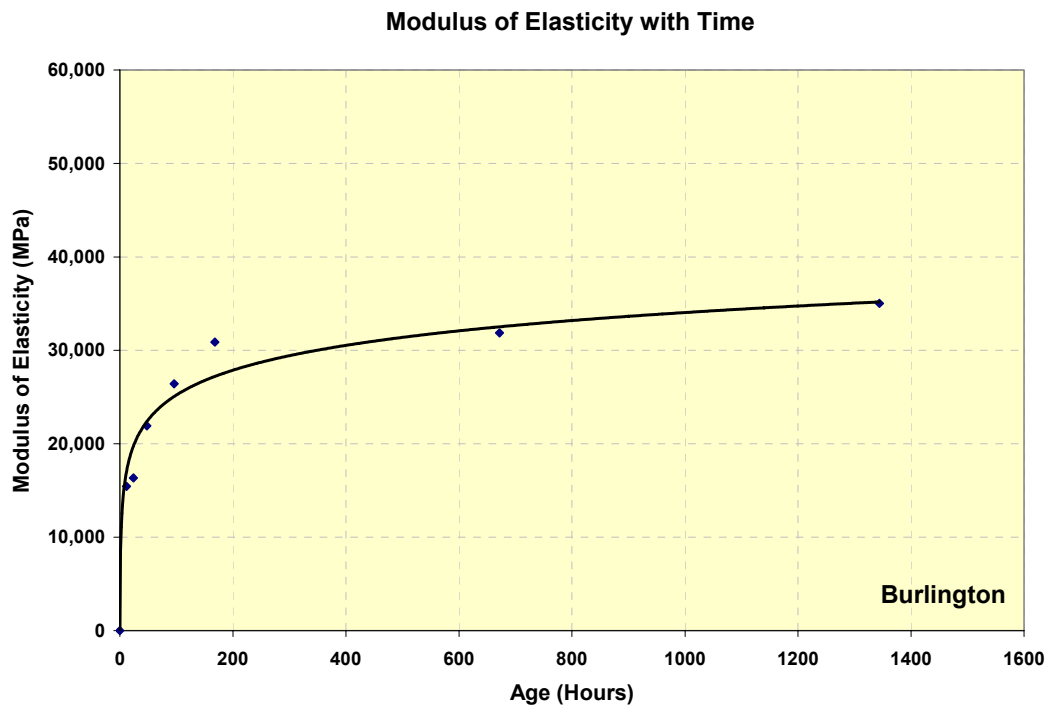
Figure A1-5 Modulus of elasticity with time for specimens in US-34, Burlington

Modulus of Elasticity with Time
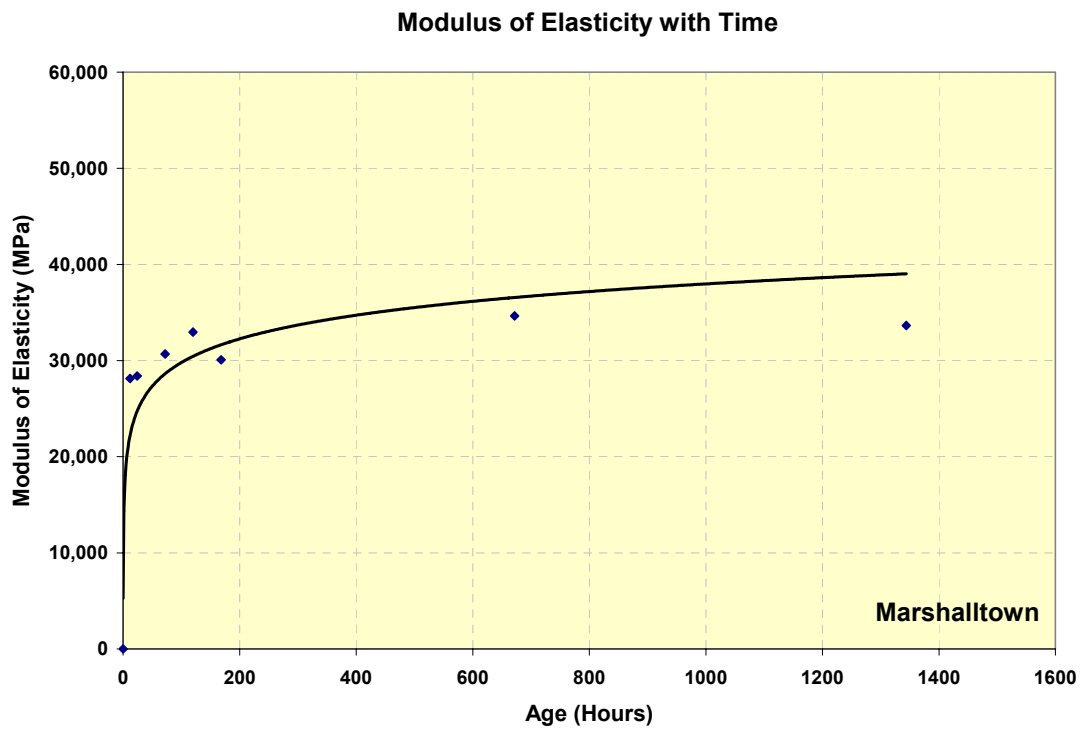
Figure A1-6 Modulus of elasticity with time for specimens in US-34, Marshalltown
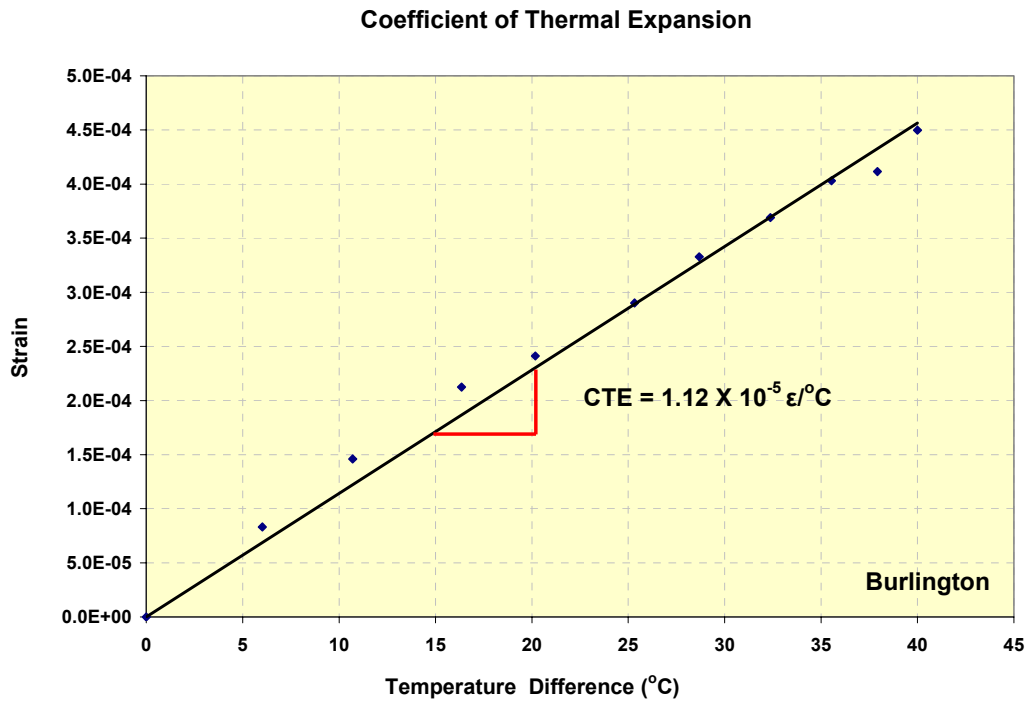
Figure A1-7 CTE for specimens in US-34, Burlington
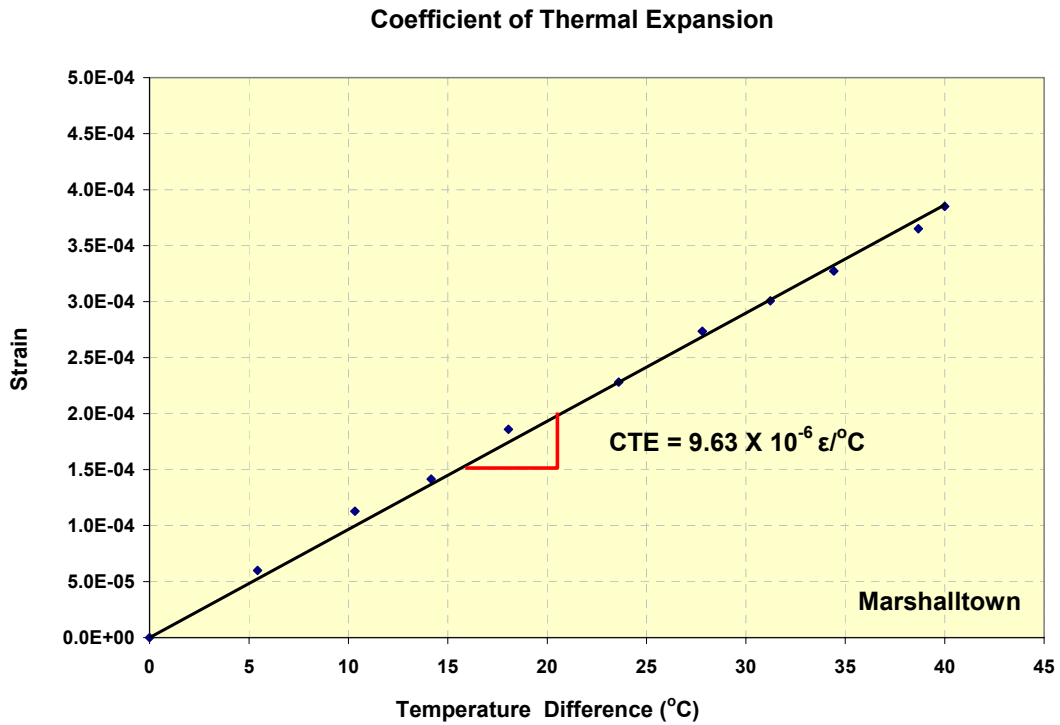
Figure A1-8 CTE for specimens in US-30, Marshalltown

Table A1-1 Summary of CTE test results for specimens in US-34, Burlington

I.D	CTE (ε/°C)	Average(ε/°C)	Range(ε/°C)
Specimen 1-1	1.20×10^{-05}	1.12×10^{-05}	1.55×10^{-06}
Specimen 1-2	1.13×10^{-05}		
Specimen 2	1.05×10^{-05}		
Specimen 3	1.12×10^{-05}		

Table A1-2 Summary of CTE test results for specimens in US-30, Marshalltown

I.D	CTE (ε/°C)	Average	Range
Specimen 1-1	9.55×10^{-06}	9.63×10^{-06}	1.57×10^{-06}
Specimen 1-2	9.66×10^{-06}		
Specimen 2	1.04×10^{-05}		
Specimen 3	8.87×10^{-06}		

APPENDIX 2 TEMPERATURE MEASUREMENT RESULTS
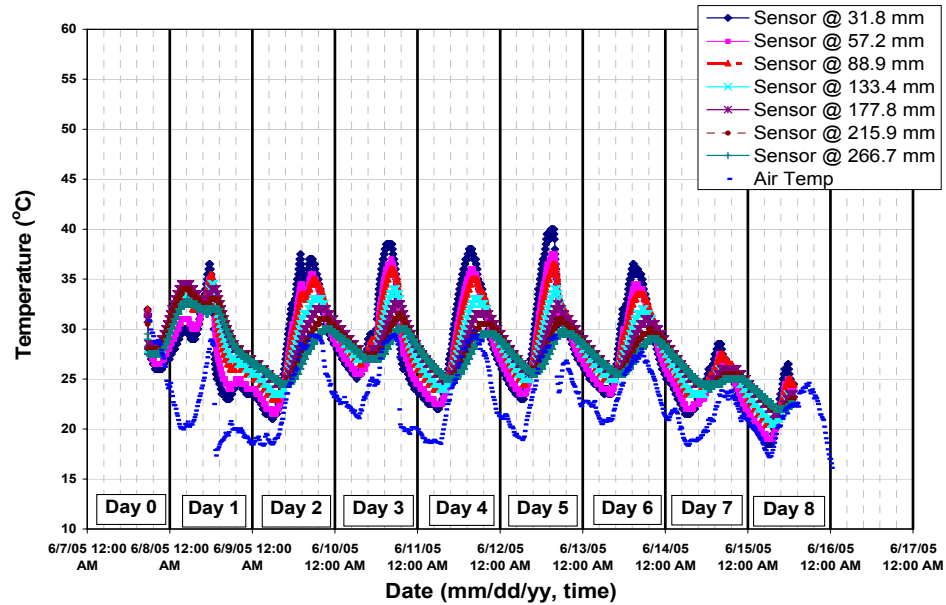
Figure A2-1 Temperature variation with time in test section 1 (afternoon paving) of US-34, Burlington
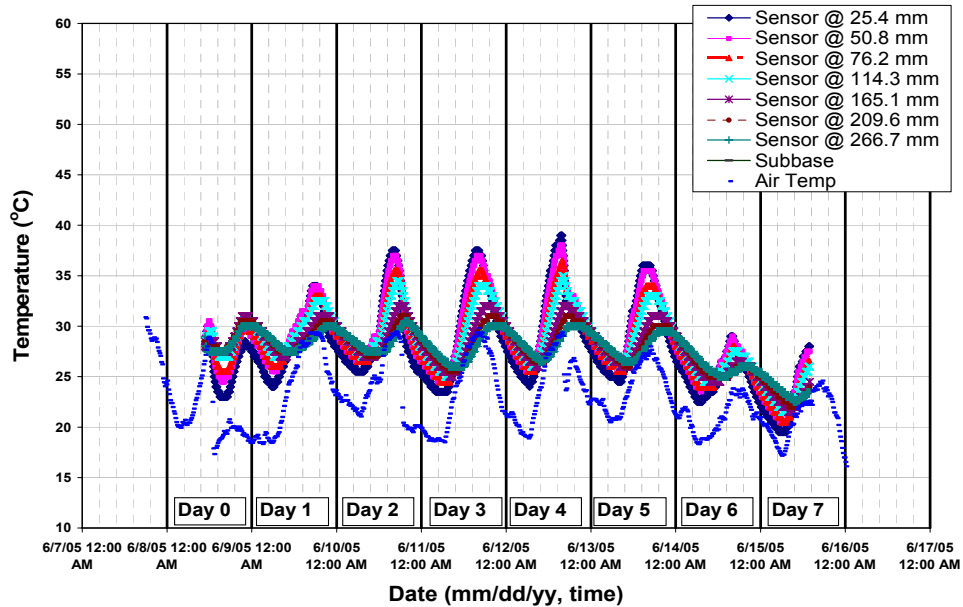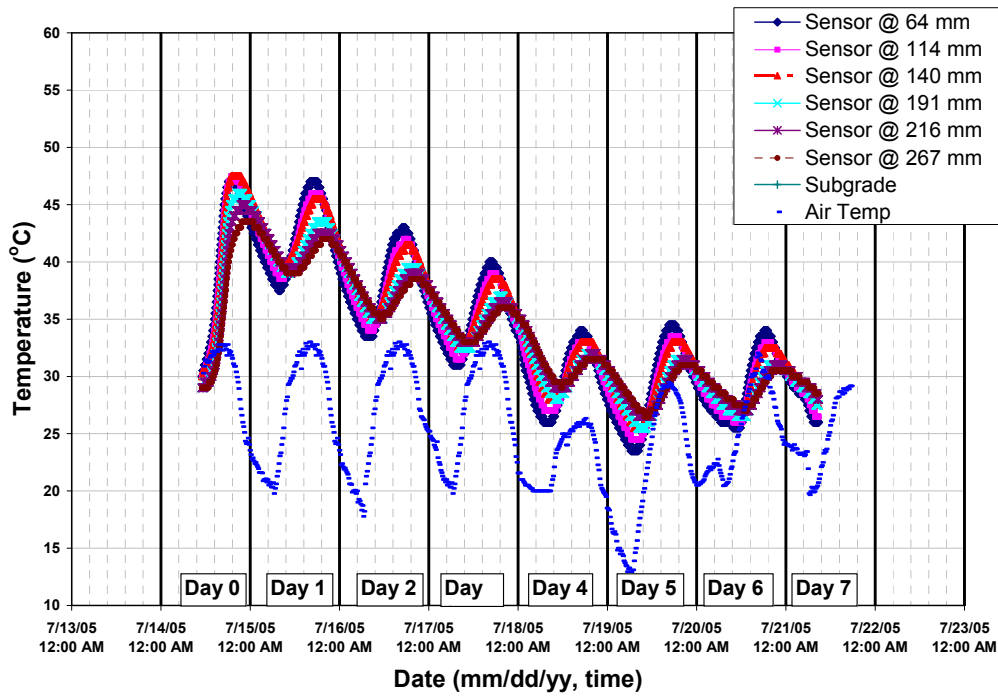

Figure A2-2 Temperature variation with time in test section 2 (morning paving) of US-34, Burlington
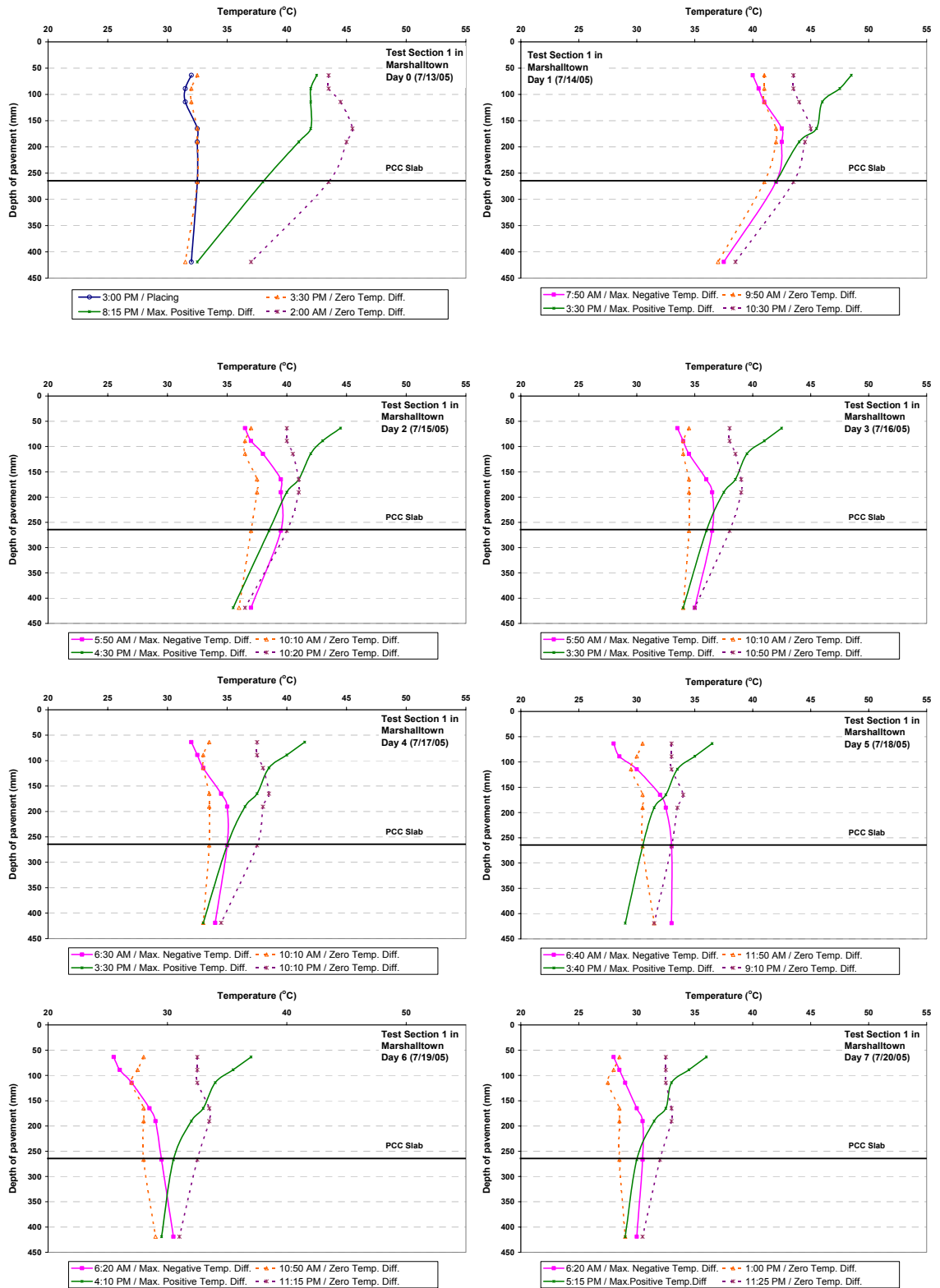
236
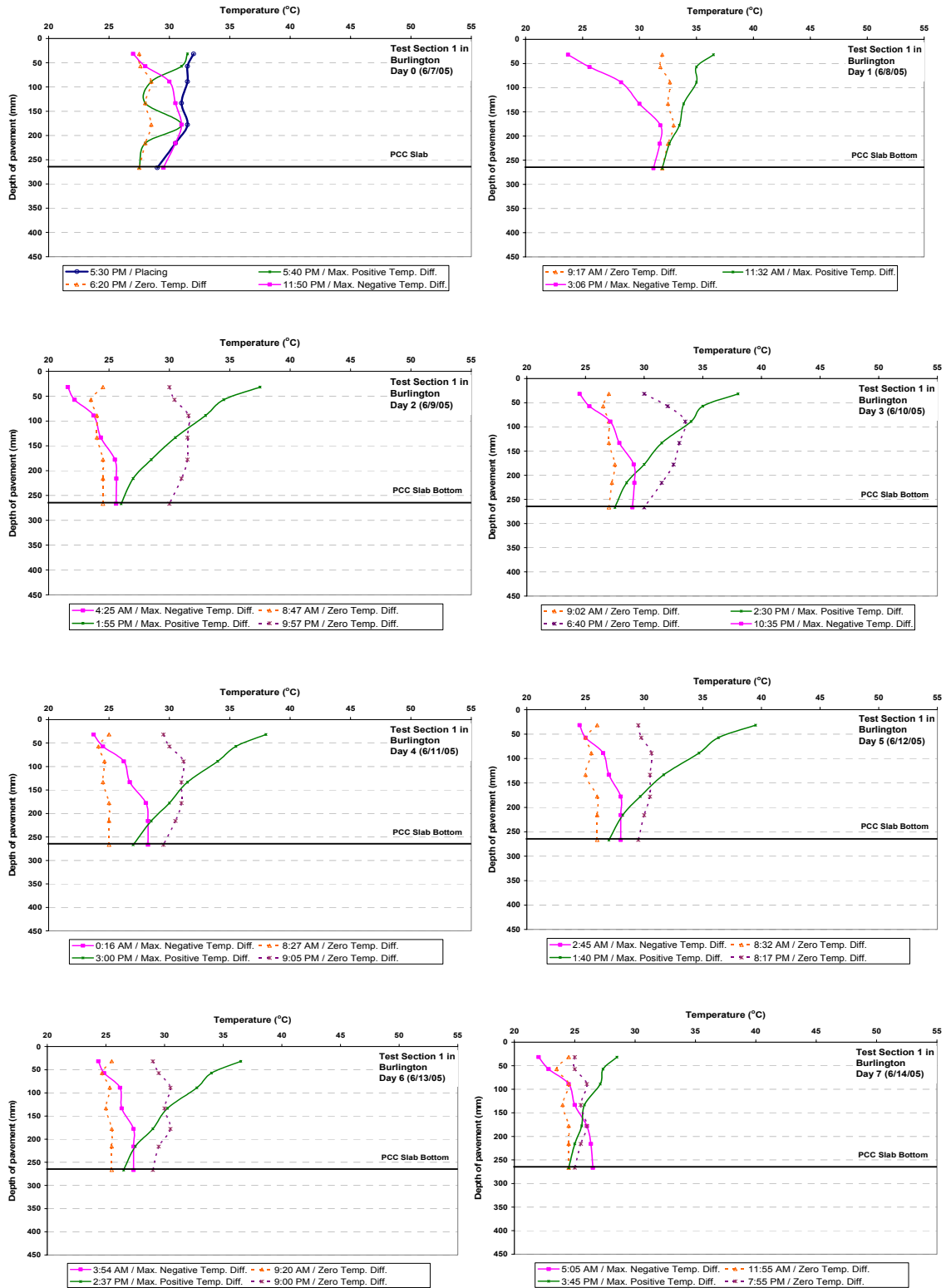
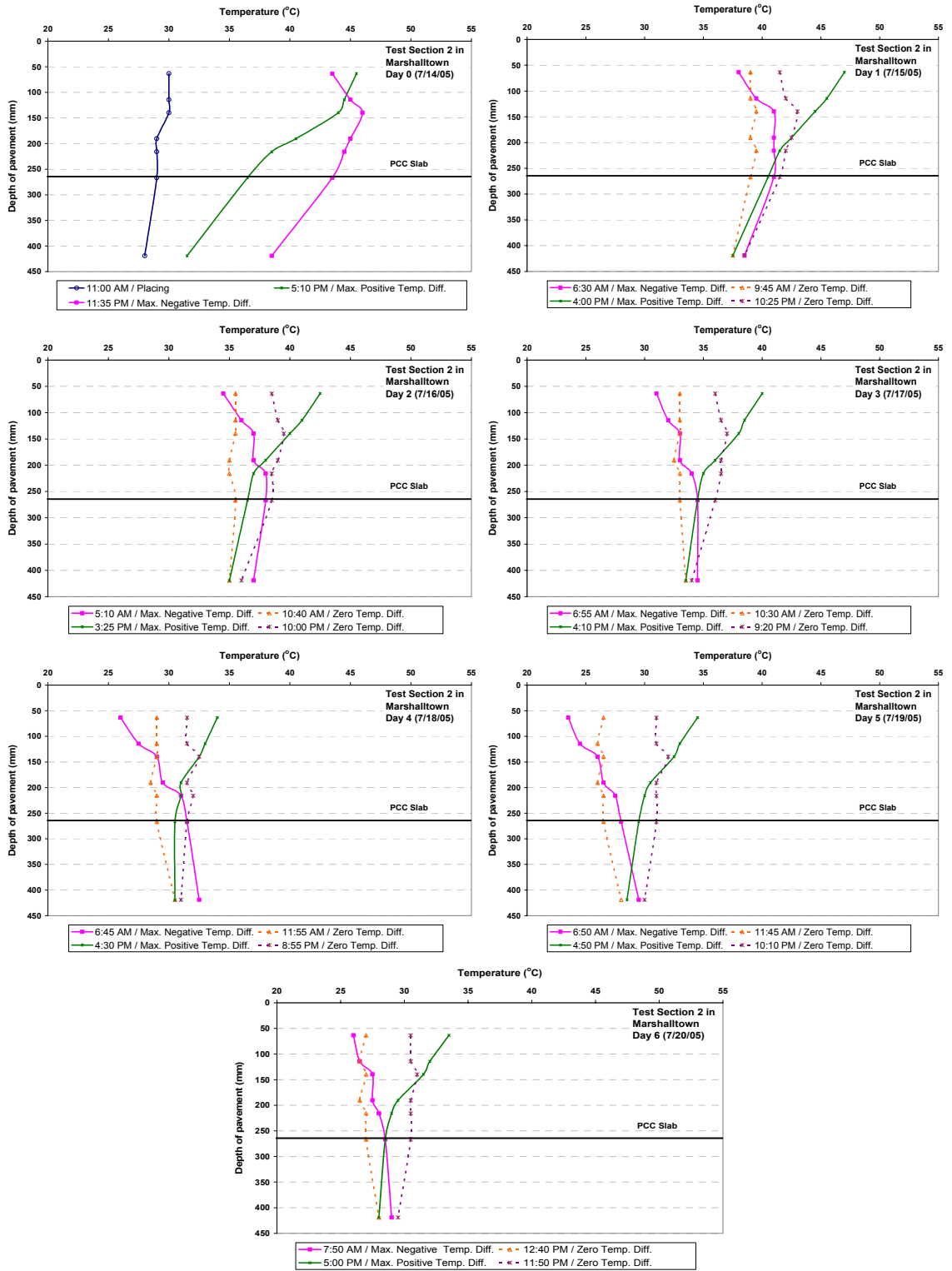**Figure A2-3 Temperature profile with depth in test section 1 (afternoon paving) of US-34, Burlington**
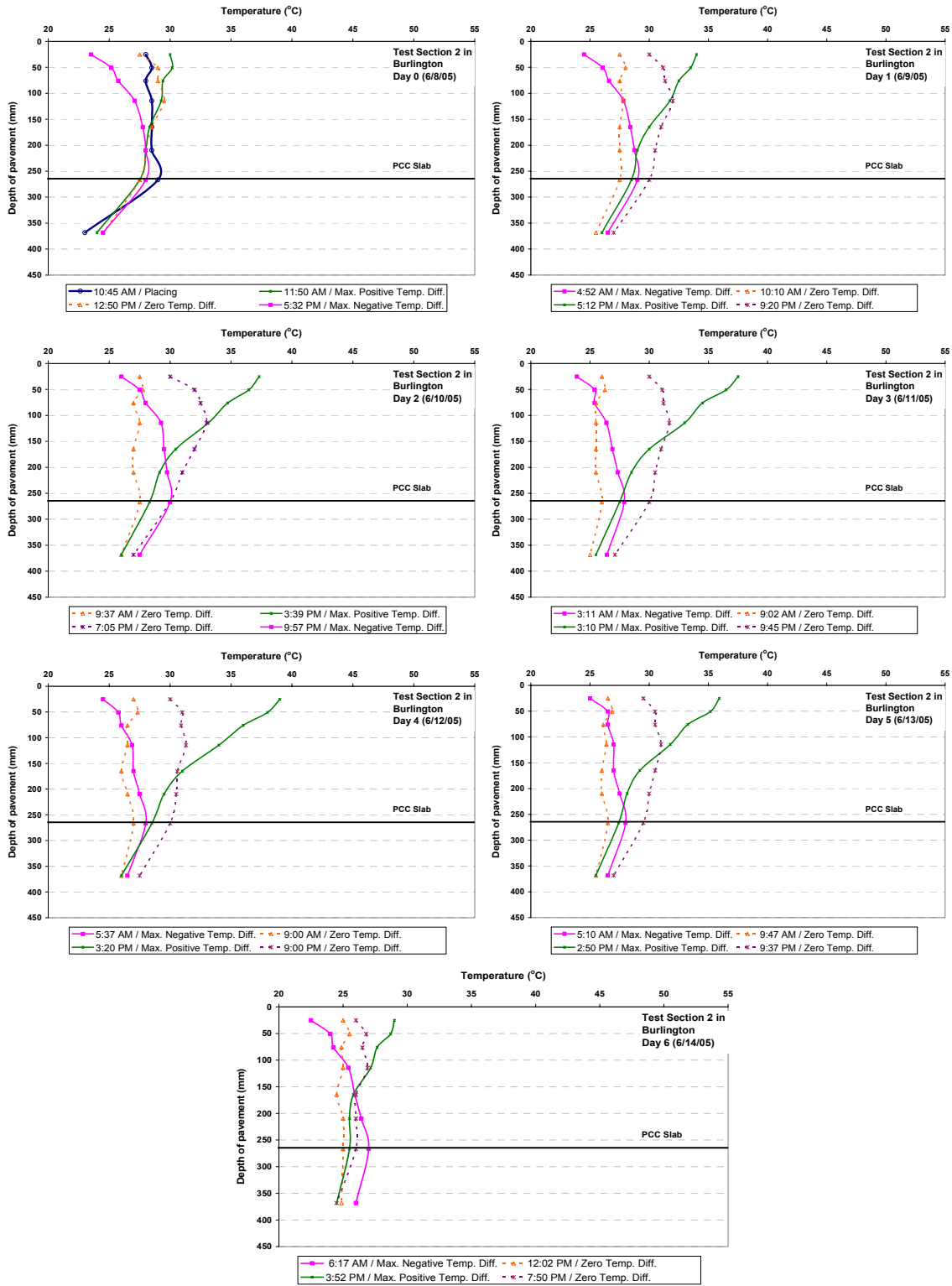
Figure A2-4 Temperature profile with depth in test section 2 (morning paving) of US-34, Burlington
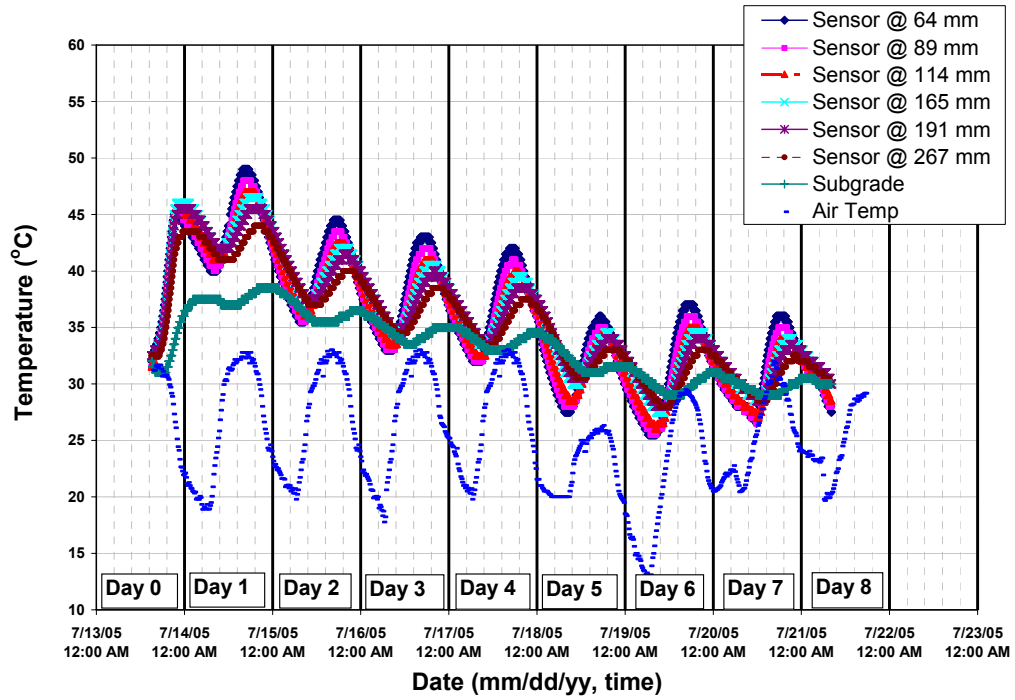
Figure A2-5 Temperature variation with time in test section 1 (afternoon paving) of US-30, Marshalltown

Figure A2-6 Temperature variation with time in test section 2 (morning paving) of US-30, Marshalltown

Figure A2-7 Temperature profile with depth in test section 1 (afternoon paving) of US-30, Marshalltown

Figure A2-8 Temperature profile with depth in test section 2(morning paving) of US-30, Marshalltown

APPENDIX 3 MOISTURE MEASUREMENT RESULTS
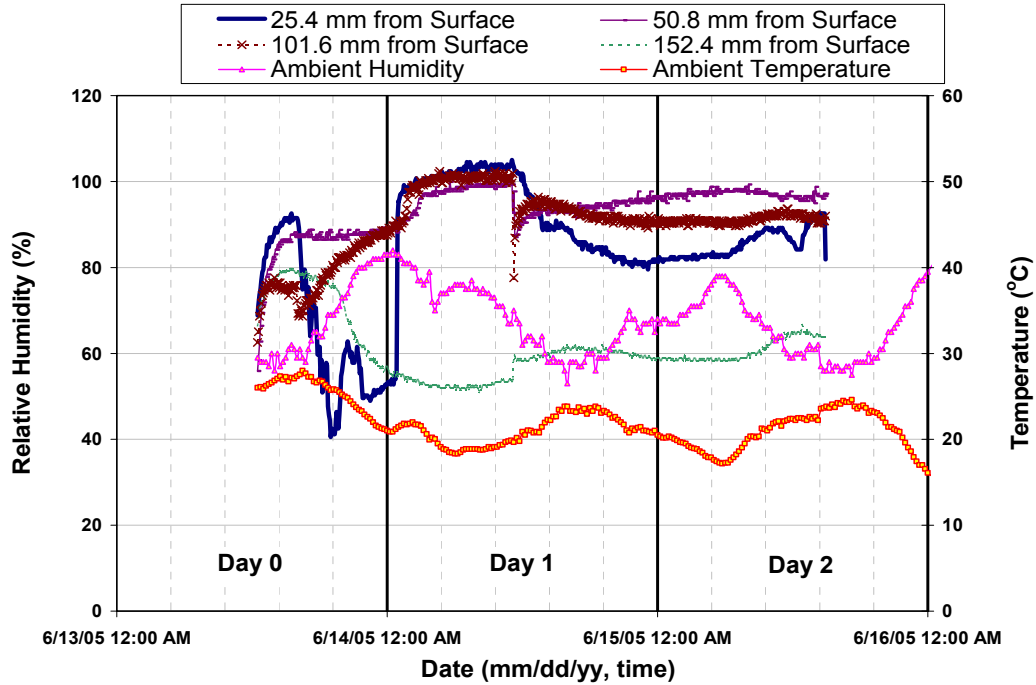
Figure A3-1 Moisture variation with time in US-34, Burlington
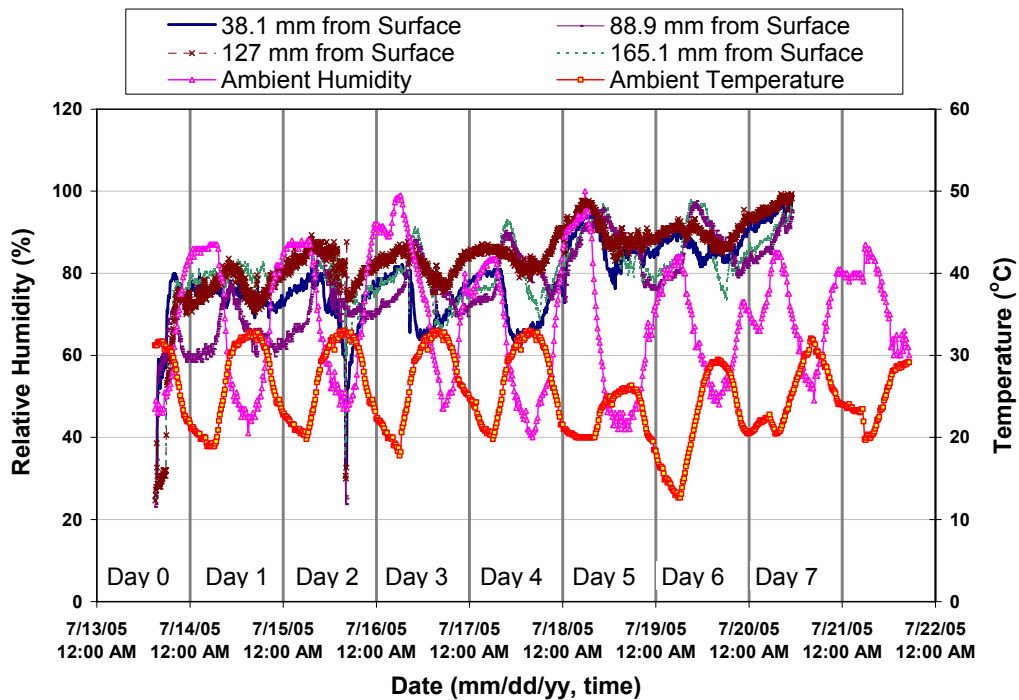
Figure A3-2 Moisture variation with time in US-30, Marshalltown
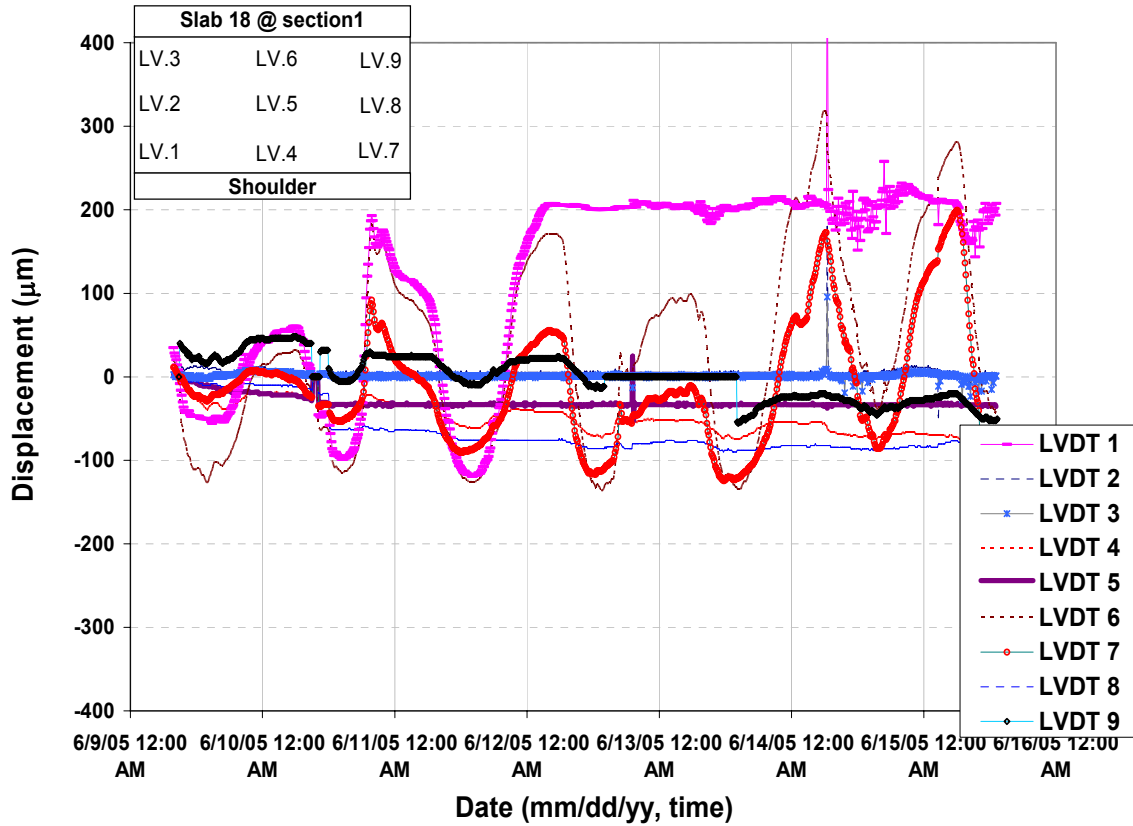
APPENDIX 4 LVDT MEASUREMENT RESULTS

Figure A4-1 LVDT measurements at slab 18 in test section 1 (afternoon paving) of US-34, Burlington
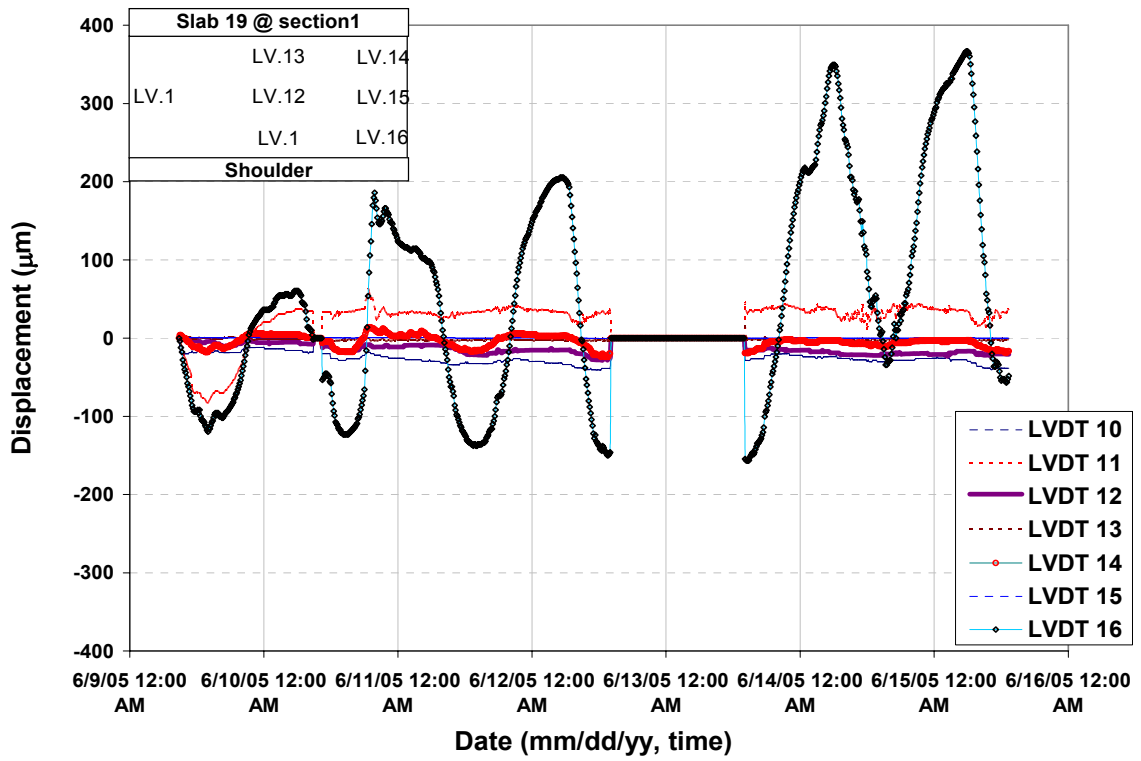
Figure A4-2 LVDT measurements at slab 19 in test section 1 (afternoon paving) of US-34, Burlington
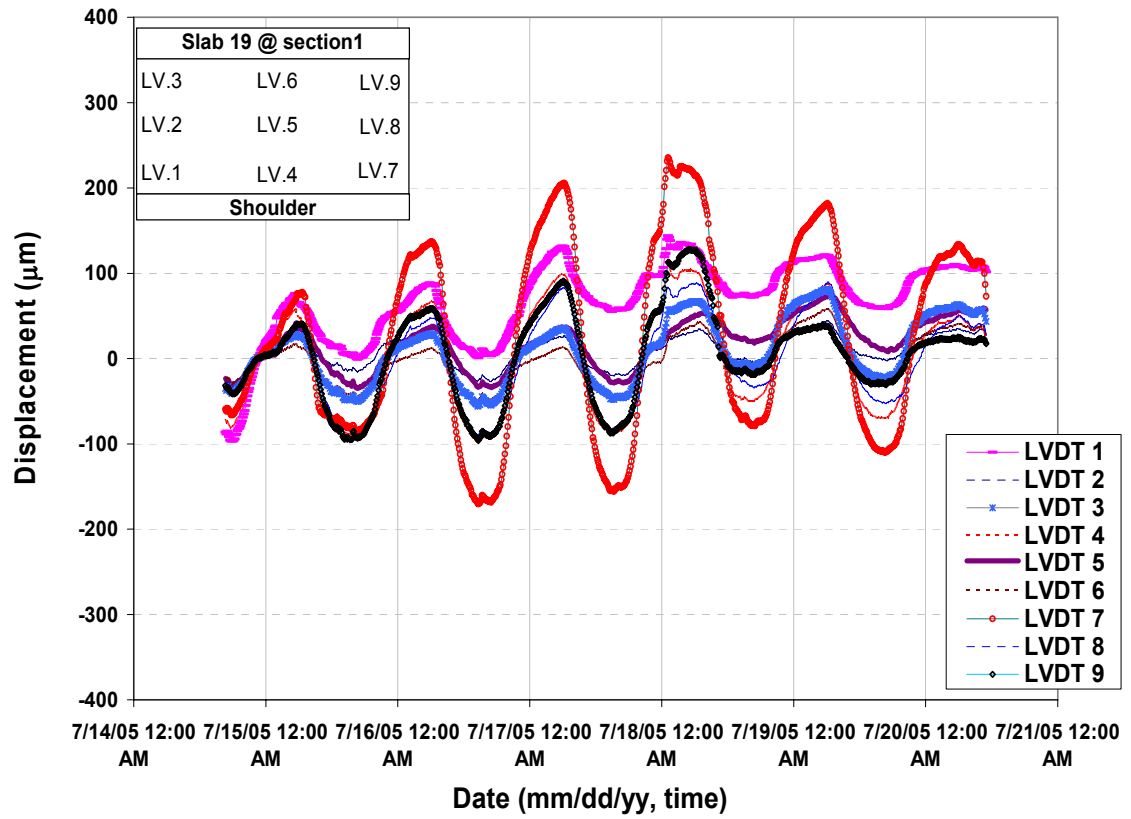
Figure A4-3 LVDT measurements at slab 19 in test section 1 (afternoon paving) of US-30, Marshalltown
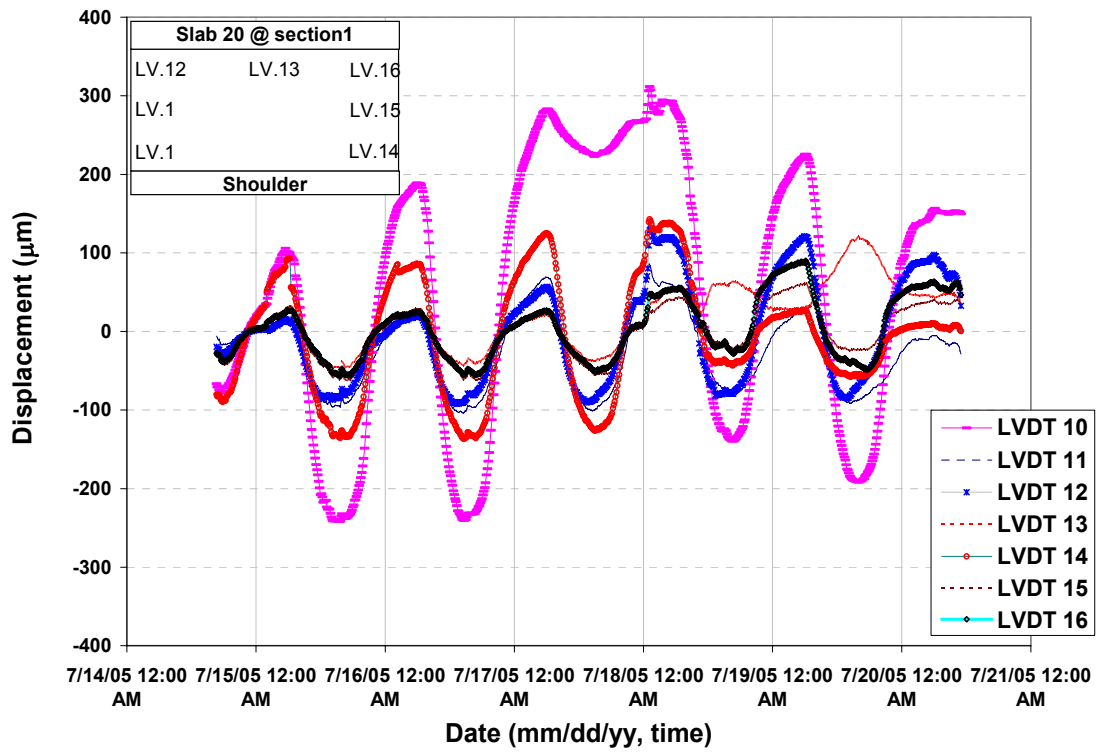
Figure A4-4 LVDT measurements at slab 20 in test section 1 (afternoon paving) of US-30, Marshalltown

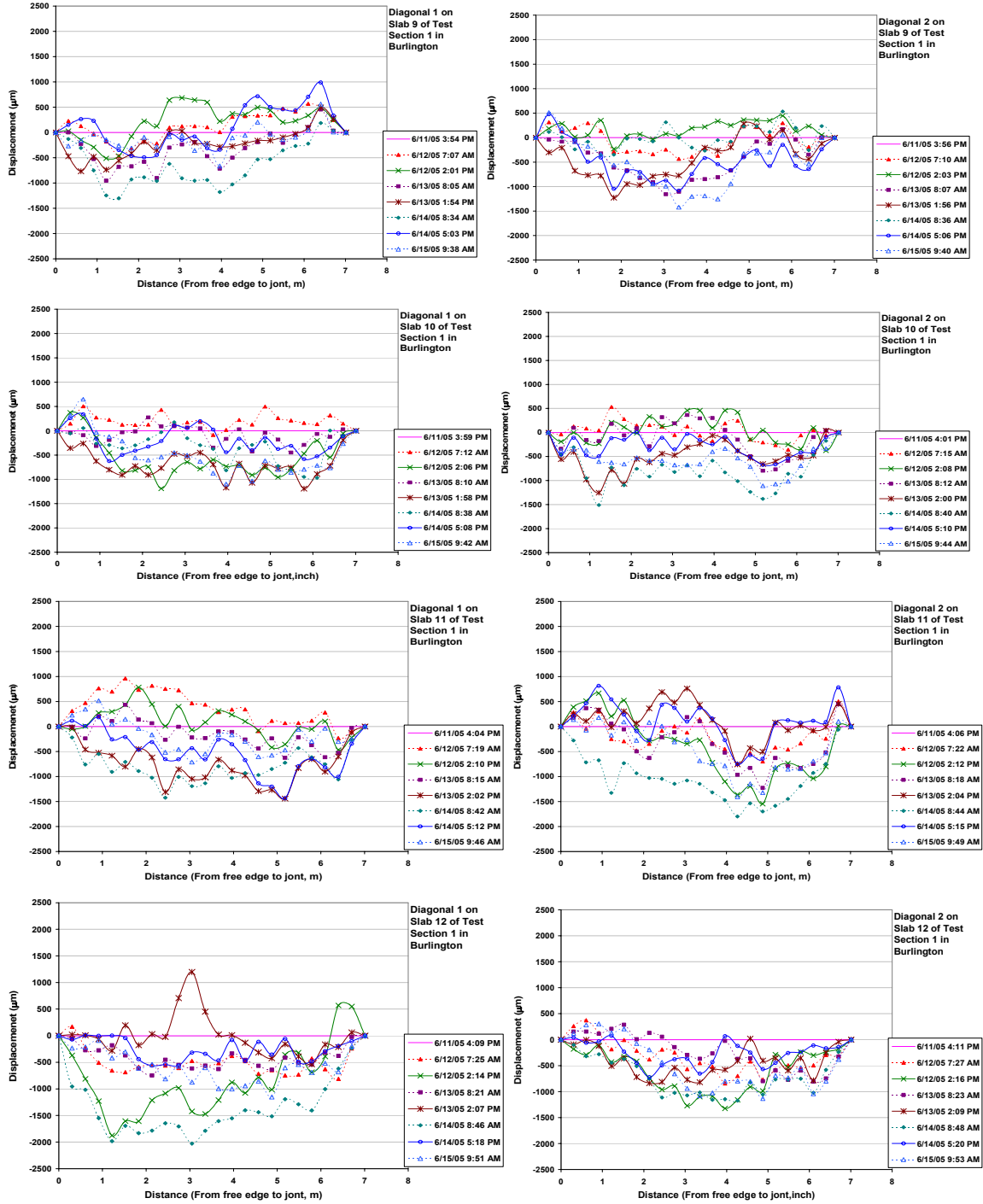# APPENDIX 5 SLAB CURVATURE PROFILE

Figure A5-1 Slab curvature profile of diagonal direction in test section 1 (afternoon paving) of US-34, Burlington
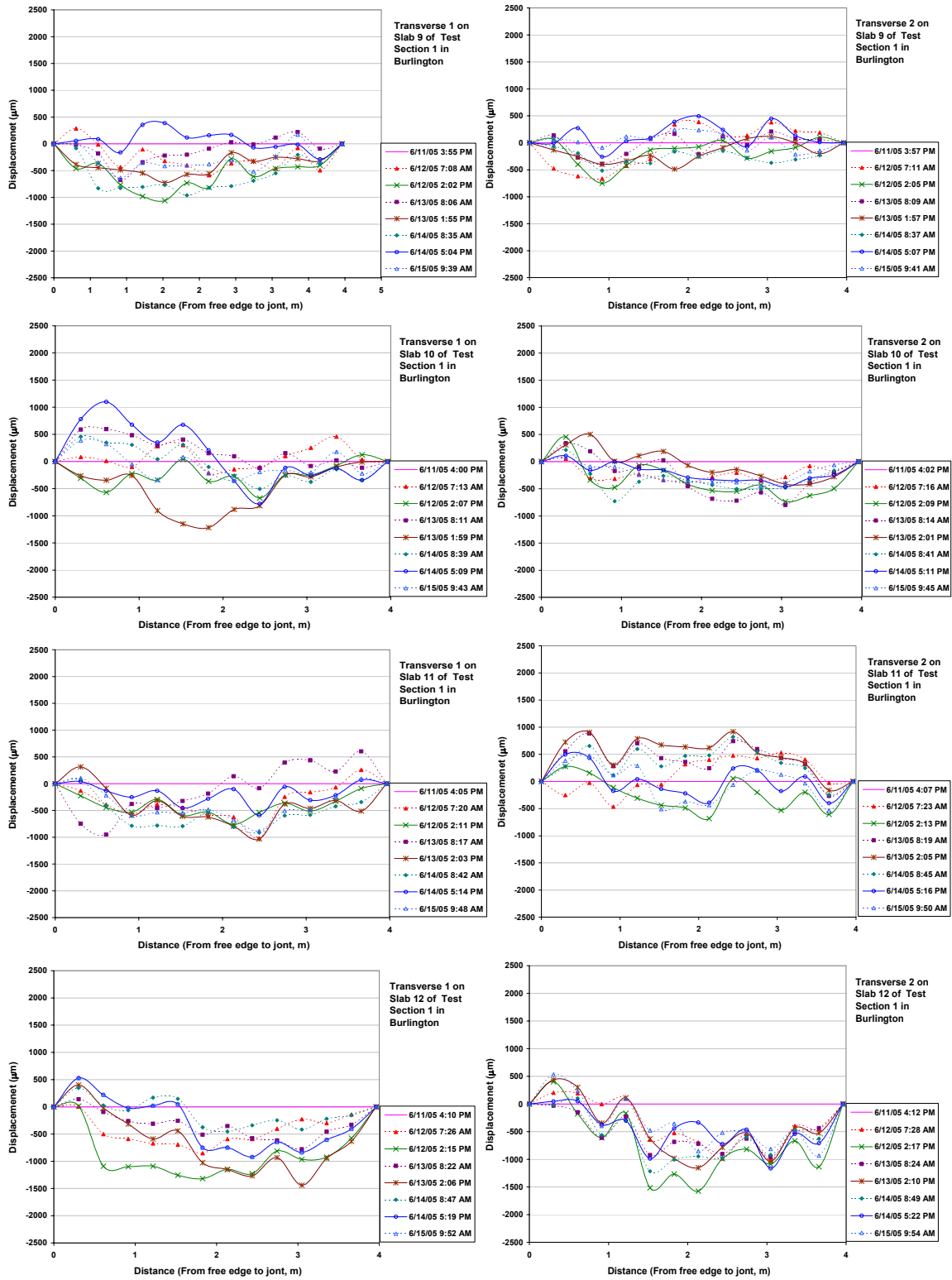
Figure A5-2 Slab curvature profile of transverse direction in test section 1 (afternoon paving) of US-34, Burlington
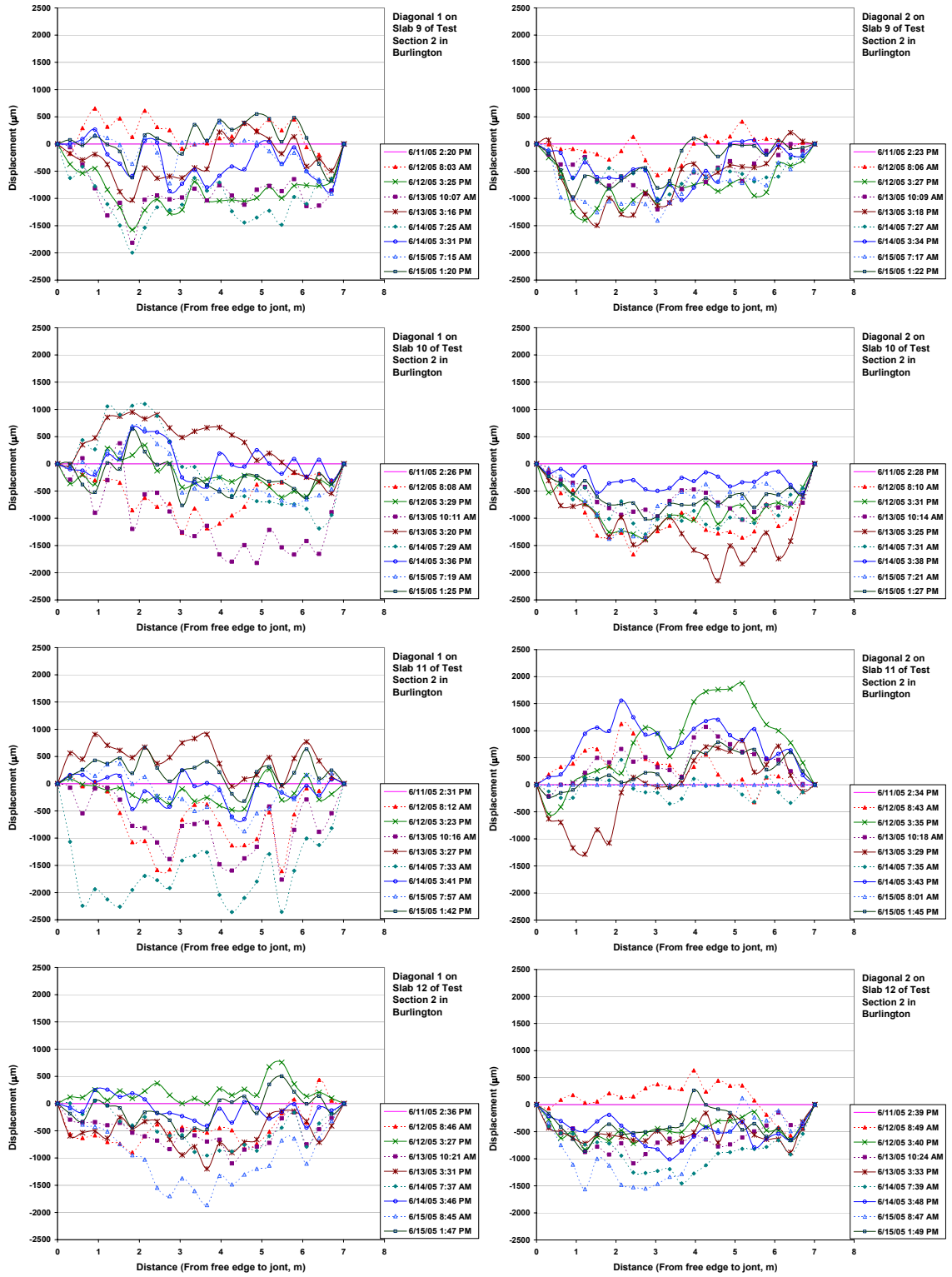
248

Figure A5-3 Slab curvature profile of diagonal direction in test section 2 (morning paving) of US-34, Burlington

Figure A5-4 Slab curvature profile of transverse direction in test section 2 (morning paving) of US-34, Burlington

Figure A5-5 Slab curvature profile of diagonal direction in test section 1 (afternoon paving) of US-30, Marshalltown
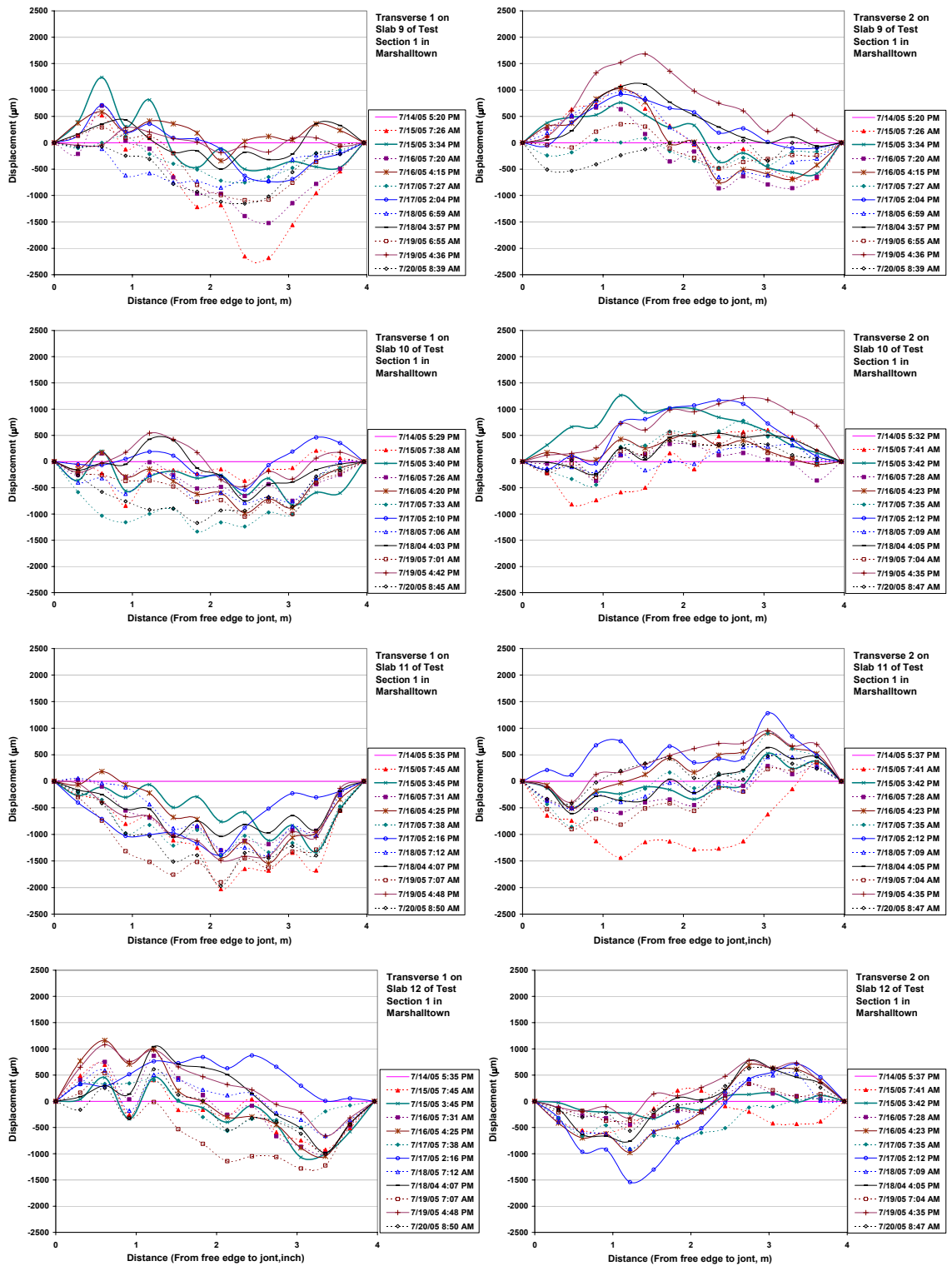
Figure A5-6 Slab curvature profile of transverse direction in test section 1 (afternoon paving) of US-30, Marshalltown

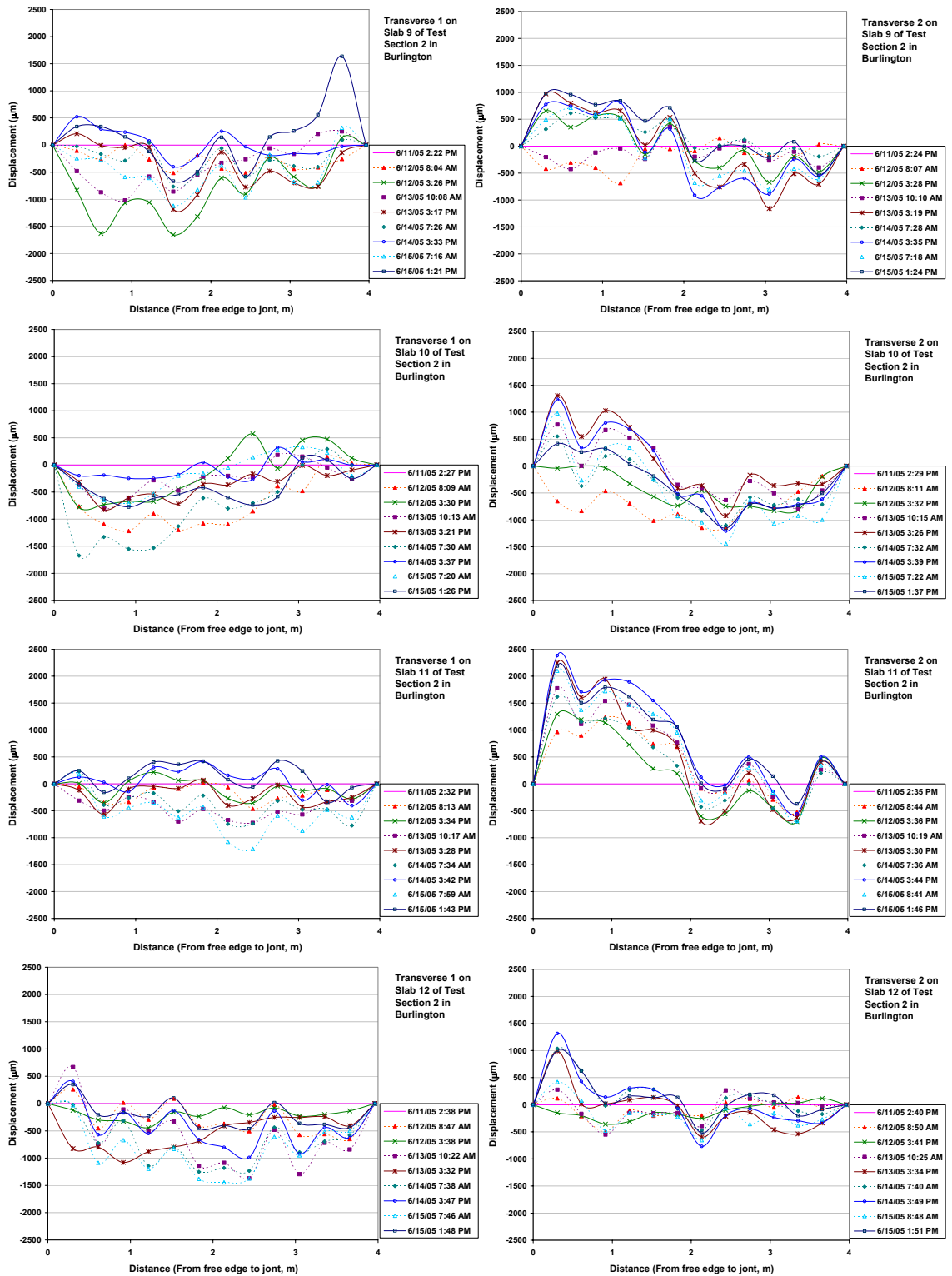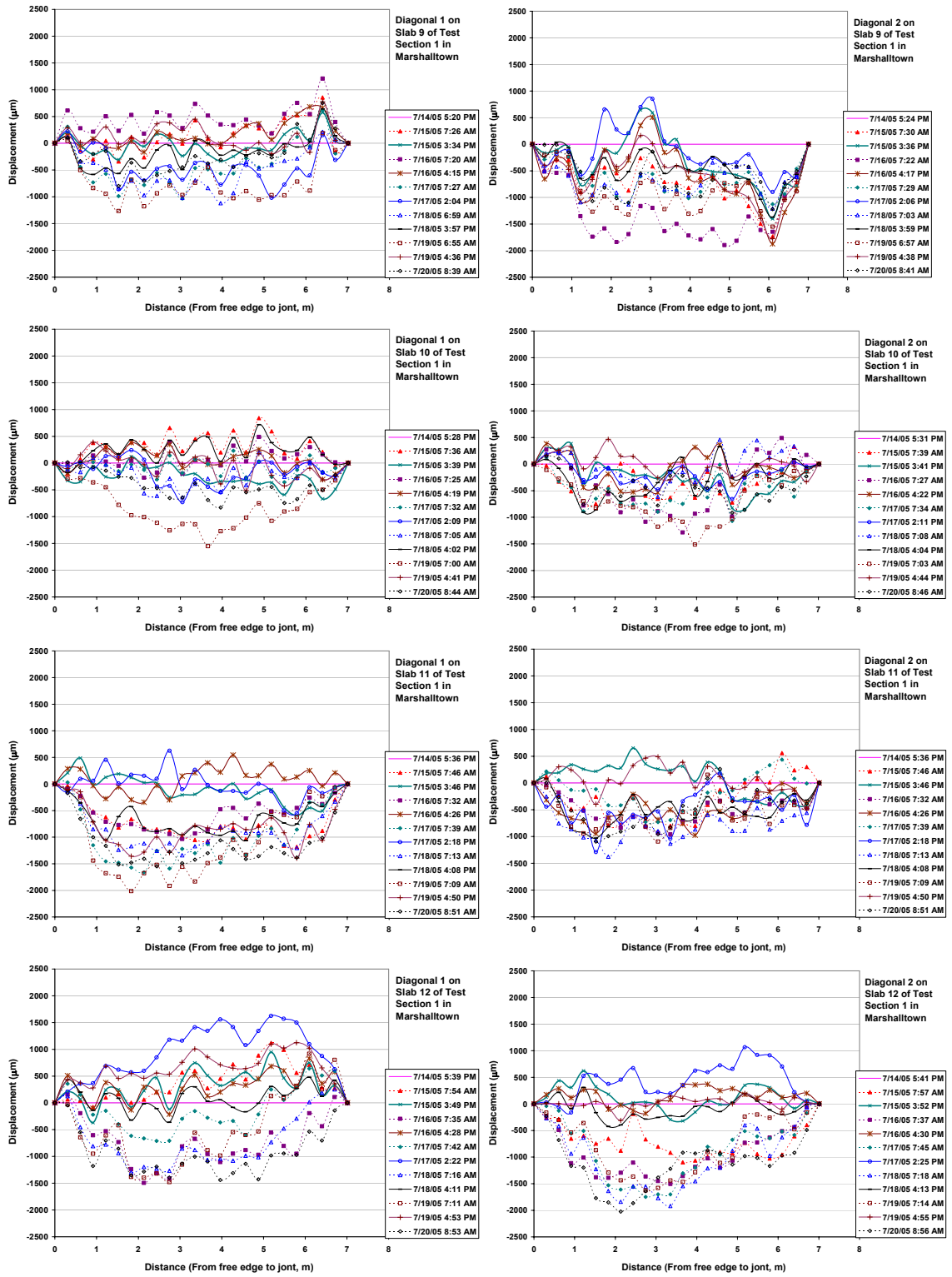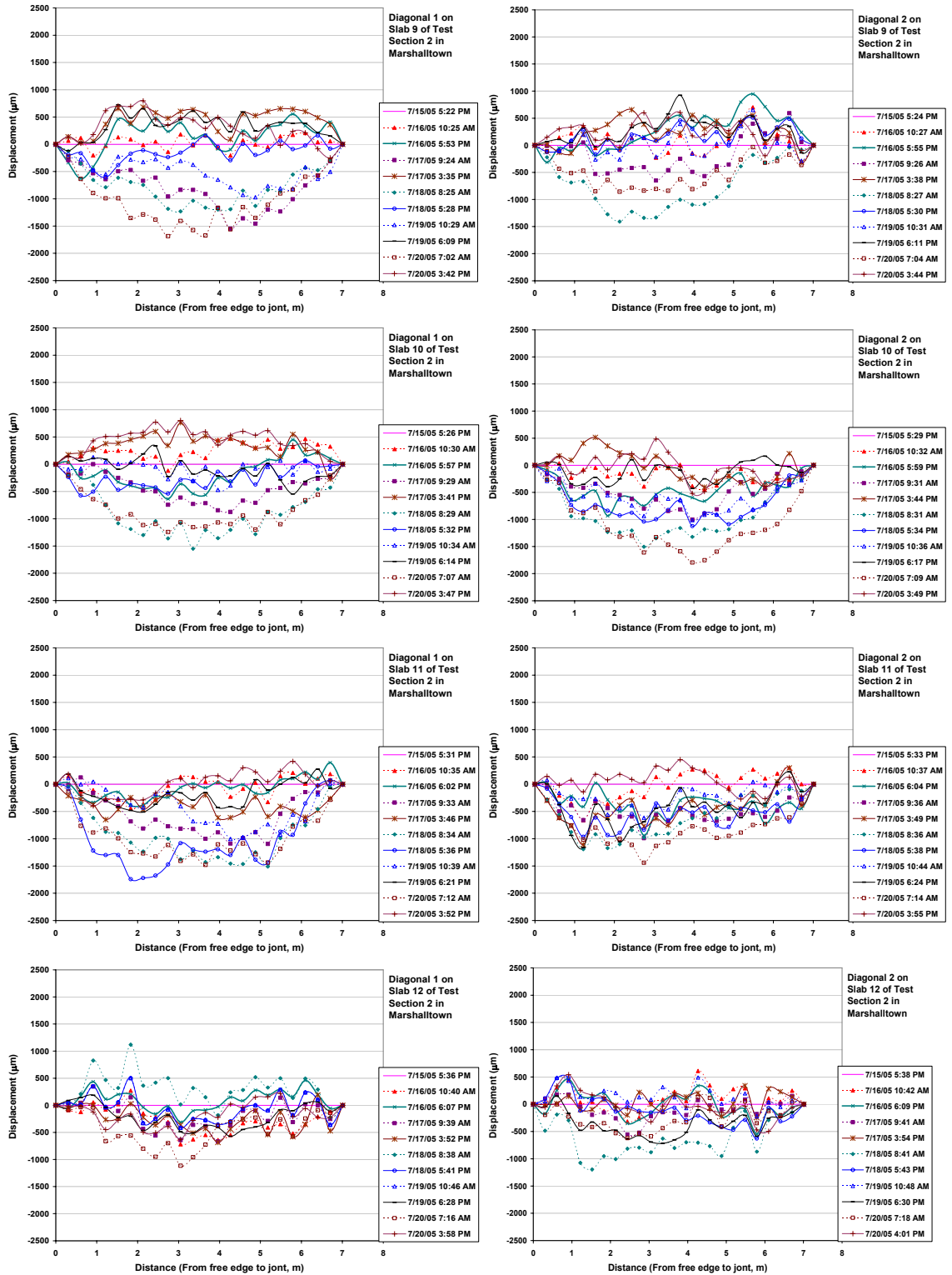**Figure A5-7 Slab curvature profile of diagonal direction in test section 2 (morning paving) of US-30, Marshalltown**
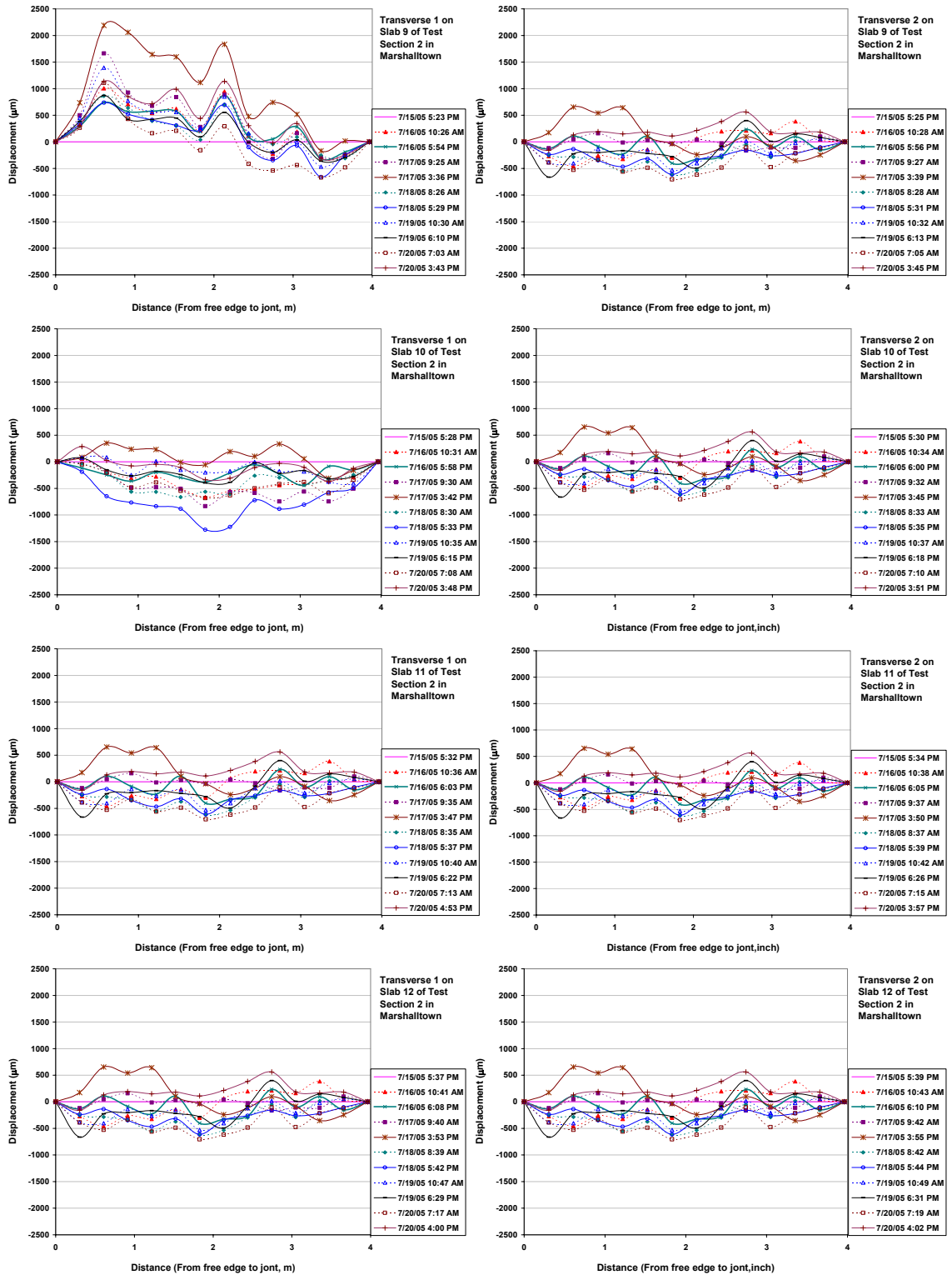
Figure A5-8 Slab curvature profile of transverse direction in test section 2 (morning paving) of US-30, Marshalltown

APPENDIX 6 FEM SIMULATION

Figure A6-1 Profile measured versus FEM (using method 2 for equivalent temperature) simulated slab curvature profile of diagonal 1 direction at negative temperature different condition in test section 1 (afternoon paving) of US-34, Burlington

Figure A6-2 Profile measured versus FEM (using method 2 for equivalent temperature) simulated slab curvature profile of diagonal 2 direction at negative temperature different condition in test section 1 (afternoon paving) of US-34, Burlington

Figure A6-3 Profile measured versus FEM (using method 2 for equivalent temperature) simulated slab curvature profile of transverse 1 direction at negative temperature different condition in test section 1 (afternoon paving) of US-34, Burlington

Date / Time : 6/12/05 7:17AM
Pavement Temp. Diff. : -2.8 °C
Equivalent Temp. Diff. : -7.1 °C
(EverFE 2.24) & -5.3 °C (ISLAB 2000)

Date / Time : 6/13/05 8:14AM
Pavement Temp. Diff. : -2.8 °C
Equivalent Temp. Diff. : -7.1 °C
(EverFE 2.24) & -5.3 °C (ISLAB 2000)

Date / Time : 6/14/05 8:41 AM
Pavement Temp. Diff. : -2.8 °C
Equivalent Temp. Diff. : -7.1 °C
(EverFE 2.24) & -5.3 °C (ISLAB 2000)

Figure A6-4 Profile measured versus FEM (using method 2 for equivalent temperature) simulated slab curvature profile of transverse 2 direction at negative temperature different condition in test section 1 (afternoon paving) of US-34, Burlington
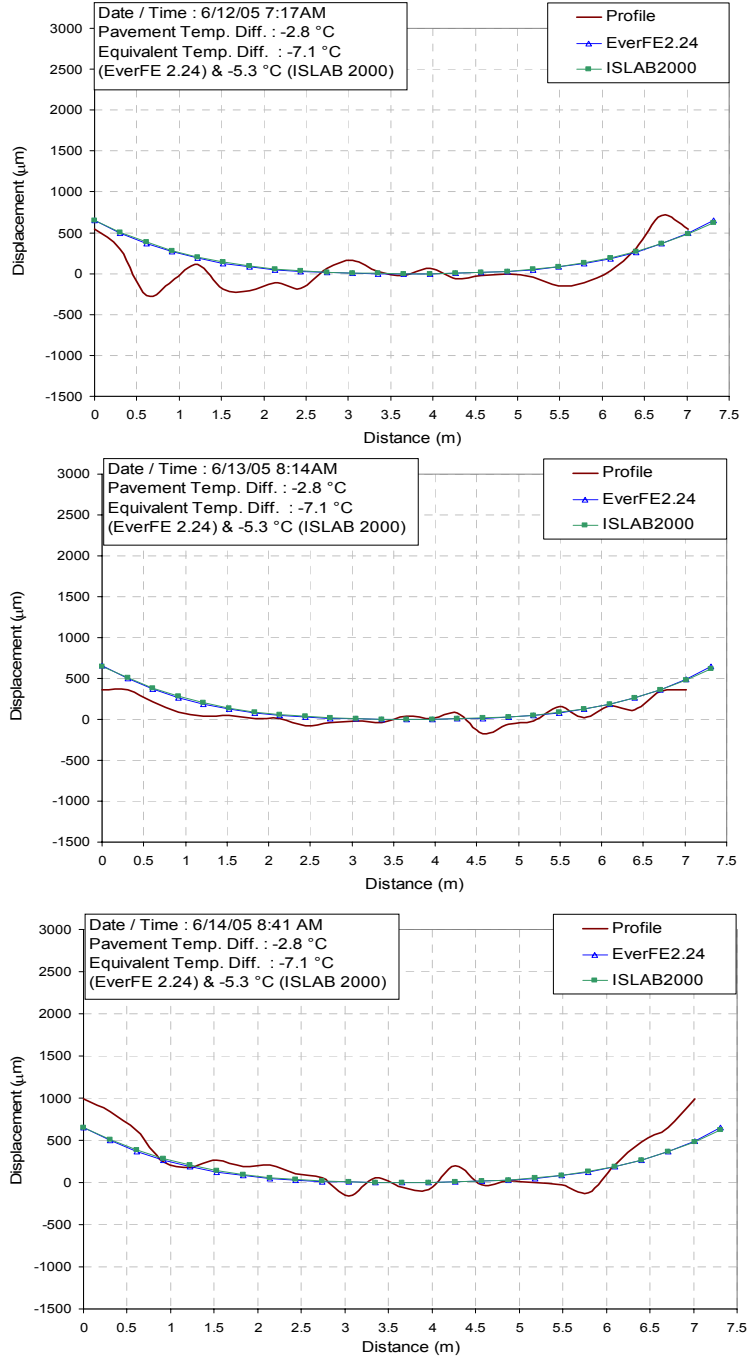
Figure A6-5 Profile measured versus FEM (using method 2 for equivalent temperature) simulated slab curvature profile of diagonal 1 direction at positive temperature different condition in test section 1 (afternoon paving) of US-34, Burlington
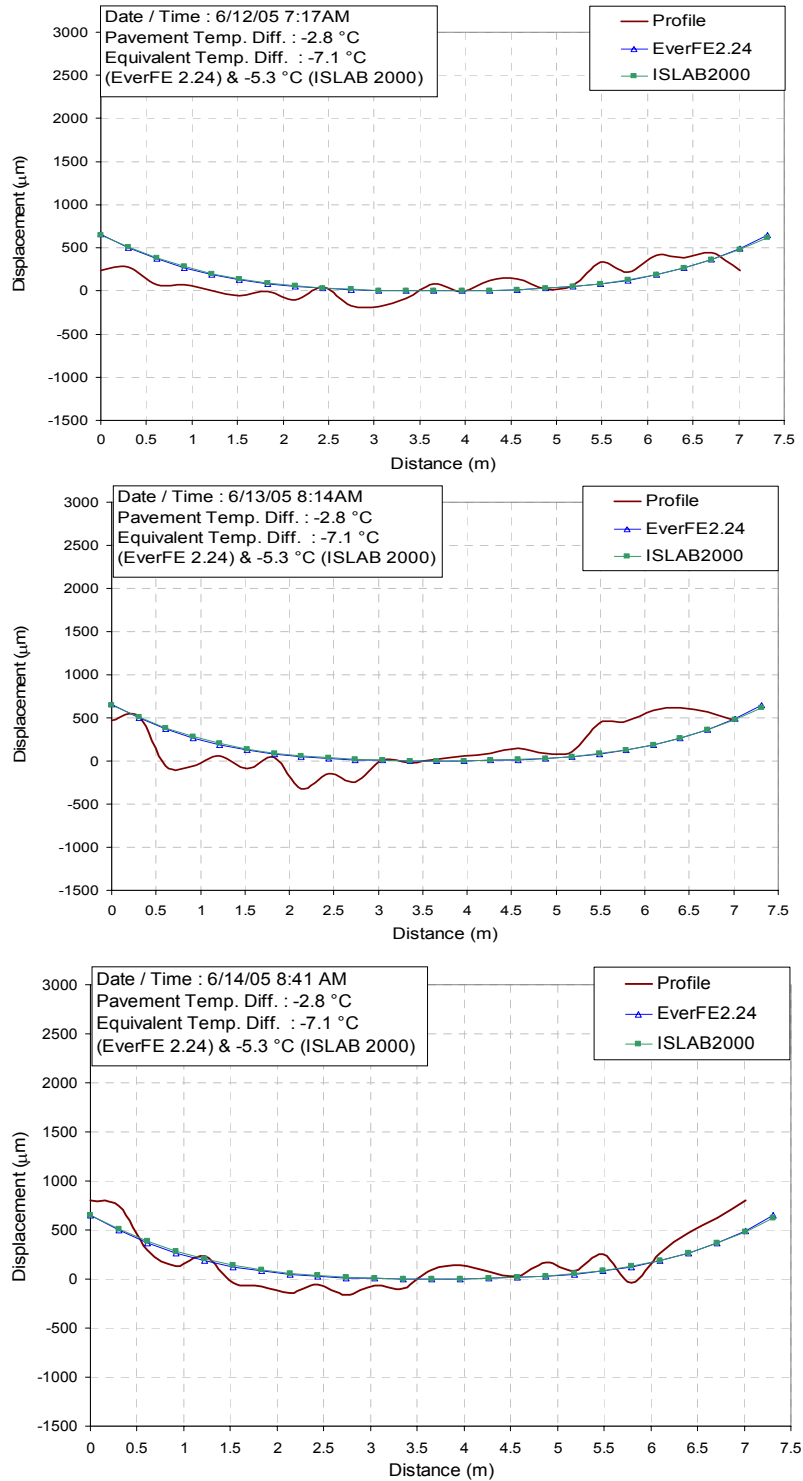
Figure A6-6 Profile measured versus FEM (using method 2 for equivalent temperature) simulated slab curvature profile of diagonal 2 direction at positive temperature different condition in test section 1 (afternoon paving) of US-34, Burlington
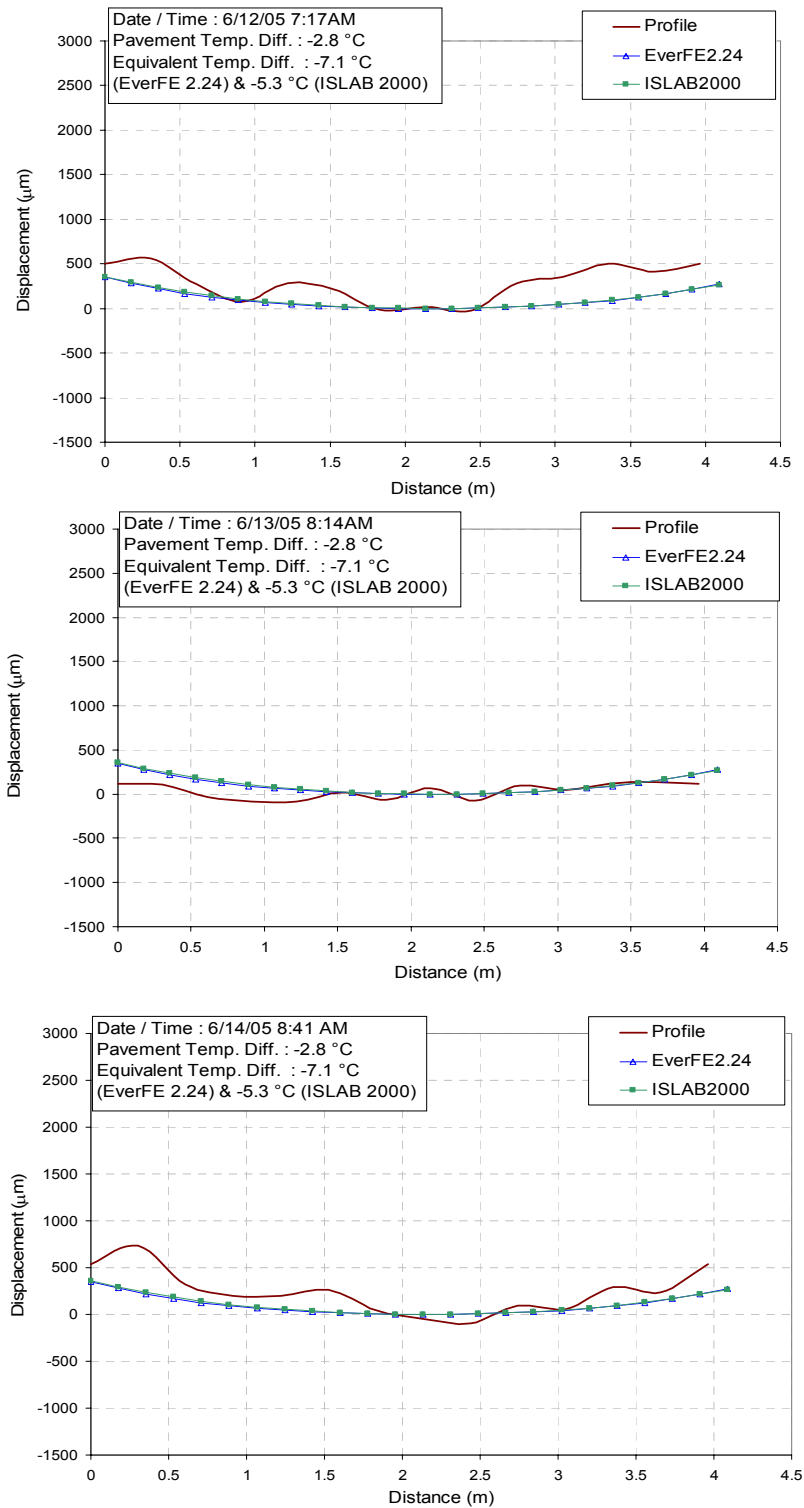
Figure A6-7 Profile measured versus FEM (using method 2 for equivalent temperature) simulated slab curvature profile of transverse 1 direction at positive temperature different condition in test section 1 (afternoon paving) of US-34, Burlington

Figure A6-8 Profile measured versus FEM (using method 2 for equivalent temperature) simulated slab curvature profile of transverse 2 direction at positive temperature different condition in test section 1 (afternoon paving) of US-34, Burlington

Figure A6-9 Profile measured versus FEM (using method 2 for equivalent temperature) simulated slab curvature profile of diagonal 1 direction at negative temperature different condition in test section 2 (morning paving) of US-34, Burlington

Figure A6-10 Profile measured versus FEM(using method 2 for equivalent temperature) simulated slab curvature profile of diagonal 2 direction at negative temperature different condition in test section 2 (morning paving) of US-34, Burlington
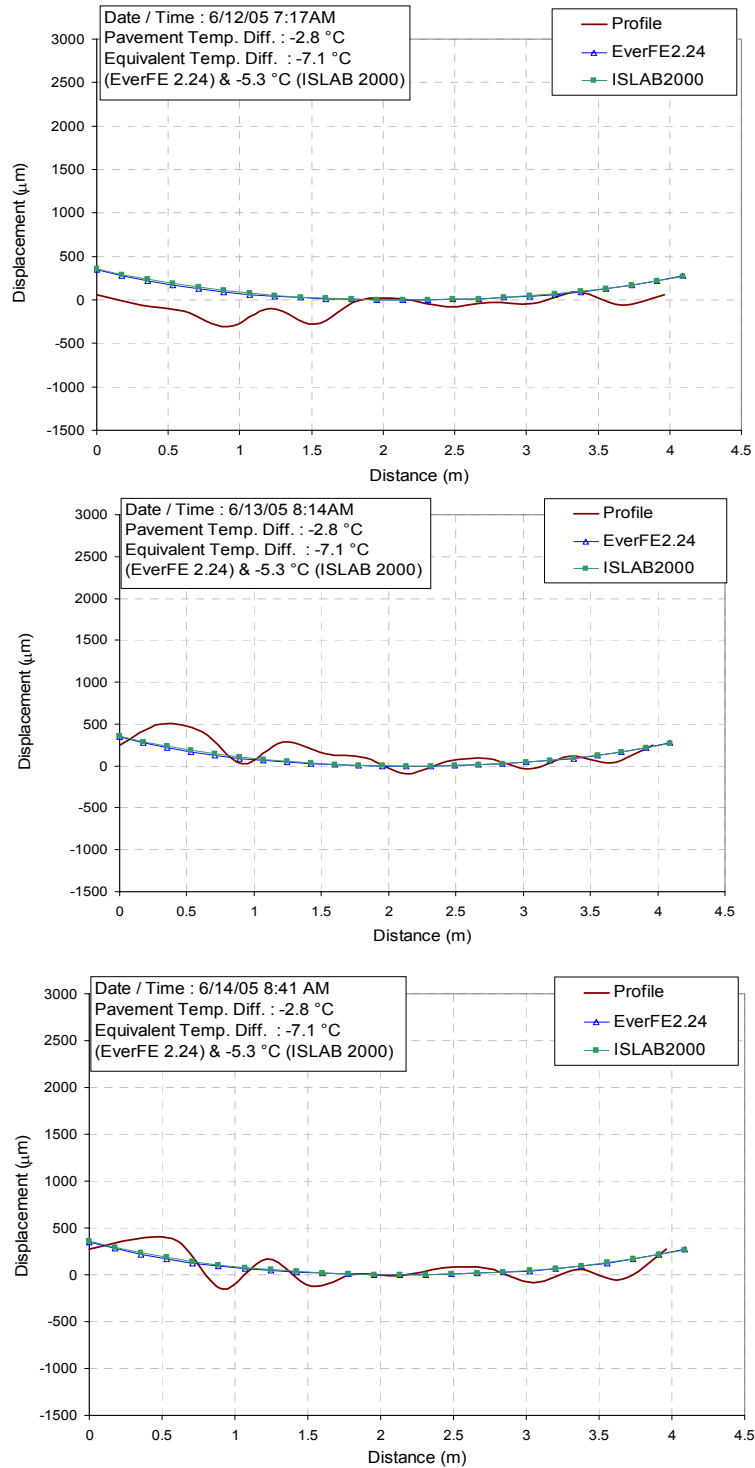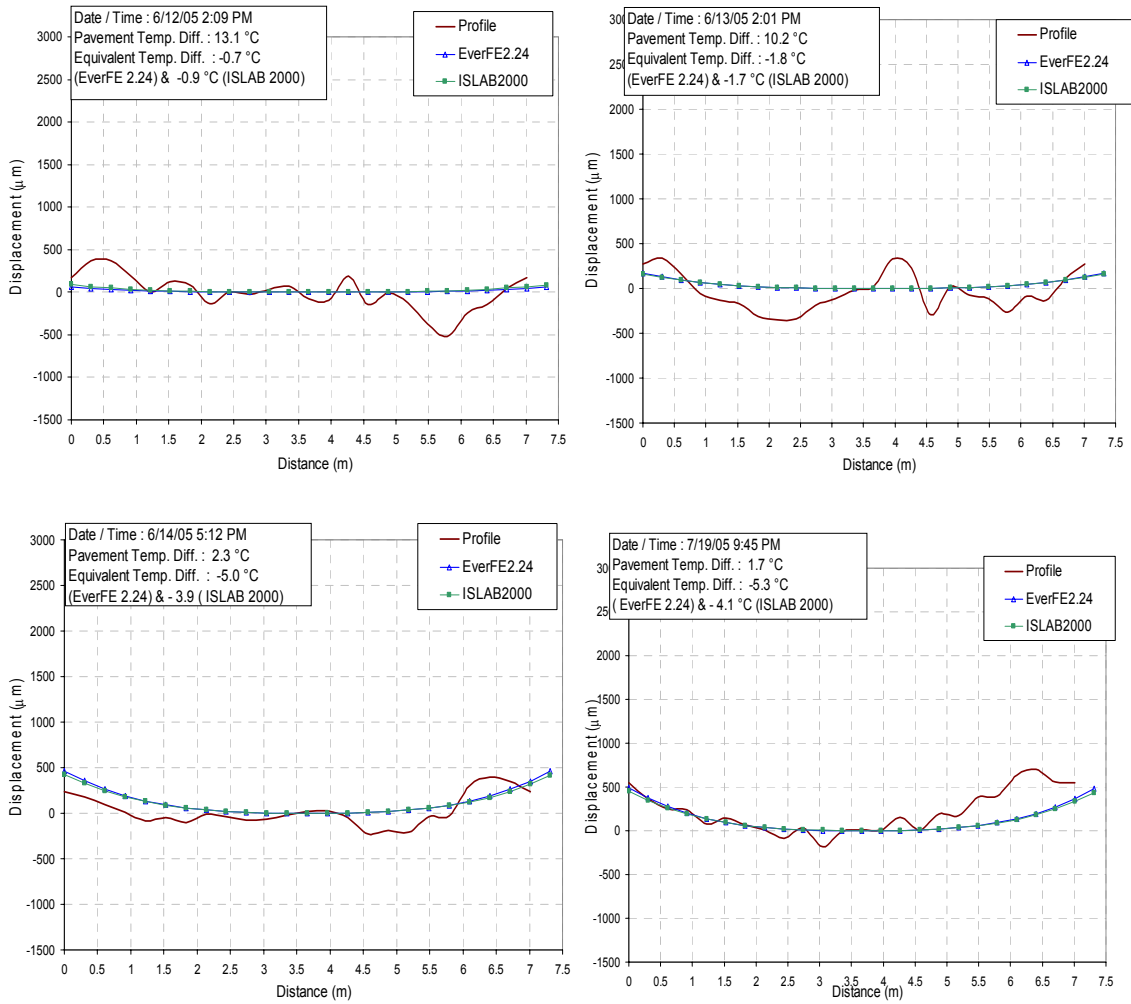
Figure A6-11 Profile measured versus FEM(using method 2 for equivalent temperature) simulated slab curvature profile of transverse 1 direction at negative temperature different condition in test section 2 (morning paving) of US-34, Burlington

Figure A6-12 Profile measured versus FEM(using method 2 for equivalent temperature) simulated slab curvature profile of transverse 2 direction at negative temperature different condition in test section 2 (morning paving) of US-34, Burlington
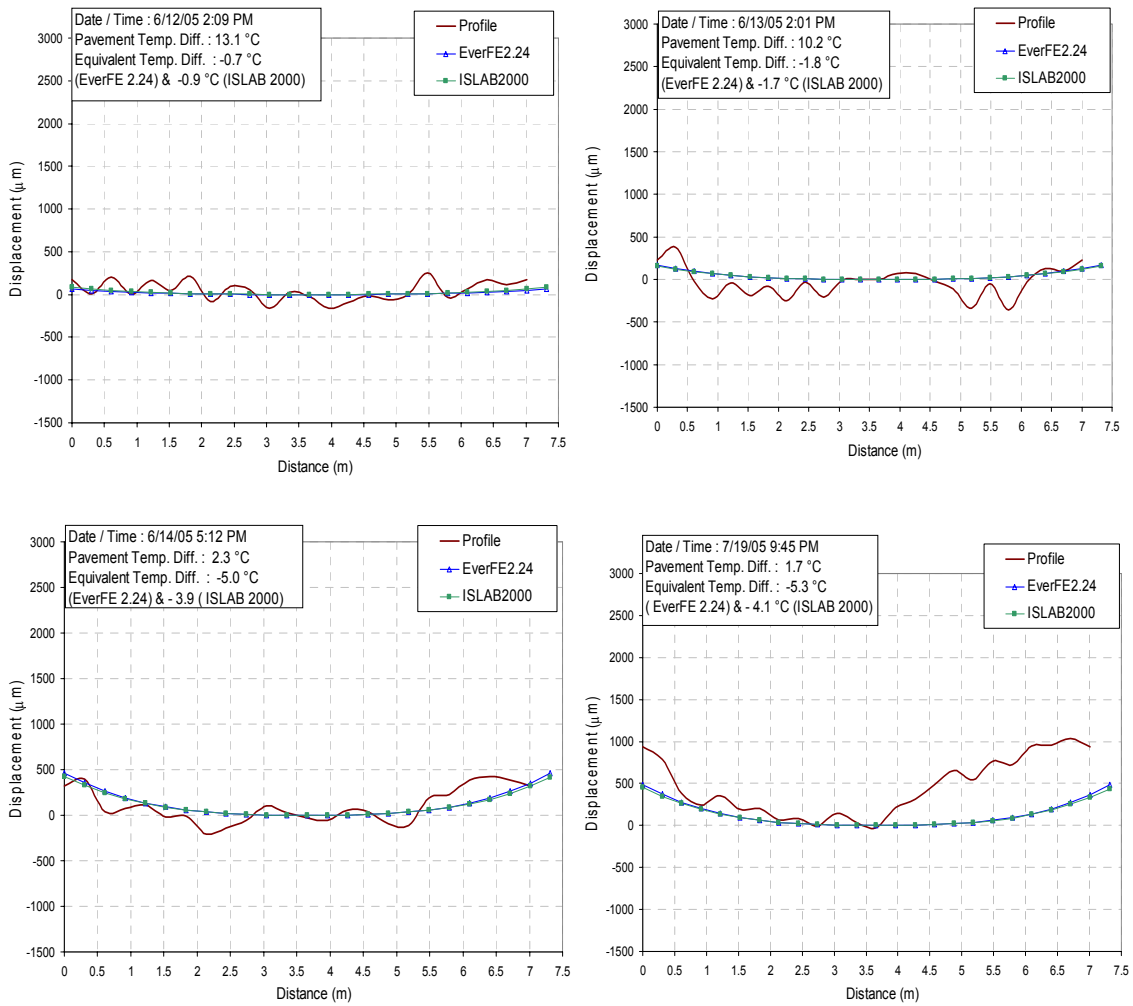
Figure A6-13 Profile measured versus FEM(using method 2 for equivalent temperature) simulated slab curvature profile of diagonal 1 direction at positive temperature different condition in test section 2 (morning paving) of US-34, Burlington

Figure A6-14 Profile measured versus FEM(using method 2 for equivalent temperature) simulated slab curvature profile of diagonal 2 direction at positive temperature different condition in test section 2 (morning paving) of US-34, Burlington
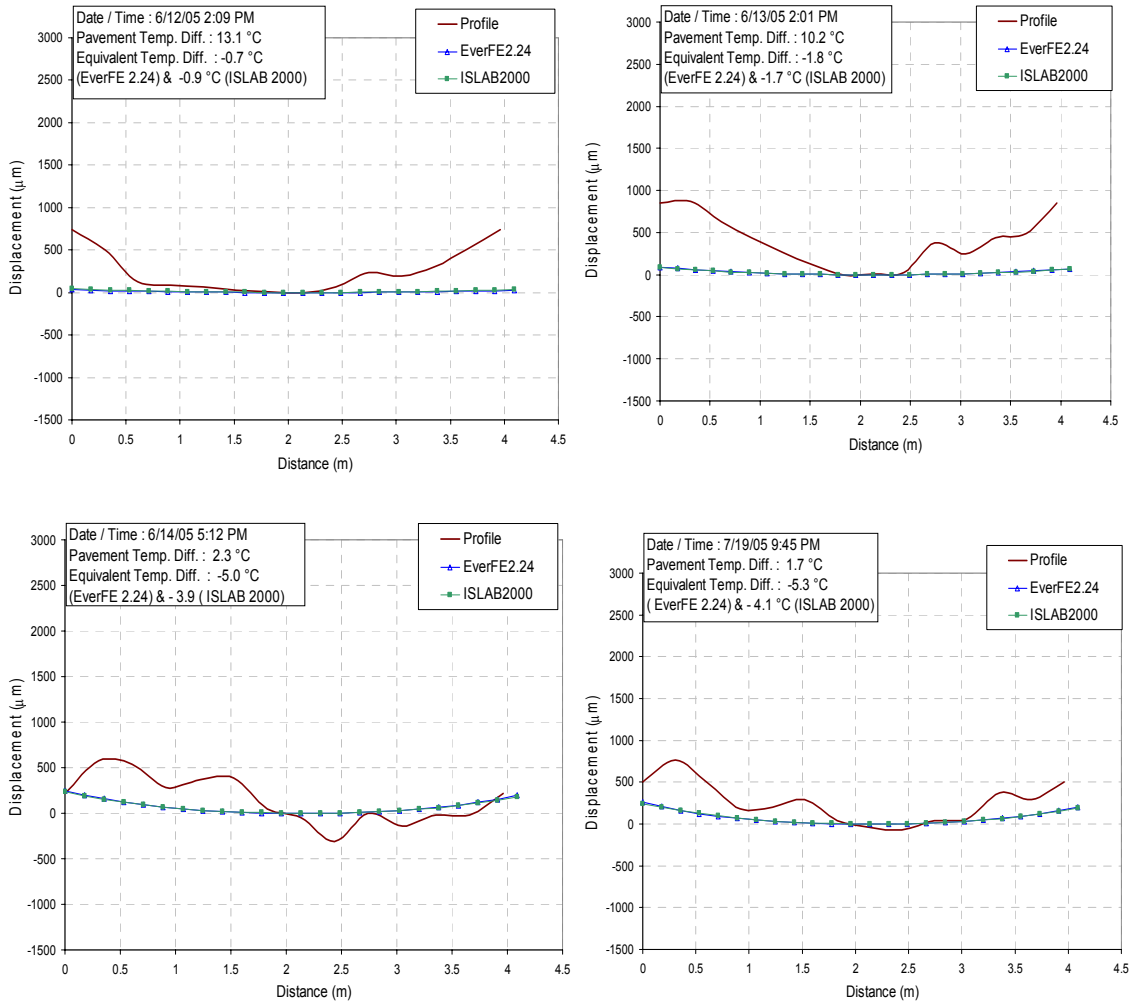
Figure A6-15 Profile measured versus FEM(using method 2 for equivalent temperature) simulated slab curvature profile of transverse 1 direction at positive temperature different condition in test section 2 (morning paving) of US-34, Burlington
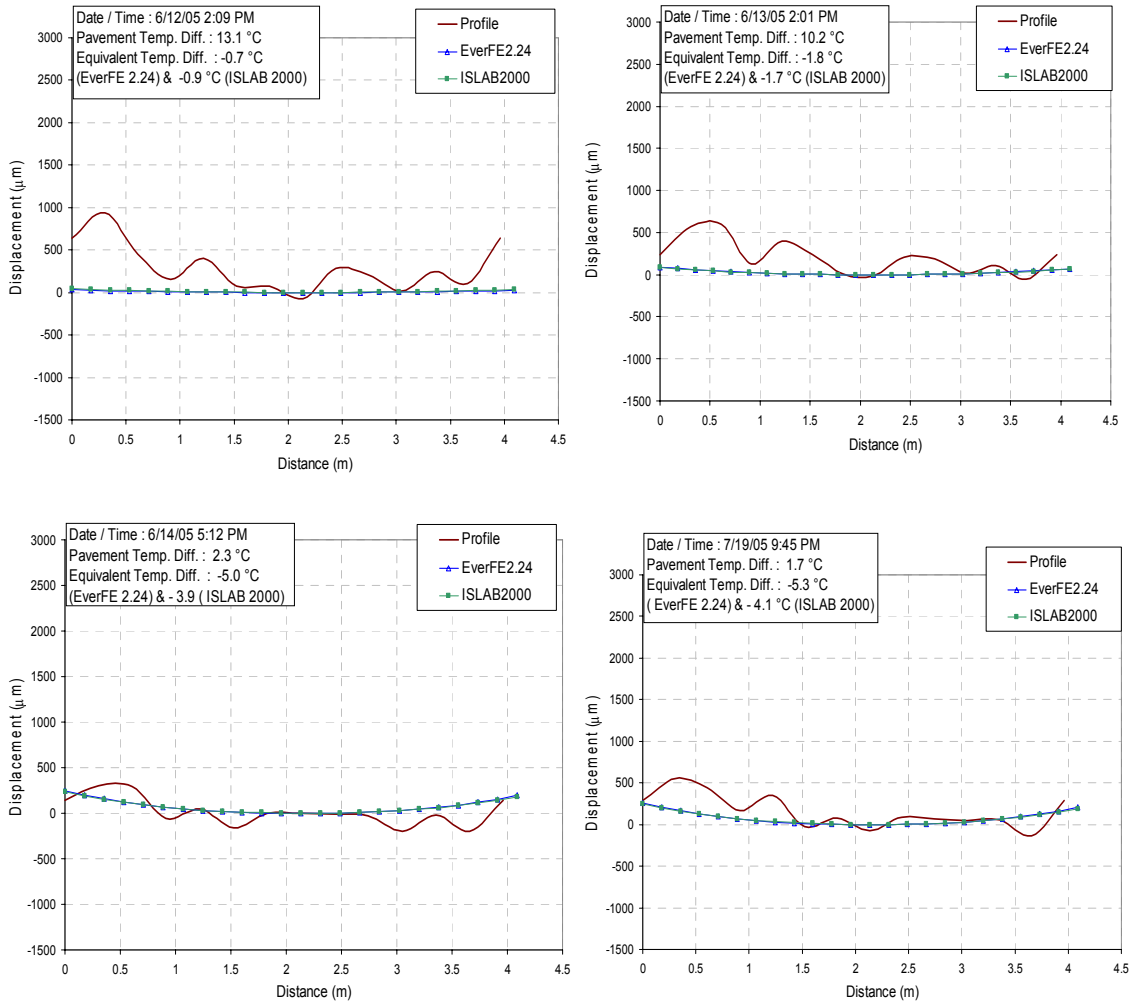
Figure A6-16 Profile measured versus FEM(using method 2 for equivalent temperature) simulated slab curvature profile of transverse 2 direction at positive temperature different condition in test section 2 (morning paving) of US-34, Burlington
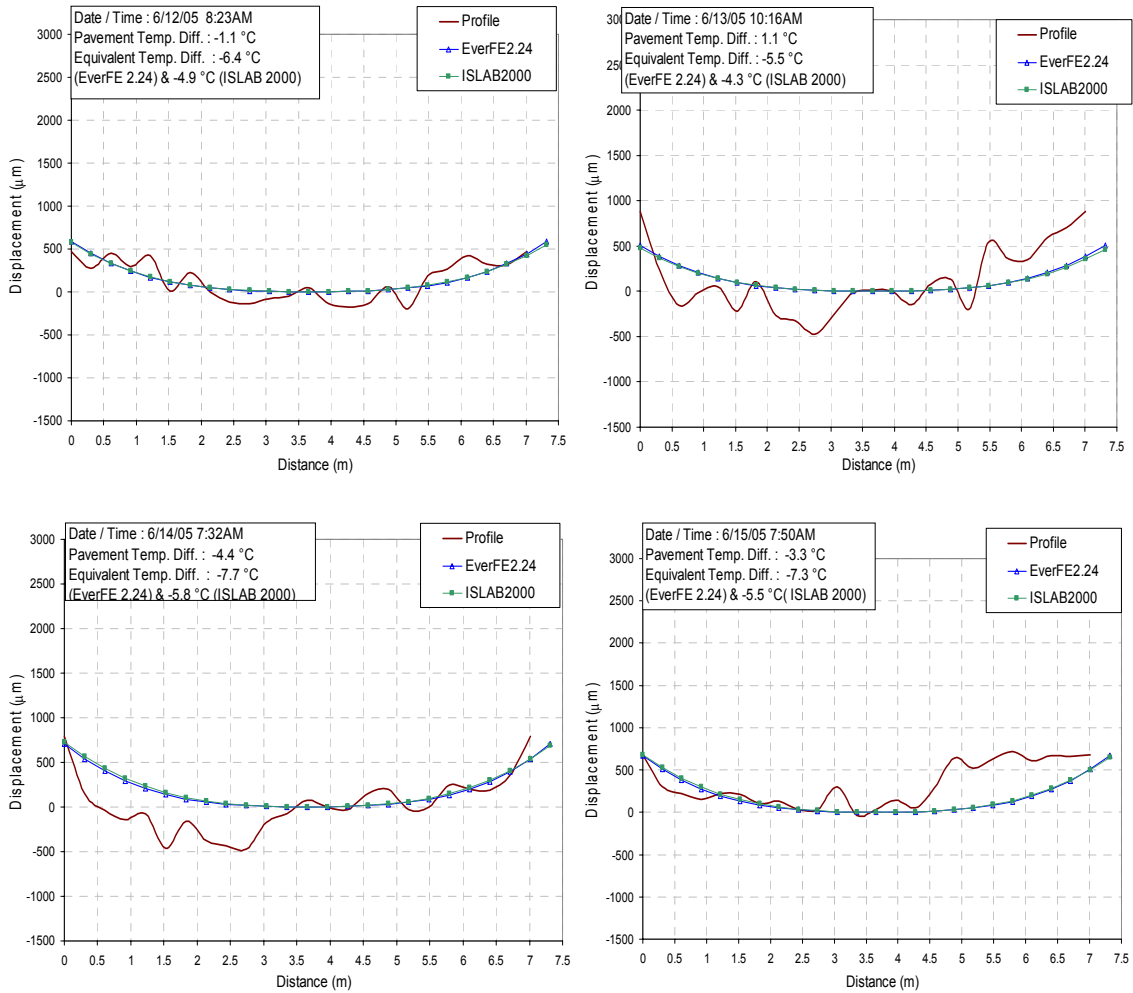
Figure A6-17 Profile measured versus FEM(using method 1 for equivalent temperature) simulated slab curvature profile of diagonal 1 direction at negative temperature different condition in test section 1 (afternoon paving) of US-30, Marshalltown
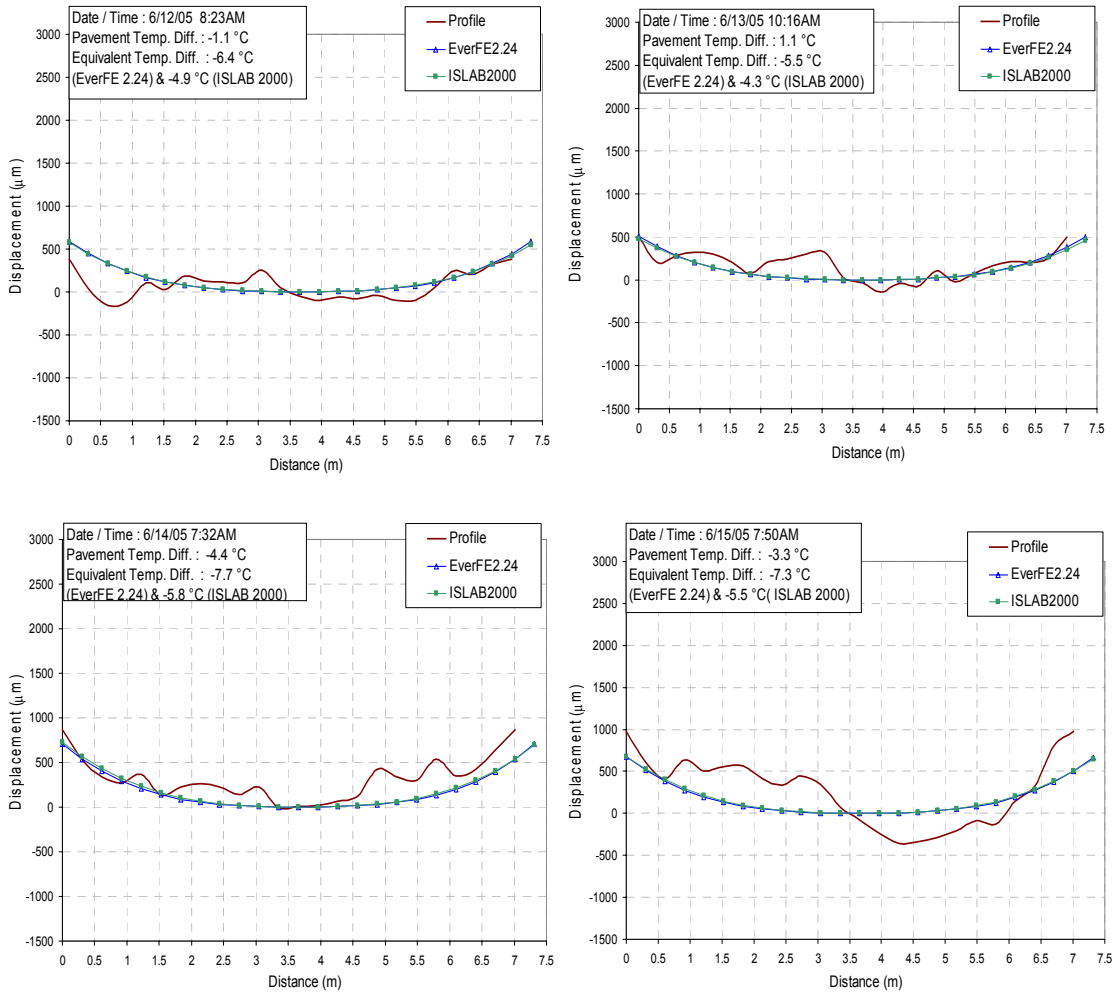
Figure A6-18 Profile measured versus FEM(using method 1 for equivalent temperature) simulated slab curvature profile of diagonal 2 direction at negative temperature different condition in test section 1 (afternoon paving) of US-30, Marshalltown

Figure A6-19 Profile measured versus FEM(using method 1 for equivalent temperature) simulated slab curvature profile of transverse 1 direction at negative temperature different condition in test section 1 (afternoon paving) of US-30, Marshalltown
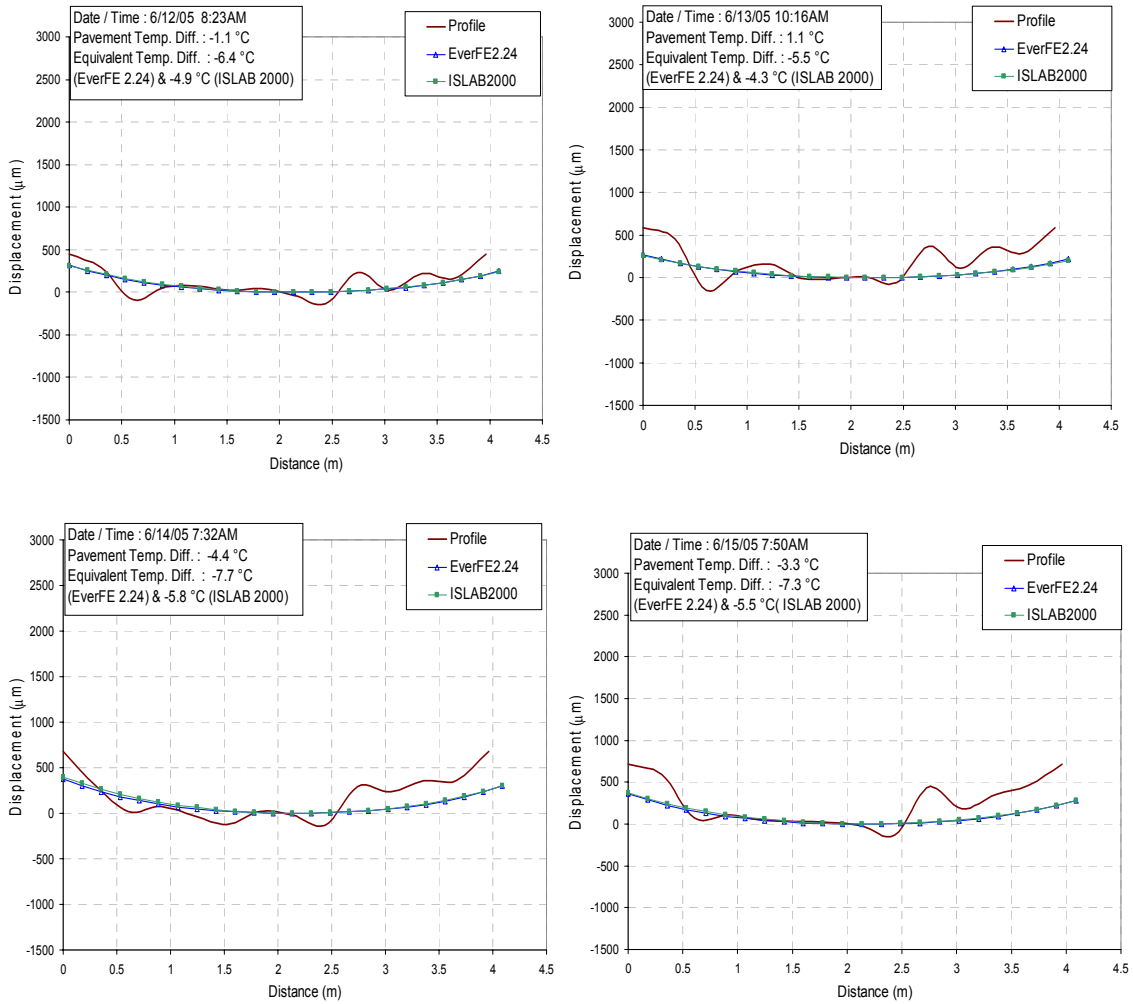
Figure A6-20 Profile measured versus FEM(using method 1 for equivalent temperature) simulated slab curvature profile of transverse 2 direction at negative temperature different condition in test section 1 (afternoon paving) of US-30, Marshalltown

Figure A6-21 Profile measured versus FEM(using method 1 for equivalent temperature) simulated slab curvature profile of diagonal 1 direction at positive temperature different condition in test section 1 (afternoon paving) of US-30, Marshalltown

Figure A6-22 Profile measured versus FEM(using method 1 for equivalent temperature) simulated slab curvature profile of diagonal 2 direction at positive temperature different condition in test section 1 (afternoon paving) of US-30, Marshalltown
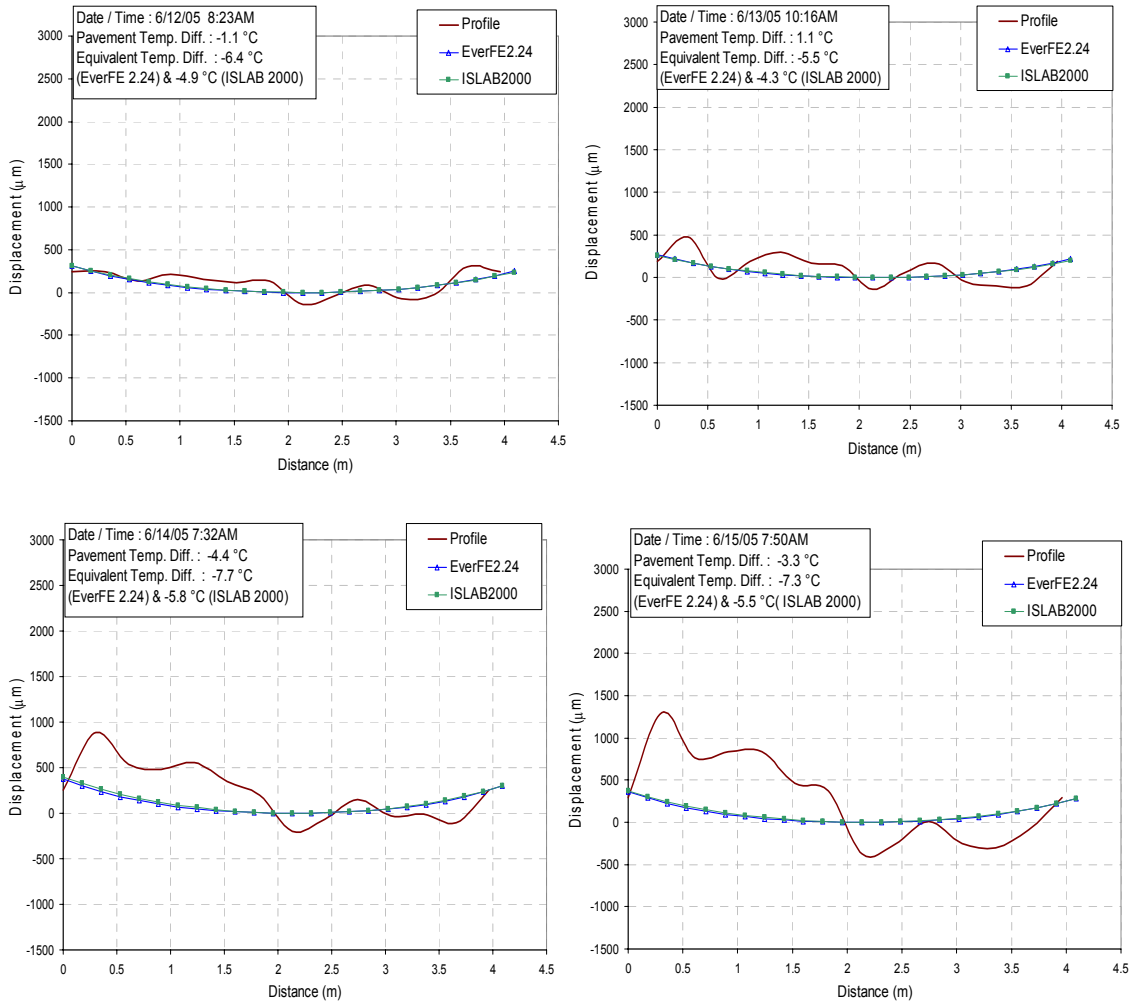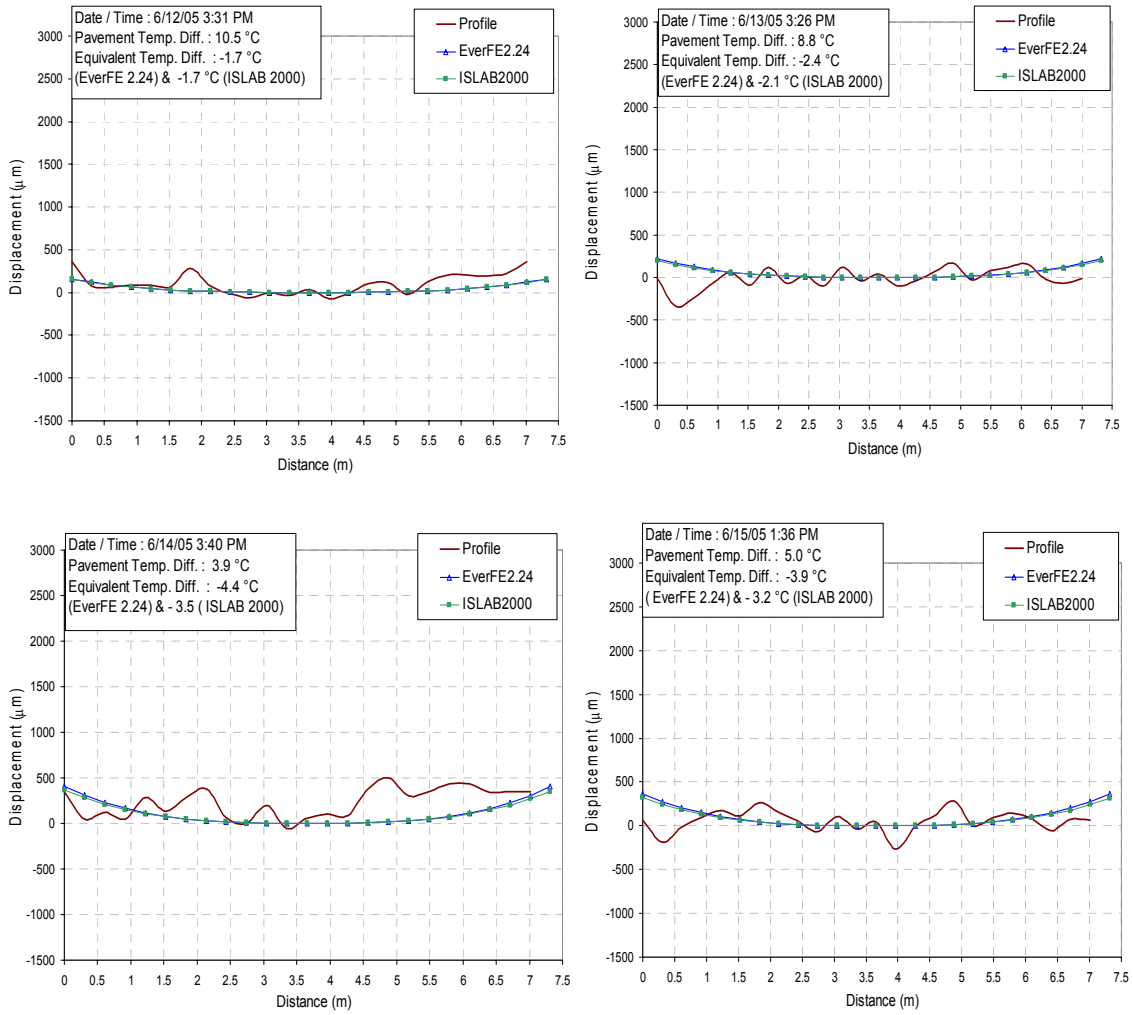
Figure A6-23 Profile measured versus FEM(using method 1 for equivalent temperature) simulated slab curvature profile of transverse 1 direction at positive temperature different condition in test section 1 (afternoon paving) of US-30, Marshalltown

Figure A6-24 Profile measured versus FEM(using method 1 for equivalent temperature) simulated slab curvature profile of transverse 2 direction at positive temperature different condition in test section 1 (afternoon paving) of US-30, Marshalltown
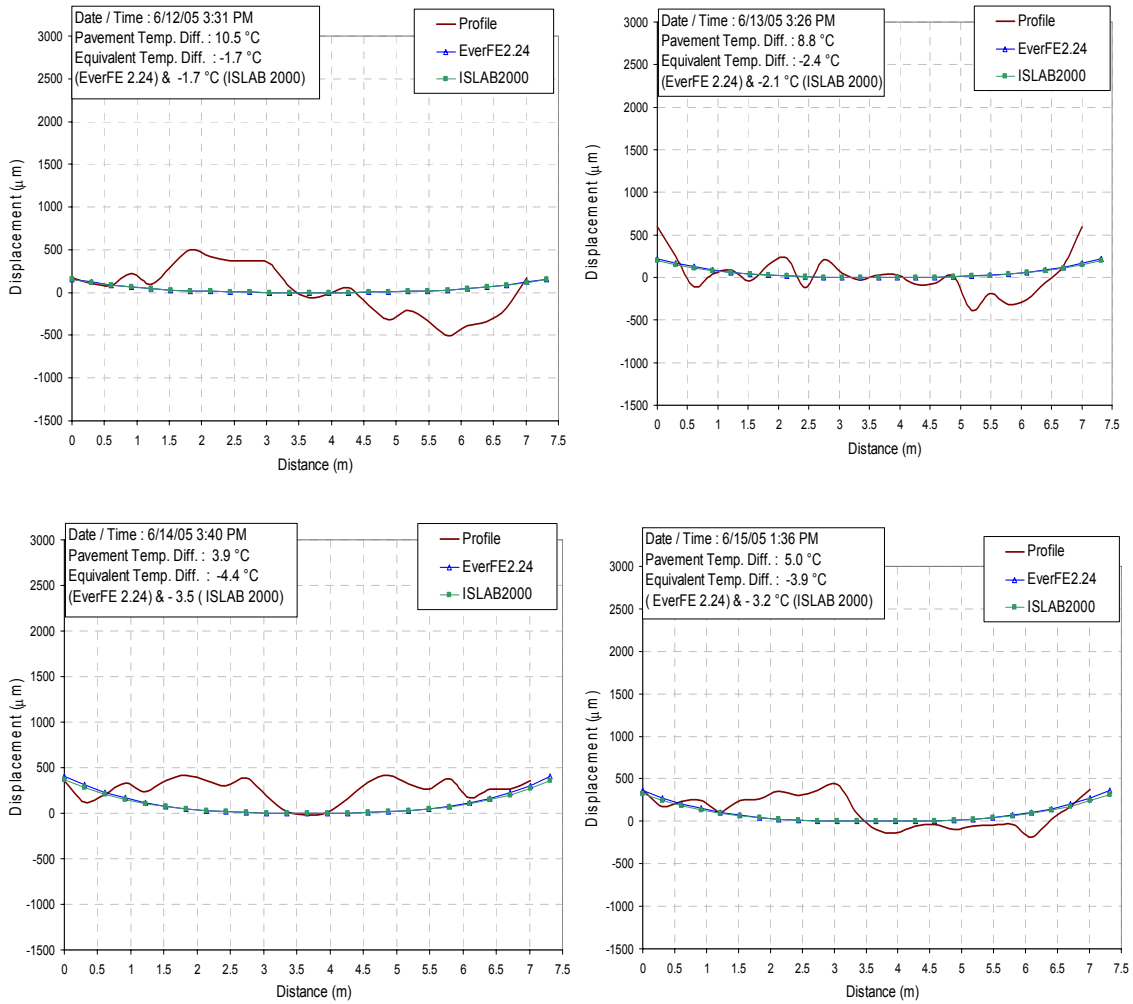
Figure A6-25 Profile measured versus FEM(using method 1 for equivalent temperature) simulated slab curvature profile of diagonal 1 direction at negative temperature different condition in test section 2 (morning paving) of US-30, Marshalltown

Figure A6-26 Profile measured versus FEM(using method 1 for equivalent temperature) simulated slab curvature profile of diagonal 2 direction at negative temperature different condition in test section 2 (morning paving) of US-30, Marshalltown
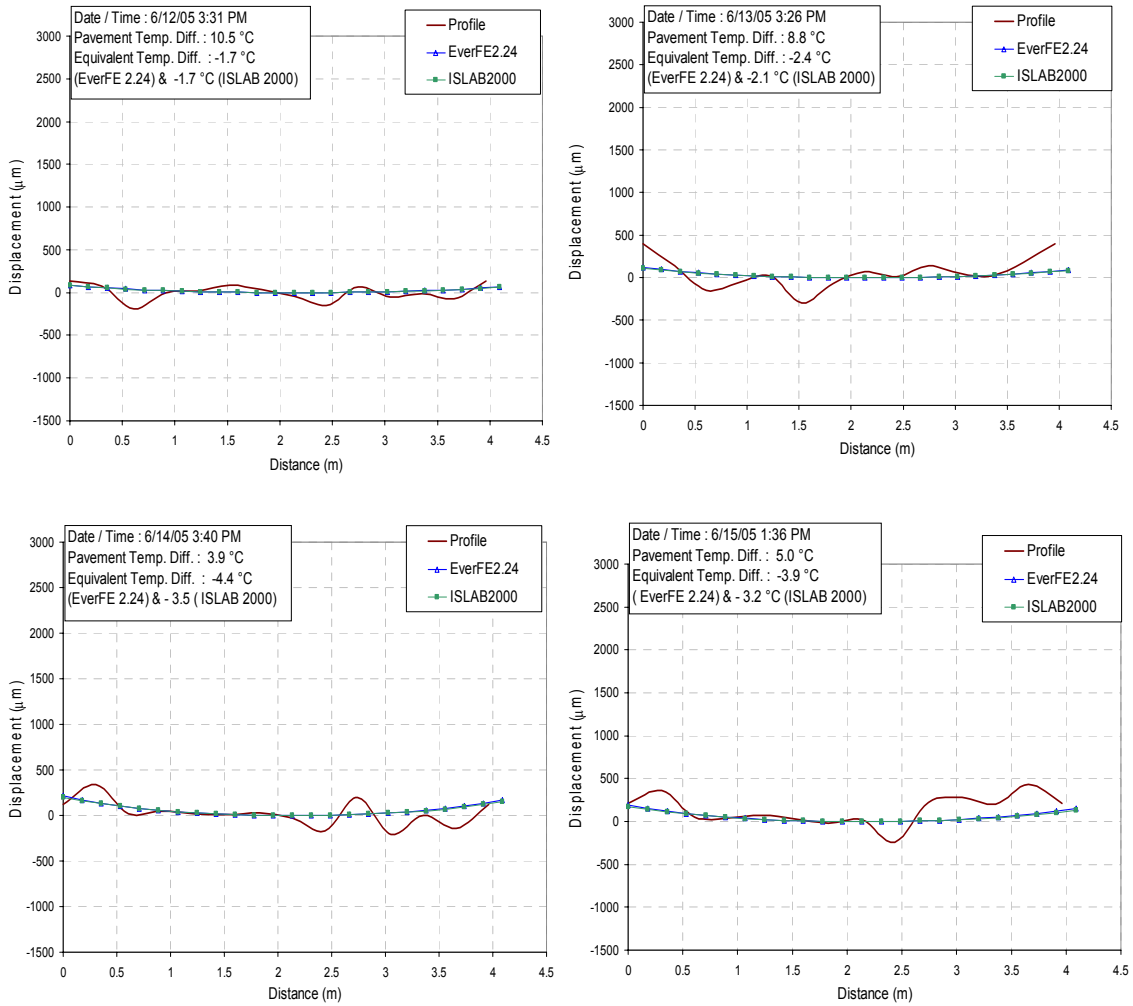
Figure A6-27 Profile measured versus FEM(using method 1 for equivalent temperature) simulated slab curvature profile of transverse 1 direction at negative temperature different condition in test section 2 (morning paving) of US-30, Marshalltown
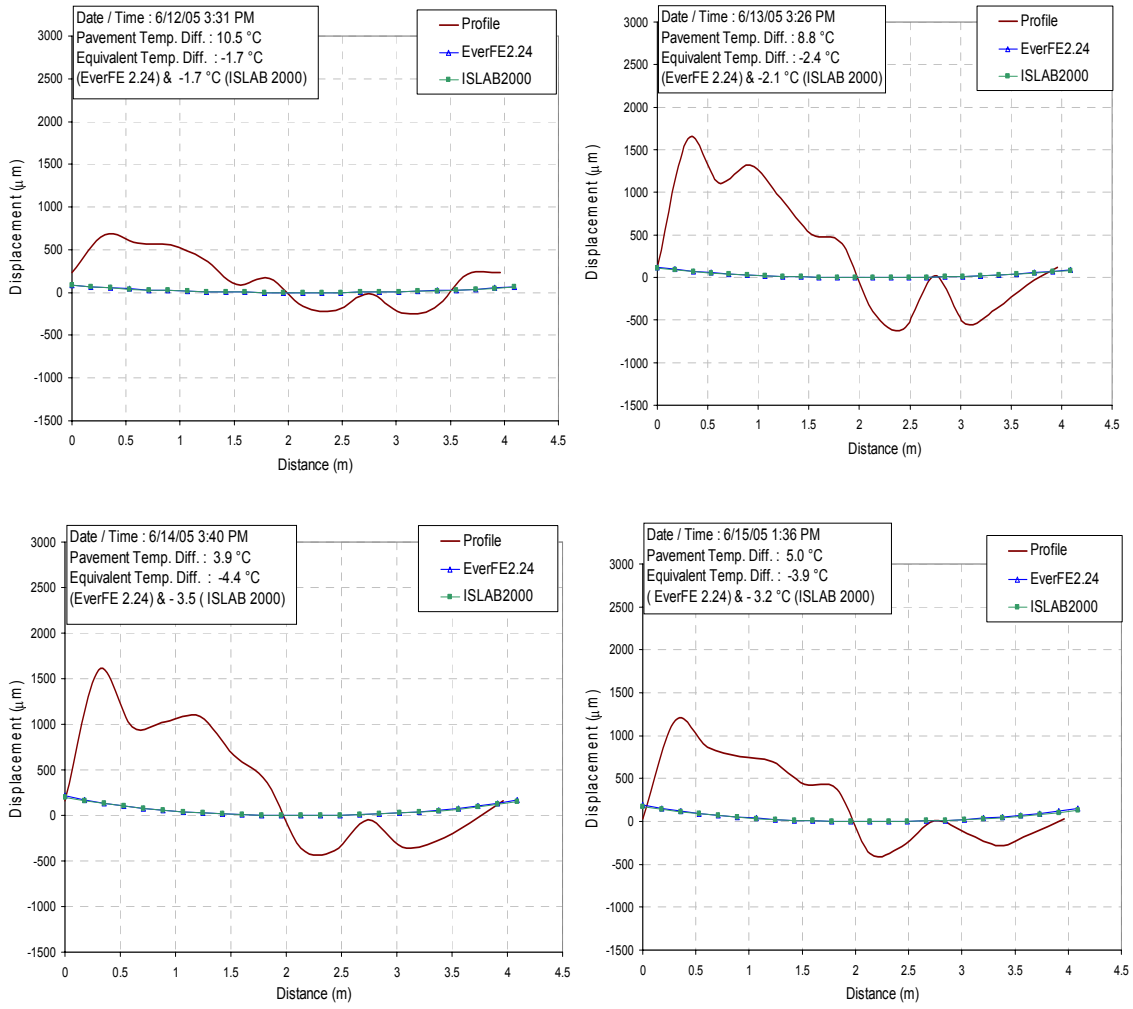
Figure A6-28 Profile measured versus FEM(using method 1 for equivalent temperature) simulated slab curvature profile of transverse 2 direction at negative temperature different condition in test section 2 (morning paving) of US-30, Marshalltown

Figure A6-29 Profile measured versus FEM(using method 1 for equivalent temperature) simulated slab curvature profile of diagonal 1 direction at positive temperature different condition in test section 2 (morning paving) of US-30, Marshalltown
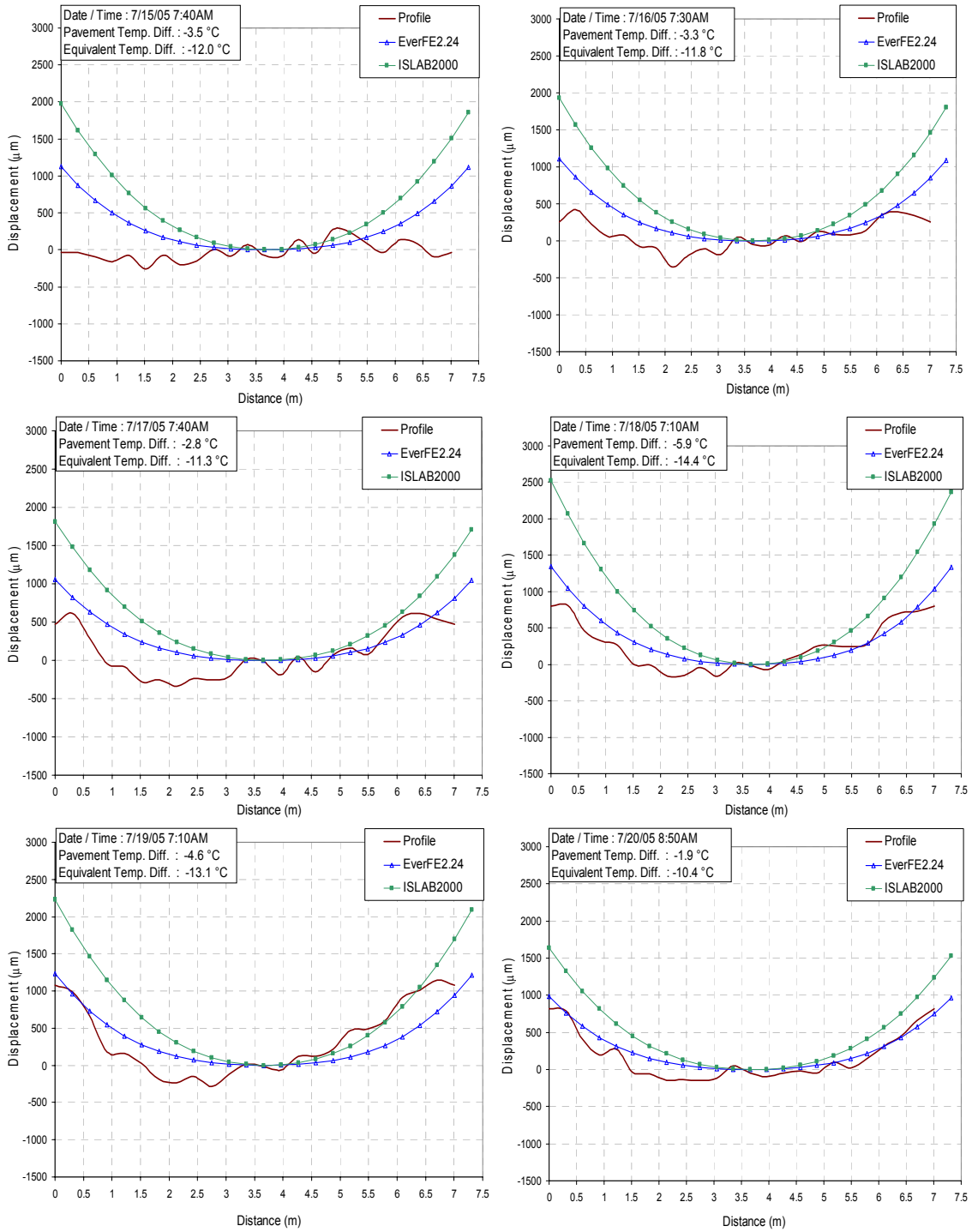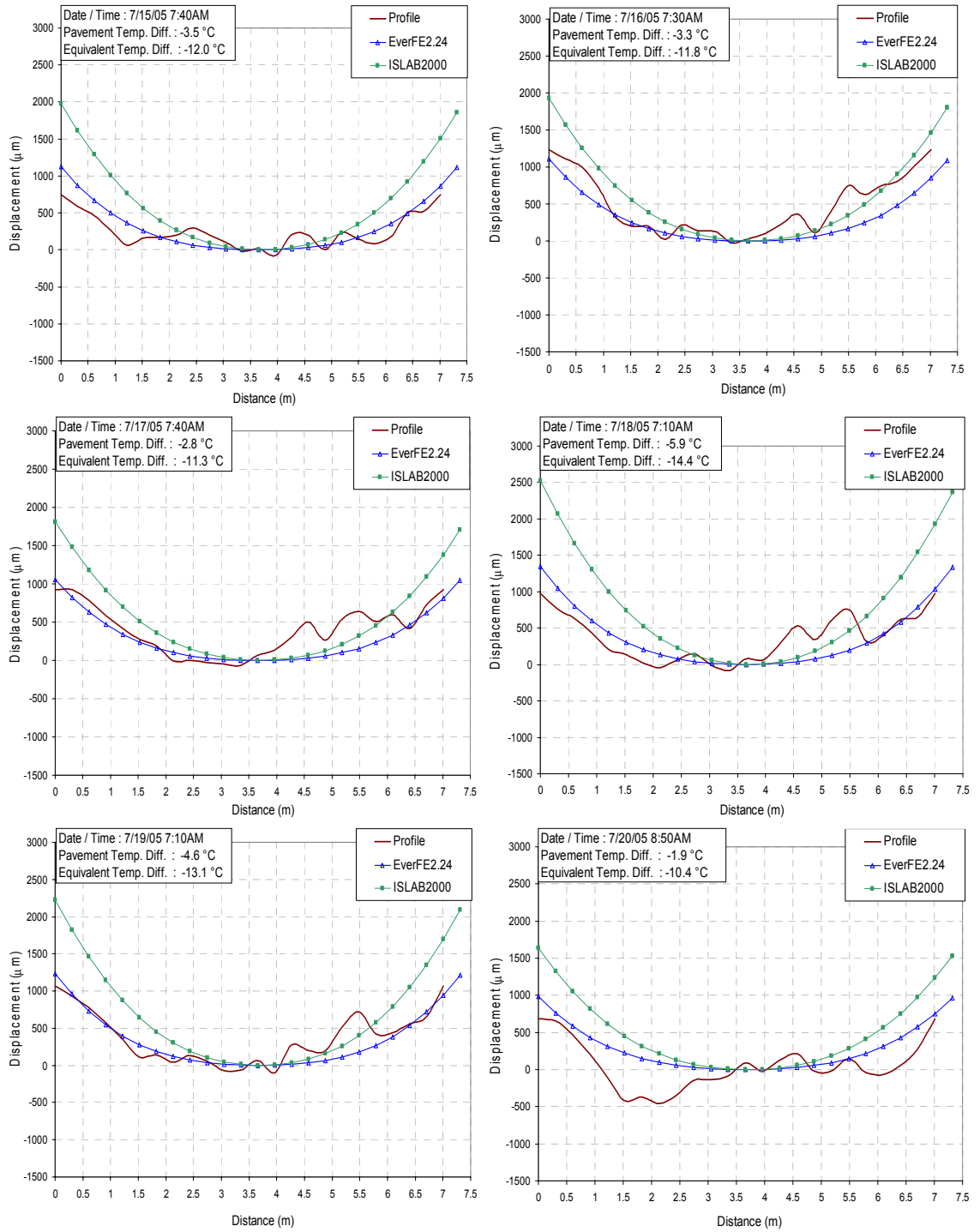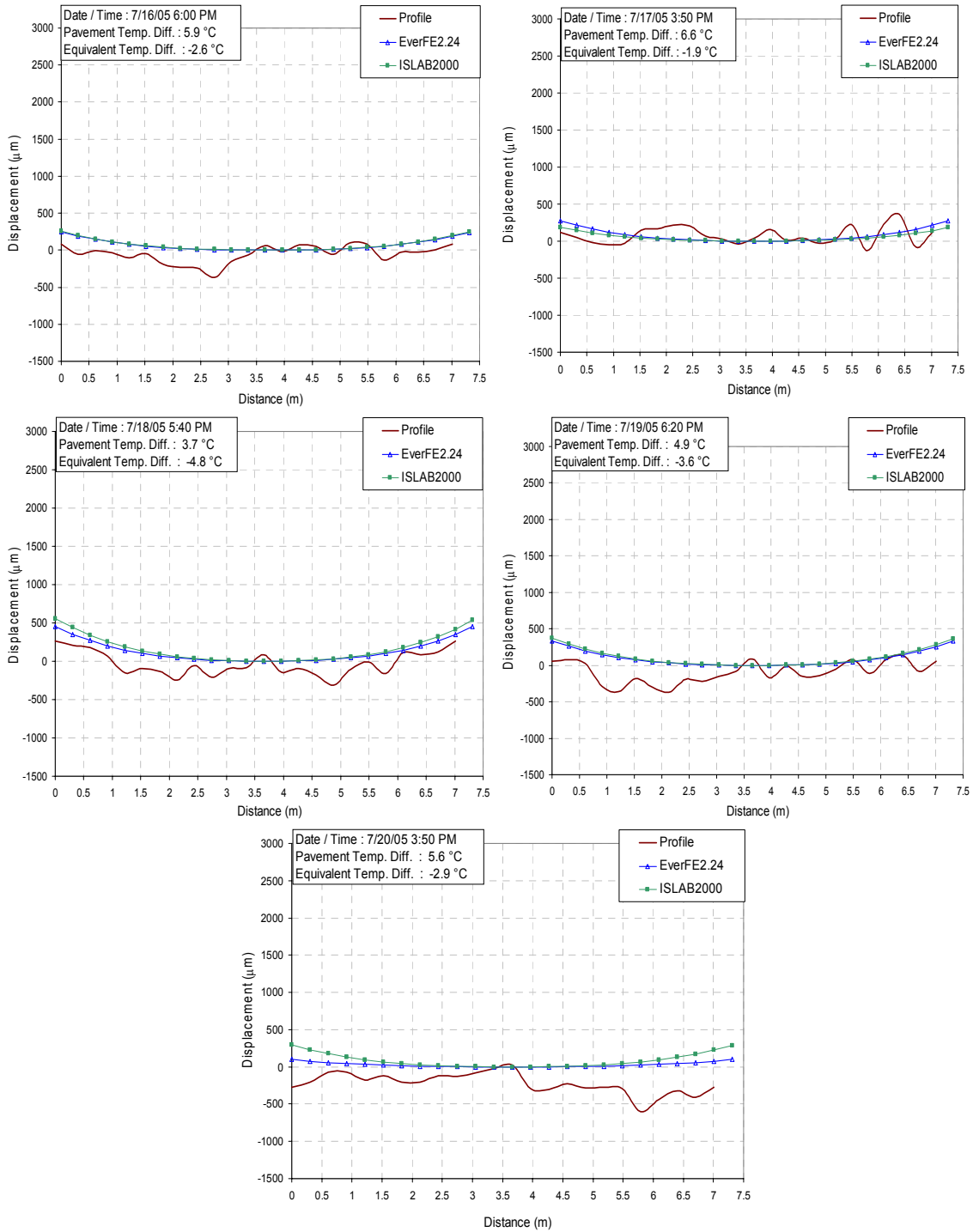
Figure A6-30 Profile measured versus FEM(using method 1 for equivalent temperature) simulated slab curvature profile of diagonal 2 direction at positive temperature different condition in test section 2 (morning paving) of US-30, Marshalltown
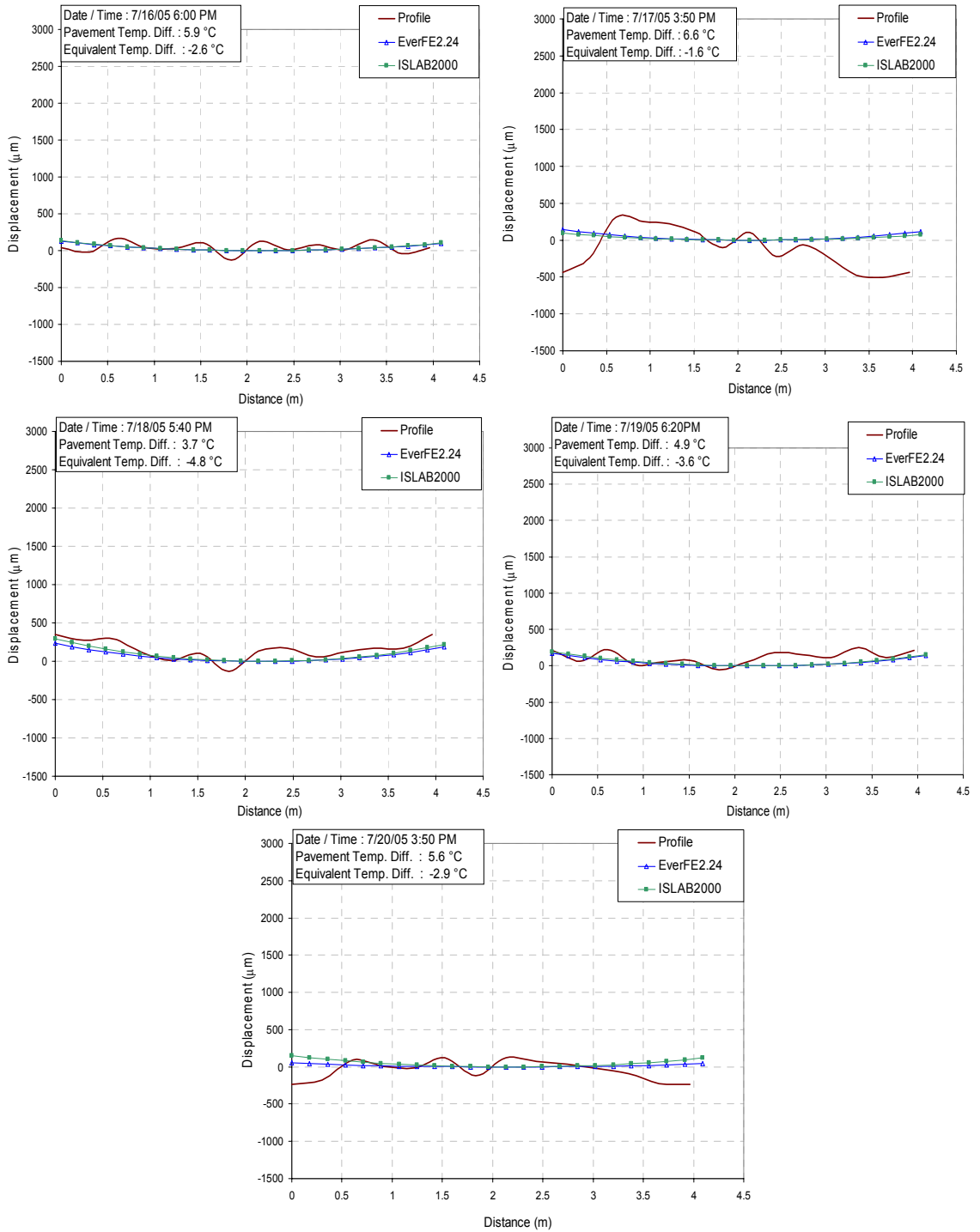
Figure A6-31 Profile measured versus FEM(using method 1 for equivalent temperature) simulated slab curvature profile of transverse 1 direction at positive temperature different condition in test section 2 (morning paving) of US-30, Marshalltown
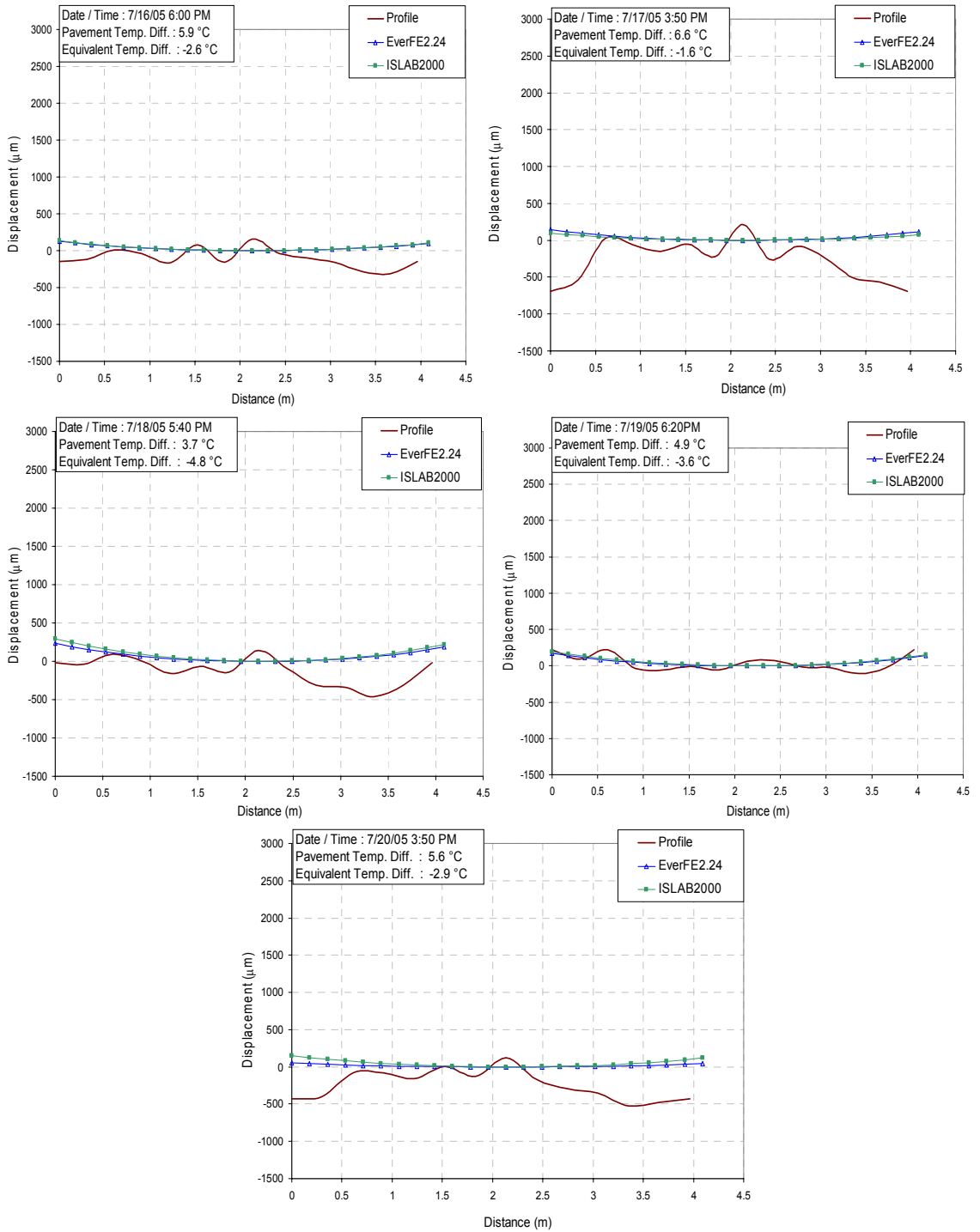
Figure A6-32 Profile measured versus FEM(using method 1 for equivalent temperature) simulated slab curvature profile of transverse 2 direction at positive temperature different condition in test section 2 (morning paving) of US-30, Marshalltown
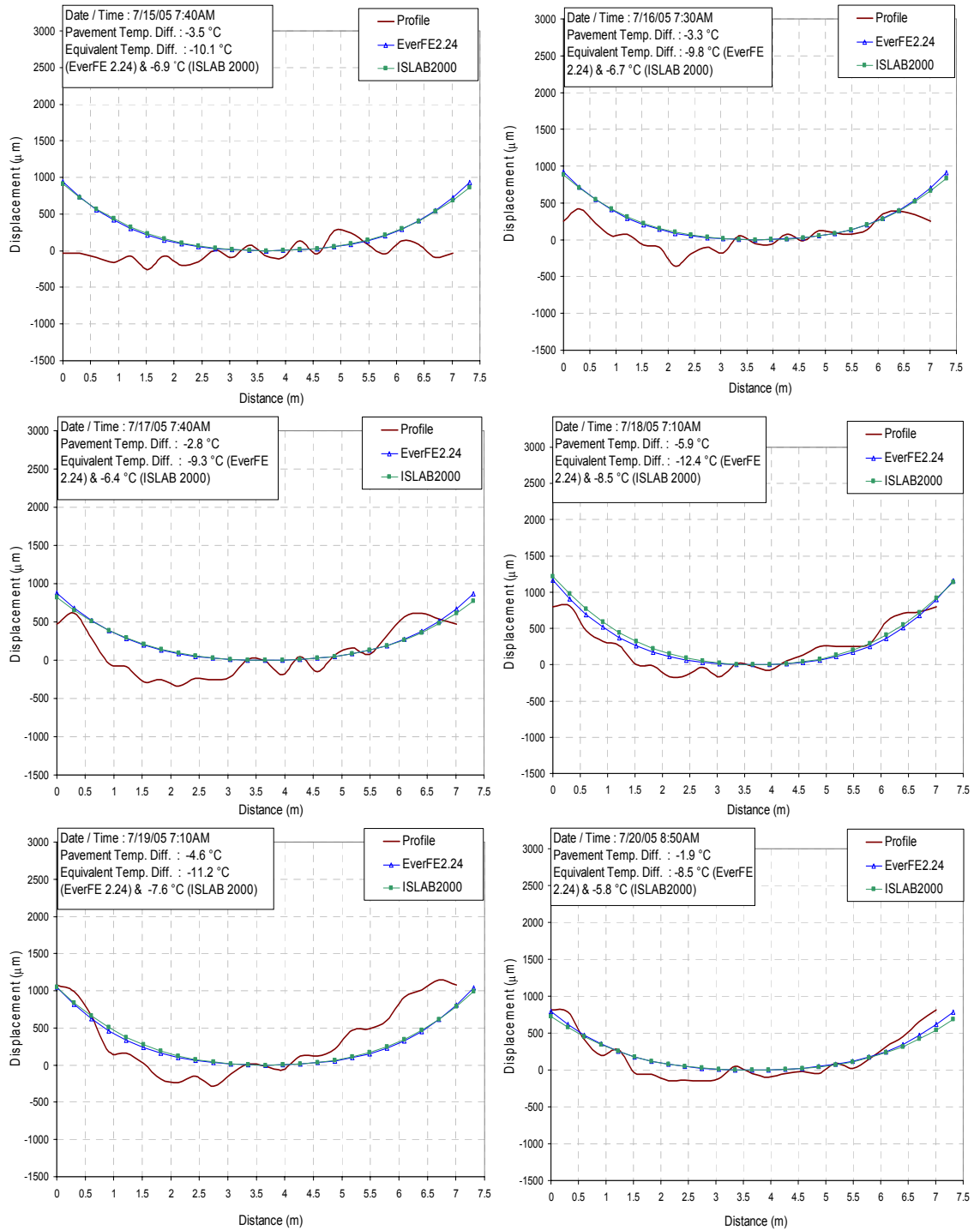
Figure A6-33 Profile measured versus FEM(using method 2 for equivalent temperature) simulated slab curvature profile of diagonal 1 direction at negative temperature different condition in test section 1 (afternoon paving) of US-30, Marshalltown
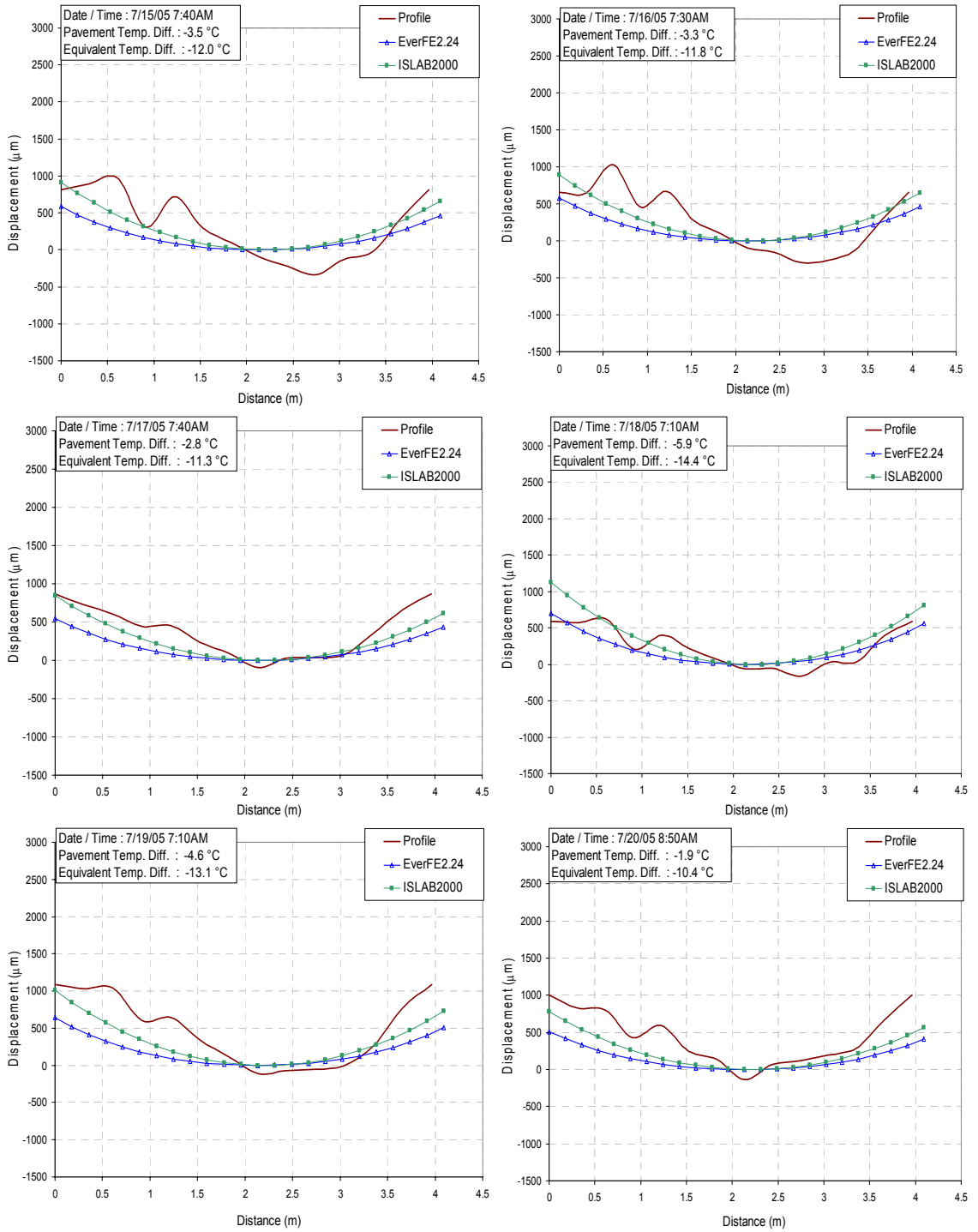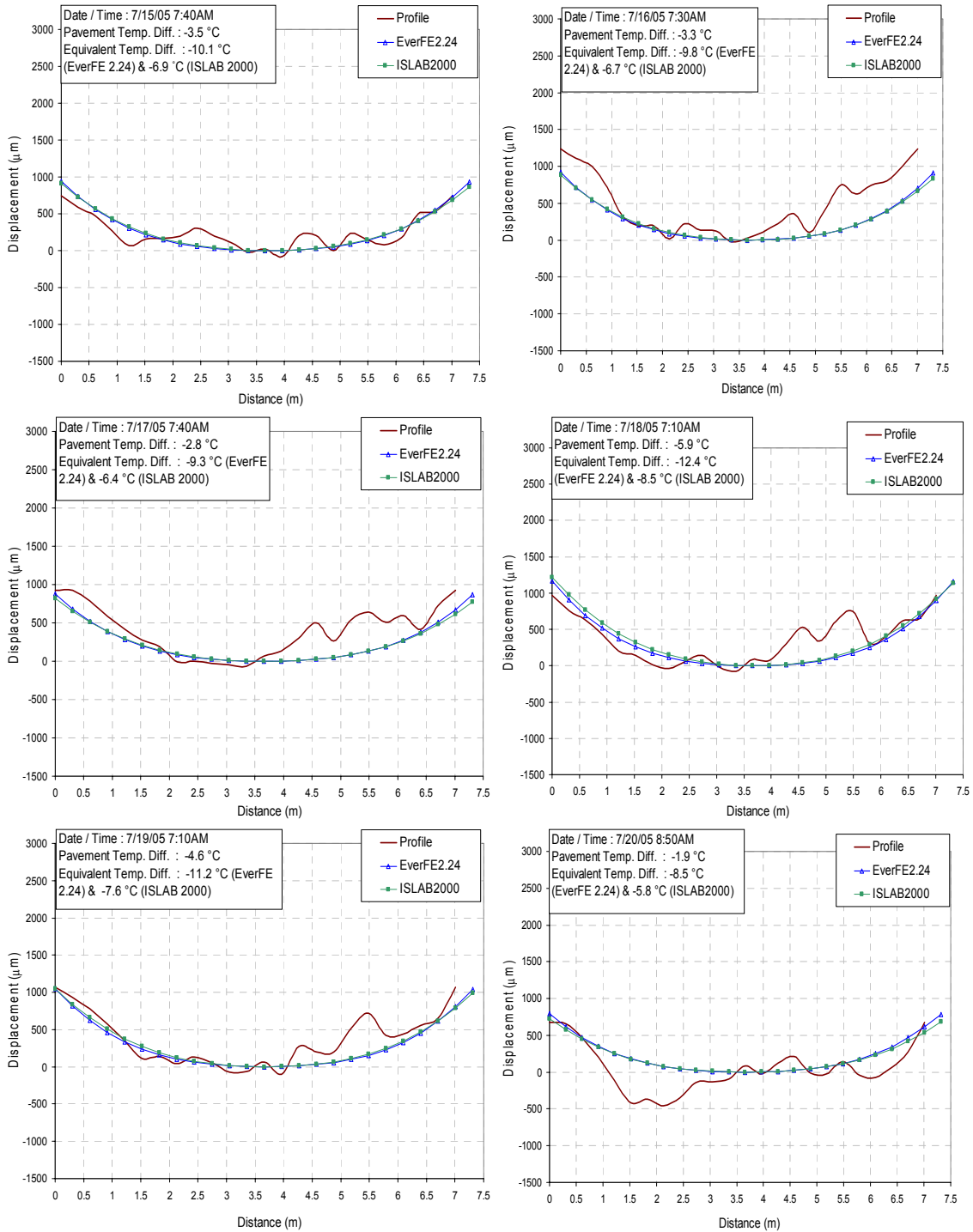
Figure A6-34 Profile measured versus FEM(using method 2 for equivalent temperature) simulated slab curvature profile of diagonal 2 direction at negative temperature different condition in test section 1 (afternoon paving) of US-30, Marshalltown
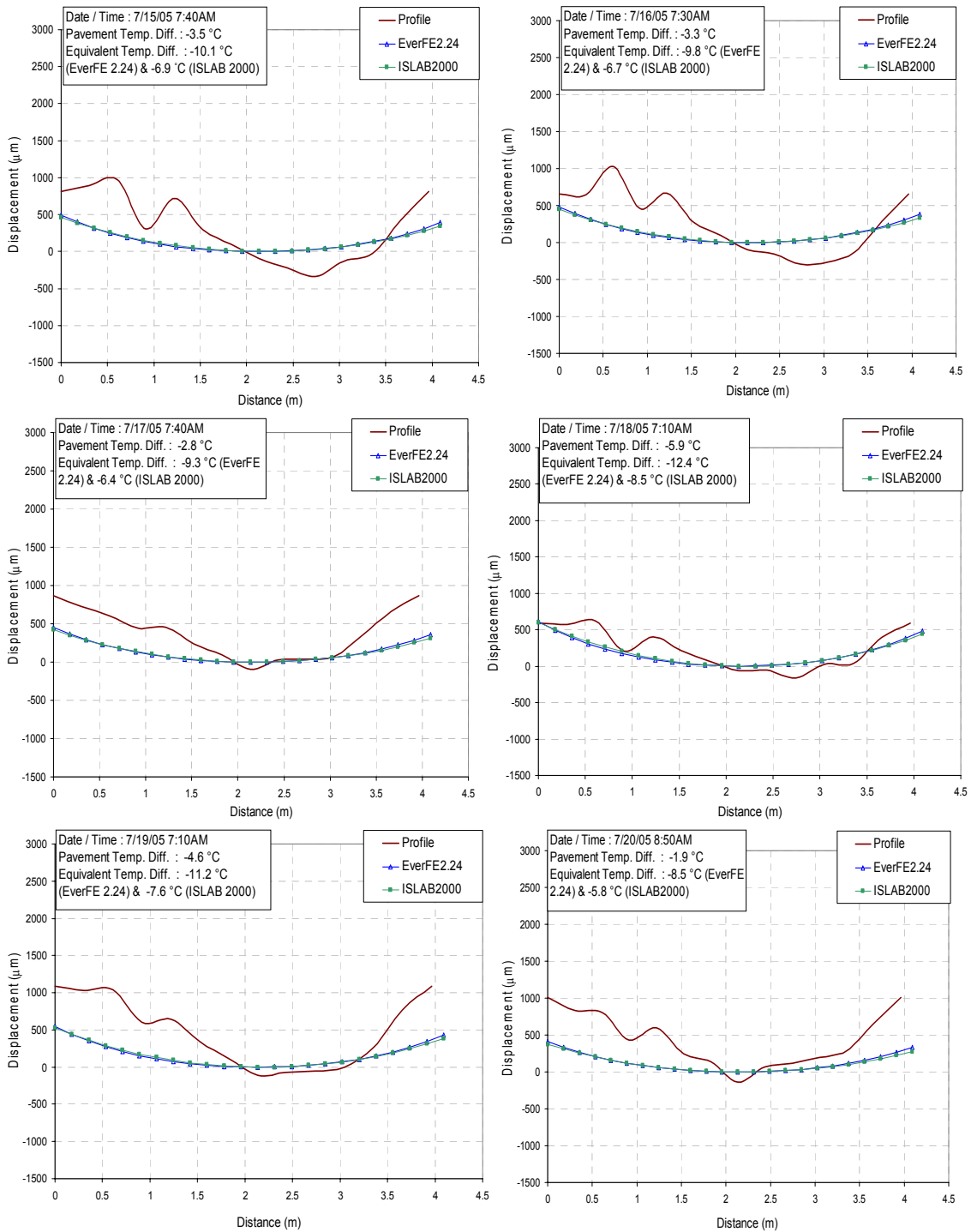
Figure A6-35 Profile measured versus FEM(using method 2 for equivalent temperature) simulated slab curvature profile of transverse 1 direction at negative temperature different condition in test section 1 (afternoon paving) of US-30, Marshalltown
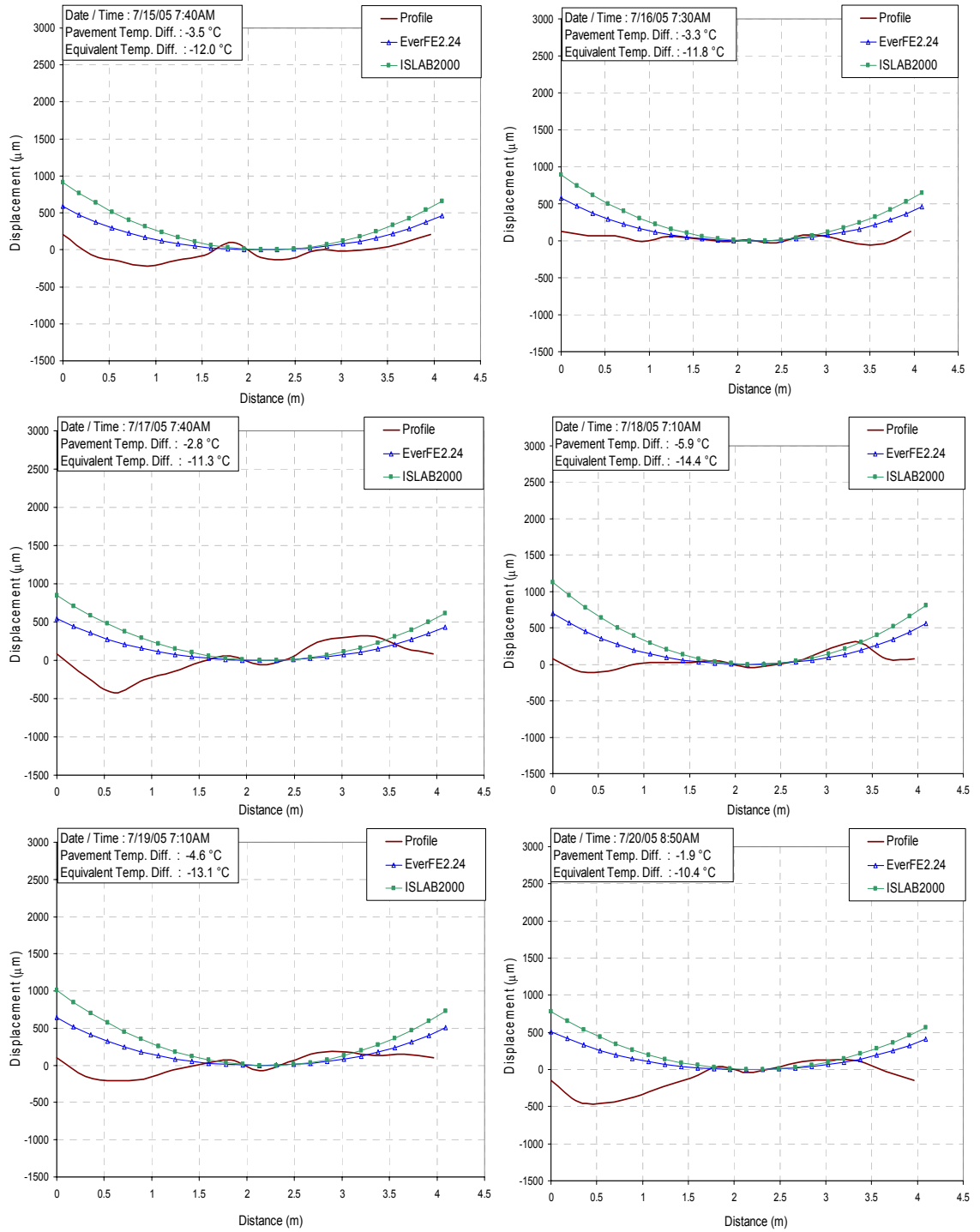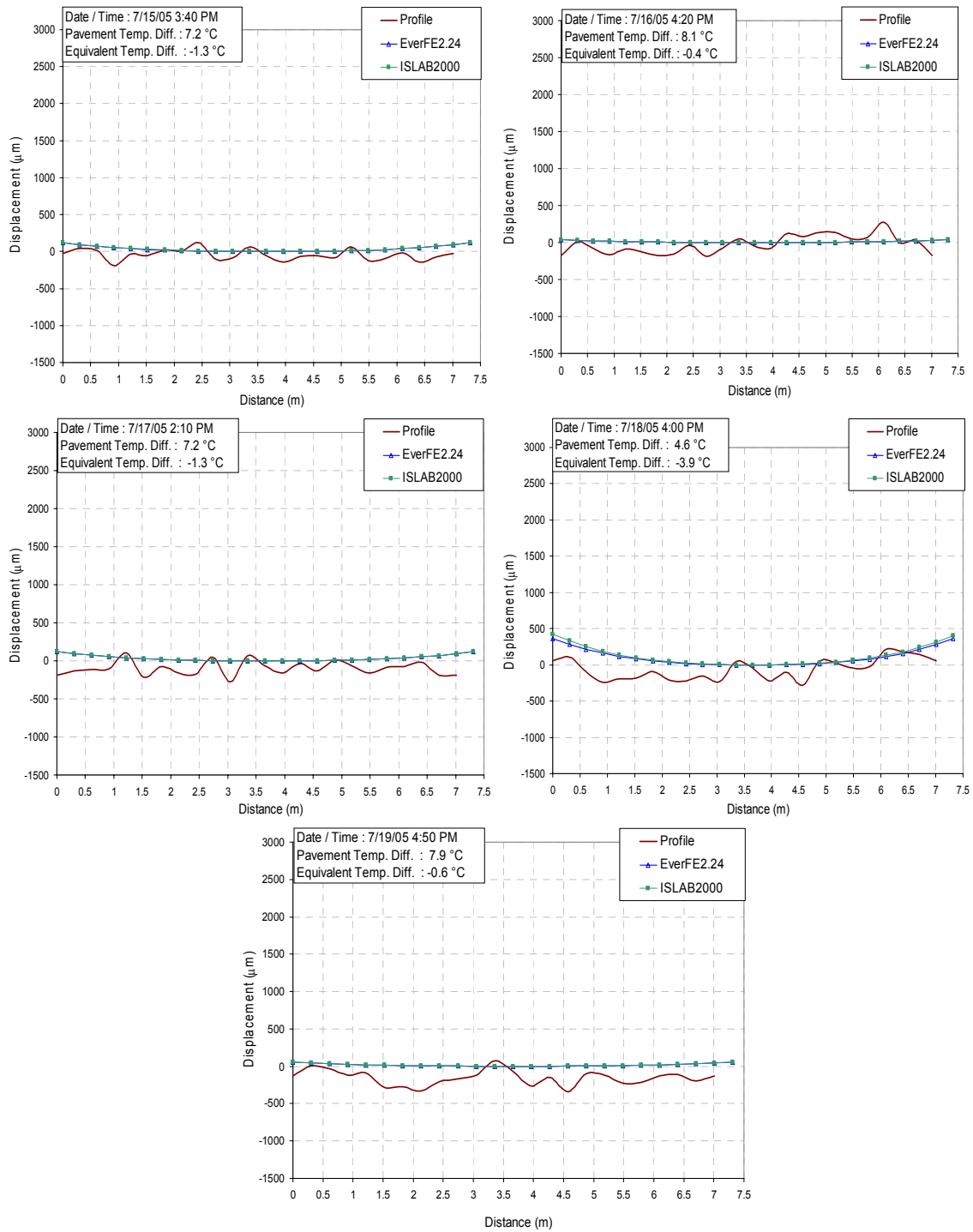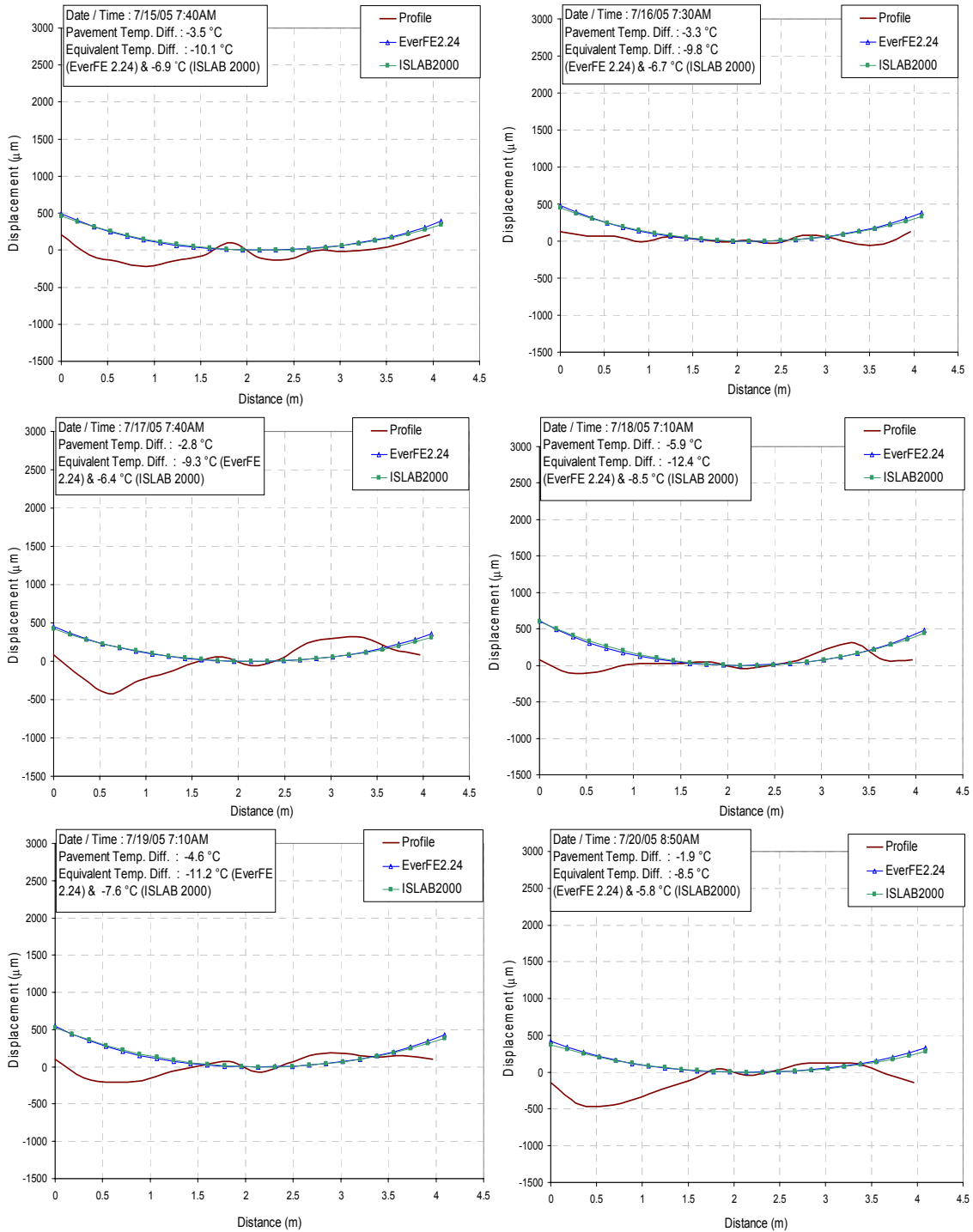
Figure A6-36 Profile measured versus FEM(using method 2 for equivalent temperature) simulated slab curvature profile of transverse 2 direction at negative temperature different condition in test section 1 (afternoon paving) of US-30, Marshalltown
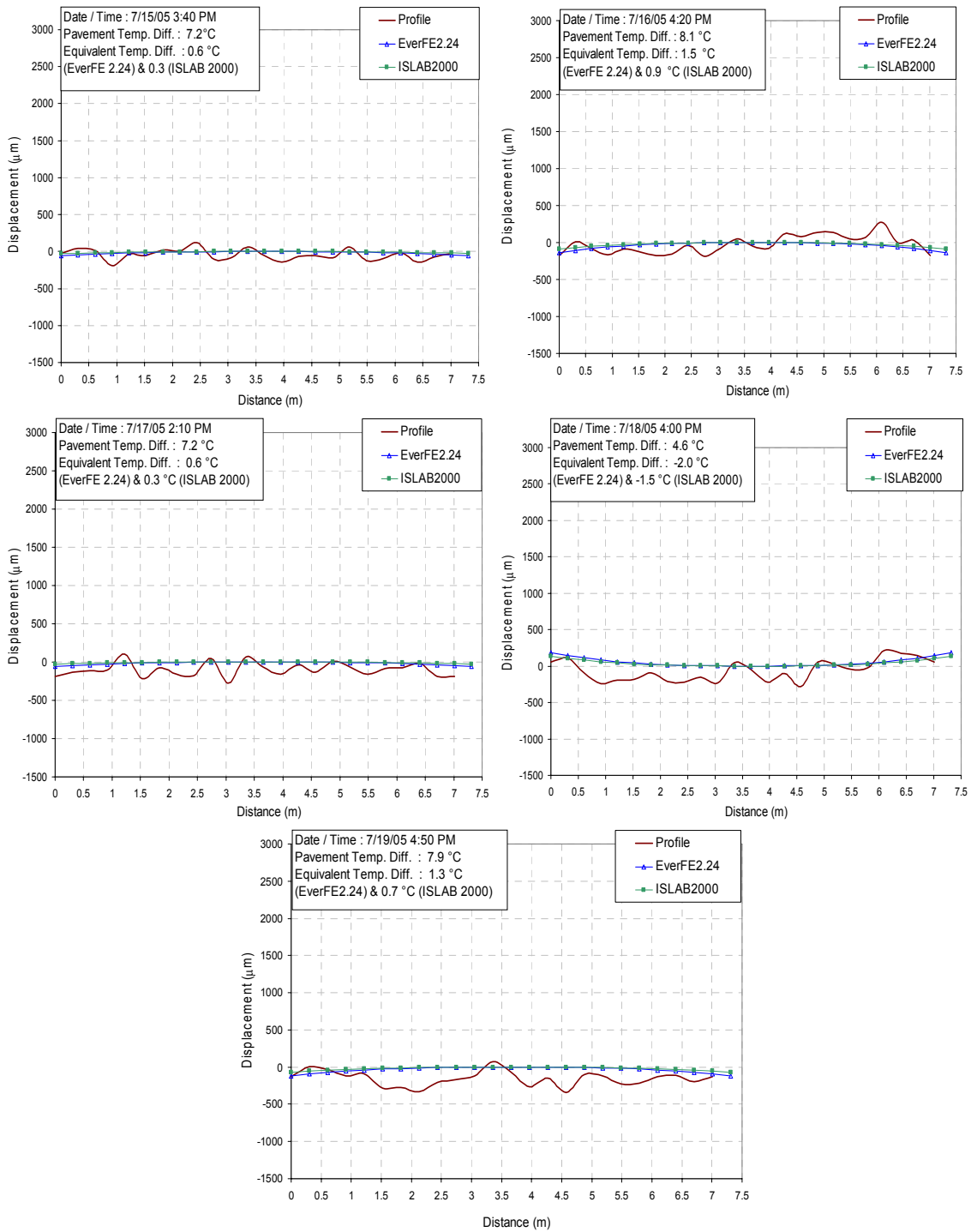
Figure A6-37 Profile measured versus FEM(using method 2 for equivalent temperature) simulated slab curvature profile of diagonal 1 direction at positive temperature different condition in test section 1 (afternoon paving) of US-30, Marshalltown
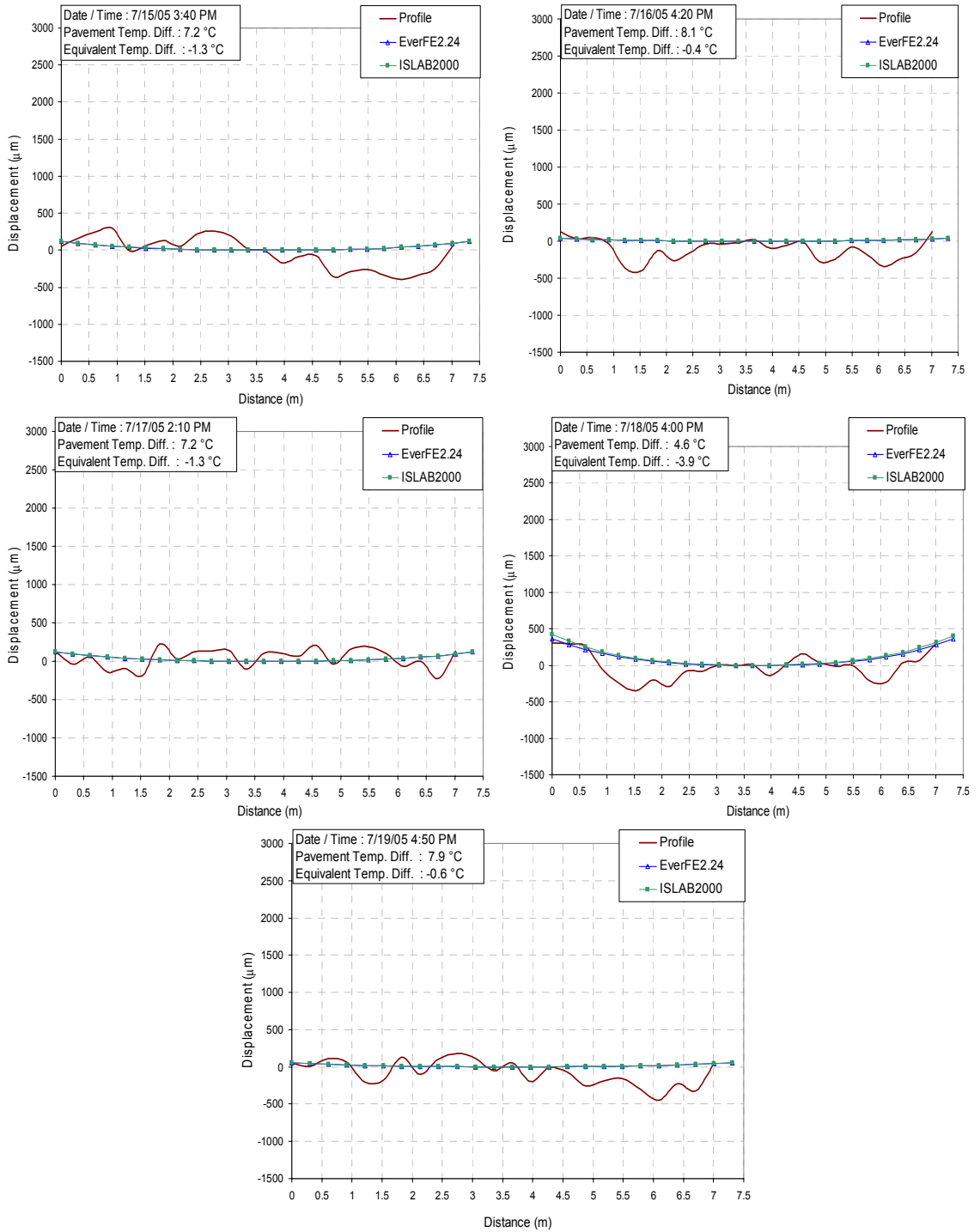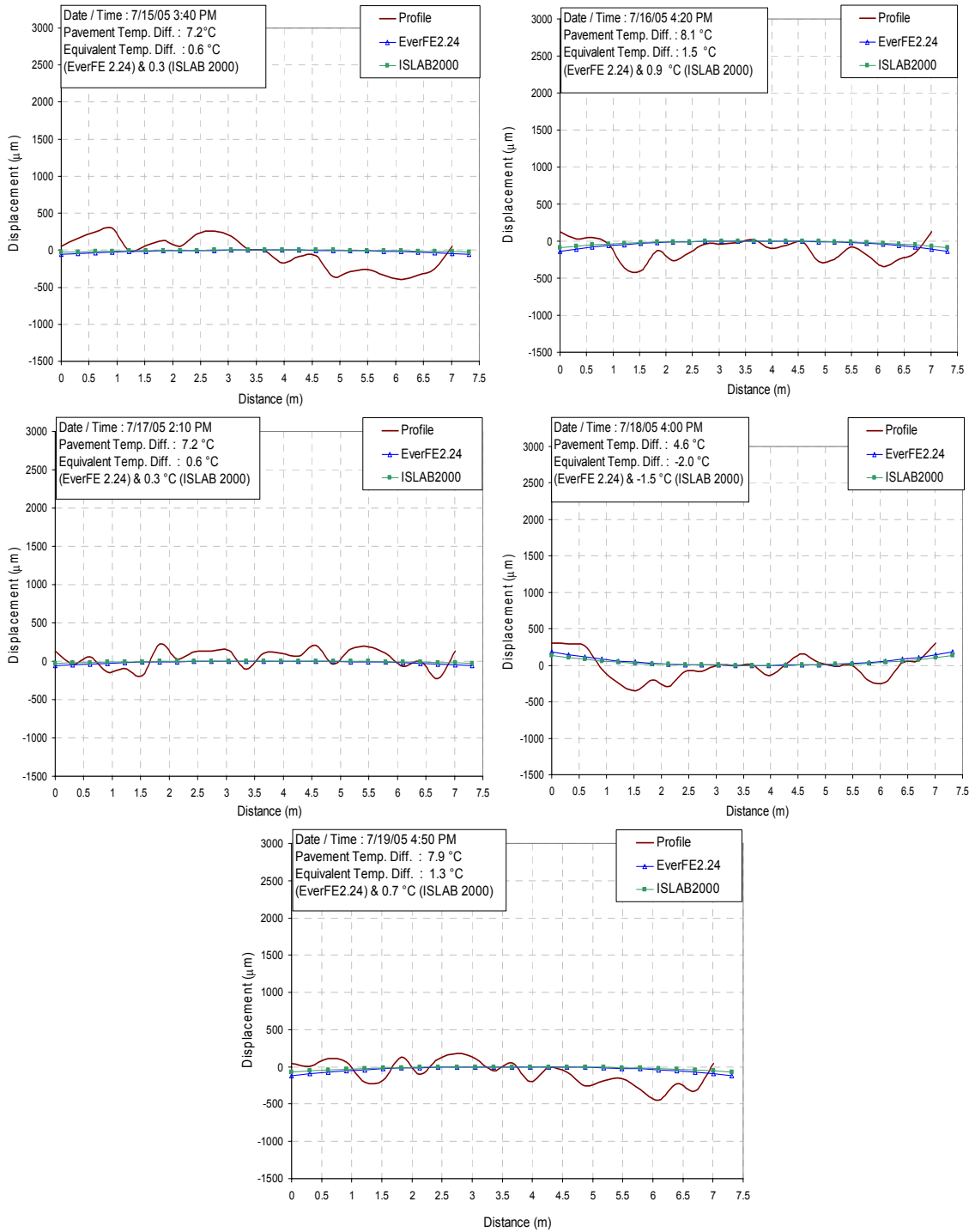
Figure A6-38 Profile measured versus FEM(using method 2 for equivalent temperature) simulated slab curvature profile of diagonal 2 direction at positive temperature different condition in test section 1 (afternoon paving) of US-30, Marshalltown
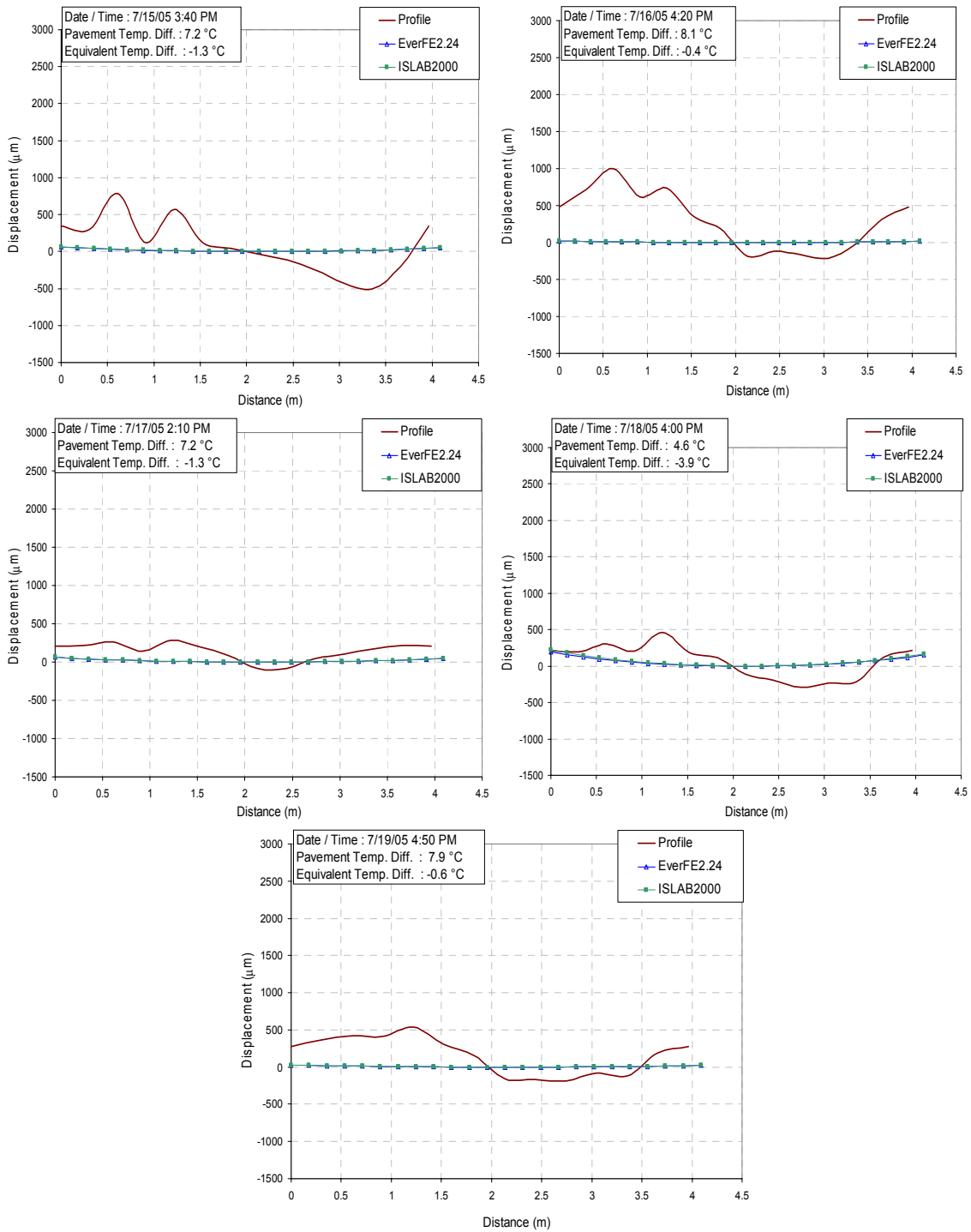
292
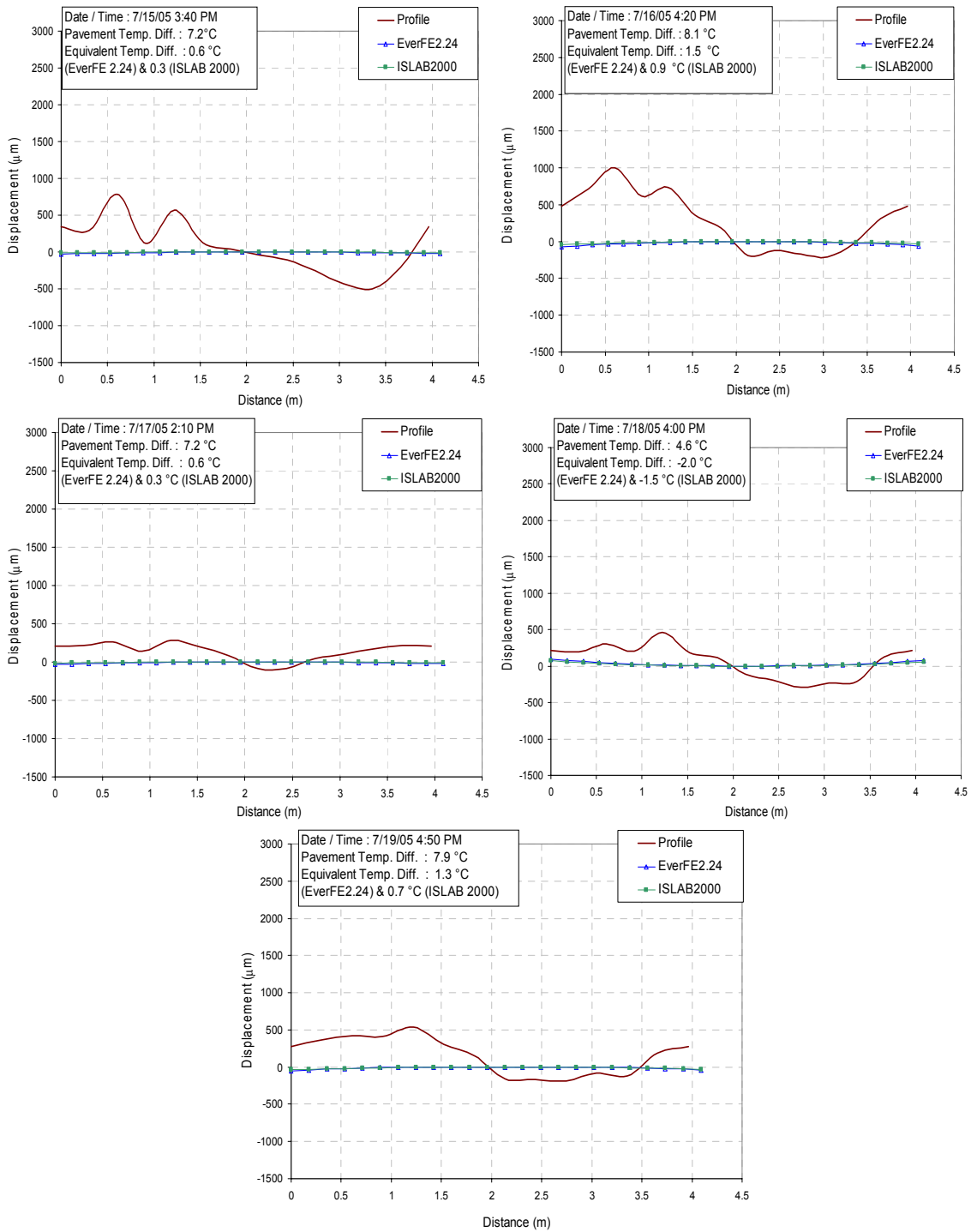
Figure A6-39 Profile measured versus FEM(using method 2 for equivalent temperature) simulated slab curvature profile of transverse 1 direction at positive temperature different condition in test section 1 (afternoon paving) of US-30, Marshalltown
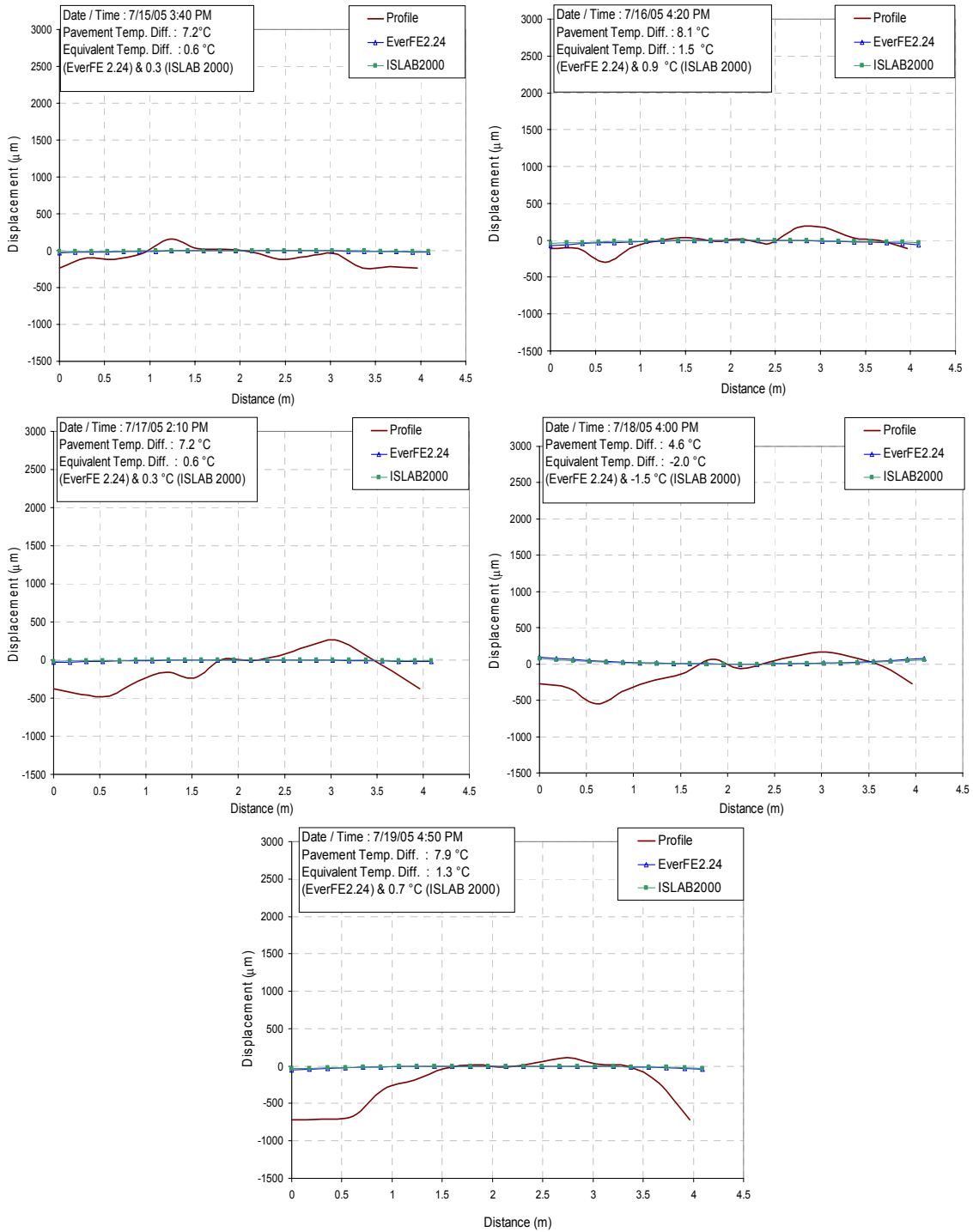
Figure A6-40 Profile measured versus FEM(using method 2 for equivalent temperature) simulated slab curvature profile of transverse 2 direction at positive temperature different condition in test section 1 (afternoon paving) of US-30, Marshalltown
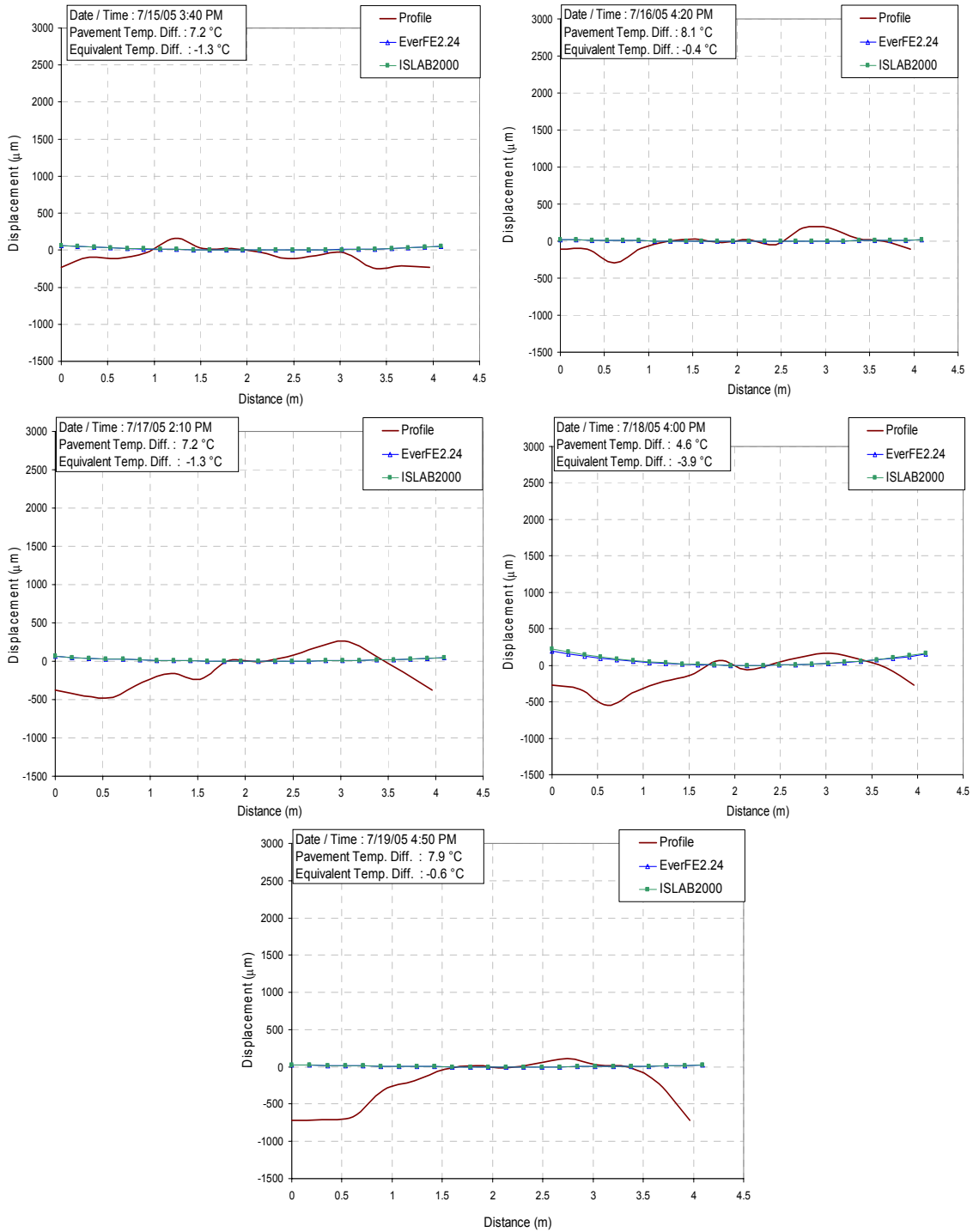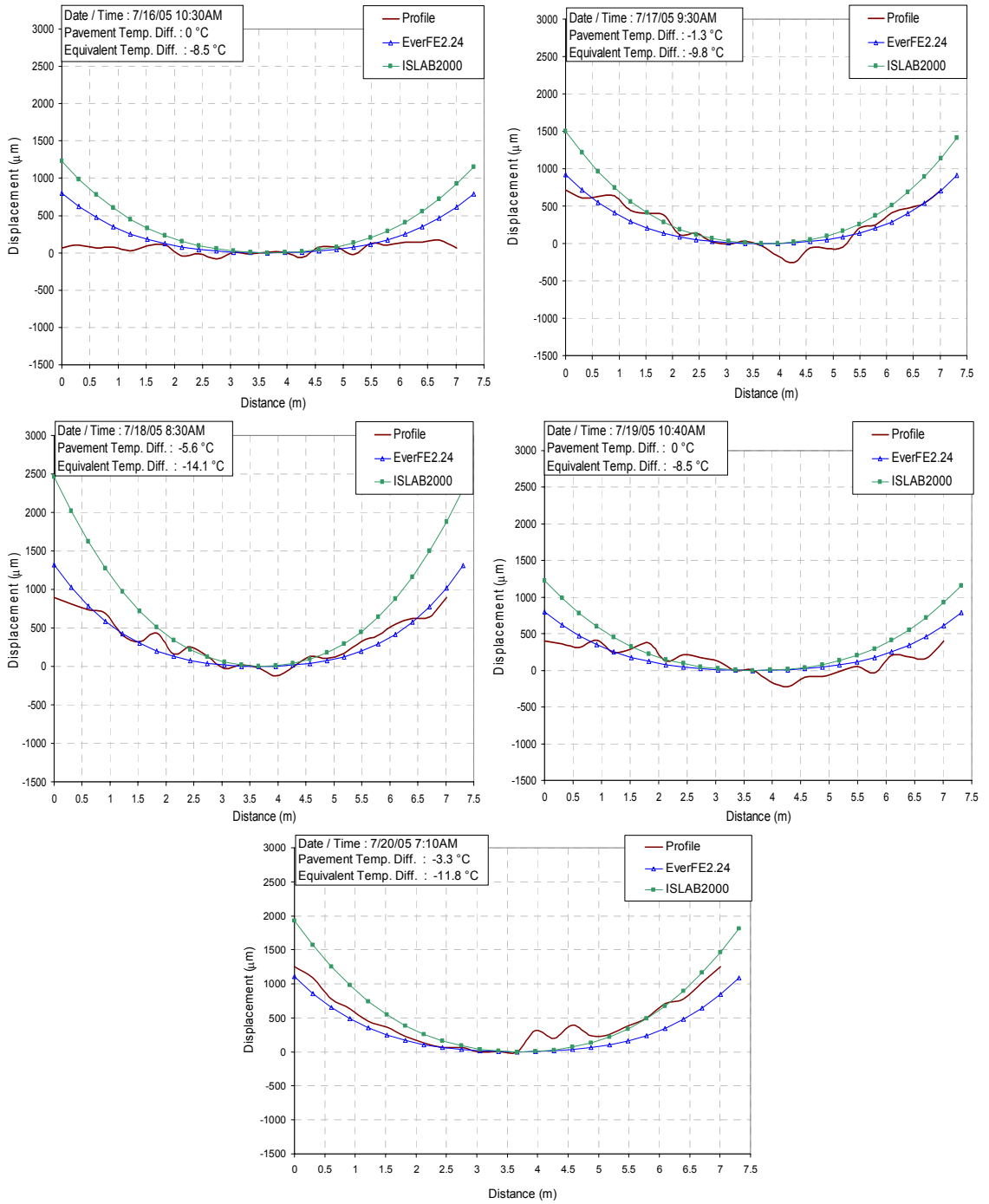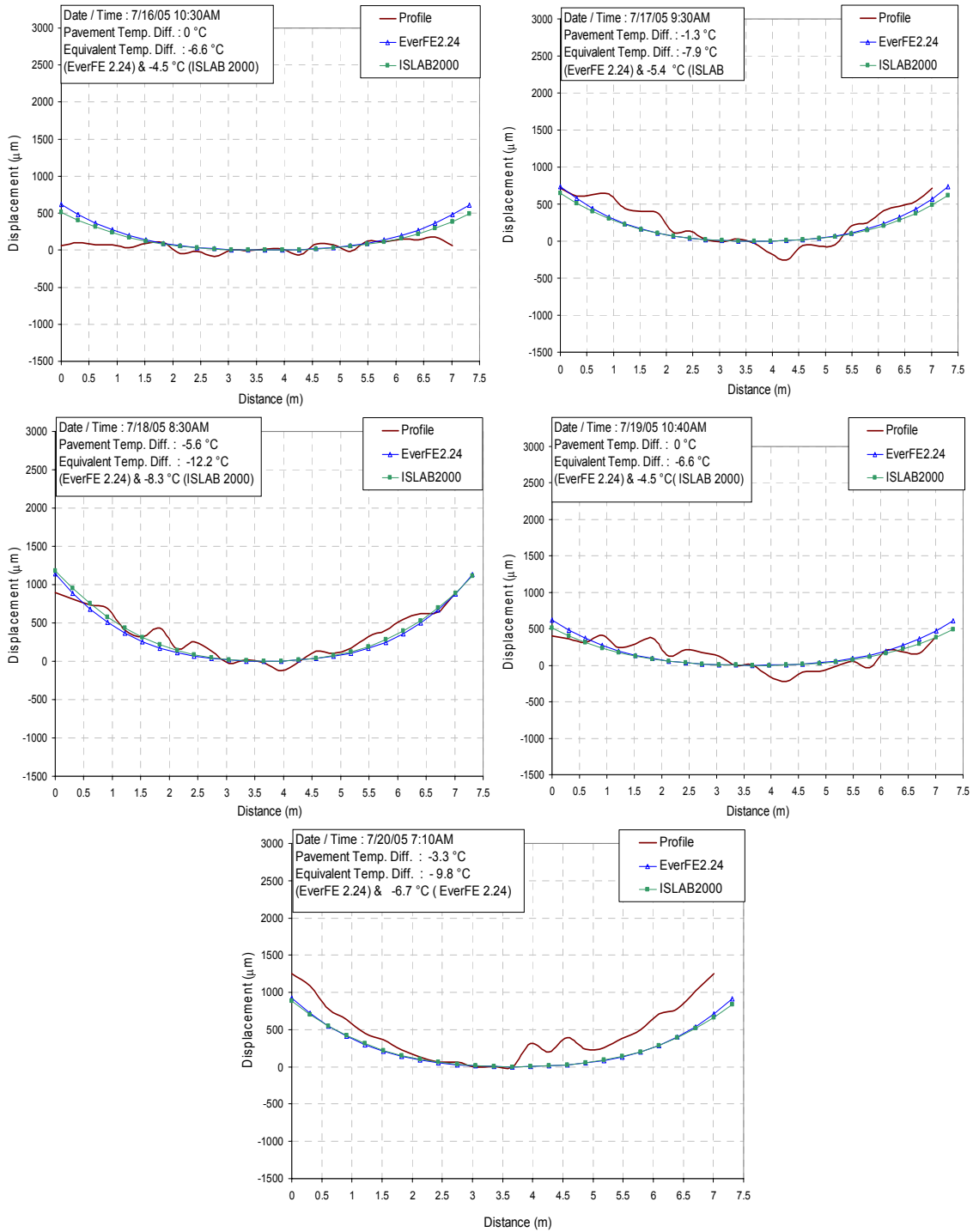
Figure A6-41 Profile measured versus FEM(using method 2 for equivalent temperature) simulated slab curvature profile of diagonal 1 direction at negative temperature different condition in test section 2 (morning paving) of US-30, Marshalltown
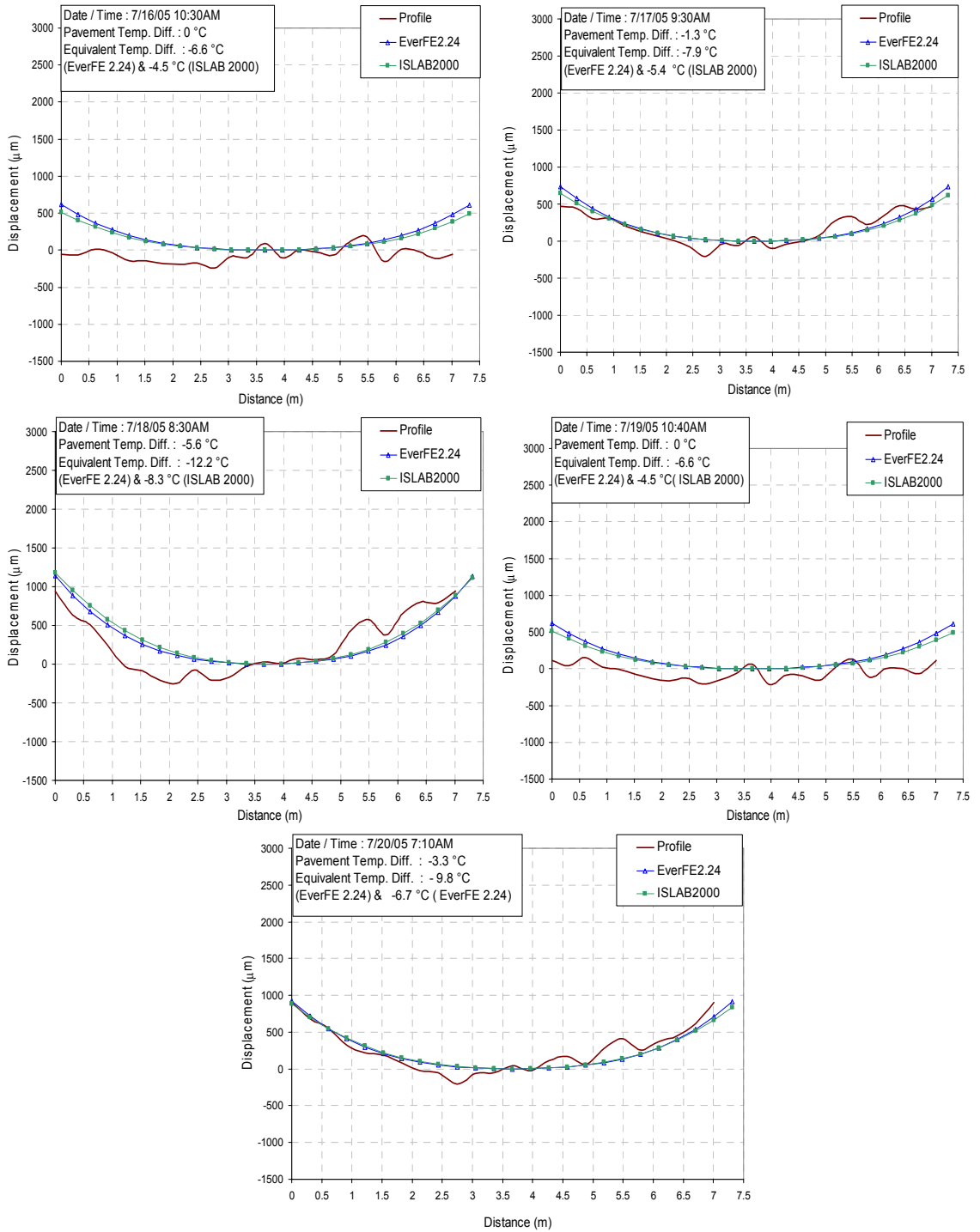
Figure A6-42 Profile measured versus FEM(using method 2 for equivalent temperature) simulated slab curvature profile of diagonal 2 direction at negative temperature different condition in test section 2 (morning paving) of US-30, Marshalltown
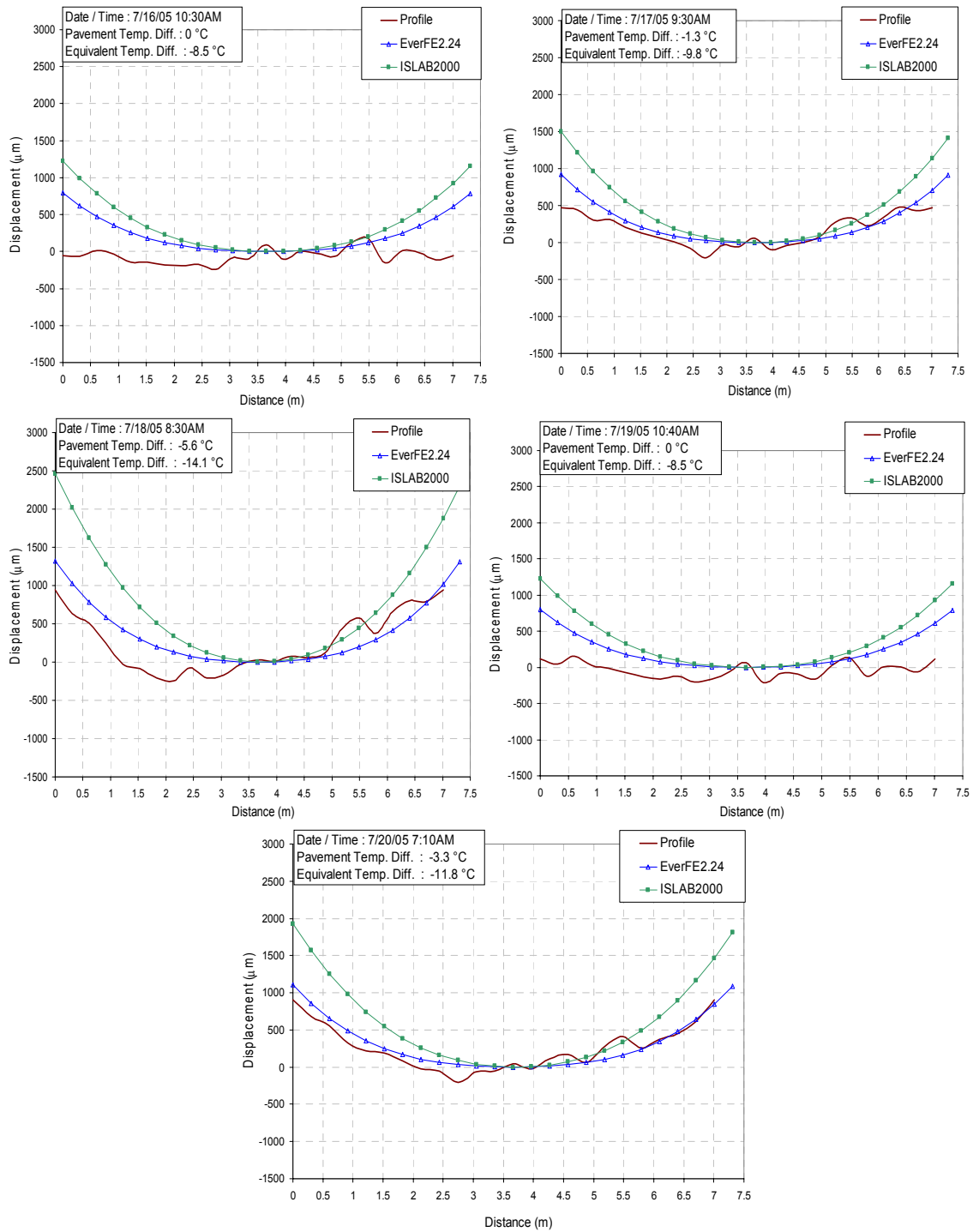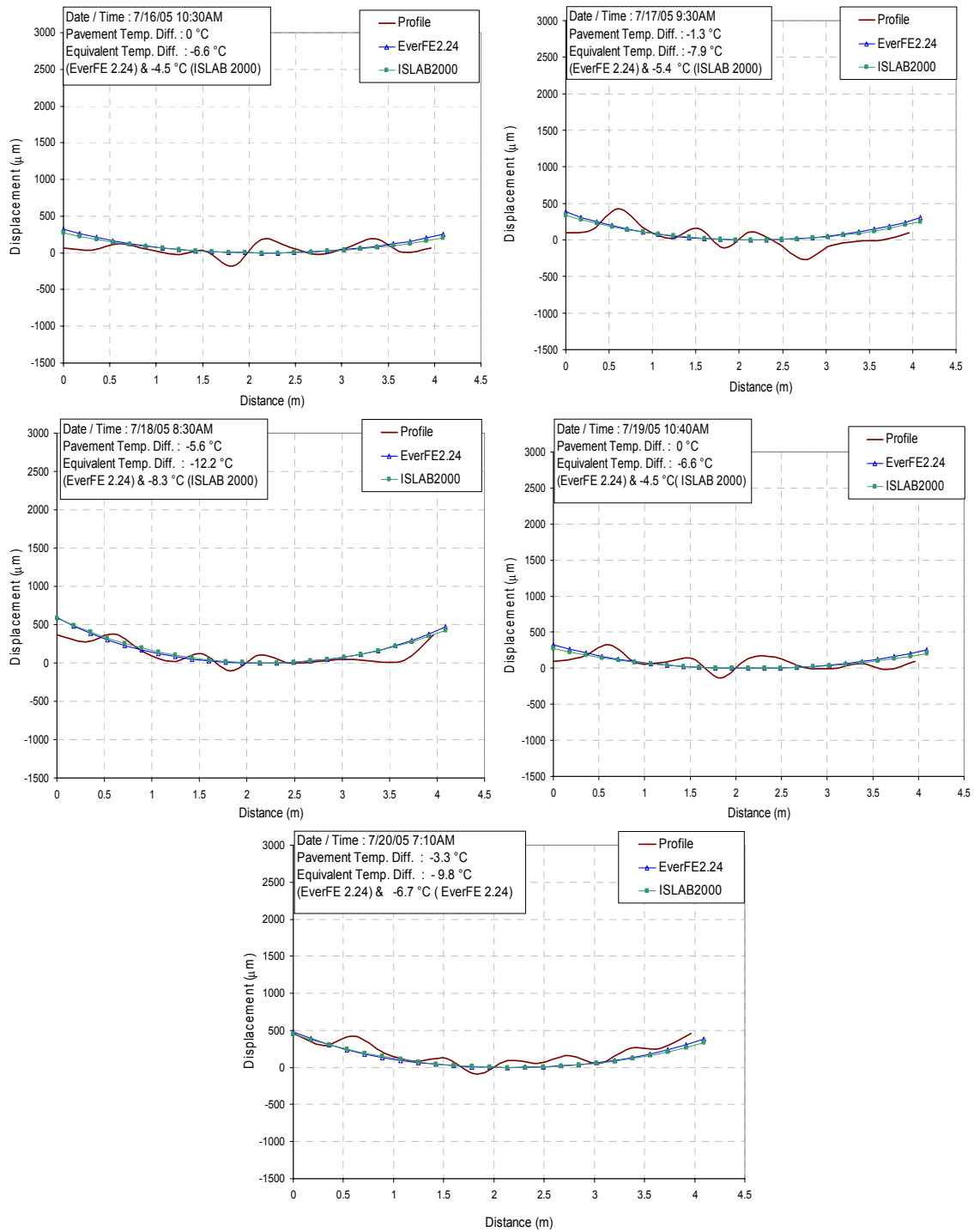
Figure A6-43 Profile measured versus FEM(using method 2 for equivalent temperature) simulated slab curvature profile of transverse 1 direction at negative temperature different condition in test section 2 (morning paving) of US-30, Marshalltown
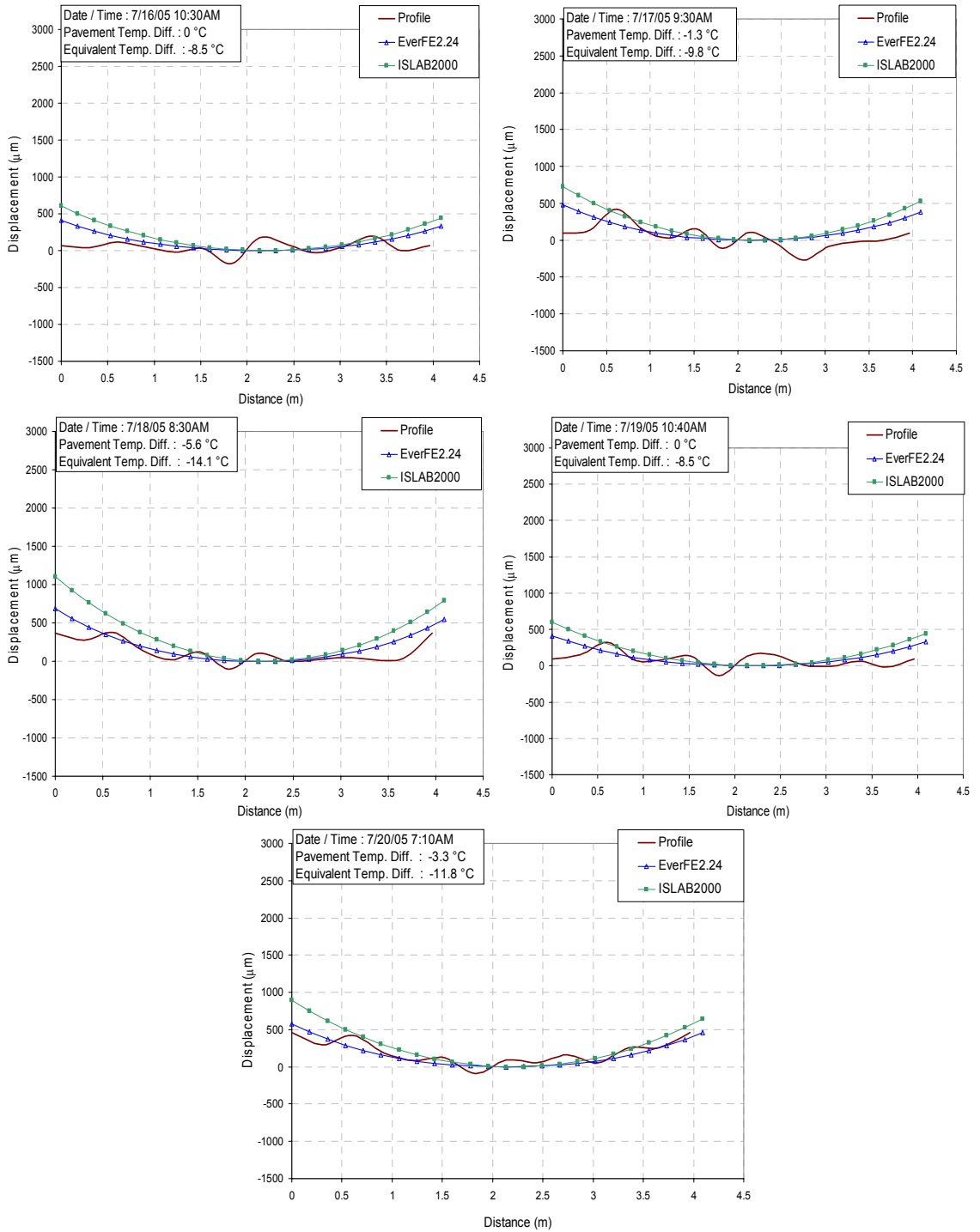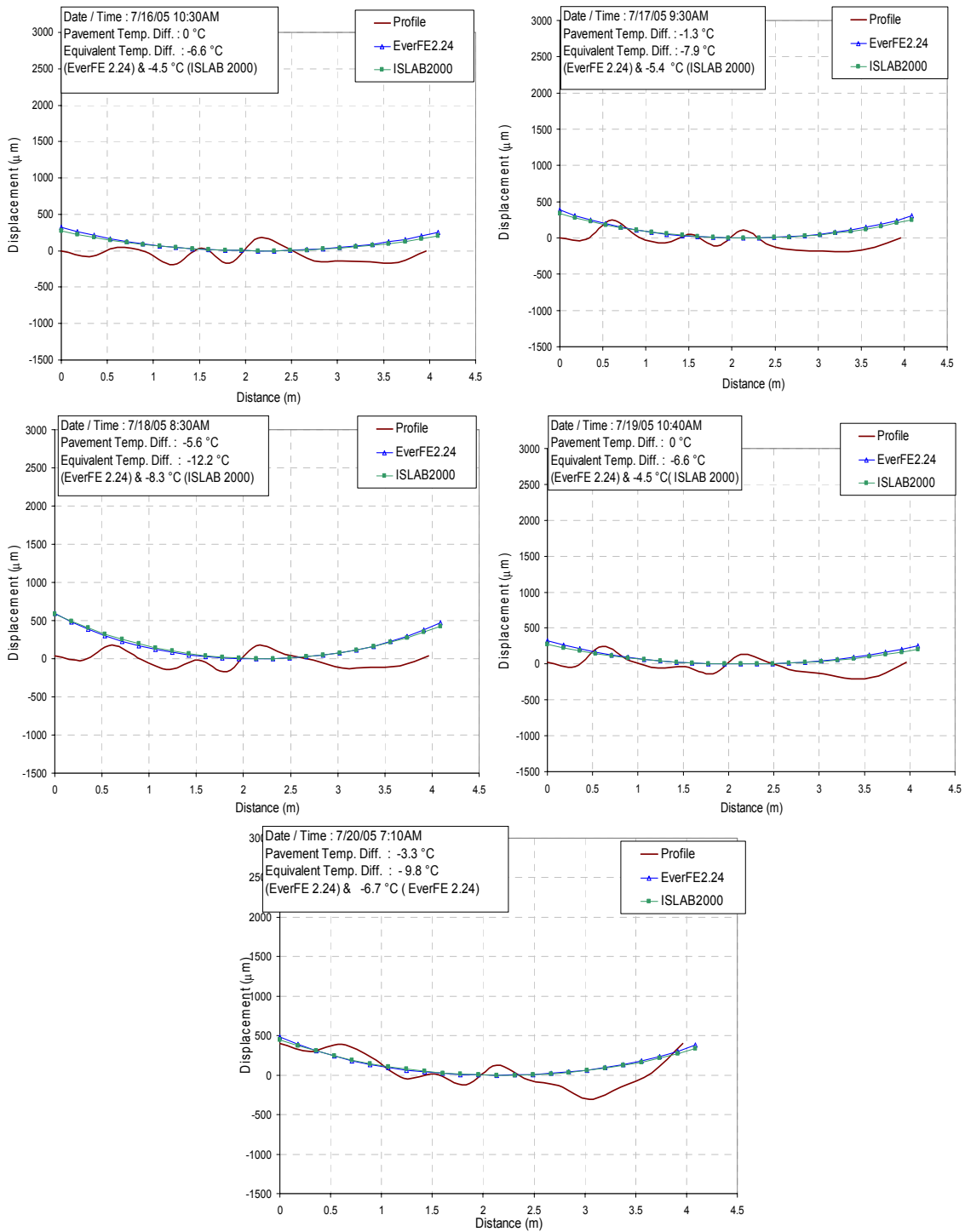
Figure A6-44 Profile measured versus FEM(using method 2 for equivalent temperature) simulated slab curvature profile of transverse 2 direction at negative temperature different condition in test section 2 (morning paving) of US-30, Marshalltown
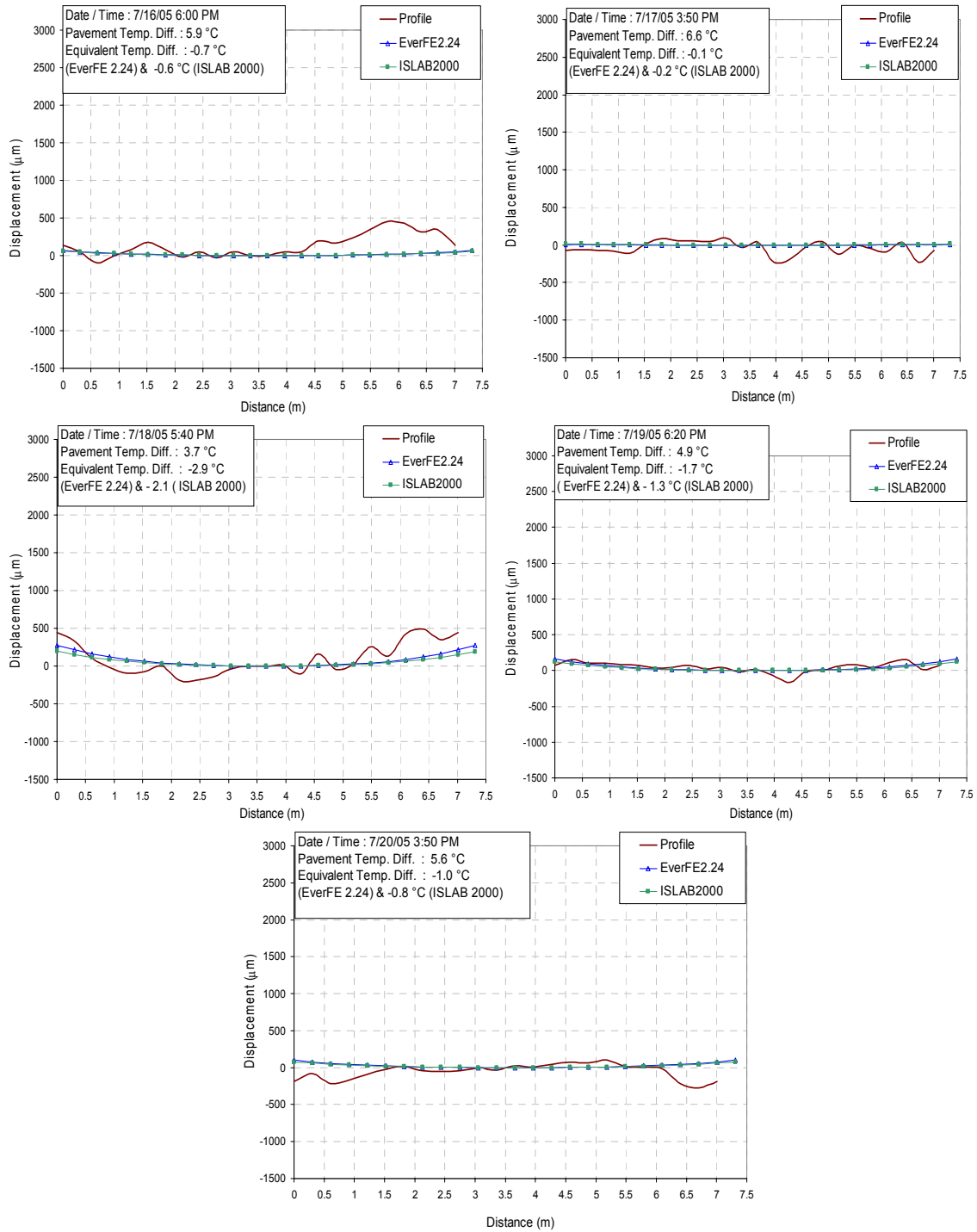
Figure A6-45 Profile measured versus FEM(using method 2 for equivalent temperature) simulated slab curvature profile of diagonal 1 direction at positive temperature different condition in test section 2 (morning paving) of US-30, Marshalltown
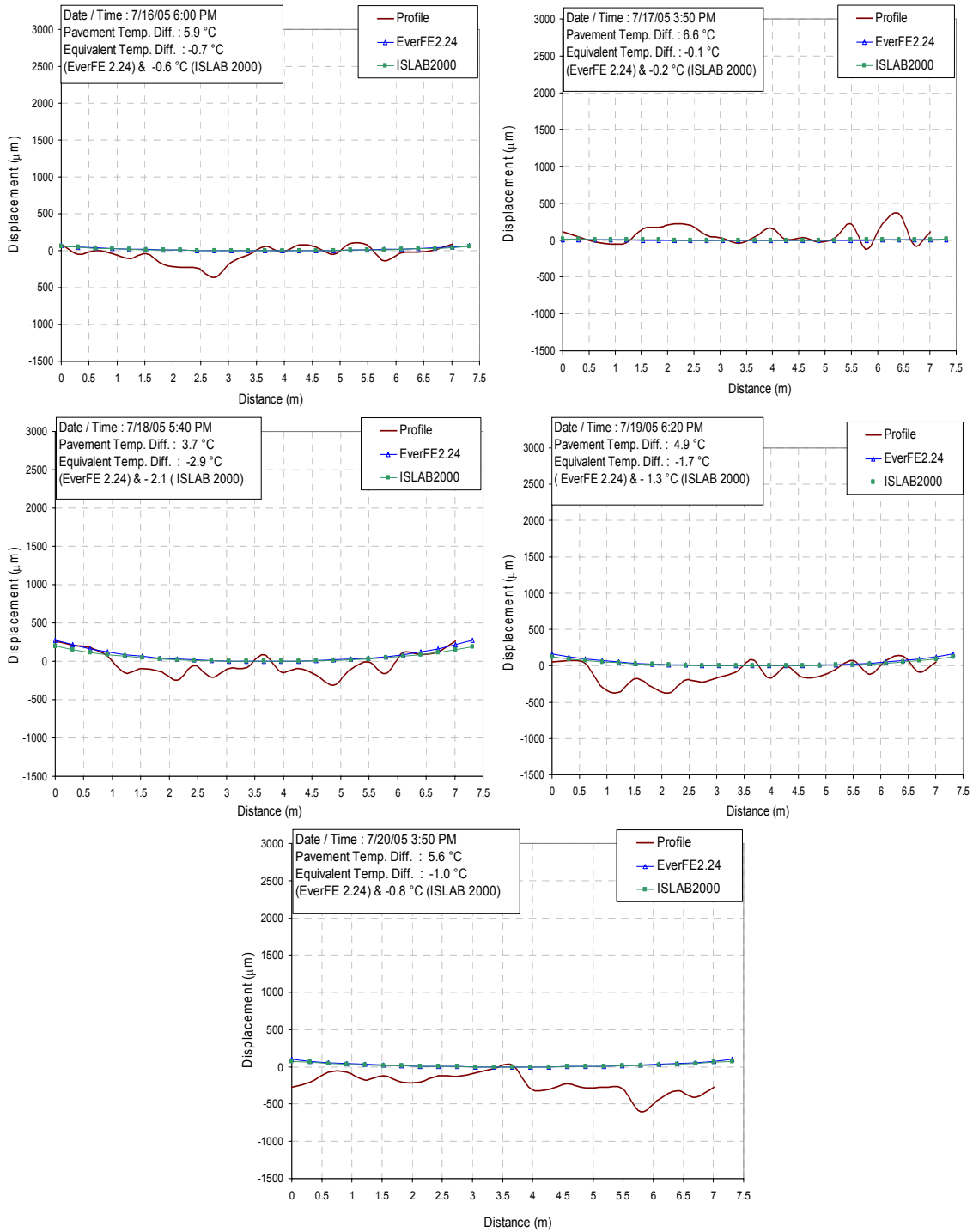
Figure A6-46 Profile measured versus FEM(using method 2 for equivalent temperature) simulated slab curvature profile of diagonal 2 direction at positive temperature different condition in test section 2 (morning paving) of US-30, Marshalltown
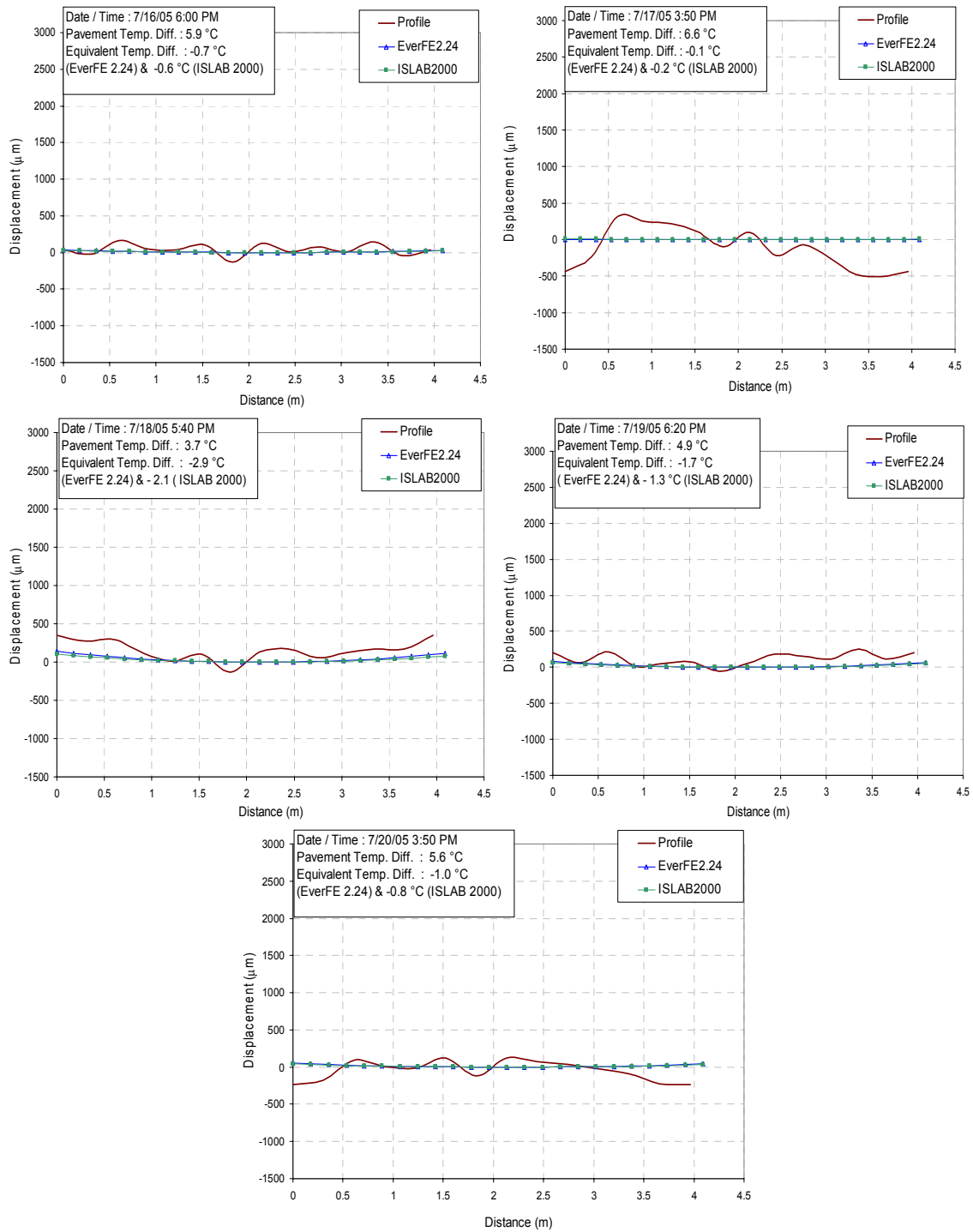
Figure A6-47 Profile measured versus FEM(using method 2 for equivalent temperature) simulated slab curvature profile of transverse 1 direction at positive temperature different condition in test section 2 (morning paving) of US-30, Marshalltown
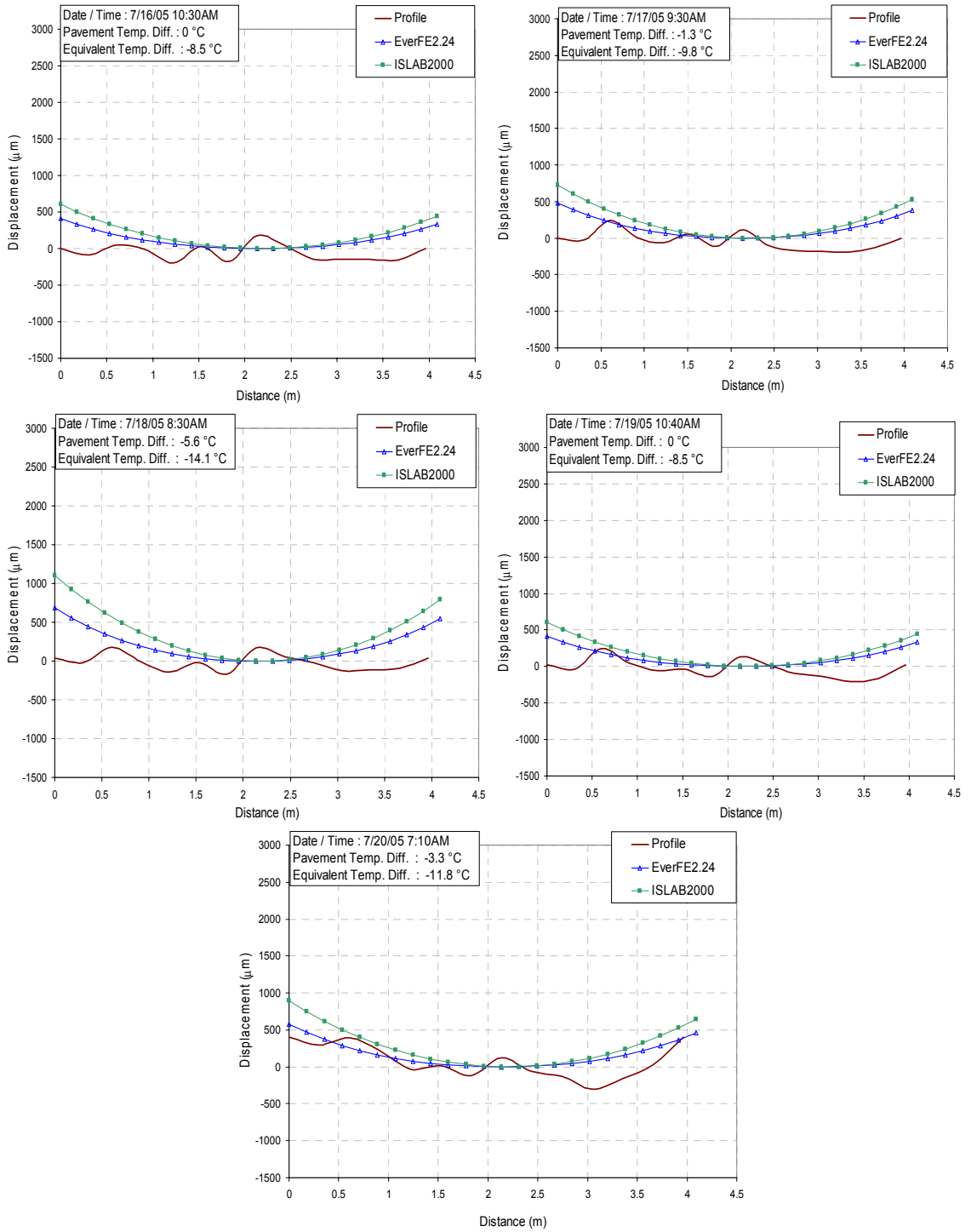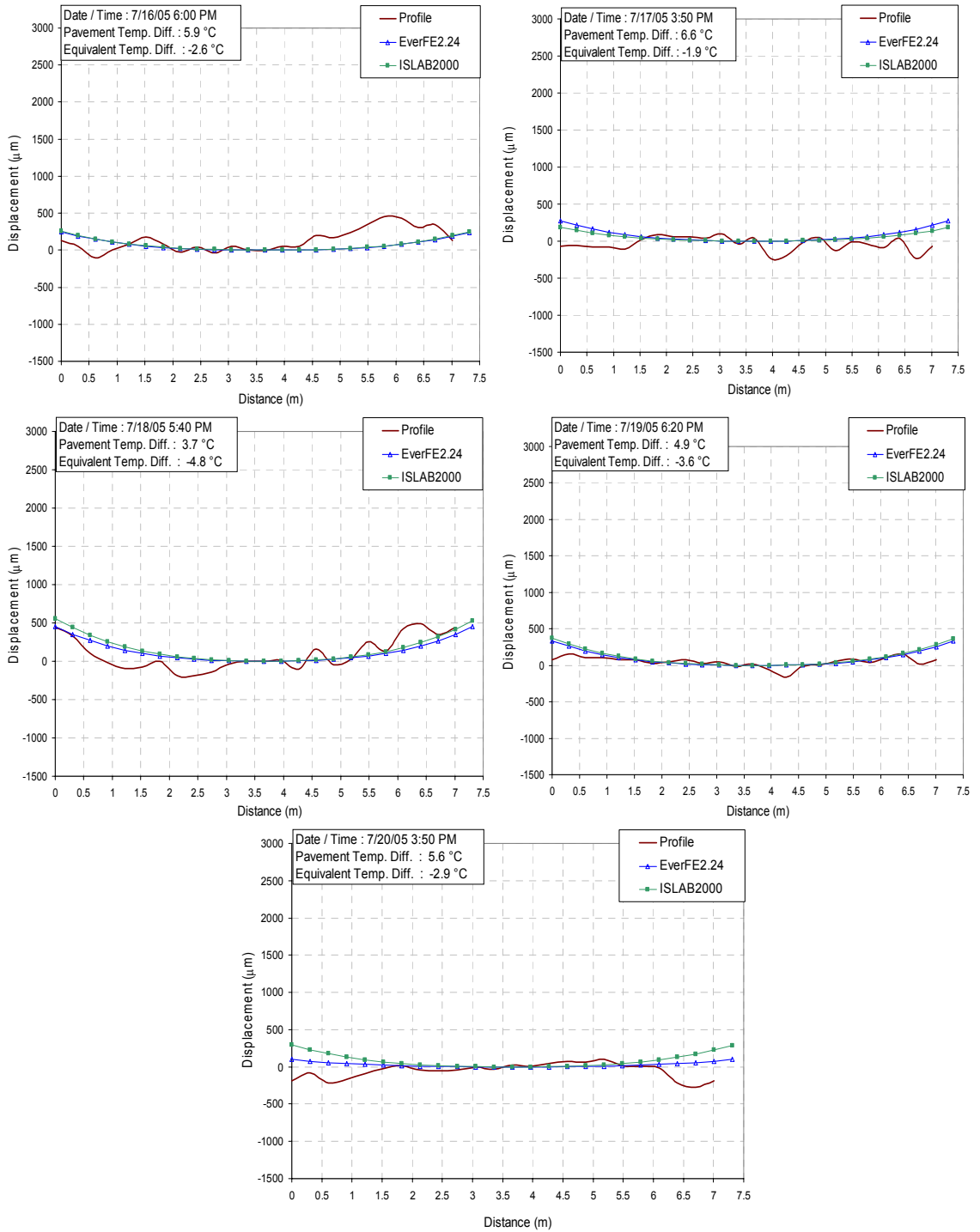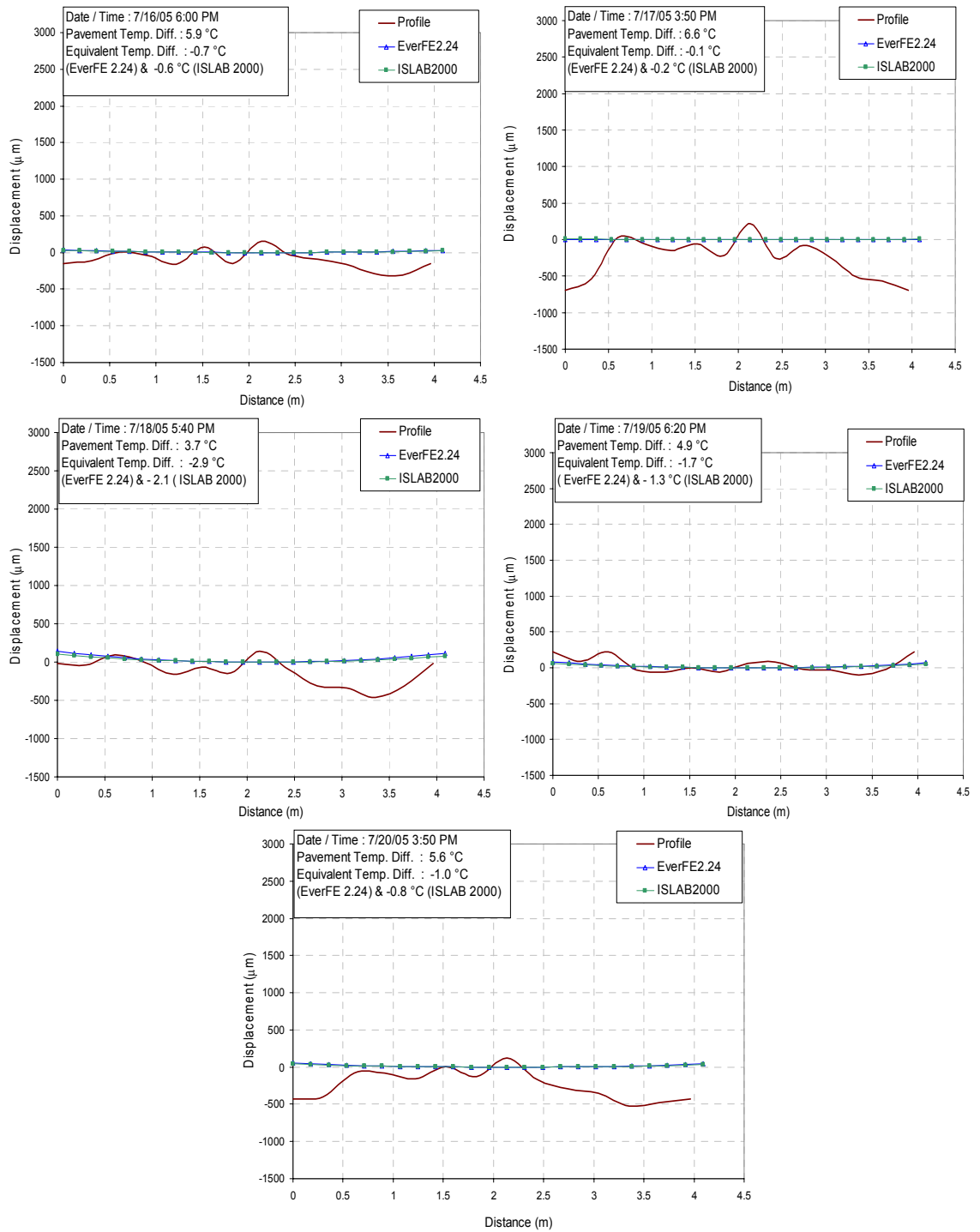
Figure A6-48 Profile measured versus FEM(using method 2 for equivalent temperature) simulated slab curvature profile of transverse 2 direction at positive temperature different condition in test section 2 (moring paving) of US-30, Marshalltown

APPENDIX 7 SMOOTHNESS INDEX

Table A7-1 Smoothness index at slab edge profile in test section 1 (afternoon paving) of US-34, Burlington

Date	Age (hr)	Amb. Temp. (°C)	Ave. Pave. Temp. (°C)	Pave. Temp. Diff. (°C)	IRI (mm/km)	PTRN (mm/km)	RN
6/8/05 6:14 PM	24.8	20.1	26.8	-5.8	1245	2619	3.29
6/9/05 8:03 AM	38.6	20.6	23.7	-1.9	1196	2554	3.32
6/9/05 2:46 PM	45.3	28.0	31.2	11.0	1275	2867	3.16
6/10/05 7:33 AM	62.1	22.4	26.7	-2.6	1259	2688	3.25
6/10/05 2:29 PM	69.0	28.7	32.1	13.5	1363	3315	2.94
6/11/05 7:34 AM	86.1	20.9	24.2	-1.9	1246	2728	3.23
6/11/05 2:59 PM	93.5	28.9	32.1	14.2	1174	2729	3.23
6/12/05 7:02 AM	109.5	20.4	24.9	-3.2	1265	2878	3.15
6/12/05 1:15 PM	115.8	28.2	31.9	14.8	1190	2800	3.19
6/13/05 7:16 AM	133.8	21.0	25.2	-2.6	1245	2731	3.23

Table A7-2 Smoothness index at mid-slab profile in test section 1 (afternoon paving) of US-34, Burlington

Date	Age (hr)	Amb. Temp. (°C)	Ave. Pave. Temp. (°C)	Pave. Temp. Diff. (°C)	IRI (mm/km)	PTRN (mm/km)	RN
6/8/05 6:36 PM	25.1	20.1	26.7	-5.8	1246	2422	3.39
6/9/05 8:14 AM	38.8	21.0	23.9	-1.3	1119	2556	3.32
6/9/05 2:56 PM	45.4	28.1	31.2	10.3	928	2284	3.47
6/10/05 7:44 AM	62.3	22.9	26.9	-1.9	1059	2516	3.34
6/10/05 2:36 PM	69.1	28.7	32.2	12.9	1074	2562	3.32
6/11/05 7:42 AM	86.2	21.3	24.2	-1.9	1022	2554	3.32
6/11/05 3:08 PM	93.7	29.4	32.3	13.5	1060	2420	3.39
6/12/05 6:53 AM	109.4	20.4	25.0	-3.9	1046	2758	3.22
6/12/05 1:23 PM	115.9	28.1	32.1	15.5	1057	2628	3.28
6/13/05 7:24 AM	133.9	20.8	25.1	-3.2	1011	2124	3.56

303

**Table A7-3 Smoothness index at 0.6m from shoulder profile in test section 1
(afternoon paving) of US-34, Burlington**

Date	Age (hr)	Amb. Temp. (˚C)	Ave. Pave. Temp. (˚C)	Pave. Temp. Diff. (˚C)	IRI (mm/km)	PTRN (mm/km)	RN
6/9/05 8:43 AM	39.3	22.1	24.2	0.0	1486	3083	3.05
6/9/05 3:09 PM	45.7	28.2	31.2	9.7	1513	3130	3.03
6/10/05 7:54 AM	62.4	23.2	27.0	-1.3	1518	3471	2.87
6/10/05 2:43 PM	69.3	28.9	32.4	12.9	1699	3577	2.82
6/11/05 3:16 PM	93.8	29.4	32.3	13.5	1642	3646	2.79
6/12/05 1:33 PM	116.1	28.1	32.3	16.1	1698	3748	2.74
6/13/05 7:33 AM	134.1	20.8	25.1	-3.2	1554	2759	3.21
6/13/05 1:26 PM	139.9	26.4	29.6	11.0	1693	3457	2.88
6/14/05 8:07 AM	158.7	18.9	23.8	-3.9	1609	3651	2.79
6/14/05 4:29 PM	167.0	23.3	26.2	3.9	1568	3341	2.93
6/15/05 9:09 AM	183.7	21.3	21.9	0.6	1516	3203	2.99

**Table A7-4 Smoothness index at 0.9 m from shoulder profile in test section 1
(afternoon paving) of US-34, Burlington**

Date	Age (hr)	Amb. Temp. (˚C)	Ave. Pave. Temp. (˚C)	Pave. Temp. Diff. (˚C)	IRI (mm/km)	PTRN (mm/km)	RN
6/9/05 8:49 AM	39.3	22.1	24.2	0.0	1363	3461	2.87
6/9/05 3:19 PM	45.8	28.2	31.2	9.0	1226	2900	3.14
6/10/05 8:11 AM	62.7	23.1	26.9	-0.6	1186	3001	3.09
6/10/05 2:50 PM	69.3	28.9	32.6	13.5	1169	2744	3.22
6/11/05 3:25 PM	93.9	29.4	32.4	13.5	1281	3117	3.04
6/12/05 1:39 PM	116.2	28.3	32.4	16.1	1142	2833	3.18
6/13/05 7:42 AM	134.2	20.9	25.1	-3.2	1079	2447	3.38
6/13/05 1:33 PM	140.1	26.4	29.6	11.0	1243	2941	3.12
6/14/05 8:14 AM	158.8	18.8	23.8	-3.9	1262	3113	3.04
6/14/05 4:41 PM	167.2	23.2	26.3	3.2	1208	2977	3.1
6/15/05 9:17 AM	183.8	21.3	22.0	1.3	1065	2527	3.34

Table A7-5 Smoothness index at 0.3m from vertical joint profile in test section 1 (afternoon paving) of US-34, Burlington

Date	Age (hr)	Amb. Temp. (°C)	Ave. Pave. Temp. (°C)	Pave. Temp. Diff. (°C)	IRI (mm/km)	PTRN (mm/km)	RN
6/9/05 9:20 AM	39.8	22.9	24.7	1.9	1130	3032	3.08
6/9/05 3:43 PM	46.3	28.8	31.4	9.7	1082	2868	3.16
6/10/05 8:34 AM	63.1	23.3	26.9	-0.6	904	2759	3.21
6/10/05 3:07 PM	69.6	28.9	32.7	13.5	895	2524	3.34
6/11/05 3:46 PM	94.3	29.1	32.7	12.9	977	2430	3.39
6/12/05 1:55 PM	116.4	28.9	32.6	14.8	984	2584	3.31
6/13/05 7:58 AM	134.5	21.0	25.0	-3.2	950	2545	3.33
6/13/05 1:48 PM	140.3	26.6	30.0	11.0	1085	2811	3.19
6/14/05 8:26 AM	158.9	18.8	23.8	-3.9	1180	2938	3.12
6/14/05 4:56 PM	167.4	23.7	26.1	1.9	1090	2519	3.34
6/15/05 9:32 AM	184.0	21.2	22.1	1.9	931	2300	3.46

Table A7-6 Smoothness index at 0.9 m from vertical joint profile in test section 1 (afternoon paving) of US-34, Burlington

Date	Age (hr)	Amb. Temp. (°C)	Ave. Pave. Temp. (°C)	Pave. Temp. Diff. (°C)	IRI (mm/km)	PTRN (mm/km)	RN
6/9/05 9:15 AM	39.8	22.9	24.7	1.9	1208	2650	3.27
6/9/05 3:31 PM	46.0	28.3	31.2	9.0	1164	2439	3.38
6/10/05 8:25 AM	62.9	23.3	26.9	-0.6	1085	2398	3.41
6/10/05 2:58 PM	69.4	28.9	32.6	13.5	1011	1966	3.65
6/11/05 3:33 PM	94.1	29.4	32.6	13.5	1041	2196	3.52
6/12/05 1:49 PM	116.3	28.3	32.6	14.8	907	2048	3.6
6/13/05 7:50 AM	134.3	20.9	25.0	-3.2	945	1792	3.75
6/13/05 1:41 PM	140.2	26.6	29.9	11.6	1218	2318	3.45
6/14/05 8:21 AM	158.8	18.8	23.8	-3.9	1025	2368	3.42
6/14/05 4:50 PM	167.3	23.2	26.1	1.9	989	2190	3.52
6/15/05 9:25 AM	183.9	21.2	22.1	1.3	921	1956	3.66

Table A7-7 Smoothness index at slab edge profile in test section 2 (morning paving) of US-34, Burlington

Date	Age (hr)	Amb. Temp. (˚C)	Ave. Pave. Temp. (˚C)	Pave. Temp. Diff. (˚C)	IRI (mm/km)	PTRN (mm/km)	RN
6/10/05 4:43 PM	54.0	29.4	33.5	10.7	1748	3955	2.65
6/11/05 6:45 AM	68.0	19.5	25.1	-3.8	1675	3640	2.79
6/11/05 1:24 PM	74.7	28.2	30.5	10.7	1636	3704	2.76
6/12/05 7:44 AM	93.0	21.6	26.0	-2.5	1778	3649	2.79
6/12/05 2:38 PM	99.9	29.1	33.1	11.9	1776	3802	2.72
6/13/05 9:58 AM	119.3	23.4	26.5	0.6	1606	3187	3
6/13/05 2:35 PM	123.8	27.3	31.4	10.7	1682	3520	2.85
6/14/05 6:42 AM	139.9	18.8	24.8	-5.0	1761	3507	2.85
6/14/05 2:49 PM	148.1	22.7	26.2	3.1	1690	3611	2.81
6/15/05 6:33 AM	163.8	17.6	21.4	-5.0	1679	3671	2.78
6/15/05 12:44 PM	170.0	22.5	25.0	5.6	1524	3471	2.87

Table A7-8 Smoothness index at mid- slab profile in test section 2 (morning paving) of US-34, Burlington

Date	Age (hr)	Amb. Temp. (˚C)	Ave. Pave. Temp. (˚C)	Pave. Temp. Diff. (˚C)	IRI (mm/km)	PTRN (mm/km)	RN
6/10/05 4:51 PM	54.1	29.4	33.4	10.0	1185	2635	3.28
6/11/05 6:52 AM	68.1	19.5	25.1	-3.8	1125	2624	3.29
6/11/05 1:32 PM	74.8	28.2	30.8	10.0	1073	2447	3.38
6/12/05 7:52 AM	93.1	21.6	26.1	-2.5	999	2325	3.45
6/12/05 2:46 PM	100.0	29.1	33.2	11.9	1035	2379	3.42
6/13/05 9:06 AM	118.3	22.4	25.9	-1.9	1136	2652	3.27
6/13/05 2:43 PM	124.0	26.9	31.6	10.7	1040	2210	3.51
6/14/05 6:50 AM	140.1	18.8	24.8	-5.0	1063	2529	3.34
6/14/05 2:56 PM	148.2	22.7	26.4	3.8	1021	2395	3.41
6/15/05 6:40 AM	163.9	17.9	21.4	-5.0	1126	2548	3.33
6/15/05 12:55 AM	170.2	22.4	25.1	5.6	1066	2434	3.39

Table A7-9 Smoothness index at 0.6m from shoulder profile in test section 2 (morning paving) of US-34, Burlington

Date	Age (hr)	Amb. Temp. (°C)	Ave. Pave. Temp. (°C)	Pave. Temp. Diff. (°C)	IRI (mm/km)	PTRN (mm/km)	RN
6/10/05 4:59 PM	54.3	29.2	33.5	10.0	1366	2720	3.24
6/11/05 1:40 PM	74.9	28.7	30.9	10.7	1328	2546	3.33
6/12/05 2:54 PM	100.2	29.2	33.4	11.9	1309	2617	3.29
6/13/05 9:13 AM	118.5	22.8	25.9	-1.3	1363	2723	3.23
6/13/05 2:50 PM	124.1	26.9	31.6	10.7	1406	2729	3.23
6/14/05 6:56 AM	140.2	18.9	24.8	-5.0	1366	2669	3.26
6/14/05 3:04 PM	148.3	22.7	26.5	3.1	1352	2561	3.32
6/15/05 6:48 AM	164.1	17.9	21.4	-5.0	1325	2622	3.29
6/15/05 1:05 PM	170.3	22.4	25.3	5.0	1322	2747	3.22

Table A7-10 Smoothness index at 0.9 m from shoulder profile in test section 2 (morning paving) of US-34, Burlington

Date	Age (hr)	Amb. Temp. (°C)	Ave. Pave. Temp. (°C)	Pave. Temp. Diff. (°C)	IRI (mm/km)	PTRN (mm/km)	RN
6/10/05 5:06 PM	54.3	29.2	33.5	9.4	1078	2581	3.31
6/11/05 1:47 PM	75.0	28.7	30.9	10.7	1049	2340	3.44
6/12/05 3:01 PM	100.3	29.2	33.5	12.5	1078	2507	3.35
6/13/05 9:20 AM	118.6	22.8	25.9	-1.3	1090	2676	3.26
6/13/05 2:57 PM	124.2	27.3	31.7	10.7	1229	2755	3.22
6/14/05 7:03 AM	140.3	18.9	24.7	-5.0	1093	2699	3.25
6/14/05 3:11 PM	148.4	23.4	26.5	3.1	1071	2456	3.37
6/15/05 6:54 AM	164.2	18.2	21.4	-5.0	1070	2412	3.4
6/15/05 1:12 PM	170.4	22.2	25.4	5.0	1103	2436	3.39

Table A7-11 Smoothness index at 0.3m from vertical joint profile in test section 2 (morning paving) of US-34, Burlington

Date	Age (hr)	Amb. Temp. (˚C)	Ave. Pave. Temp. (˚C)	Pave. Temp. Diff. (˚C)	IRI (mm/km)	PTRN (mm/km)	RN
6/10/05 5:21 PM	54.6	28.9	33.6	8.8	1472	3327	2.94
6/11/05 2:04 PM	75.3	28.8	31.3	11.3	1407	3231	2.98
6/12/05 3:15 PM	100.5	29.2	33.6	12.5	1467	3681	2.77
6/13/05 9:35 AM	118.8	22.9	26.1	-0.6	1336	3106	3.04
6/13/05 3:10 PM	124.4	26.7	31.8	10.7	1434	3341	2.93
6/14/05 7:18 AM	140.6	18.9	24.7	-5.0	1164	2606	3.29
6/14/05 3:25 PM	148.7	23.3	26.9	3.8	1344	2915	3.14
6/15/05 7:08 AM	164.4	18.6	21.4	-4.4	1322	3024	3.08

Table A7-12 Smoothness index at 0.9 m from vertical joint profile in test section 2 (morning paving) of US-34, Burlington

Date	Age (hr)	Amb. Temp. (˚C)	Ave. Pave. Temp. (˚C)	Pave. Temp. Diff. (˚C)	IRI (mm/km)	PTRN (mm/km)	RN
6/10/05 5:14 PM	54.5	28.9	33.6	8.8	1254	2744	3.22
6/11/05 1:55 PM	75.2	28.8	31.1	10.7	1185	2567	3.32
6/12/05 3:08 PM	100.4	29.2	33.5	12.5	1109	2874	3.16
6/13/05 9:28 AM	118.8	22.9	26.1	-0.6	1134	2273	3.48
6/13/05 3:03 PM	124.3	27.3	31.8	10.7	1163	2636	3.28
6/14/05 7:10 AM	140.4	18.9	24.8	-5.0	1261	2731	3.23
6/14/05 3:18 PM	148.6	23.4	26.6	3.8	1186	2616	3.29
6/15/05 7:01 AM	164.3	18.2	21.4	-5.0	1303	2729	3.23

Table A7-13 Smoothness index at slab edge profile in test section 1 (afternoon paving) of US-30, Marshalltown

Date	Age (hr)	Amb. Temp. (˚C)	Ave. Pave. Temp. (˚C)	Pave. Temp. Diff. (˚C)	IRI (mm/km)	PTRN (mm/km)	RN
7/14/05 10:11 AM	20.25	29.9	41.4	0.7	1311	2994	3.1
7/14/05 4:14 PM	26.33	32.3	46.1	8.5	1513	3324	2.94
7/15/05 6:23 AM	40.5	20.4	37.8	-3.9	1336	2897	3.14
7/15/05 2:30 PM	48.58	32.9	40.0	6.6	1491	3356	2.92
7/16/05 6:33 AM	64.67	21.1	34.7	-3.9	1497	3188	3
7/16/05 3:19 PM	73.42	32.8	39.2	8.5	1357	3105	3.04
7/17/05 6:43 AM	88.83	21.7	33.5	-3.3	1541	3406	2.9
7/17/05 1:15 PM	95.33	32.8	36.0	5.9	1431	3169	3.01
7/18/05 6:05 AM	112.17	20.0	31.0	-5.9	1485	3144	3.02
7/18/05 2:58 PM	121.08	27.0	33.0	4.6	1440	3042	3.07
7/19/05 6:06 AM	136.17	16.2	27.7	-4.6	1529	3330	2.93
7/19/05 3:44 PM	145.83	29.4	33.3	7.9	1384	3070	3.06
7/20/05 7:43 AM	161.83	23.9	29.0	-2.6	1352	2931	3.13

Table A7-14 Smoothness index at mid-slab profile in test section 1 (afternoon paving) of US-30, Marshalltown

Date	Age (hr)	Amb. Temp. (˚C)	Ave. Pave. Temp. (˚C)	Pave. Temp. Diff. (˚C)	IRI (mm/km)	PTRN (mm/km)	RN
7/14/05 10:27 AM	20.58	30.3	41.6	0.7	1567	2379	3.42
7/14/05 4:23 PM	26.5	32.5	46.3	8.2	1617	2404	3.4
7/15/05 6:32 AM	40.58	20.6	37.8	-3.9	1551	2316	3.45
7/15/05 2:40 PM	48.75	32.6	40.3	6.2	1584	2359	3.43
7/16/05 6:41 AM	64.75	21.1	34.7	-3.9	1551	2354	3.43
7/16/05 3:28 PM	73.58	32.8	39.2	8.5	1518	2160	3.54
7/17/05 6:50 AM	88.92	21.7	33.4	-3.3	1617	2671	3.26
7/17/05 1:24 PM	95.5	32.8	36.2	6.6	1522	2253	3.49
7/18/05 6:17 AM	112.33	20.0	30.8	-5.9	1634	2378	3.42
7/18/05 3:06 PM	121.17	27.0	33.0	4.6	1666	2477	3.36
7/19/05 6:13 AM	136.33	16.2	27.7	-4.6	1644	2406	3.4
7/19/05 3:55 PM	146	29.4	33.4	7.9	1527	2142	3.55
7/20/05 7:51 AM	161.92	23.9	29.0	-2.6	1549	2161	3.54

Table A7-15 Smoothness index at 0.6m from shoulder profile in test section 1 (afternoon paving) of US-30, Marshalltown

Date	Age (hr)	Amb. Temp. (˚C)	Ave. Pave. Temp. (˚C)	Pave. Temp. Diff. (˚C)	IRI (mm/km)	PTRN (mm/km)	RN
7/14/05 10:40 AM	20.75	30.4	41.7	1.3	1863	3510	2.85
7/14/05 4:34 PM	26.67	32.8	46.3	7.9	1874	3823	2.71
7/15/05 6:46 AM	40.83	21.3	37.6	-3.6	1983	3539	2.84
7/15/05 2:49 PM	48.92	32.6	40.4	6.6	1899	3804	2.72
7/16/05 6:50 AM	64.92	21.1	34.7	-3.9	1917	3870	2.69
7/16/05 3:37 PM	73.67	32.8	39.3	8.2	1904	3750	2.74
7/17/05 6:58 AM	89.08	21.7	33.4	-3.3	1866	3682	2.77
7/17/05 1:33 PM	95.67	32.8	36.3	6.6	1858	3599	2.81
7/18/05 6:27 AM	112.5	20.0	30.8	-5.9	1840	3782	2.73
7/18/05 3:14 PM	121.33	27.0	33.1	4.6	1922	3760	2.74
7/19/05 6:21 AM	136.42	16.2	27.6	-5.2	1836	3679	2.77
7/19/05 4:04 PM	146.17	29.4	33.6	7.9	1825	3408	2.9
7/20/05 8:01 AM	162.08	23.9	28.9	-2.3	1836	3455	2.88

Table A7-16 Smoothness index at 0.9 m from shoulder profile in test section 1 (afternoon paving) of US-30, Marshalltown

Date	Age (hr)	Amb. Temp. (˚C)	Ave. Pave. Temp. (˚C)	Pave. Temp. Diff. (˚C)	IRI (mm/km)	PTRN (mm/km)	RN
7/14/05 4:41 PM	26.75	32.6	46.3	7.9	1672	2956	3.12
7/15/05 6:58 AM	41.08	21.7	37.5	-3.3	1679	2822	3.18
7/15/05 3:07 PM	49.17	32.4	40.5	6.9	1595	2744	3.22
7/16/05 6:57 AM	65.08	21.1	34.5	-3.6	1688	2980	3.1
7/16/05 3:51 PM	73.92	32.8	39.6	7.9	1641	2941	3.12
7/17/05 7:05 AM	89.17	21.7	33.3	-3.3	1617	2706	3.24
7/17/05 1:40 PM	95.75	32.8	36.5	6.9	1592	2663	3.27
7/18/05 6:35 AM	112.67	20.0	30.8	-6.2	1597	2654	3.27
7/18/05 3:23 PM	121.47	27.0	33.2	4.6	2018	4236	2.54
7/19/05 6:28 AM	136.58	16.2	27.6	-5.2	1696	2756	3.22
7/19/05 4:13 PM	146.33	29.4	33.7	8.5	1560	2543	3.33
7/20/05 8:16 AM	162.33	23.9	28.8	-2.0	1679	2748	3.22

**Table A7-17 Smoothness index at 0.3m from vertical joint profile in test section 1
(afternoon paving) of US-30, Marshalltown**

Date	Age (hr)	Amb. Temp. (°C)	Ave. Pave. Temp. (°C)	Pave. Temp. Diff. (°C)	IRI (mm/km)	PTRN (mm/km)	RN
7/14/05 4:57 PM	27	32.4	46.3	7.9	1499	2945	3.12
7/15/05 7:08 AM	41.25	22.4	37.3	-3.9	1376	2448	3.38
7/15/05 3:18 PM	49.42	32.6	40.7	7.2	1412	2657	3.27
7/16/05 7:05 AM	65.20	21.1	34.4	-3.3	1639	2947	3.12
7/16/05 3:58 PM	74.08	32.8	39.6	7.9	1403	2717	3.24
7/17/05 7:12 AM	89.25	21.7	33.3	-3.3	1388	2581	3.31
7/17/05 1:49 PM	95.92	32.8	36.5	7.2	1357	2611	3.29
7/18/05 6:44 AM	112.83	20.0	30.5	-6.2	1380	2496	3.35
7/18/05 3:31 PM	121.58	27.0	33.2	4.6	1330	2407	3.4
7/19/05 6:37 AM	136.67	16.2	27.5	-5.2	1462	2598	3.3
7/19/05 4:20 PM	146.42	29.4	33.8	7.9	1325	2428	3.39
7/20/05 8:24 AM	162.5	23.9	28.7	-2.0	1379	2513	3.34

**Table A7-18 Smoothness index at 0.9 m from vertical joint profile in test section 1
(afternoon paving) of US-30, Marshalltown**

Date	Age (hr)	Amb. Temp. (°C)	Ave. Pave. Temp. (°C)	Pave. Temp. Diff. (°C)	IRI (mm/km)	PTRN (mm/km)	RN
7/14/05 5:06 PM	27.17	32.4	46.4	7.9	1696	2649	3.27
7/15/05 7:16 AM	41.33	22.4	37.3	-3.9	1647	2643	3.28
7/15/05 3:26 PM	49.5	33.0	40.8	7.2	1628	2639	3.28
7/16/05 7:12 AM	65.25	21.1	34.4	-3.3	1709	2786	3.2
7/16/05 4:07 PM	74.17	32.8	39.6	7.9	1633	2477	3.36
7/17/05 7:20 AM	89.42	21.7	33.3	-3.3	1677	2638	3.28
7/17/05 1:56 PM	96	32.8	36.7	7.2	1639	2518	3.34
7/18/05 6:52 AM	112.92	20.0	30.3	-5.9	1669	2485	3.36
7/18/05 3:39 PM	121.75	27.0	33.3	4.6	1545	2335	3.44
7/19/05 6:44 AM	136.83	16.2	27.4	-4.6	1611	2442	3.38
7/19/05 4:29 PM	146.58	29.4	34.0	7.9	1567	2318	3.45
7/20/05 8:31 AM	162.58	23.9	28.7	-2.0	1622	2384	3.41

Table A7-19 Smoothness index at slab edge profile in test section 2 (morning paving) of US-30, Marshalltown

Date	Age (hr)	Amb. Temp. (°C)	Ave. Pave. Temp. (°C)	Pave. Temp. Diff. (°C)	IRI (mm/km)	PTRN (mm/km)	RN
7/15/05 10:29 AM	24.67	29.9	39.5	1.3	1156	2608	3.29
7/15/05 4:35 PM	30.75	32.7	43.8	8.5	1065	2430	3.39
7/16/05 9:22 AM	47.5	27.8	34.9	-2.0	1272	2879	3.15
7/16/05 4:58 PM	55.17	32.2	40.0	7.2	1191	2699	3.25
7/17/05 8:27 AM	70.67	26.7	32.3	-3.3	1267	2677	3.26
7/17/05 2:47 PM	76.92	33.3	36.1	6.2	1223	2939	3.12
7/18/05 7:38 AM	93.83	20.6	28.5	-5.9	1182	2751	3.22
7/18/05 4:36 PM	102.75	26.7	32.0	4.3	1226	2731	3.23
7/19/05 9:38 AM	119.83	25.0	25.8	-2.6	1204	2575	3.31
7/19/05 5:19 PM	127.5	28.9	32.0	5.9	1156	2348	3.43
7/20/05 6:16 AM	140.42	23.3	27.8	-2.6	1232	2789	3.2
7/20/05 2:48 PM	149	31.1	28.8	4.6	1178	2680	3.26

Table A7-20 Smoothness index at mid-slab profile in test section 2 (morning paving) of US-30, Marshalltown

Date	Age (hr)	Amb. Temp. (°C)	Ave. Pave. Temp. (°C)	Pave. Temp. Diff. (°C)	IRI (mm/km)	PTRN (mm/km)	RN
7/15/05 10:37 AM	24.75	29.9	39.5	1.3	1082	1814	3.74
7/15/05 4:45 PM	30.92	32.6	44.0	7.9	1076	1945	3.66
7/16/05 9:33 AM	47.75	27.8	35.0	-1.6	1043	1704	3.81
7/16/05 5:07 PM	55.25	32.2	40.0	7.2	1055	1803	3.75
7/17/05 8:40 AM	70.83	26.7	32.3	-3.3	1040	1764	3.77
7/17/05 2:55 PM	77.08	33.3	36.2	6.6	1059	1743	3.78
7/18/05 7:46 AM	93.92	20.6	28.5	-5.9	1063	1851	3.72
7/18/05 4:46 PM	102.92	26.7	32.2	3.9	1044	1754	3.78
7/19/05 9:46 AM	119.92	25.0	25.8	-2.6	1070	1756	3.78
7/19/05 5:29 PM	127.67	28.9	32.1	5.9	1035	1726	3.79
7/20/05 6:25 AM	140.58	23.3	27.6	-3.3	1087	1885	3.7
7/20/05 2:56 PM	149.08	31.1	28.9	4.6	1038	1827	3.73

Table A7-21 Smoothness index at 0.6m from shoulder profile in test section 2 (morning paving) of US-30, Marshalltown

Date	Age (hr)	Amb. Temp. (°C)	Ave. Pave. Temp. (°C)	Pave. Temp. Diff. (°C)	IRI (mm/km)	PTRN (mm/km)	RN
7/15/05 4:52 PM	31	32.2	44.1	7.9	1257	2348	3.43
7/16/05 9:42 AM	47.83	27.8	35.0	-1.3	1213	2176	3.53
7/16/05 5:15 PM	55.42	32.2	40.1	7.2	1201	2144	3.55
7/17/05 8:48 AM	71	26.7	32.4	-2.6	1155	2103	3.57
7/17/05 3:03 PM	77.25	33.3	36.3	6.6	1183	2179	3.53
7/18/05 7:55 AM	94.08	20.6	28.5	-5.9	1223	2064	3.59
7/18/05 4:54 PM	103.08	26.7	32.3	3.9	1177	2135	3.55
7/19/05 9:55 AM	120.08	25.0	26.0	-1.6	1193	2092	3.58
7/19/05 5:38 PM	127.83	28.9	32.1	5.9	1152	2051	3.6
7/20/05 6:32 AM	140.67	23.3	27.6	-3.3	1202	2258	3.48
7/20/05 3:04 PM	149.25	31.1	29.1	5.3	1259	2308	3.46

Table A7-22 Smoothness index at 0.9 m from shoulder profile in test section 2 (morning paving) of US-30, Marshalltown

Date	Age (hr)	Amb. Temp. (°C)	Ave. Pave. Temp. (°C)	Pave. Temp. Diff. (°C)	IRI (mm/km)	PTRN (mm/km)	RN
7/15/05 4:59 PM	31.17	32.2	44.1	7.9	1193	2251	3.49
7/16/05 9:50 AM	48	27.8	35.0	-1.3	1190	2005	3.63
7/16/05 5:23 PM	55.58	32.2	40.2	7.2	1190	2166	3.53
7/17/05 8:56 AM	71.08	26.7	32.4	-2.6	1186	2119	3.56
7/17/05 3:11 PM	77.33	33.3	36.3	6.2	1177	2122	3.56
7/18/05 8:02 AM	94.17	20.6	28.5	-5.9	1163	2147	3.55
7/18/05 5:02 PM	103.17	26.7	32.3	3.9	1111	2177	3.53
7/19/05 10:03 AM	120.25	25.0	25.9	-1.3	1137	2002	3.63
7/19/05 5:45 PM	127.92	28.9	32.1	5.9	1145	2021	3.62
7/20/05 6:39 AM	140.83	23.3	27.5	-3.3	1153	2070	3.59
7/20/05 3:13 PM	149.42	31.1	29.3	4.6	1172	2117	3.56

Table A7-23 Smoothness index at 0.3m from vertical joint profile in test section 2 (morning paving) of US-30, Marshalltown

Date	Age (hr)	Amb. Temp. (°C)	Ave. Pave. Temp. (°C)	Pave. Temp. Diff. (°C)	IRI (mm/km)	PTRN (mm/km)	RN
7/15/05 5:14 PM	31.42	32.2	44.1	7.9	778	2010	3.62
7/16/05 9:59 AM	48.17	27.8	35.0	-0.7	705	1694	3.81
7/16/05 5:31 PM	55.67	31.7	40.2	7.2	824	2026	3.62
7/17/05 9:05 AM	71.25	26.7	32.5	-2.6	817	1978	3.64
7/17/05 3:19 PM	77.5	33.3	36.5	5.9	753	1841	3.72
7/18/05 8:10 AM	94.33	20.6	28.4	-5.9	880	2038	3.61
7/18/05 5:13 PM	103.42	26.7	32.3	3.9	719	1690	3.81
7/19/05 10:12 AM	120.33	25.0	26.0	-0.7	693	1590	3.88
7/19/05 5:55 PM	128.08	28.9	32.1	5.9	704	1862	3.71
7/20/05 6:47 AM	140.92	23.3	27.4	-3.3	795	1890	3.69
7/20/05 3:21 PM	149.5	31.1	29.4	4.9	795	1929	3.67

Table A7-24 Smoothness index at 0.9 m from vertical joint profile in test section 2 (morning paving) of US-30, Marshalltown

Date	Age (hr)	Amb. Temp. (°C)	Ave. Pave. Temp. (°C)	Pave. Temp. Diff. (°C)	IRI (mm/km)	PTRN (mm/km)	RN
7/15/05 5:06 PM	31.25	32.2	44.1	7.9	1117	2220	3.5
7/16/05 10:06 AM	48.25	27.8	35.2	-0.7	1046	1917	3.68
7/16/05 5:38 PM	55.83	31.7	40.3	6.2	1066	1899	3.69
7/17/05 9:12 AM	71.33	26.7	32.5	-2.6	1071	1879	3.7
7/17/05 3:27 PM	77.58	33.3	36.7	6.6	1071	1914	3.68
7/18/05 8:17 AM	94.42	20.6	28.4	-5.9	1035	1816	3.74
7/18/05 5:20 PM	103.5	26.7	32.3	3.9	1021	1805	3.75
7/19/05 10:21 AM	120.5	25.0	26.0	-0.7	1035	1769	3.77
7/19/05 6:02 PM	128.17	28.9	32.1	5.9	1055	1854	3.72
7/20/05 6:55 AM	141.08	23.3	27.3	-3.3	999	1791	3.75
7/20/05 3:28 PM	149.67	31.1	29.5	5.2	1054	1923	3.67

ACKNOWLEDGEMENTS

I would like to express my deepest gratitude to my major advisor, Dr. Halil Ceylan and Dr. Kejin Wang, for their support, advice, and direction during this study. I am also very grateful for Dr. Charles T. Jahren, Dr. R. Chris Williams and Dr. Tomas J. Rudophi's time and efforts on serving my Ph.D. committee and providing valuable comments on my dissertation. I would also like to thank Dr. Kasthurirangan Gopalakrishnan for the many helpful discussions during this study, as well as for reviewing this thesis.

I like to acknowledge the crew of PCC lab and Dennis J. Turner in the Transtec Group, Inc. Without their assistants, much of this work would not have been possible. I also gratefully acknowledge the Federal Highway Administration (FHWA) for the financial assistance which made this research possible.

Special thanks are extended to Dr. Jiong Hu, Dr. Dong Chen, Dr. Zhi Ge, Satish Reddy Chintakunta, Fatih Bektas and Chetan Hazaree for theirs constant helps and supports.

I would like to express my deep gratitude and sincere tank to my wife, Jung-Sue Kwon for her unlimited patience, encouragement, and love. I am deeply indebted to her continuous support and extraordinary efforts to share the bulk of responsibility and raising our two kids Ki-June and Leslie. Without her efforts, this study could not have been completed. I want to thank my parents, family and friends for their love, support and encouragement.

Sunghwan Kim Ames, November 2006